Earth & Ocean Sciences
School of Natural Sciences

NUI Galway
OÉ Gaillimh

Lateral transport of suspended particulate matter in nepheloid layers along the Irish continental margin - A case study of the Whittard Canyon, North-East Atlantic Ocean.

A thesis submitted to the National University of Ireland, Galway for the degree of Doctor of Philosophy

Annette M. Wilson (B.Sc)

Supervisors: Dr. Martin White & Dr. Robin Raine

Earth & Ocean Sciences
School of Natural Sciences
National University of Ireland, Galway

June 2016

Internal examiner

Dr. Rachel Cave

Earth & Ocean Sciences

School of Natural Sciences

National University of Ireland, Galway

Ireland

External examiner

Dr. Furu Mienis

Ocean Systems Sciences

NIOZ Royal Netherlands Institute for Sea Research, Texel

The Netherlands

Table of Contents

Declaration

I, Annette Wilson, certify that this thesis is all my own work and that the results presented here are to best of my knowledge correct. I have not obtained a degree in this University or elsewhere on the basis of any of this work. Contributions by other authors were made to the articles presented here, as outlined on the cover page of each chapter.

Signed:

Date:

Funding

The Hardiman Research Scholarship programme, NUI Galway is gratefully acknowledged for its support and for enabling me to carry out the research for this thesis.

The samples and data collected for the research presented in this thesis were collected over three research surveys carried out under the Sea Change strategy with the support of the Marine Institute and the Marine Research Sub-Programme of the National Development Plan 2007–2013.

Funding from the Thomas Crawford Hayes Award Trust, NUI Galway, Marine Institute Networking and Travel Grant Scheme, Challenger Society and AGU Student travel grant scheme are also gratefully acknowledged.

Abstract

Nepheloid layers, defined by their increased concentration of suspended particulate material (SPM), are an important transport mechanism in the pelagic to benthic coupling of material, including rich organic matter. Fortuitously located at the edge of the Celtic Sea shelf along the NE Atlantic margin; an area of high energy and primary production–the Whittard Canyon is recognised as a refuge for benthic and suspension feeding fauna. The formation and composition of material in benthic (BNL) and intermediate nepheloid layers (INLs) in the Whittard Canyon were investigated over the course of three research surveys between 2011 and 2013, in order to investigate the extent and significance of this transport pathway. BNLs were detected in the four surveyed branches, to water depths greater than 2500 m, with INLs occurring as extensions from the benthic source and stretching distances of 25 km off the slope. Hotspots for nepheloid layer generation were identified at depths of critical and supercritical conditions for semidiurnal internal tide reflection and at the boundaries of the permanent thermocline and Mediterranean Outflow Water. Seasonal variations in primary productivity and, temporal variations induced by the combined effects of (seasonal) stratification and storm activity, influenced nepheloid layer generation and the distribution patterns of SPM. Recently, bottom trawling activity has also become a recognised and legitimate mechanism for sediment transport, feeding thick or enhanced nepheloid layers (ENLs). ENLs, with concentrations of SPM typically an order of magnitude higher than normal nepheloid layers, were detected during the survey in June 2013. High spatial and temporal coverage of bottom trawlers, identified using Vessel Monitoring System data, coincided with the occurrence of these events. Material collected from (normal) BNLs and INLs in 2013 showed enrichment of fresh particulate organic material (molar C/N, pigments, SEMs, lipid biomarkers). BNLs in the upper reaches of the canyon (650–750 m) had high concentrations of labile lipids and showed high contributions of chlorophyll *a* and other compounds derived from primary production in the surface waters. Considerable compositional heterogeneity was also observed in the nepheloid layers, indicative of the inherent natural, spatial and temporal variance of settling organic and resuspended material that is influenced by different processes in the

different branches. Localised variations in energy fluxes in the different canyon branches partly explain the frequency, location and level of turbidity of the nepheloid layers. However, the differing degree of trawling activity adjacent to the canyon branches is also likely to have an influence, particularly on the compositional components. Qualitative analysis (lipid biomarkers) from benthic nepheloid layers (1300–1400 m) showed an apparent eastern and western differentiation which is likely associated with the alteration of material by trawling activity. In terms of sediment transport rates, the magnitude of the fishing activity adjacent to the Whittard Canyon is shown to have impacts on human rather than geological timescales. Furthermore, a unique assemblage of limid bivalves and deep-sea oysters was found in association with nepheloid layers in the canyon. Changes to the distribution and delivery of rich organic matter by nepheloid layers are likely to affect faunal feeding, distribution patterns and, the functioning of these canyon ecosystems.

Chapter 1
Introduction

1.1 General introduction

From shelf seas to the deep abyss

The deep-sea is one of the largest, most diverse and poorly understood ecosystems on the Earth's surface. The deep-sea (i.e. water depths >1000 m), occupies approximately 60% of the Earth's surface, covering an area of approximately 360 million km^2 (Glover and Smith, 2003). Variable habitats from seamounts, hydrothermal vents and cold seeps to submarine canyons and flat abyssal plains are numerous but widely spaced on the seafloor. Topographic highs, rising 1000 to 4000 m above the seafloor and lows as deep at 11,000 m encourage complex oceanographic and sedimentology patterns and promote richly diverse ecosystems.

Previous perceptions of the deep-sea have changed dramatically over the last two centuries. The idea that the deep sea was barren, with increasing pressures, coldness and darkness inhibiting any organisms from living there, was put to rest with early expeditions such as the *HMS Challenger* (1872–1876). We now know that the deep ocean hosts some of the most unique habitats and valuable commodities in the world (e.g. Thiel, 2001; Ramirez-Llodra et al., 2011). In recent years we are increasingly turning to the deep-sea for commercial uses and commodities (e.g. mineral extraction and nodule mining, communication cables, pharmaceuticals and, storage of waste (see Thiel, 2001; Glover and Smith, 2003; Ramirez-Llodra et al., 2011 and references therein). The vast diversity of the deep ocean creates conservational challenges. Therefore research on production pathways to the deep can aid our understanding of how the resident ecosystems function.

Although there is life in the deep sea, due to the light limitations below the euphotic zone, this part of the open ocean is generally considered food limited. Many organisms have adapted to such conditions, however the export and sinking of organic particles from the surface and shelf environments supports (most) life at great depths (Lampitt and Anita, 1997; Puig et al., 2001; Smith et al., 2009). In these environments, terrestrial, fluvial and glacial erosion can introduce particles into the ocean (Fig. 1.1). While organic matter can be derived from these particles, they tend to be refractory sources with a high potential for preservation in marine sediments. Marine algae are autotrophic organisms with phytoplankton in surface water and shelf seas, particularly diatoms and coccolithophorids,

forming the base of the ocean food chain. These microscopic plants globally produce ~45–50 Gt C yr^{-1} (e.g. Longhurst et al., 1995). Detritus; ranging from fresh phyto- and zoo- plankton remains and faecal material to whale falls, are the most important source of labile marine particulate organic matter (Smith, 2006). Marine snow (particles with diameters >5 mm) also contribute to higher sinking velocities due to the larger size and as marine snow escapes degradation processes, it can also rapidly transport rich organic matter, triggering an awakening response of benthic organisms after a spring bloom (e.g. Allredge and Silver, 1988; Graf, 1989; Lampitt et al., 1993). The density of pure organic matter is lower than water and it has been shown that calcite, opal and lithogenic material serve as ballast to achieve particle densities high enough to allow sinking (Iversen and Ploug, 2010). Generally the sinking velocity of ocean particles ranges between 10 and 150 m d^{-1} (McDonnell and Buesseler, 2010 and references therein). In the deep North Atlantic Ocean higher sinking velocities of ~3000 m d^{-1} have been estimated (Lampitt, 1985) thus inferring high levels of production, high velocity sinking events and/or other processes increasing vertical transport here.

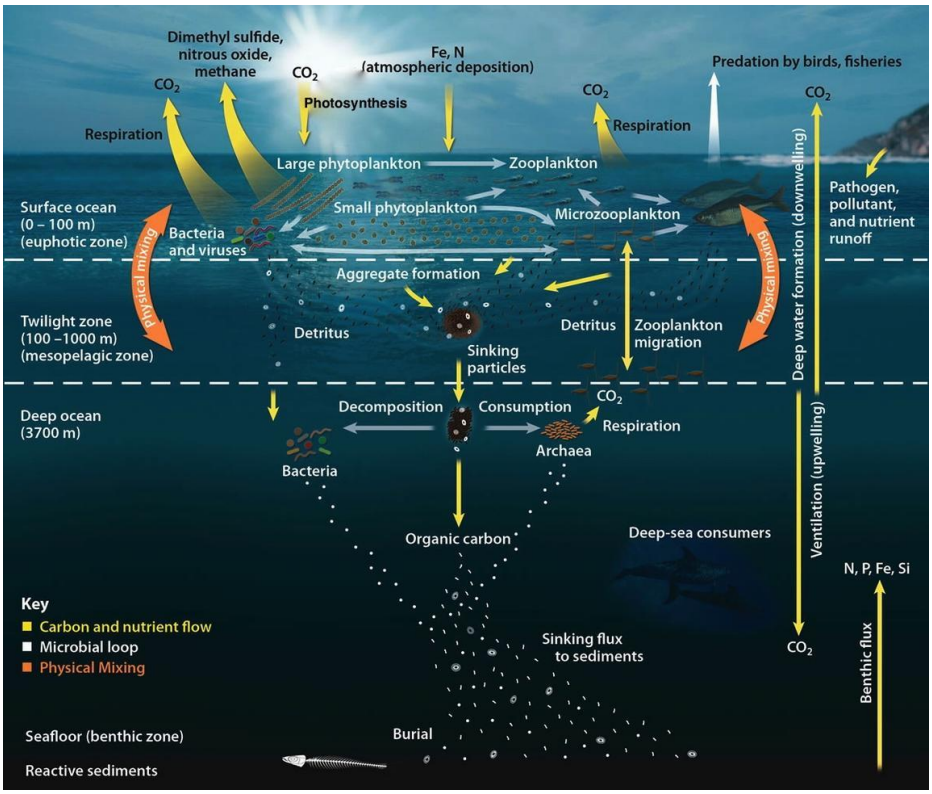

Fig. 1.1 Sources of particles and the ocean carbon cycle (Image credit: Oak Ridge National Laboratory Source: http://serc.carleton.edu/eslabs/carbon/6a.html)

Transport at the continental margin

In most areas of the open ocean, surface production is the most significant source of particles to the deep. An attenuated 'rain' of detritus from remote surface water typically delivers 1–10 g C_{org} $m^{-2}yr^{-1}$, (Glover and Smith, 2003) but a significant proportion of organic matter is also delivered through lateral advection of particles (e.g. Wollast, 1998; Jahnke et al., 1990; Inthorn et al., 2006a). Furthermore, primary production is not evenly distributed across the ocean. Although the highest production occurs in the shallow coastal and shelf environments (rich in light and nutrients), continental margins are important areas of export. The margins are the ocean's gateway, forming a transitional zone, separating the generally productive shelf seas and the deep ocean; mediating transfer of water, energy, sediments, organisms, and contaminants between the continents and the open sea (e.g. Levin and Dayton, 2009). High nutrient fluxes and upwelling often occur here due to the interaction of wind, tides and the dramatic changes in topography (Fig. 1.2). As such the continental margins of the oceans worldwide are areas of high productivity and play a significant role in global biogeochemical cycles including carbon cycling in the ocean (e.g. Walsh, et al., 1981; Lampitt and Anita, 1997; Wollast, 1998). Although continental margins represent only ~15–20% of the surface area of the marine system 50% of the global marine production takes place there (Wollast, 1998). In addition, approximately half of the organic production in coastal zones is exported to the continental slope and open ocean at the margin, with approximately 80% of the total exported organic carbon is buried in the margin sediments (Wollast, 1998). More recent studies have estimated that 90% of the ocean's carbon is buried in continental margin sediments (e.g. Hartnett et al., 1998; Sarmiento and Gruber, 2006).

The significant role of lateral advection and transport from continental shelves was first suggested by Walsh et al. (1981). A tentative global marine carbon cycle published by Wollast (1998) indicated lateral particle fluxes between shelf, slope and the open ocean only by question marks. However, lateral transport has since been investigated by many large international projects e.g. Shelf Edge Exchange Processes I and II (SEEP), Ocean Margin EXchange I and II (OMEX) and STRATA FORmation on Margins (STRATAFORM). The importance of

considering continental margins and lateral transport when assessing the relative role in the marine environment was conclusively demonstrated by such projects (see publications from these projects e.g. Walsh et al., 1988; Lampitt et al., 1995; van Weering et al., 1998; Nittrourer, 1999; van Weering and McCave, 2002).

Lateral advection and export likely explain discrepancy in models and vertical flux studies. Remote sensing data on primary production coupled with sediment trap data have been used with assumptions on decomposition of organic matter to model and estimate organic carbon fluxes and clarify the amount of fixation of organic carbon by marine phytoplankton in the euphotic zone with benthic recycling and burial rates at the underlying sediment (e.g. Antia et al., 2001). However, these models are only vertically adjusted for particle transport and there are remarkable differences observed when rates of benthic remineralisation are used to calculate the organic flux (Seiter et al., 2005). Sediment traps deployed across the Goban Spur area during OMEX also confirmed the existence of an important lateral transport of material (Wollast and Chou, 2001; Antia et al., 2001). Even after correction for trap efficiencies, particulate fluxes increased at 3000 m. The expected decrease in organic carbon content was significantly lower than could be explained by remineralisation and normal decay during settling. Joint et al. (2001) suggested that not all the exportable carbon estimated from new production is exported as a vertical POC flux and part may be exported out of the area by lateral advective transport of either POC or DOC.

Submarine canyons are geomorphological features that incise continental shelves and slopes at margins around the world. Although submarine canyons are rare, covering 1.21% of the global ocean sea floor (4,393,650 km^2; Harris et al. 2014), their local bathymetry naturally supports the downslope transport of particles. Canyons violate the low-energy deep-sea 'rule' by focusing flow and organic matter flux and sediments and acting as conduits across the continental slope (Glover and Smith, 2003). Greater hydrodynamic activity in the canyon leads to enhanced transport processes through turbidity currents, sediment slides and slumps (Puig et al., 2014). These sites, therefore, can be quantitatively important pathways for carbon and enhanced food availability (e.g. Rowe, 1971; Kiriakoulakis et al., 2011; Puig et al., 2014). Many examples portraying canyons as biodiversity and biomass hotspots are found in the literature (e.g. Vetter and Dayton, 1988; Smith and Demopoulos, 2003; De Leo et al., 2010) but there is no

consensus on this as of yet and there are reports of lower biodiversity/mass for some species at some sites (e.g. Robertson et al., 2014).

From a conservationperspective, continental margins and canyons have also become increasingly important in recent years. These “hotspot ecosystems” provide a variety of resources, marine goods and services that humans are increasingly dependent on (e.g. Weaver et al., 2004 and COMARGE programme). Enhanced food and energy resources at the margin create high species and habitat diversity (Levin and Dayton, 2009) in many marine animals, that are now known to contain bioactive compounds with pharmaceutical and medical uses (e.g. Munro et al., 1999). Species diversity has also attracted fisheries to the continental margin and deeper waters (Ramirez-Llodra et al., 2011). Pauly et al. (2005) describes how our interactions with fisheries resources have come to resemble the wars of extermination that newly arrived hunters conducted 40000–50000 years ago in Australia, and 11000–13000 years ago against large terrestrial mammals in North America. Continental margins have become repositories for anthropogenic wastes (Levin and Sibuet, 2012 and references therein) and submarine canyons and the deep sea are now considered a major sink for marine litter (e.g. Mordecai et al., 2011; Pham et al., 2014) and micoplastic debris (e.g. Woodall et al., 2014). Recently, the average plastic abundance in the Northeast Atlantic was calculated as 2.46 particles m^{-3} (Lusher et al., 2014). Monitoring for natural disasters and climate change patterns in large seafloor observatory networks (e.g. ESONET; ESONIM; MARS; NEPTUNE; VENUS; ARENA; H2O; HUGO; Favali and Beranzoli, 2006) at continental margins has also become increasingly important. Increasing human-disturbances at these sites requires greater scientific knowledge of the setting surrounding these habitats in order to implement appropriate management strategies and the proper assignment of vulnerable marine ecosystems VMEs and special area of conservation (SAC) status (FAO, 2009, Davies et al., 2007). In understanding the deep-sea ecosystems; submarine canyons and lateral transport processes need to be considered as a carbon pathway.

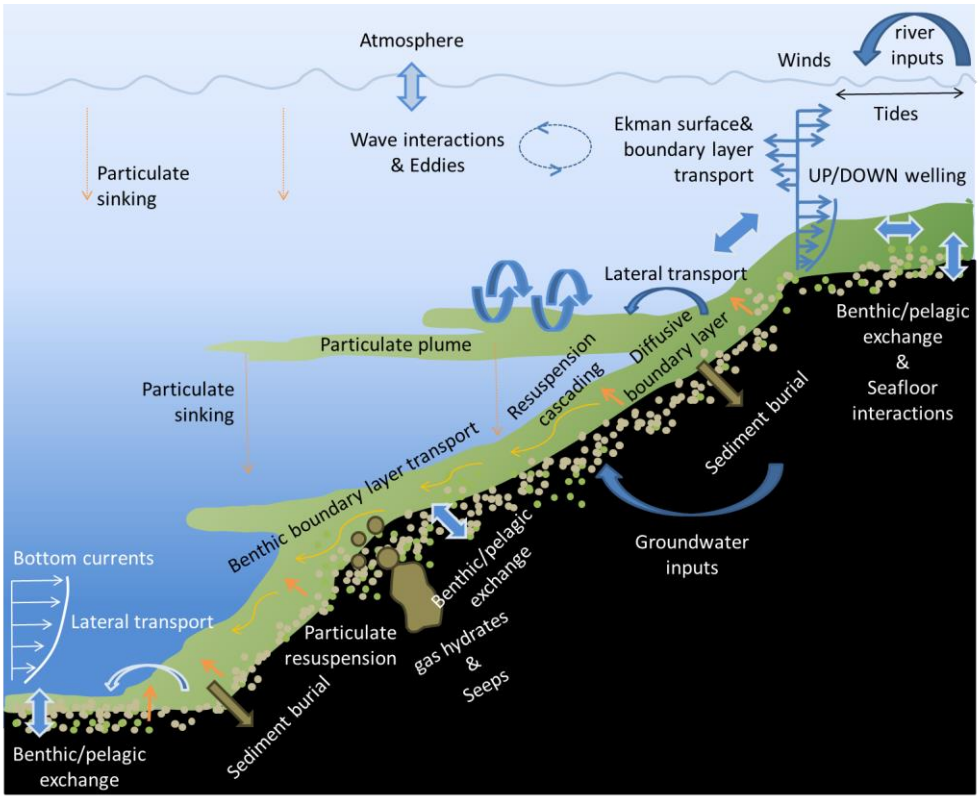

Fig. 1.2 Schematic representation of major exchange processes and factors affecting energy and material fluxes at continental margins. (Adapted from Wollast, 1998 and figure by Boyette, 2005).

Nepheloid layers transporters of food and fuel

Nepheloid layers are distinct cloudy layers of suspended particulate matter and particles at the seabed and at intermediate water depths (Fig. 1.3). They are a significant contributor to the shelf edge exchange of material (Amin and Huthnance, 1999), present at the continental margins of our oceans world-wide and, serve as a physical link between pelagic and abyssal environments (Puig et al., 2001). Formed by a balance between settling and resuspension processes they are important lateral transporters of sediment and organic matter.

It has been suggested that nepheloid layers can act as a fast-track route for labile organic matter to the deep, supporting suspension and benthic deposition feeding fauna. Food rich marine snow particles can accumulate in nepheloid layers (Ransom et al., 1998) and trigger reproductive processes in flora and fauna (Tyler and Gage, 1984). This in turn can affect species abundance, biomass and richness of associated ecosystems.

At continental margins, lateral particle displacement in intermediate and bottom nepheloid layers has also been proposed as a potential reason for the discrepancy in local marine carbon cycles (e.g. Jahnke et al., 1990; Biscay and

Anderson, 1994). The importance of organic carbon transport in semi-permanent bottom nepheloid layers and intermediate layers at the Goban spur area has been previously suggested (van Weering et al., 1998). Whilst this area is not a major carbon depocenter, Wollast and Chou (2001) suggest that organic carbon that is exported from the euphotic zone at the shelf break, which is remineralised in intermediate and deep water, can be considered as a temporary sink on a time scale of a few hundred years.

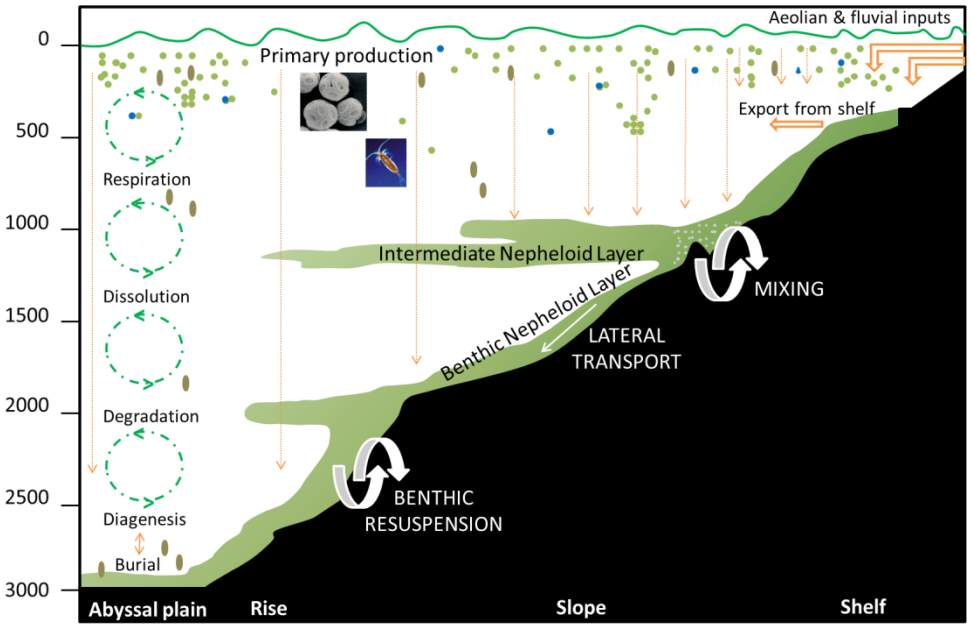

Fig. 1.3 Schematic of nepheloid layers as lateral transporters along a sloping continental margin; sources of material, transport and degradation. (Adapted from Inthorn, M., 2006b Fig. 1.2)

The quality and the quantity of deposited organic matter transported by these layers are strongly influenced by physical and biological processes; seasonal dynamics and spring blooms (Lampitt et al., 1995), hydrodynamic processes (Thorpe and White, 1988), shorter term events (e.g., internal waves; storms; anthropogenic activity) and microbial and benthic activity in the water column (Graf et al., 1995; Thomsen, 1999; Thomsen et al., 2001). Sedimentation rates ultimately determine the amount of organic matter preserved during burial (Armstrong et al., 2002). High particle sinking velocities through aggregation processes and inorganic mineral ballast can protect organic matter from degradation (Hedges et al., 2001). However, particles laterally transported in suspension (i.e. in nepheloid layers) also undergo repeated sedimentation, resuspension loops, aggregation and disaggregation processes (Thomsen and van Weering, 1998). Lateral transport and the processes undergone during this form

of transport therefore have a significant role in determining the proportion of organic matter preserved and in the formation of depocenters and, is often neglected (e.g. Inthorn et al., 2006a).

The mechanisms by which continental margins trap or bypass particulate material is closely related to the distribution and dynamics of particles (Durrieu de Madron, 1994); thus there is a need to delineate nepheloid layer formation, dispersion and compositional characteristics.

1.2 Motivation & Aims

The potential of nepheloid layers to provide a source of fresh, high-quality organic material to abyssal sediments cannot be overstated. Their redistribution and recycling of organic matter and supply of rich food may provide explanations for variations in marine carbon flux calculations and faunal distribution patterns. They also hold important implications for quantitative modelling; biological prediction models for biodiscovery; carbon burial for climate change and biogeochemical cycling for ocean acidification.

The research presented in this thesis explores nepheloid layer as a pathway in the pelagic to benthic coupling of suspended particle matter. This work focuses on nepheloid layers in a submarine canyon along the NE Atlantic margin. This study envisages clarifying the quality of material transported in nepheloid layers and defining the oceanographic conditions affecting the formation, under the hypothesis that nepheloid layers are a lateral transport mechanism, aiding canyon transport and provide a rapid pathway in the benthic to pelagic coupling of labile organic material in the Whittard Canyon. In order to assess the temporal, spatial and qualitative characteristics of nepheloid layers in the Whittard Canyon, the aims of this thesis are to;

- Delineate the distribution of nepheloid layers within Whittard Canyon
- Identify the oceanographic regimes and processes that influence nepheloid layer dynamics at Whittard Canyon
- Investigate the organic content of nepheloid layers in the Whittard Canyon

- Assess the influence of these layers in the distribution and quality of organic matter in the canyon system that influences benthic habitats and carbon cycling
- Assess the influence of human exploitation on material transported through the Whittard Canyon

1.3 Summary and structure of thesis

This thesis is primarily structured around five research papers; three first author papers (two published) and two co-author papers (both published; Fig. 1.4).

A broad literature review and background is provided in Chapter 2. This includes a broad overview of nepheloid layer formation processes and composition, history of instrumentation and methods used to describe them and their context along the NE Atlantic margin. A brief description of the study area, the Whittard Canyon, is also provided here while an extensive review of this system is provided in Appendix B.

Chapter 3 details the research surveys and gives details of the methodologies not covered in the papers. The results chapters (chapter 4, 5, 6) are written as three journal articles. Chapter 4 covers the physical generation of nepheloid layers, describing the distribution and dynamics of benthic and intermediate nepheloid layer. Chapter 5 examines the possibility of anthropogenic influence on sediment transport in enhanced nepheloid layers. Chapter 6 addresses the compositional components and biogeochemical quality of material transported in the layers. Chapter 7 is a synthesis of the thesis. The main finding are summarised and discussed, and possibilities for future work are outlined.

Two other manuscripts relate to this thesis and they are presented in appendices. Appendix A describes the discovery of a unique faunal community on a vertical wall in the Whittard Canyon and an association with intermediate nepheloid layers. Appendix B is an international multi-disciplinary review paper, collaborating old and current research to give a broad and deep insight into the function of the Whittard Canyon.

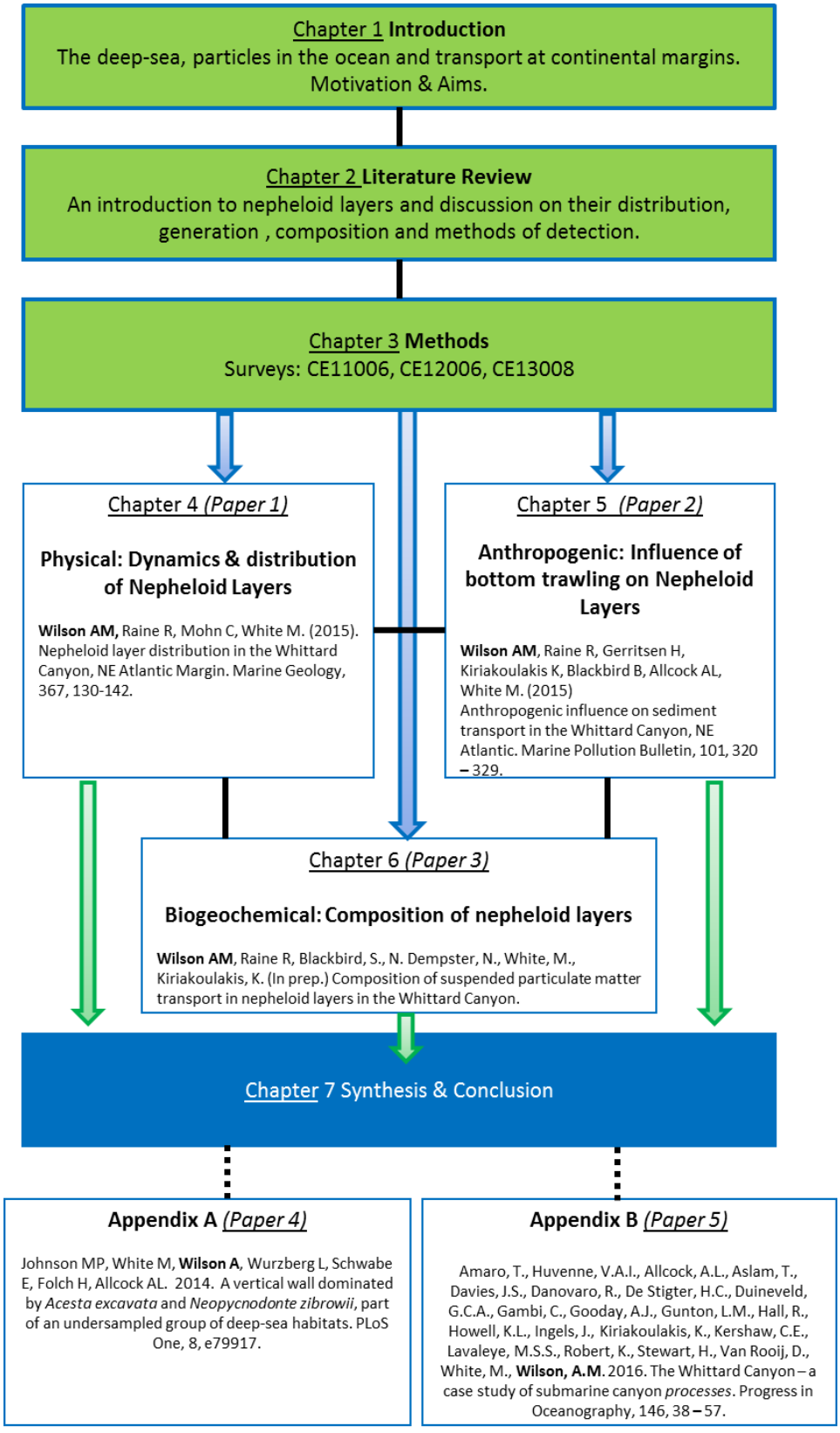

Figure 1.4. Structure of the PhD thesis.

References

Alldredge, A.L. and Silver, M.W., 1988. Characteristics, dynamics and significance of marine snow. Progress in oceanography, 20, 41-82.

Amin, M. and Huthnance, J.M., 1999. The pattern of cross-slope depositional fluxes. Deep Sea Research Part I: Oceanographic Research Papers, 46, 1565-1591.

Boyette, A. 2005. Skidaway Institute of Oceanography; developed for CoOP's Coastal Benthic Exchange Dynamics (CBED) Workshop. Source: http://www.whoi.edu/ooi_cgsn/page.do?pid=53281

Antia, A.N., Maaßen, J., Herman, P., Voß, M., Scholten, J., Groom, S. and Miller, P., 2001. Spatial and temporal variability of particle flux at the NW European continental margin. Deep Sea Research Part II: Topical Studies in Oceanography, 48, 3083-3106.

Armstrong, R.A., Lee, C., Hedges, J.I., Honjo, S. and Wakeham, S.G., 2002. A new, mechanistic model for organic carbon fluxes in the ocean based on the quantitative association of POC with ballast minerals. Deep-Sea Research II, 49, 219-236.

Biscaye, P.E. and Anderson, R.F., 1994. Fluxes of particulate matter on the slope of the southern Middle Atlantic Bight: SEEP-II. Deep-Sea Research II, 41, 459-509.

Davies, A.J., Roberts, J.M. and Hall-Spencer, J., 2007. Preserving deep-sea natural heritage: emerging issues in offshore conservation and management. Biological Conservation, 138, 299-312.

De Leo, F.C., Smith, C.R., Rowden, A.A., Bowden, D.A. and Clark, M.R., 2010. Submarine canyons: hotspots of benthic biomass and productivity in the deep sea. Proceedings of the Royal Society of London B: Biological Sciences, p.rspb20100462.

Durrieu de Madron, X., 1994. Hydrography and nepheloid structures in the Grand-Rhône canyon. Continental Shelf Research, 14, 457-477.

FAO, 2009. International guidelines for the management of deep-sea fisheries in the High Seas. Food and Agriculture Organisation, United Nations, Rome, Italy. 73 p.

Favali, P. and Beranzoli, L., 2006. Seafloor observatory science: A review. Annals of Geophysics, 49, 515-567.

Frederiksen, R., Jensen, A. and Westerberg, H., 1992. The distribution of the scleractinian coral Lophelia pertusa around the Faroe Islands and the relation to internal tidal mixing. Sarsia, 77, 157-171.

Glover, A.G. and Smith, C.R., 2003. The deep-sea floor ecosystem: current status and prospects of anthropogenic change by the year 2025.Environmental Conservation, 30, 219-241.

Graf, G., 1989. Benthic-pelagic coupling in a deep-sea benthic community. Nature, 341, 437-439.

Graf, G., Gerlach, S.A., Linke, P., Queisser, W., Ritzrau, W., Scheltz, A., Thomsen, L., Witte, U., 1995. Benthic-pelagic coupling in the Greenland-Norwegian Sea and its effect on the geological record. Geologische Rundschau 84, 49-58.

Harris, P.T., Macmillan-Lawler, M., Rupp, J. and Baker, E.K., 2014. Geomorphology of the oceans. Marine Geology, 352, 4-24.

Hartnett, H.E., Keil, R.G., Hedges, J.I. and Devol, A.H., 1998. Influence of oxygen exposure time on organic carbon preservation in continental margin sediments. Nature, 391, 572-575.

Hedges, J.I. et al., 2001. Evidence for non-selective preservation of organic matter in sinking marine particles. Nature, 409, 801-804.

Inthorn, M., Wagner, T., Scheeder, G. and Zabel, M., 2006a. Lateral transport controls distribution, quality, and burial of organic matter along continental slopes in high-productivity areas. Geology, 34, 205-208.

Inthorn, M. 2006b Lateral particle transport in nepheloid layers – a key factor for organic matter distribution and quality in the Benguela high-productivity area. Berichte, Fachbereich Geowissenschaften, Universität Bremen, No. 244, 124 pages, Bremen, 2006. ISSN 0931-0800.

Iversen, M.H. and Ploug, H., 2010. Ballast minerals and the sinking carbon flux in the ocean: carbon-specific respiration rates and sinking velocity of marine snow aggregates. Biogeosciences, 7, 2613-2624.

Jahnke, R.A., Reimers, C.E. and Craven, D.B., 1990. Intensification of recycling of organic matter at the sea floor near ocean margins. Nature, 348, 50-54. doi: 10.1038/348050a0.

Joint, I., Wollast, R., Chou, L., Batten, S., Elskens, M., Edwards, E., Hirst, A., Burkill, P., Groom, S., Gibb, S. and Miller, A., 2001. Pelagic production at the Celtic Sea shelf break. Deep Sea Research Part II: Topical Studies in Oceanography, 48, 3049-3081.

Kiriakoulakis, K., Blackbird, S., Ingels, J., Vanreusel, A., Wolff, G.A., 2011. Organic geochemistry of submarine canyons: The Portuguese Margin. Deep Sea Research Part II: Topical Studies in Oceanography, 58, 2477-2488.

Lampitt, R., 1985. Evidence for the seasonal deposition of detritus to the deep-sea floor and its subsequent resuspension. Deep Sea Research Part A. Oceanographic Research Papers, 32, 885-897.

Lampitt, R.S., Hillier, W.R. and Challenor, P.G., 1993. Seasonal and diel variation in the open ocean concentration of marine snow aggregates. Nature, 362, 737-739.

Lampitt, R.S., Raine, R.C.T., Billett, D.S.M., Rice, A.L., 1995. Material supply to the European continental slope: A budget based on benthic oxygen demand and organic supply. Deep Sea Research Part I: Oceanographic Research Papers 42, 1865-1880.

Lampitt, R.S. and Antia, A.N., 1997. Particle flux in deep seas: regional characteristics and temporal variability. Deep Sea Research Part I: Oceanographic Research Papers, 44, 1377-1403.

Levin, L.A. and Dayton, P.K., 2009. Ecological theory and continental margins: where shallow meets deep. Trends in ecology & evolution, 24, 606-617.

Levin, L.A. and Sibuet, M., 2012. Understanding continental margin biodiversity: a new imperative. Annual Review of Marine Science, 4, 79-112.

Longhurst, A., Sathyendranath, S., Platt, T. and Caverhill, C., 1995. An estimate of global primary production in the ocean from satellite radiometer data. Journal of Plankton Research, 17, 1245-1271.

Lusher, A.L., Burke, A., O'Connor, I. and Officer, R., 2014. Microplastic pollution in the Northeast Atlantic Ocean: validated and opportunistic sampling. Marine pollution bulletin, 88, pp.325-333.

McDonnell, A.M. and Buesseler, K.O., 2010. Variability in the average sinking velocity of marine particles. Limnology and Oceanography, 55, 2085-2096.

Mordecai, G., Tyler, P.A., Masson, D.G. and Huvenne, V.A., 2011. Litter in submarine canyons off the west coast of Portugal. Deep Sea Research Part II: Topical Studies in Oceanography, 58, 2489-2496.

Munro, M.H., Blunt, J.W., Dumdei, E.J., Hickford, S.J., Lill, R.E., Li, S., Battershill, C.N. and Duckworth, A.R., 1999. The discovery and development of marine compounds with pharmaceutical potential. Journal of Biotechnology, 70, 15-25.

Nittrouer, C.A., 1999. STRATAFORM: overview of its design and synthesis of its results. Marine Geology, 154,3-12.

Pauly, D., Watson, R. and Alder, J., 2005. Global trends in world fisheries: impacts on marine ecosystems and food security. Philosophical Transactions of the Royal Society of London B: Biological Sciences, 360, 5-12.

Pham, C.K., Ramirez-Llodra, E., Alt, C.H., Amaro, T., Bergmann, M., Canals, M., Davies, J., Duineveld, G., Galgani, F., Howell, K.L. and Huvenne, V.A., 2014. Marine litter distribution and density in European seas, from the shelves to deep basins. PLoS ONE, 9, e95839.

Puig, P., Company, J.B., Sardà, F., Palanques, A., 2001. Responses of deep-water shrimp populations to intermediate nepheloid layer detachments on the Northwestern Mediterranean continental margin. Deep Sea Research Part I: Oceanographic Research Papers, 48, 2195-2207.

Puig, P., Palanques, A. and Martín, J., 2014. Contemporary sediment-transport processes in submarine canyons. Annual review of marine science, 6, 53-77.

Ramirez-Llodra, E., Tyler, P.A., Baker, M.C., Bergstad, O.A., Clark, M.R., Escobar, E., Levin, L.A., Menot, L., Rowden, A.A., Smith, C.R. and Van Dover, C.L., 2011. Man and the last great wilderness: human impact on the deep sea. PLoS ONE, 6, e22588.

Ransom, B., Shea, K.F., Burkett, P.J., Bennett, R.H., Baerwald, R., 1998. Comparison of pelagic and nepheloid layer marine snow: implications for carbon cycling. Marine Geology 150, 39-50.

Robertson, C.M., Demopoulos, A.J.W., Bourque, J.R., Mienis, F., Duineveld, G., Davies, A.J., Ross, S., Brooke, S. 2014. Distinct benthic community trends driven by an enrichment paradox in the Mid-Atlantic Bight Canyons, NW Atlantic, Paper presented at 2nd International Symposium on Submarine Canyon, Edinburgh, October 2014.

Rowe, G.T., 1971 Observations on bottom currents and epibenthic populations in Hatteras Submarine Canyon. Deep Sea Research and Oceanographic, 18, 569-581.

Sarmiento, J.L. and Gruber, N., 2006. Remineralization and Burial in Sediment, In Ocean Biogeochemical Dynamics, Princeton University Press (2006), pp.227-268.

Seiter, K., Hensen, C. and Zabel, M., 2005. Benthic carbon mineralization on a global scale. Global Biogeochemical Cycles, 19. doi: 10.1029/2004GB002225.

Smith, C.R. and Demopoulos, A.W., 2003. The deep Pacific ocean floor. In Ecosystems of the World, (Eds. Tyler P.A.), Elsevier (2003) pp.179-218.

Smith, C.R., 2006. Bigger is better: the role of whales as detritus in marine ecosystems. In Whales, whaling and ocean ecosystems, (Eds. Estes, J.A., DeMaster, D.P., Brownell Jr, R.L., Doak, D.F., William, T.M., Berkeley, D.) University of California Press (2006), pp. 286-301.

Smith, K., Ruhl, H., Bett, B., Billett, D., Lampitt, R., Kaufmann, R., 2009. Climate, carbon cycling, and deep-ocean ecosystems. Proceedings of the National Academy of Sciences 106, 19211-19218.

Thiel, H., 2001. Use and protection of the deep sea—an introduction. Deep Sea Research Part II: Topical Studies in Oceanography, 48, 3427-3431.

Thomsen, L. and van Weering, T.C., 1998. Spatial and temporal variability of particulate matter in the benthic boundary layer at the NW European Continental Margin (Goban Spur). Progress in Oceanography, 42, 61-76.

Thomsen, L., 1999. Processes in the benthic boundary layer at continental margins and their implication for the benthic carbon cycle. Journal of Sea Research, 41, 73-86.

Thomsen, C., Blaume, F., Fohrmann, H., Peeken, I., Zeller, U., 2001. Particle transport processes at slope environments — event driven flux across the Barents Sea continental margin. Marine Geology, 175, 237-250.

Thorpe, S.A., White, M., 1988. A deep intermediate nepheloid layer. Deep Sea Research Part A. Oceanographic Research Papers, 35, 1665-1671.

Tyler, P.A., Gage, J.D., 1984. Seasonal reproduction of Echinus affinis (Echinodermata: Echinoidea) in the Rockall trough, northeast Atlantic Ocean. Deep Sea Research Part A. Oceanographic Research Papers, 31, 387-402.

Van Weering, T.C.E., McCave, I.N. and Hall, I.R., 1998. Ocean Margin Exchange (Omex I) benthic processes study. Progress in Oceanography, 42, 1-4.

Van Weering, T.C.E. and McCave, I.N., 2002. Benthic processes and dynamics at the NW Iberian margin: an introduction. Progress in Oceanography, 52, 123-128.

Vetter, E.W. and Dayton, P.K., 1998. Macrofaunal communities within and adjacent to a detritus-rich submarine canyon system. Deep Sea Research Part II: Topical Studies in Oceanography, 45, 25-54.

Walsh, J.J., Rowe, G.T., Iverson, R.L. and McRoy, C.P., 1981. Biological export of shelf carbon is a sink of the global CO2 cycle. Nature, 291, 196-201.

Walsh, J.J., Biscaye, P.E. and Csanady, G.T., 1988. The 1983-1984 Shelf Edge Exchange Processes (SEEP)-1 experiment: hypotheses and highlights. Continental Shelf Research, 8, 435–457.

Walsh, J.J., 1991. Importance of continental margins in the marine biogeochemical cycling of carbon and nitrogen. Nature 350, 53-55.

Weaver, P.P., Billett, D.S., Boetius, A., Danovaro, R., Freiwald, A., and Sibuet, M. 2004. Hotspot ecosystem research on Europe's deep-ocean margins. Oceanography, 17, 132-143.

Wollast, R., 1998. Evaluation and comparison of the global carbon cycle in the coastal zone and in the open ocean. In The Sea, (Eds) K.H. Brink and A.R. Robinson. Wiley & Sons (1998), pp. 213–252.

Wollast, R. and Chou, L., 2001. The carbon cycle at the ocean margin in the northern Gulf of Biscay. Deep Sea Research Part II: Topical Studies in Oceanography, 48, 3265-3293.

Woodall, L.C., Sanchez-Vidal, A., Canals, M., Paterson, G.L., Coppock, R., Sleight, V., Calafat, A., Rogers, A.D., Narayanaswamy, B.E. and Thompson, R.C., 2014. The deep sea is a major sink for microplastic debris. Royal Society open science, 1, 140317.

Chapter 2

A review of nepheloid layer generation, composition and their context along the Irish continental margin.

2.1 Nepheloid layers: history and general description

The term “nepheloid layer” originating from the Greek “nephos” meaning cloudy, accurately describes the appearance of turbid layers of suspended particulate matter (SPM) that cover most parts of the deep ocean (McCave, 1986). Reports of this remarkable feature date back as far as Kalle (1937) and Jerlov (1953) with intermittent research on its source and composition since. In 1977, Biscaye and Eittreim (1977) identified distinct vertical and horizontal features in the distributions of SPM in the Atlantic Ocean. They proposed a three-layer model to describe their findings with three main features (1) a surface-water turbid layer, (2) a clear water minimum and (3) a deep-water turbid layer (Fig. 2.1). Definitions of the nepheloid layer in the 1980’s and 1990’s were more semi-quantitative and focused on the generation mechanisms. Dickson and McCave, (1986) described nepheloid layers as distinct layers of water with reduced optical transmittance, increased light scattering and attenuation relative to minimum values found at mid-water depth and surrounding clear water. Naudin and Cauwet (1996) define the benthic nepheloid layer as a (steady state) vertical concentration gradient, from the assumed balance between the gravitational settling velocity of particles coming from the surface and the turbulent mixing velocity induced by current friction on the bottom stripping sediment from the ocean floor. More recently, nepheloid layers have also been classified as erosional features (Rebeseco et al., 2014).

While benthic nepheloid layers (BNLs) are detected adjacent to the seafloor, intermediate nepheloid layers (INLs) at mid-water depths also exist (Fig. 2.1). Descriptions and detection of INLs were first reported in the literature in the 1980’s (e.g. Pak et al., 1980, Dickson and McCave, 1986; Thorpe and White, 1988). They are often detected near ocean (topographic and water mass) boundaries (Gardner and Walsh, 1990) and are frequently observed in high abundance near continental shelves, offshore on the upper slope and at the depth off the shelf-edge (Pak et al., 1980; Puig et al., 2004a). In flatter (non-sloping) environments and away from the sides of the ocean basin, between 1000–3000 m, nepheloid layer formation is at a minimum; a lack of primary production, weak stratification and few zones of strong currents impede/limit their formation (McCave, 1986). BNLs are associated with the local scouring of bottom sediments at the seabed by currents that maintain and transport a resuspension layer. INLs are detached

mixed layers from the BNL, the result of an accumulation and/or the transport of particles in intermediate waters in association with strong density gradients and ocean dynamics, particularly internal waves (Cacchione and Drake, 1986; Dickson and McCave, 1986; Thorpe and White, 1988). INLs have also been described as sub-layers within the BNL, originating in regions of strong currents and gaining material by fall-out from above (McCave, 1986). They can also be advected across adjacent abyssal plains.

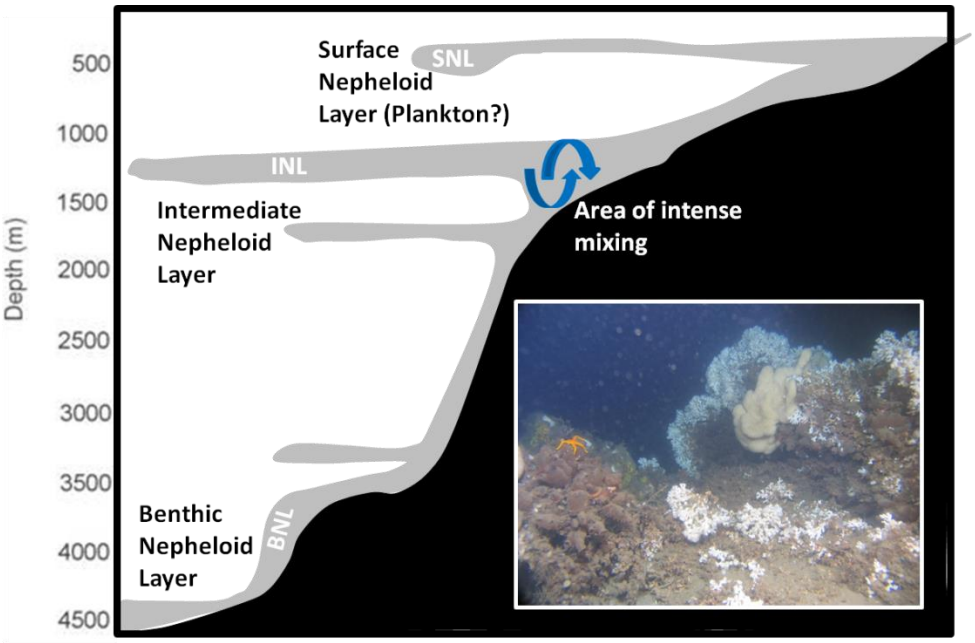

Fig. 2.1. Schematic of the three types of nepheloid layer described in the literature and inset shows photograph of nepheloid layer at a benthic ecosystem.

Similar to Biscaye and Eittreim's (1977) model, some authors describe a surface nepheloid layer (e.g. Gardner et al., 1993; Oliveria et al., 2002), (Fig. 2.1). These tend to be found in areas of increased primary production and terrestrial or fluvial input and are (often) associated with the biological active surface layer and/or the floatation of particles (Oliveira et al., 2002). Some studies have described sediment from the BNL transported by upwelling events to the surface as an SNL (Agrawal, 2004). Others have described the possibility of INLs being transported to the surface to form SNLs that fuel plankton blooms under favourable conditions (Shatova, 2008). There is some ambiguity over what the SNL is, as the SNL described by McCave (1986); the upper ocean layer in which particles are produced by biological activity, is difficult to differentiate from the region of phytoplankton primary production in the euphotic zone.

Nepheloid layers have a global distribution. They have been detected in higher latitudes in both the Arctic (Hunkins et al., 1969) and Indian-Pacific Antarctic Sea (Eittreim, 1972), to mid and equatorial latitudes e.g. Guinea and Angola Basins (Connary and Ewing, 1972), off Namibia (Inthorn et al., 2006), and the Gulf of Mexico (Feely, 1975). Reports span from the Americas (Lorenzoni et al., 2009; Cacchione and Drake, 1986; McPhee-Shaw et al., 2004), to the north western European continental margin (Dickson and McCave, 1986; Thorpe and White, 1988; McCave et al., 2001), the Gulf of Lions (Durrieu de Madron et al., 1990), the Iberian peninsula (Oliveira et al., 2002; Puig and Palanques, 1998a; van Weering et al., 2002), the Mediterranean margin (Chronis et al., 2000; Puig et al., 2013), China Sea (Yanagi et al., 1996), and Taiwan (Liu et al., 2010) to coastal Australian waters (Wolanski et al., 2003). They have been observed in freshwater bodies in the Great Lakes e.g. Michigan (Chambers and Eadie, 1981), Ontario (Sandilands and Mudroch, 1983), and Superior (Qaker et al., 1985). In the ocean, they have been observed in a range of settings from the abyssal Atlantic Ocean (Biscay and Eittreim, 1977) and smooth topographic settings (e.g. PAP site) (Vangriesheim, 1988) to open continental shelves (Cacchione and Drake, 1986; Puig et al., 2001; van Weering et al., 2001; McCave and Hall, 2002; Oliveira et al., 2002), areas of upwelling (McPhee-Shaw et al., 2004; Inthorn et al., 2006) to submarine canyons (Baker and Hickey, 1986; Durrieu de Madron, 1994; Puig et al., 2004a; Liu et al., 2010) and marginal seas (e.g. Chronis et al., 2000).

Particles are introduced into the ocean by biological production, fluvial and glacial input and reintroduced by resuspension of bottom sediments (Gardner and Walsh, 1990). Biological, chemical and gravitational processes act to remove, modify and redistribute such particles and, these have important implications for biogeochemcical processes in the ocean. Nepheloid layers vary significantly in intensity and dimension, spatially and temporally, being both transient and permanent features. Their intensity and thickness, features and patterns will depend on local conditions. Deep-ocean nepheloid layers often follow local circulation patterns (Gardner and Sullivan, 1981) and the characteristics of the BNL are strongly correlated with those of the benthic boundary layer (Naudin and Cauwet, 1996). The shape of nepheloid layers often fits that of the local water column density structure, as their development is closely related to the density field and water column stratification (Oliveira et al., 2002). However, BNLs are

also seen to transcend water masses of different sources (McCave, 1986). Chronis et al. (2000) have also shown that the distribution of nepheloid layers closely agree with vertical distributions of chlorophyll *a*, particularly at deep chlorophyll maximums associated with the seasonal pycnocline. It is generally perceived that the thickness of the BNL ranges from a few metres to frequently several ten or even hundreds of metres (Thorpe and White, 1988); 50–200m (McCave, 1983); 500–1500 m (Puig et al., 2013a). Greater thicknesses have been reported at particular sites e.g. in trenches and passages where they can be 2600 m thick (McCave, 1986). INLs are smaller with thicknesses of ~10–50 m (Oliveira et al., 2002).

Concentrations of SPM in nepheloid layers vary greatly from location to location, again depending on the local dynamics and source of particles. McCave et al. (2001) report 0.05– 0.13 mg l^{-1} off the North Western Atlantic, while in the NE Mediterranean higher concentrations of 0.2–1.5 mg l^{-1} are reported (Chronis et al., 2000). More concentrated layers are found closer to shore, in estuarine and other terrestrially influenced environments. On the Northern Portuguese shelf, an area that is heavily influenced by the Douro River, Oliveira et al. (2002) reports nepheloid layers with concentrations of 0.1–19 mg l^{-1}. Palanques and Drake (1990) report concentrations <1 mg l^{-1} along the continental margin offshore of the River Ebro. Concentrations of SPM will also vary depending on the rate of decay, time and distance from the generating source. In the BNL, distance above the seabed will also affect the SPM concentration and BNLs generally display a basal uniform region concentration with a logarithmic fall-off in intensity from the seabed (McCave, 1986). INLs progressively decay depending on the rate of settling and aggregation and maintenance of turbulence by boundary friction and shear velocity from their original source in the BNL. INLs generally lose particles by thinning and mixing at their boundaries as a result of lateral spread, eventually yielding a uniform stratification (McCave, 1986), often detaching from their source.

Nepheloid layers are often the end-point of oceanographic processes and biological reworking. Their distribution therefore often indicates an active area with the resuspension, dispersal and deposition of SPM. However the initial source of the nepheloid layer will depend on the local setting and processes,

which also determine the composition of the nepheloid layer. These processes will now be considered in turn.

2.2 Transport of OM, generation and formation of NLs.

The primary source of particles will vary depending on geographic location, depth in the water column and the local processes dictating the formation of the nepheloid layer. Nepheloid layer formation therefore cannot be easily explained by any single source and/or mechanism (Azetsu-Scott et al., 1993; McCave et al., 2001; Wells and Deming 2003). However, in general terms, nepheloid layer formation can be described as a result of a balance between the *settling* (gravitational, scavenging and aggregation) of particles and *turbulent mixing and re-suspension* of bottom sediments, commonly in zones where a strong density gradient is present (Dickson and McCave, 1986; McCave, 1986; Thorpe and White, 1988; Cacchione and Drake, 1986; Pak et al., 1980). Similar topography and oceanographic settings are likely to promote NL formation at similar sites. The generation of nepheloid layers in the case study presented here looks at a submarine canyon, Whittard Canyon on the NE Atlantic and will be addressed in Chapter 4.

2.2.1 Settling and sinking and marine snow

Surface nepheloid layers and shallow intermediate nepheloid layers are strongly influenced by the flocculation and floatation of particles associated with planktonic activity and primary production, atmospheric dust and fluvial particle input. However, the rain of particulate matter from the upper water column also influences the benthic nepheloid layer.

The settling velocity of a particle can be approximated by Stoke's Law (McCave, 1986); which states that for a particle the settling velocity is proportional to the radius squared (r^2), assuming spherical particles, that there is no interaction/ hindering /impact between particles and boundaries and that the flow is laminar. However the (real) settling velocity of particles is dependent on the sedimentological characteristic of the particles; size, shape, density, porosity, concentration, composition, and on flow and these must be accounted for. Furthermore, the impact of both viscous drag and impact must be considered depending on the type of flow and is determined by the Reynolds number. For

laminar flows, friction will be the dominant force, whilst for turbulent flows impact is the dominant force and the drag coefficient is constant.

Large variability in settling velocities has been reported in the literature. Azetsu-Scott et al. (1993) reported settling velocities of 2 m day^{-1}, for the particles of silty-clay pelagic deposits (mean grain size 4 µm) in the Emerald basin. According to McCave, (1984), particles ranging from 10–20 µm take approximately 20 to 50 days to settle from an average NL (~60 m thick) and larger particles taking a few weeks. Extremely high settling velocities of ~3000 m d^{-1} have been reported from the North Atlantic Ocean (Lampitt, 1985), while more moderate estimates between ~50 to 150 m d^{-1} have been reported by others (Alldredge and Gotschalk, 1988). Sinking velocities of diatoms and coccolithophores are generally negligible as pure organic matter has a lower density than water. Ballasting by lithogenic material often assists particle densities to be high enough to sink through the water column (Armstrong et al., 2002). Substantial proportions of the sedimentary flux are made up of "marine snow" (Turner, 2002) with large particles (>5 mm) of marine aggregates (faecal matter, microorganisms, minerals) connected by sticky transparent exopolymer particles called TEP. This marine snow has high sinking velocities and often escapes degradation and contributes to the close coupling of ocean surface and deep-sea organic carbon fluxes (Lampitt, 1985). Porosity can be an important factor. Calculated settling speeds by Asper, (1987) showed that on average larger aggregates (4–5 mm) had slower settling velocities (1 m day^{-1}) than smaller aggregates (1–2.5 mm; 36 m day^{-1}) and suggested that the larger aggregates were less dense (i.e. more porous) than smaller aggregates .

2.2.2 Turbulent mixing and resuspension

Resuspended particles compose the largest component of the nepheloid layer according to Gardner et al. (1985). Although vertical sinking does play an important role in the delivery of fresh material to the seafloor, seasonally variable input of resuspended material directly related to annual variability in near-bed current regimes diminishes seasonal settling signals in the maximum flux and bulk composition of material near the seabed (Mienis et al., 2009). Velocities at the seabed inducing resuspension and turbulent mixing are affected by density currents, as well as barotropic currents and intermittent processes such as dense

shelf water cascading, internal waves and episodic events (e.g. tsunami, rogue waves, anthropogenic activity) with influences from meteorologically driven up/down welling, storms and spin off eddies. Intensity of the local current velocity and bottom roughness can induce modifications to the kinematic viscosity, fluid density and turbulent eddy viscosity (diffusion co-efficient) ratio, which are critical to the settling and maintain of particles in suspension. Therefore, BNL distributions share a very similar pattern with global abyssal circulation patterns (McCave, 1986). The effect of these parameters will decrease logarithmically, both horizontally and vertically, from the site of source. Fig. 2.2 shows some of the erosion, deposition and oceanographic processes in continental margins and deep basins that can affect and influence NLs.

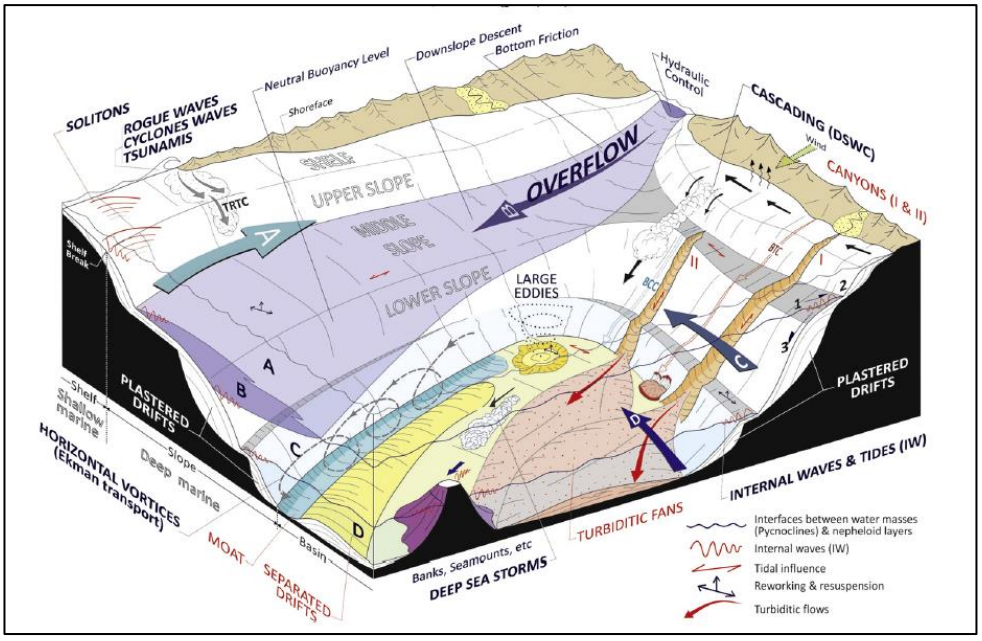

Fig. 2.2 Sketch depicting erosive and depositional oceanographic processes in deep-water environments that can influence NL formation (Rebesco et al., 2014).

2.2.2.1 Deep energetic and boundary flows (Bottom and density currents)

The most turbid benthic nepheloid layers are found in deep regions with water depths >3000 m, associated with strong bottom flows (Eittreim et al., 1976; McCave, 1983). Studies show that the broad patterns of inflowing cold bottom water in the southern Indian and Atlantic oceans are very similar to the extent of the BNL coverage (Eittreim et al., 1976; Biscaye and Eittreim, 1977). It was suggested by these authors that the Antarctic Bottom Water was contributing particles to the formation of the nepheloid layer there. However, later McCave, (1986) reported that the high velocity inflows of cold bottom water and the

influence of bottom topography inducing strong bottom currents, generated the nepheloid layers in these regions.

Bottom currents are typically baroclinic and their velocity at the seabed is correlated with the strength of their density gradients. Boundary currents and thermohaline bottom flows result in significant particle transport, particularly along western ocean margins (McCave, 1986; Anderson et al., 1994; Fohrmann et al., 2001). Density-driven bottom currents that flow parallel to depth contours and large bathymetric features (i.e. continental margin) are in (quasi-)geostrophic balance. The earth's rotation steers these large scale flows to the right (in the northern hemisphere) and when they encounter small scale topographic features (e.g. seamounts, canyons, mounds), the disrupted flow can have much higher velocities (Allen and Durrieu de Madron et al., 2009). These currents and outflowing water masses often exit through narrow straits into wider basins where their scale is proportional to the slope of the seabed and to the density difference between the density current and overlying water mass (e.g. Borenäs and Wåhlin, 2000; Legg et al., 2009), thus accelerating their velocity according to;

$$U = \frac{g.\frac{\Delta\rho}{\rho_0}.\alpha}{f} \qquad (2.1)$$

where $\Delta\rho = \rho - \rho_0$ is the difference in density, α is the slope of the seabed and f is the Coriolis frequency.

Before deposition, these erosive flows transport sediment laden water, often through NLs (Rebesco et al., 2014). For example, in deep western boundary currents; SPM can be 10 times greater than in overlying water masses (Ewing et al., 1971; Rebesco et al., 2014). These bottom currents generate shear stresses that resuspend fine-grained sediment and/or can induce a "winnowing effect" that efficiently prevents or reduces the accumulation of smaller and lighter particles in the sediments i.e. keeping them in suspension. Values in the range of 10–15 cm s^{-1} have been reported as a typical threshold speed for the re-suspension of fresh matter (Thomsen and Gust, 2000; Chronis et al., 2000).

Deep energetic flows and boundary currents also induce Ekman transport in the bottom boundary layer (directed to the left of the flow velocity in the northern hemisphere). Dense water flowing into the region will adjust to the divergence of the frictional transport. As water is expelled through Ekman

transport, the density interface levels out, widening the flow (Borenäs and Wåhlin, 2000, in Rebesco et al., 2014). If the topography is uneven, the density flow can be broken up into eddies and overturns, further enhancing vertical mixing (Cenedese et al. 2004). In particular, eddies are now considered a significant mechanism for the long-distance transport of sediment and the formation of NLs (Rebesco et al., 2014). Closely related to eddy formation, benthic/deep storms have also been related to NL formation, sediment transport and redistribution of particles as demonstrated by the HEBBLE project (e.g. Hollister and McCave, 1984). These can last between two to twenty days (but typically three to five) and increase velocities between two to five times, typically reaching >20 cm s^{-1}. Hollister and McCave (1984) reported benthic storms associated with "rings" from the Gulf Stream and concentrations of SPM = 5 µg L^{-1} during the resultant benthic storms. Furthermore, benthic storms have been shown to have longer-lasting effects on the suspension of bottom sediment, phytoplankton bloom production and supply of OM (Richardson et al., 1993; Von Lom–Keil et al., 2002).

2.2.2.2 Meteorological driven flows: storms, down welling and DSWC

Similar to friction in in the boundary layer, high kinetic energy in the surface can propagate downwards, causing patches of intermittently high abyssal eddy kinetic energy and delineating paths of high turbidity and benthic nepheloid layers (McCave, 1986). Prevailing weather and circulation patterns, frequency and timing and the orientation of the local topography will determine the extent of particle resuspension (Hickey et al., 1986). Storm-induced down-welling can transport large amounts of resuspended shelf material. For example, at Blanes Canyon (Sanchez-Vidal et al., 2012), a massive storm initiated the transport of up to 28 g m^{-3} of sediment. Surface storms and hurricanes can also trigger turbidity currents that carry significant amounts of particles and in sloping environments or canyons can transport sediment downslope for nepheloid layer formation. In the Portuguese Nazaré Canyon, the distal end of storm-induced turbidity currents (10–20 cm s^{-1}) have been interpreted as the means of generating concentrated benthic nepheloid layers (Martín et al., 2011). Similarly Masson et al. (2011) have reported the lateral advection of nepheloid layers that have been formed by turbidity currents triggered by storms.

The formation of nepheloid layers have also been related to up/down-welling Hickey et al. (1986) observed the variation in resuspension according to these patterns along-isobath flow over the upper slope at Quinault Canyon. Dickson and McCave (1986) found internal wave resonance, created by the movement of the vertical stratification (N) was responsible for INL formation. Intense BNLs have also been observed over the Portuguese shelf under dominant down-welling conditions (Oliveira et al., 2002) where particles are sourced from river borne supply or remobilised at mid-shelf. They also reported the dispersion of particles and formation of a SNL with changes in the predominant circulation to upwelling combined with seasonal stratification.

Another meteorologically driven oceanographic phenomenon is the formation of dense shelf water cascading (DSWC) by the cooling, evaporation or freezing in the surface layer over continental shelves (e.g. Puig et al., 2008). Under the influence of the earth's rotation and gravity, these can propagate along-slope by the formation of spiral waves, meanders and eddies (Shapiro et al., 2003); or across/down-slope, passing mainly through submarine canyons until they reach their hydrostatic equilibrium level (Canals et al., 2006; Palanques et al., 2008; Ribó et al., 2011). The descent of these waters down the continental slope to greater depths as gravity currents can generate high sediment fluxes and has been reported to generate massive sand beds (Gaudin et al., 2006). These events can also be induced by storms such as that described by Palanques et al. (2008) at Cap de Creus Canyon. Cooling of the shelf waters by a long storm (in the spring rather than typical winter) caused the formation of dense water that flushed through the canyon, reaching velocities of >80 cm s^{-1}, amplifying down-canyon sediment fluxes (Palanques et al., 2008; 2012). The cold, dry winter winds in the Gulf of Lions and the preferential along-shelf circulation (toward the west), narrowing shelf and topography of the Cap de Creus peninsula forces many DSWC events through Lacaze-Duthiers and Cap de Creus canyons (Durrieu de Madron et al., 2005; 2008; Canals et al., 2009). Béthoux et al. (2002) first suggested that the formation of a BNL was attributed to DSWC events that transported turbid shelf water and re-suspended sediment in the SW part of the Gulf of Lions. Puig et al. (2013a) showed that indeed the thick BNL there is generated by the mixture of dense water formed by deep convection in the open sea by deep cascading and that this process plays a significant role in transporting material from coastal regions in to

the basin. At the mouth of the Cap de Creus Canyon, Canals et al. (2006) has also shown that a well-developed BNL corresponded with the thickness of a bottom layer of cold dense shelf water transported to the basin due to a major cascading event.

2.2.2.3 Internal tides and waves

Internal waves and tides are energetic and ubiquitous in the ocean, containing huge amounts of energy that regularly mix water as they move back and forth along continental slopes, scouring the bottom and resuspending sediment. The intensification of baroclinic energy at sloping boundaries can restrict and govern the movement of material in the water column by dominating the flow field and holding material in suspension (Gardner, 1989a, b; Hotchkiss and Wunsch, 1982). Lab experiments by Cacchione and Wunsch (1974) first demonstrated that varying frequency internal waves could break by upslope, shoaling and generating intensified velocities. At the same time Shepard et al. (1974) revealed the first evidence of internal waves propagating along submarine canyons axes off California.

Baroclinic tides play a substantial role in mixing and in global meridional overturning circulation (Munk and Wunsch, 1998). These baroclinic tidal currents (internal waves with tidal periods) are commonly generated above areas of steep topography (e.g. the shelf break; Baines, 1982) and reflected from complex topography (e.g. submarine canyons; Shepard, 1976; Hickey, 1995).

Rectification (scattering) of barotropic (surface) flows can generate baroclinic (internal) tides at continental slopes where the tidal flow is perpendicular to the shelf (Baines, 1982). The perturbation of isopycnal surfaces can also result in the formation of internal waves and can oscillate along the interface with the beams (β) having lower frequencies, higher amplitudes and enhanced energy (Dickson and McCave, 1986; Apel, 2000; 2004). Tidally transformed barotropic flows and locally generated baroclinic motions can take two forms; (a) bottom trapped baroclinic waves or (b) reflected freely propagating internal waves that can become trapped or focused, particularly at sloping boundaries (Hotchkiss and Wunsch, 1982). Matching of the forcing diurnal frequency and natural oscillation period within the water column, determined by N and the slope of the seabed (α) will determine the extent of amplification whereby;

$$N * \sin(\alpha) = maximum \quad (2.2)$$

(Rhines, 1970; Huthnance, 1981). N the vertical stratification is approximated by;

$$N = -\left({}^{g}/_{\rho_0}\right) * \delta_\rho/\delta_z \quad (2.3)$$

where g is the gravitational acceleration (~9.8 m/s^2) and ρ is the average fluid density over a pycnocline whose vertical ρ gradient is δ_ρ/δ_z. Bottom current enhancement might therefore be expected from baroclinic motions driven at tidal frequencies at slopes where there are large N values (White and Dorschel, 2010), and increased amplitudes, wave numbers and shorter horizontal wavelengths cause increased velocities.

The type of reflection (Fig. 2.3) that occurs is determined by the topographic slope (α) and the internal wave characteristic slope gradient/angle of energy propagation/internal wave ray slope (β) which is expressed by:

$$\tan(\beta) = [(\sigma^2 - f^2)/(N^2 - \sigma^2)]^{\frac{1}{2}} \quad (2.4)$$

and is dependent on N, σ and f where N is the buoyancy frequency, σ is the internal wave frequency and f is the Coriolis parameter (Thorpe, 1987; 2005). Three scenarios are possible;

i. *Transmissive conditions/Subcritical reflection.* Where the angle of propagation (β) is greater than the slope of the seabed (α/β <1), the wave is reflected and the offshore waves and energy will propagate up slope, bouncing between the mixed layer and the seafloor (Fig. 2.3i).
ii. *Reflective conditions/Supercritical reflection.* Where the angle of propagation is smaller than the slope of the seabed (α/β>1), energy rebounds off the slope and travels towards the seabed and back into deeper water after it is reflected. These conditions are common in canyons where internal waves above the canyon rim are focused toward the canyon floor and steep vertical walls focus energy towards the seafloor (Hotchkiss and Wunsch, 1982).

iii. *Critical conditions/reflection.* Where the angles are equal ($\alpha/\beta \cong 1$), (near) critical reflection occurs. Energy is trapped/grazes against the boundary and potentially results in non-linear effects such as wave breaking, solitons, internal bores and turbulent mixing (Nash et al., 2004).

Reflection of internal energy rays occurs about the direction of the local gravity vector and thus the waves can propagate in any direction (i.e. the frequency of the wave is preserved upon reflection). The energy reflected can induce strong shear forces, mixing and possible boundary-instabilities that result in strong turbulent mixing and diffusivity (Cacchione and Wunsch, 1974; Cacchione and Drake, 1986; Wunsch, 1969; McPhee-Shaw et al., 2004). These instabilities cause mixing cells/vortices to develop which intensify breaking and shoaling (Cacchione and Wunsch, 1974). The increased velocities, shear and bottom stresses and turbulent overturns in these vortices can resuspend and can hold material in suspension (Cacchione and Drake, 1986; McPhee-Shaw and Kunze, 2002).

The energy associated with internal waves has been postulated as a major mechanism in the production and the maintenance of INLs and BNLs (McCave, 1986; Dickson and McCave, 1986; Cacchione et al., 2002; Puig et al., 2004b) both along- and across- slope(s) and has been well documented, particularly in sloping environments and canyons. Cacchione and Drake (1986) first suggested that the elevated velocities and stresses caused by shoaling or breaking internal waves might explain the generation and maintenance of near-bottom nepheloid zones and turbid detachments at the shelf and slope off California. On the east coast of the U.S.A, Gardner, (1989b) similarly showed that internal waves breaking at internal tide frequencies, like a bore of cold water with a turbulent head in Baltimore canyon, produced periodic sediment resuspension events that generate INLs. Later Cacchione et al. (2002) demonstrated that bottom shear velocities caused by semi-diurnal tides on the northern California continental slope were high enough to inhibit deposition of fine-grained sediment and keep it in suspension and they proposed that this situation could be reached on many continental slopes. Since then, many other studies have periodic resuspension and transport of material to internal waves (e.g. Drake and Gorsline, 1973; Dickson and McCave, 1986; Thorpe and White, 1988; Puig and Palanques, 1988a;

Durrieu de Madron et al., 1990; Chronis et al., 2000; McCave et al., 2001; Puig et al., 2004b; Mienis et al., 2007). Internal waves can also promote increased primary production at the shelf edge via vertical mixing (Frederiksen et al., 1992; Sharples et al., 2007) and increased concentrations of fresh food particles at carbonate mounds in conjunction with BNL and INL formation (Mienis et al., 2007) and thus contributing to organic sediment fluxes.

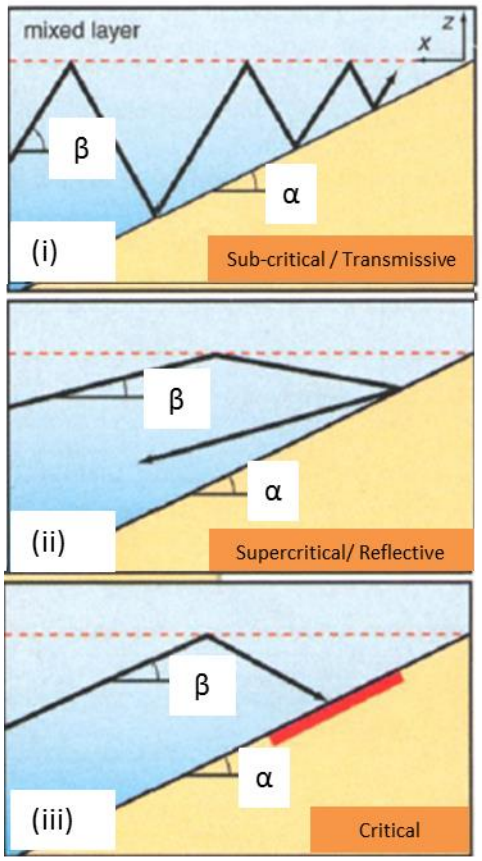

Fig. 2.3 Three classes of internal wave reflection and propagation from bottom slope, in a linearly stratified fluid (i) $\alpha/\beta<1$; transmissive or subcritical (ii) $\alpha/\beta>1$; reflective or super critical (iii) $\alpha/\beta = 1$; critical conditions (Adapted from Cacchione et al. 2002).

2.2.3 Lateral dispersion and INL formation

The presence of BNLs hundreds of metres thick indicates that (some) particles must be sourced from far upslope. These BNLs infer the role of horizontal advection in addition to boundary turbulence in maintaining NLs (McCave, 1984). Furthermore, the formation of INLs is supported by the lateral advection (Gardner et al., 1985) and detachment of material from the benthic nepheloid layer by turbulent processes along a density gradient.

Propagating and reflecting internal waves

As described above, the enhanced energy internal waves (lower frequencies, high amplitudes) can prevent deposition and maintain material in suspension. At the site of internal wave breaking and reflection, entrainment and expulsion of fluid in mixing cells can produce thin horizontal layers (Cacchione and Wunsch, 1974). Many studies have suggested that boundary-layer intrusions due to internal wave reflection are a mechanism for the detachment and growth if INLs (McPhee-Shaw, 2006; McPhee-Shaw and Kunze, 2002). In the Emerald Basin, Azetsu-Scott et al. (1993) observed the depth of INL occurrence matching the 'critical depth' of the M_2 internal tide. Similarly, the locations of slope-depth INLs on the northern California continental margin were observed at regions where the topographic slope angle was critical for internal tide reflection (McPhee-Shaw et al., 2004). In the North Western Alboran Sea, (benthic and) INL formation within and around Guadiaro Canyon were also attributed to the critical conditions of internal tide reflection (Puig et al., 2004b). Similarly at the European Margin, McCave et al. (2001) reported intermittent INLs associated with periodic internal-wave driven resuspension.

Density gradients and fronts

Stratification and isopycnal surfaces are of key importance to the formation of INLs (Fig. 2.4). Internal waves can be formed by the perturbation of isopyncal surfaces (e.g. Dickson and McCave, 1986). Furthermore, these (and other flows) can oscillate along the interface between two water masses of different densities (Apel, 2000; 2004; Cacchione et al., 2002). As early as 1989, INLs were reported moving seaward along isopycnals after internal tides had caused periodic sediment resuspension (Gardner, 1989a). De Silva et al. (1997) also showed this in the lab where fine particles migrated seaward along isopycnals and this mechanism has been observed in the field by many other studies (see above).

Frontal systems also favour the detachment and development of INLs. In shelf-slope environments where lower salinity shelf waters are separated from more saline offshore waters, resuspended material from the shelf can be advected down the slope and be retained along the front (Puig et al., 2001b). Thus

the intersection of the front with the seabed provides an interface for the nepheloid layer to detach and INLs are commonly observed in shelf-slope environments (Puig and Palanques, 1998a). At Quinault Canyon, Hickey et al. (1986) showed shelf-break INLs detachments formed after resuspended sediment by storm activity on the shelf was advected over the canyon. Durrieu de Madron, (1994) and Martín et al. (2006) have also reported similar INL development processes and detachments in Grand Rhone and La Fonera submarine canyons.

In a similar manner, the inflow of different water masses can cause INL detachments. In the Cretan Sea for example, Chronis et al. (2000) found a clear relationship between INLs and density stratification between Modified Atlantic waters (MAW) and the denser Cretan Intermediate Water that underlies it. Similarly, as well as resuspending material in the BNL, slope water intrusions at certain times of year (up- down- welling) can also induce INLs (e.g. Azetsu-Scott et al., 1993). Instabilities by intense water circulation (strong jets and eddies) have also been found to coincide with the appearance of INLs in Monterey Bay, (McPhee-Shaw and Kunze, 2002).

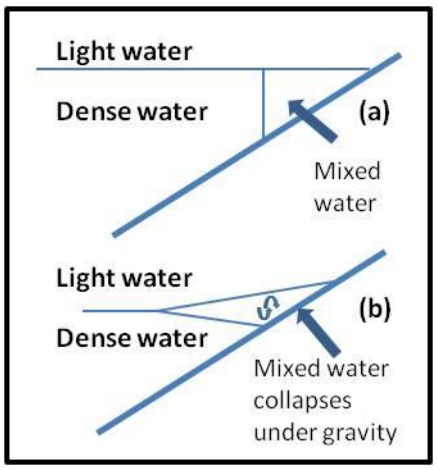

Fig. 2.4 Generation of intermediate nepheloid layer in a stratified area due to turbulent processes (a) turbulent processes cause mixing and a resultant patch of intermediate density mixed fluid (b) the newly homogenous patch will collapse under gravity and be advected from the boundary forming a layer. (Adapted from White, 1990).

In a stratified fluid the turbulence causes irreversible mixing (McPhee-Shaw and Kunze, 2002). The change in potential energy makes a locally mixed fluid patch at the boundary unstable with respect to the density gradient in the interior. Following this, a horizontal pressure gradient can form and induce horizontal flow (McPhee-Shaw and Kunze, 2002). This newly formed homogenous water mass ($\rho_1/\rho+\rho_2/\rho$) as a result of the mixing will then collapse under gravity (Thorpe and White, 1988), (Fig. 2.4). The fluid will then lead to the spread of material along the isopyncal boundary/gradient between the two original water

masses and result in an INL. Even for low Reynolds numbers, when diapycnal mixing is weak, horizontal intrusions can be generated and can advect fluid horizontally. INLs can extend and detach from the seabed, settling in deeper waters and contributing to sediment transport in the area.

2.2.4 Episodic events

Many of the processes transporting sediment and creating NLs can also be triggered by episodic events. Reports of tsunami triggering sediment failure and traction currents are presented in the literature e.g. Wright and Rathje (2003);(Rebesco et al. 2014). Tsunami comprise a wave or series of waves that have long wave lengths and long periods caused by an impulsive vertical displacement of water by earthquakes, volcanoes etc. (Shanmugam, 2006; 2011). Tsunami do not transport sediment (or water-just energy) but during the transformation stage they can erode and incorporate sediment into the incoming wave.

Rogue and cyclonic waves can trigger bottom currents, submarine mudflows and slope instabilities (Pomar et al., 2012). Rebesco et al. (2014) has proposed that these intermittent processes, considered in the context of contourites, may be accelerating deep-water sedimentation. These sedimentary deposits gain material through the same processes as NLs and therefore these triggers also need to be considered for increased suspended material.

Recently bottom trawling has been recognised as a mechanism of sediment transport. Previously Chronis et al. (2000) suggested that anthropogenic activity could be contributing to the formation of nepheloid layers in the Cretan sea. They hypothesised that fisheries in the Cretan Sea cause resuspension, which may explain the irregular occurrence of exceptionally high values of SPM very close to the seabed (within 3–4 m). The effects of this activity can be seen down to the depth of 300 m and is expected to be higher in areas where there is a stronger slope gradient. Martín et al. (2014) also showed daily resuspension by bottom trawling at La Fonera (Palamós) Canyon. Their work clearly demonstrated that deep bottom trawling can effectively replace natural processes as the main driving force of sediment resuspension on continental slope regions and generate increased near-bottom water turbidity that propagates from fishing grounds to

wider and deeper areas via sediment gravity flows and NL development. This topic will be investigated in Chapter 5.

2.3 Composition

In the open ocean surface production is generally the most significant source of particles, but near the continental margins seafloor sediments can also be an important source as a result of resuspension and lateral advection (e.g. Gardner and Walsh, 1990; Puig et al., 2014). Material within nepheloid layers therefore can be suspended and/or dissolved fine-grained solids of organic and inorganic origin. Layers fed by vertical settling will hold particles representative of the water column (i.e. detritus), while those formed by resuspension will have compositional similarities to the seabed (i.e. reworked sediments). Layers more than 500 m above the seabed are thought to be sourced from the sides of the ocean basins, slope or in protrusions (McCave, 1986). As particles settle or are advected, their concentrations, sizes and compositions will be altered and modified by aggregation, scavenging, decomposition and other processes (Gardner et al., 1985). The composition, shape and other features of the nepheloid layer are antagonistically related to both the initial site and source and physical generation mechanism (Chronis et al., 2000). Settling rates and residence times of particles will ultimately be determined by these factors, with accumulation and recycling of organic matter and heavy metals having important implications for pollutant contamination and carbon cycling (Puig et al., 1999). The generation mechanism and composition of material are therefore intimately linked and the processes involved in both have important implications for biogeochemical cycles in the ocean. The possibility of nepheloid layers contributing to the benthic-pelagic coupling of organic matter (OM) has been previously suggested (e.g. Boetius et al., 2000). The possible association of benthic and suspension feeders with nepheloid layers, due to the increased availability of nutritionally rich material, is addressed in Chapter 6 and Appendix A. The compositional nature; particle size, range, origins and some modification processes will first be outlined here.

2.3.1 Particle size

The size-fraction of particles varies from study to study indicating the significance of local sources and processes. In a global overview of nepheloid layers, McCave (1986) reports that the size of particles typically range from 8 to 40 µm, while Puig et al. (2013a) found large aggregates mostly 150 µm and up to 1 mm in the BNLs in the western Mediterranean. Gardner et al. (1985) reported that 80–90% of particles in the NLs on the continental slope and rise of the western North Atlantic are <63 µm with a mean size of ~ 22 µm. In the Northern Portuguese shelf, SPM in the NL is much finer with >50% of particulate matter <10 µm in size (Oliveria et al., 2002). In their study, Oliveria et al. (2002) have also shown that grain sizes showed normal bi- or tri-modal distributions. In their study a fine mode (5 µm), an intermediate mode (10 µm) and a coarser peak (18 µm) was observed for both SNL and BNLs. The coarser modes corresponded to biogenic debris and they found increasing mean grain sizes toward the shelf break due to the increasing importance of the biogenic components (Oliveria et al., 2002). Their work again emphasises the control of local settings and influence on the composition of NLs.

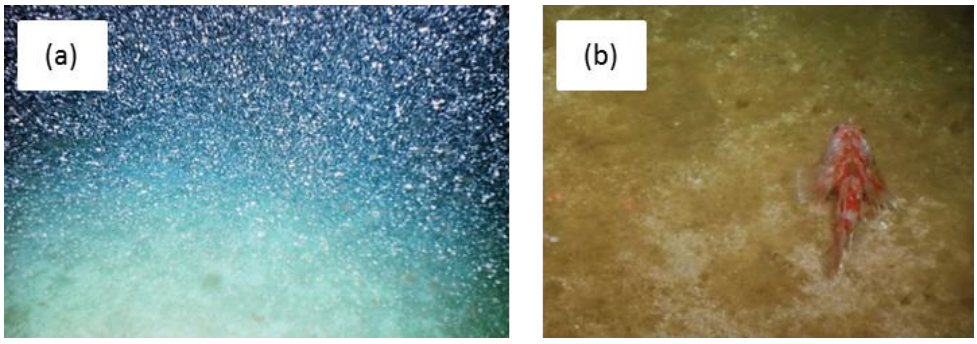

Fig. 2.5 (a) Marine snow in the water column and (b) phytodetritus on the seabed during survey CE13008 to the Whittard Canyon, June 2013.

2.3.2 Inorganic components

Inorganic material of heterogenous size consisting of mineral grains and carbonate particles constitutes a significant proportion of material in the nepheloid layer. Both BNLs and INLs, particularly influenced by the BBL, contain high amounts of lithogenic particles (McPhee-Shaw and Kunze, 2002). Generally, terrigenous mineralogical components increase with depth in the BNL (Chronis et al., 2000; Oliveira et al., 2002). This can be explained by the significance of

resuspension/erosive processes incorporating material from the sea bed. DSWC events in the Gulf of Lions scour the seabed and resultant BNLs there were composed mainly of resuspended superficial sediment from slope and basin regions, consisting predominantly of clays, fine silts with a clear absence of coarser particles in the aggregates (Puig et al. 2013a).

Distance from terrigenous sources (land, mountains and rivers) will also significantly impact the quantity of inorganic material. Chronis et al. (2000) reported high concentrations of quartz and clay minerals, material originating from aeolian and rock inputs from the Cretan mainland and North Africa in BNL and INLs in the Cretan Sea. Similarly, Oliveria et al. (2002) found that particulate matter from the northern Portuguese shelf was heavily influenced by fluvial input with high lithogenic material at the inner shelf and close to river mouths. High concentrations of calcite ($CaCo_3$) from skeletal remains were also observed here, with high terrigenous components of clay minerals (illite, kaolinite, chlorite and smectite) and other mineral grains (quartz, micra, K-feldspar and plagioclase) in smaller amounts in both BNLs and SNLs. They found that at maximum turbidity in the BNL, the particles were almost exclusively quartz and phyllosilicates. Silts and clays predominately observed were derived directly from the weathering of the high (1000 m) Minho Mountains, illustrating that although particles are locally derived they can also be transported considerable distances.

Scanning electron microscope images of material within nepheloid layers (Fig. 2.6a) have confirmed mineralogy analysis by diffractometer and radiation. Images revealing minerals, rock, silt particles, lumps of seabed and sediment remains from erosion as well nutrients (iron, manganese, phosphate) have been presented in the literature (e.g. Chronis et al., 2000; McCave et al., 2001).

Inorganic trace elements (Pb, Zn, Cu, Cr, Ni PCBs) have also been reported to accumulate in particulate matter and NLs (Mudroch and Mudroch, 1992; Puig et al., 1999). Inorganic dissolved particulate material and gases (e.g. CO_2), contributing to the maintenance of ocean pH may also be transported through NLs before deposition at greater distances and depths from their source (Holt et al. 2009). It has also been suggested that (inorganic) illite-vermiculite mixed-layer clay minerals deposited in NLs contribute to Heinrich layers in the northwest Atlantic (Bout-Roumazeilles et al., 1999).

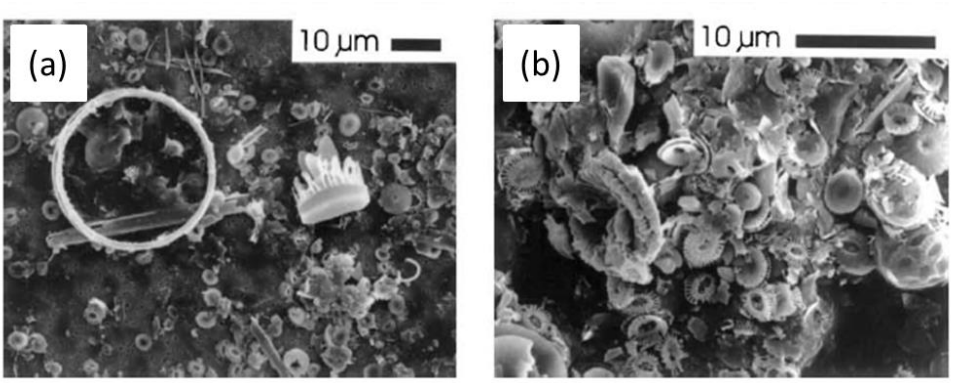

Fig. 2.6 Example SEM images of suspended particles in nepheloid layers of organic and inorganic origin. Both samples are from BNLs at 1186 m at Goban Spur (a) shows inorganic silt and clay particles and aggregates and (b) shows faecal pellets, organic debris mucus, aggregates (images from McCave et al., 2001).

2.3.3 Organic particles

Organic particles are usually transported from the surface as detritus (i.e. dead organic material). About 10–20% of the carbon fixed by photosynthesis in the euphotic zone sinks into midwater, and about 2–3% eventually reaches benthic communities at abyssal depths (e.g. Gardner et al., 1985; Tyler, 2003). Many studies have shown that NLs in the upper water column, and also in the lower water column, contain high amounts of phytodetritus and clay aggregates rich in organic matter (e.g. Naudin and Cauwet, 1996; Ransom et al., 1997; 1998; Oliveria et al., 2002). Thus, NLs provide a pathway and possibly a rapid transport mechanism for the delivery of this material to the seabed.

Material from the surface transported through the water consists primarily of organic aggregates; coccolithophores, diatoms and other phytoplankton, skeletal remains and a mixture of biogenic calcite and opaline silica. Visual inspection through a light microscope of filters from NLs commonly show aggregates of coccoliths (Oliveira et al., 1999), while scanning electron microscope images of material within NLs (Fig. 2.6b) have shown intact diatoms , dinoflagellates, silicoflagellates, grains of coccoliths skeletal fragments of these phytoplankton cells, resting spores, organic debris, organic mucus, , radiolarian, sponges, sponge remains and spicules, faecal pellets, tight closed and open aggregates, and foraminifera (,although rare) (e.g. Chronis et al., 2000, McCave et al., 2001; Oliveira et al., 2002; Mienis et al., 2007). Aggregates within NLs also have high levels of microbial activity and concentrations of bacterial communities (Epping et al., 2002; Boetius et al., 2000).

The organic constituents of the NL also display seasonality related to the seasonal pulse of phytodetritus to the benthos in temperate latitudes (e.g. Billet et al., 1983; Gooday et al., 1990). For example, Oliveria et al. (2002) observed such seasonality in the particulate organic carbon concentrations in BNLs and SNLs, related to the spring bloom input. Similarly local phytoplankton ecology and grazing zooplankton activity will affect the composition of NLs both spatially and temporally. Oliveria et al. (2002) also observed increasing organic components with increasing distance off the Portuguese shelf and decreasing influence of river and terrestrial sources, further highlighting the influence of local coastal and marine environments.

These organic particles and aggregates can contain labile lipids such as polyunsaturated fatty acids and low molecular weight alcohols which are key nutritional constituents and important food sources to many benthic ecosystems (Kiriakoulakis et al., 2004; Kiriakoulakis et al., 2007). Some studies have suggested that NLs may be important transporters of organic carbon, accumulating rich marine snow particles (e.g. van Weering et al., 2000; Puig et al., 2001b). Indeed other studies have attributed local enrichment of labile material to NLs (Kiriakoulakis et al. 2011). In the Nazaré Canyon, Kiriakoulakis et al. (2011) found the highest total lipid values (~294 mg g^{-1} OC) in mid-water depths due to to the presence of NLs associated with the upper (~600 m) and lower boundaries (~1500 m) of Mediterranean Outflow water. They found high concentrations of zooplankton lipid biomarkers, monounsaturated fatty acids $C_{20:1}$ and $C_{22:1}$ and their alkenol counterparts, at these depth ranges and suggested zooplankton were feeding on accumulated material in the NLs at these boundaries. A limited number of studies incorporating both physical profiles showing NLs and accompanying chemical analysis exist and there is some discrepancy between those that do. For example, Wells and Deming (2003) found no distinguishable nutritional advantage between nepheloid layers and surrounding clear waters. Although they found a positive correlation between nepheloid particles and chlorophyll *a* concentrations, macro-nutrient, particulate organic carbon and nitrogen concentrations were statistically indistinguishable. Contrary to this, Huvenne et al. (2011) reported high concentrations of particulate organic carbon and high proportions of labile lipids including the essential fatty acids docosahexaenoic acid (DHA) and eicosapentaenoic acid (EPA) and monosaturated

fatty acids in BNLs in water depths >1700 m. The BNLs detected in the Huvenne et al. (2011) study were also found close to coral communities and indicate the potential importance of NL in the transport of rich organic matter.

The intimate relationship between material in the NL and surface sediments is demonstrated in the Huvenne et al (2011) study whereby high proportions of labile lipids (EPA, DHA, 9(Z)-octadecenoic acid) were also found in sediment samples. Puig et al. (2001b) have also suggested that nepheloid layers are responsible for the rapid transfer of high-energy material of planktonic origin to the sediment interface in the Northwestern Mediterranean. Thus material transported by the NL is deposited on the seafloor and has potential implications for organic (and inorganic) carbon burial.

2.3.4 Decay and modification

The composition of typical NL aggregates differs from pelagic marine snow thus indicating that significant modifications of the material occurs (Ransom et al., 1998). Material can be significantly modified in transit with the rate of decay governed by the initial sources (generation and composition) (Wollast, 1998; Lampitt et al., 1995; Inthorn, 2006).

Organic sedimentation takes approximately four to six weeks to reach the sea-bed at depths of 4000 m from the surface. However, as particles settle downward or are advected laterally, their concentration and composition can be altered (Gardner et al., 1985). Biological aggregations and scavenging can alter material on its descent while at the seabed microbial and benthic activity (Graf, 1989; Tyler, 1988; Thomsen and Graff, 1994; Ritzrau, 1996; Boetius et al., 2000) and hydrodynamic processes controlling the exchange of material between the water column and the seafloor (Thomsen and Gust, 2000; Dickson and McCave, 1986) will affect the quality and quantity of material transported further or deposited.

The rate of modification (aggregation) and removal (deposition) of particles is determined by the Brownian or random motion of particles given by;

$$t_B = \frac{3\mu}{4kTN_0 E} \qquad (2.5)$$

where μ is viscosity, k is Boltzmann's constant, T is absolute temperature, N_0 is the initial number of particles and E is coalescence efficiency, the proportion of particle collisions that result in sticking (McCave, 1984). The rate of collisions of particles suspended in a liquid will be governed by the turbulent dissipation rate, mean flow speed, sediment concentration, size distribution and seabed geometry (Dickson and McCave, 1986; Hill et al., 1990). McCave (1984) showed for a (concentrated) NL of 0.3 mg L^{-1} (4 x 10^5 particles cm^3 and coalescence efficiency of 0.1) the 0.5–1 μm fraction has a coagulation time of 3 months. McCave (1984) reported that less concentrated layers have longer coagulation times and that material therefore is therefore in suspension longer allowing for greater medication and reworking of the particles. Furthermore, the rate of deposition of fine particles in a layer that remains in contact with the seabed will also be slower and fine material in dilute NLs can have residence times measured in years. Thus as the rate of decay is dependent on spatial and temporal conditions and cannot be universalised at any one site.

Aggregated phytodetritus, typically associated with high concentrations of chlorophyll, originates in the surface and has high settling velocities 0.1–0.2 cm s^{-1} (Alldrege and Silver, 1988). Lampitt, (1985) showed (experimentally) that once the material is concentrated and aggregated on to the surface of sediment the settling rates of organic fluff can increase to 0.35–1.2 cm s^{-1}. BNL aggregates tend to be assemblages of clay particles, clay floc and relatively dense organic rich micro-aggregates in a microbial exocellular organic matrix (Ransom et al., 1998). After an initial period of flocculation and settling, particles become stranded in suspension (Gonzalez and Hill, 1988). These "microflocs" can be transported long distances as shown by Milligan et al. (2007). Stranded particles in the BNL in the north western Mediterranean were shown to remain in suspension as far as the water mass extends (Puig et al., 2013a), thus the final point of deposition may be far removed from the original input zone.

BNLs and INLs originating from the BNL are heavily influenced by the BBL dynamics (McCave, 1986; McPhee-Shaw and Kunze, 2002). Hydro-dynamic sorting in the BBL and consequent dispersion also play an importance role in the modification of material (e.g. Thomsen et al., 1994; Thomsen and Graf, 1994; Thomsen and van Weering, 1998). Thomsen et al. (1994) found that in the Western Barents Sea, the chlorophyll content of the bottom water decreased

above the sea-floor from 0.13 to 0.01 μg L^{-1}, while the particulate organic matter content of the bottom water increased above the sea-floor. Hydrodynamic sorting of the organic fraction of the SPM in the BBL produced flux profiles with two maxima of the organic components; "top heavy" for the lighter fraction (organic debris) and "bottom heavy" for the fraction with higher settling rates (phytodetritus). They also showed that the BBL (in the Barents Sea) is critically important for the dispersion of material with low settling velocities.

Spatial changes and the addition and deposition of material with progression of the BNL particularly from coastal to marine environments can alter the composition. Naudin and Cauwet (1996) reported with a seaward transfer, material was progressively enriched with particulate inorganic carbon and organic nitrogen. They also observed that particulate organic carbon concentrations remained relatively constant and attribute this to plankton consuming organic material already present and settling of the mineral phase. Naudin and Cauwet, (1996) also found that temporal changes in river discharges affected the concentration of particulate organic carbon and total suspended material, although this may also be related to production in the euphotic zone. They also observed rapid modifications of the BNL content on hourly scales which they attributed to flood discharge. Temporal variability in the generation mechanism (e.g. storm activity) will also impact these rates with variable concentrations observed with inter-annual (daily, monthly, seasonal) variability (e.g. Chronis et al. 2000). Similarly, heavy rains can increase local sediment loads, affecting the composition (Oliveria et al., 2002). Seasonal changes in primary production at the surface and in the vertical supply of material will also affect the initial composition and subsequent modification of particles (Lampitt et al., 1995).

The dynamic nature of nepheloid layers makes it possible for particles to be resuspended many times before they are finally buried (Fig. 2.7). The residence time for particulate material in deep nepheloid layers is estimated to last several days to weeks for the first 15 m above the seafloor, and weeks to months in layers ~100 m above the seafloor (Kennett, 1982). The residence time driven by the physical generation will also govern these in a feedback loop, with smaller particles remaining in suspension longer and undergoing further modifications (Naudin and Cauwet, 1996). Repeated sedimentation and resuspension loops, exposes particles to dissolution and decomposition for longer (Gardner et al.,

1985; Thomsen and van Weering, 1998). Many studies have suggested that oxygen-deficient waters enhance organic matter preservation (e.g. Dean and Gardner, 1998). Thomsen and Graf (1994) however found low oxygen concentrations near the seabed due to the influence of filter feeders, while other studies have reported that there may not be a difference in the rate or extent of degradation in oxic and anoxic environments (e.g. Arthur et al., 1998). Lateral transport processes also have a significant impact on the quality of organic matter, its preservation potential during diagenesis and sequestration of organic carbon (Wollast, 1998; Inthorn, 2006). Kiel et al. (2004) showed that the oxygen exposure time during lateral transport could double for organic matter transported across the Washington margin.

Dissolved organic carbon is the primary energy source for bacteria in the BNL (Boetius et al., 2000) and microbial exudates are responsible for the formation and strengthening of aggregates in resuspension loops (Ransom et al., 1998). In turn, these laterally transported aggregates are utilised as a food source by microbenthic animals (Graf and Rosenberg, 1997). Thus lower oxygen rates in the NL may preserve material in suspension for longer periods fuelling bacteria and microbenthic animals and/or may contribute to sediment deposits for petroleum source rocks.

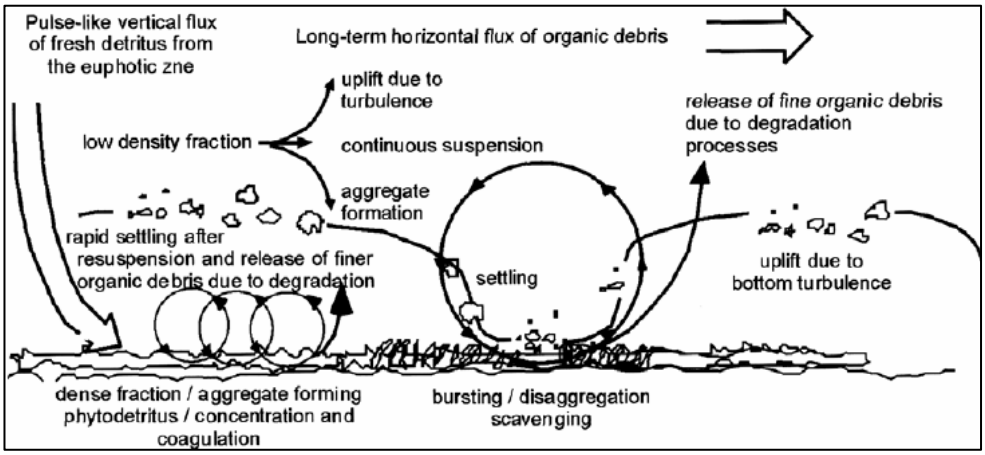

Fig. 2.7 Schematic of resuspension loops of aggregated particles (from Thomsen, 2003).

2.4 Detection and methods of measurement

Detection and methods of measurement of NLs and suspended particles vary from study to study and from site to site (Gibbs, 1974). Sampling methods therefore vary according to the problem being investigated and/or being

assessed. An array of techniques and technologies (e.g. time lapse or video camera, autonomous vertical profiles, BIOPROBE), have been utilised to measure the extent of NLs and turbidity through the water column. Sensors and underwater vision profilers (Puig et al., 2013a) have been used to "see" these turbid layers, while moored traps offer more information on the overall flux and concentration of materials reaching the seabed. Hydrodynamics and oceanographic processes generating NLs can be measured by in situ point samples and/or moorings on the seafloor. While material collected in traps on moored platforms can also be analysed for compositional components, large scale in situ pumps and filtration of water at discrete depths are used to assess particles in suspension at a point in time. More recently, modern analytical chemistry methods (i.e. elemental and molecular analysis) have been employed to assess the nature of this material, while the visualisation and mapping of the spatial and temporal extent of NLs has been carried out by point sampling or moored measurements by acoustics and more commonly optical sensors.

2.4.1 Optical sensors and acoustics

The concentration of suspended material or turbidity in the water column can be directly and quantitatively measured by optical and acoustical methods (Bloesch, 1994). Several types of instruments are available for deployment from moving ships/platforms or mounted on/close to the seabed e.g. Turbidity meters: transmissometers, back scatter sensors, nephelometers and high frequency echo sounders.

Acoustic instruments (acoustic Doppler meters) use echo sounding or the back scattering signals from particles to visualise them in the water column. While these instruments generally measure water velocity, the returned beam can indicate the concentration of SPM after correction for sound absorption and beam spread. Using a water column mass concentration equation, resuspension can be quantified. Orr and Hess, (1978) first showed that high frequency acoustic backscattering data can be a valuable tool in the remote monitoring of suspended particle distributions. This was later confirmed by Holdaway et al. (1999) who demonstrated that backscatter signals from ADCP can be comparable with transmissometer observations. Similarly, Puig et al. (2004b) and Puig et al. (2013b)

used the mean backscatter signal from ADCP transducers to estimate suspended sediment concentrations.

Although the use of acoustics has proved successful, optical sensors i.e. turbidimeters remains the most popular method for the measurement of suspended particles, providing fast, accurate turbidity measurements. Optical measurements of SPM in the ocean date back to early studies such as Ewing and Thorndike, (1965) and Biscay and Eittreim (1974) and are now considered to be the standard method of mapping and detecting NL structures and have been used globally (e.g. Pak et al., 1980; Dickson and McCave, 1986; Puig and Palanques, 1998a; Liu et al., 2010; Karageorgis et al., 2012). Optical sensors have proven to be sensitive in both high concentration environments and clear waters depending on the particular instrument used (Gibbs, 1974). The major advantage of (optical) sensors over other methods (primarily filtration) is the higher spatial resolution that can be achieved with continuous vertical or horizontal profiles. Therefore optical measurements are better suited in the study of patchy distributions of SPM.

All turbidimeters; nephelometers, backscatter sensors and transmissometers operate on a similar principle, measuring the loss of light from a light emitter (LED or LASER diode) as it propagates through the water column to a light detector (a photodiode). The loss of light can be attributed to scattering and absorption which are proportional to the temporal and spatial changes in concentration of SPM (Bloesch, 1994). Certain size ranges of particles are responsible for dominant light scattering at specific angles. Therefore, to measure the light scattered at all angles at the same time, specific-angle meters that measure the integrated light from a low forward angle to the back scattering angle are used. Using the effects of particle size and composition in the scattering of light; the composition of particles can be inferred from the index of refraction between water and the particles (Gibbs, 1974).

Three main types of optical turbidity sensor exist which can be distinguished on the relative angular position between the emitter and detector (Fig. 2.8). While nephelometers and backscatter sensors are considered true turbidimeters, transmissometers were designed to be different using visible rather than infrared light.

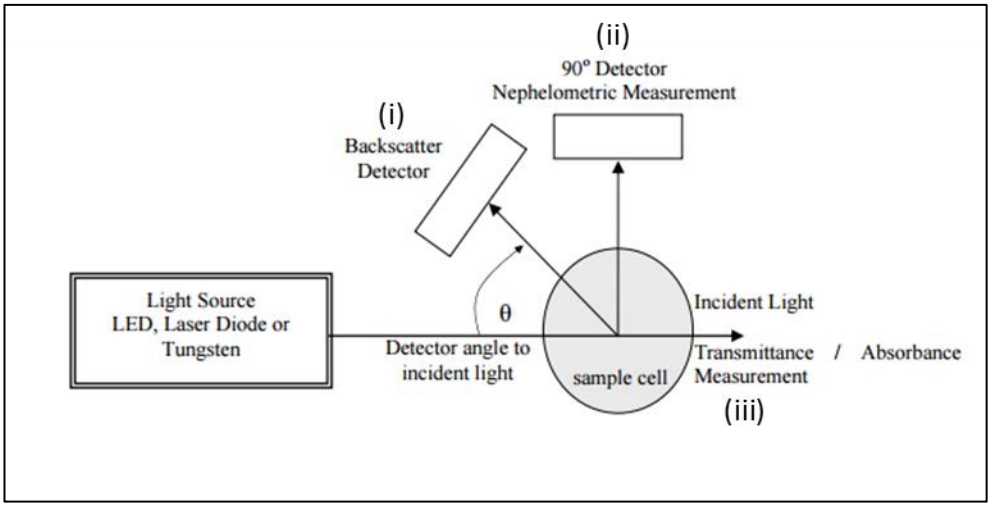

Fig. 2.8 Diagram showing different set-ups of three turbidity instruments; (i) Optical Backscatter; (ii) Nephelometer; (iii) Transmissometer. (Source: http://www.mdpi.com/1424-8220/9/10/8311?trendmd-shared=0).

Nephelometers

Nephelometers consist of a near infrared emitter and detector that are positioned at 90° to each other. Nephelometers measure the scattered light which is proportional to the total cross-section of the particles and does not suffer absorption issues (Gibbs, 1974). These instruments resolve changes in turbidity from glacier-fed streams to plumes of sediment generated during dredging operations (AML, 2016). Nephelometer measurements are usually expressed in nephelometric turbidity units (NTU) and can measure as low as 0.1 NTU (drinking water ≈ 0.3 NTU) to as high as 3000 NTU (e.g. dairy milk), (AML, 2016).

Optical backscatter sensors

The near infrared emitter and photodetector are adjacent to each other and positioned in the same direction. The USGS classify these as turbidity sensors with a 0–45° detection angle (135–180°; AML, 2016). They measure light that is scattered by greater than 90° and can therefore measure turbidity greater than 3000 NTU. However, as a direct consequence they have poor sensitivity at low turbidity levels (AML, 2016). Advantages of optical backscatter sensors include; their wider measurement range, tolerance to ranging particle sizes and accuracy in high turbidities (AML, 2016).

Transmissometers

The light source (light emitting diode) and (silicon photodioide) detector in the transmissometers are positioned at 180° facing each other with a path way separating them ~10 to 25 cm apart (Fig. 2.9). Transmissometers use visible light (usually 650–660 nm; red light) rather than near infrared as they are used to determine the depth of penetration of visible light through the water column. Transmissometers measure the attenuation of light. Output values are given as an attenuation co-efficient. Both a limitation and advantage of use; transmissometers are sensitive to low range turbidity and only practical in such environments (AML, 2016).

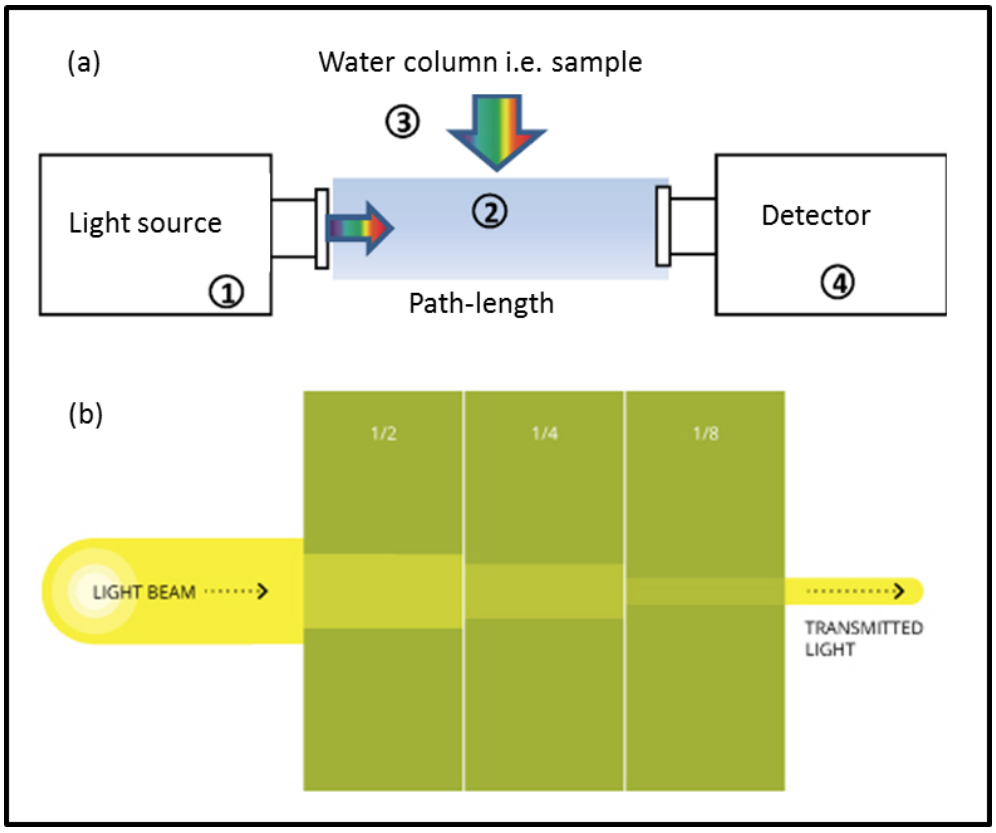

Fig. 2.9 Schematic of most popular instrument; a transmissometer. (a) Set up; (b) as light passes through the sample in the pathway, it will lose intensity due to scattering and absorption. (Adpated from Kember, 2014).

In the past, nephelometer measurements were most commonly used to delineate the distribution of particulate matter in ocean water (Jerlov, 1968; McCave, 1986). The majority of work was carried out using the Lamont

Nephelometer (McCave, 1986). Traditionally this instrument used an incandescent bulb as the source and photographic film as the detector, with light scattered between 8 and 24° from the axis of the light beam. The film was continuously wound on as the instrument was lowered, resulting in an average of the received signal over approximately 25 m depth. Throughout the years, instruments have been modified and changes to the angular domain of the detected scattered light that governs the sensitivity to particle concentrations have been made.

More recently transmissometers have been the popular choice, serving as good sensors (Fig. 2.9). Modern instruments (e.g. Wet Labs C-star) have adopted the convention that the measured beam c is relative to the clean water calibration value and hence does not include the beam attenuation coefficient for pure water at a given wavelength and temperature. The value of c for pure sea water is generally taken to be 0.40 for instruments operating at 660 nm and excess is due to particle effects (WET Labs, 2008; 2011).These instruments are simple and manufactured by many companies such as Sea Tech Inc. and Wet Labs. The accuracy of transmission and sensitivity can be adjusted by changing the length of the pathway. A major disadvantage of transmissometers is that some dissolved substances absorb light, particularly dissolved organic matter, and can therefore be inferred as increased SPM (Gibbs, 1974).

Varying light sources, detectors and angles of measurement for each instrument have resulted in an array of different and incomparable units being used (e.g. NTU, FNU, BU etc.) The output signal of each instrument is based on the relationship between the light and particle, size, colour and concentration, determined by the effect of the set-up of the instrument. Furthermore, a limitation for optical sensors exists in that their units are measurements of light scattering, attenuation or other instrument parameters (e.g. film density, volts). Units such as NTU have no intrinsic physical, chemical or biological significance, however, Biscaye and Eittreim (1977) showed that nephelometer data could be converted to absolute SPM concentration allowing for the identification of distinct features. Although there is no standard conversion between instruments and quantitative mass measurements (mg L^{-1}), correlations between difference turbidity sensors have been shown (e.g. Gardner et al., 1985). Gardner et al. (1985) found that both the LDGO nephelometer and OSU transmissometer were

effective in the study of NLs. Hall et al., (2000) also found similar results when comparing different types of sensors (transmissometer and backscatter). Similar nepheloid layer structures were found despite the fact that backscatter is more affected by fine particles and transmission by coarse particles. However, such correlations and calibrations will only be adequate for specific locations. Many factors influence optical measurements (size, shape, composition, aggregation and flocculation); (Gardner et al., 1985; Hill et al., 2011). Guillén et al. (2000) showed that turbidity measurements using the same sensor with different calibration ranges can only give descriptive or semi-quantitative data and highlighted the advantage of simultaneously combing two instruments calibrated in different ranges when significant changes in the suspended sediment concentrations are expected.

2.4.2 Calibrations, gravimetric and SPM analysis

Depending on the topic being investigated, various methods are employed for the analysis of biological components of SPM within NLs. In comparison to continuous time-series data and vertical profiles of optical instruments, water sampling provides discrete point measurements. Gravimetric analysis of SPM is however required for the calibration of optical sensors. Turbidity readings by sensors can be affected by coloured dissolved organic matter therefore measuring suspended particles by weight is the most accurate method for estimates on the concentration of particles. Calibrations are critical to obtaining accurate information from any instrument measuring SPM.

Direct filtration of SPM dates back to early studies in the 1960's and 1970's (Ewing and Thorndike, 1965; Biscay and Eittreim, 1974). The wide variability in concentrations from location to location and surface tension can incur difficulties in terms of contamination and calibrations (Gibbs, 1974). Although there are many sampling issues, and some remain unresolved, filtering discrete water samples is still the superior method and most frequently used for both calibrations purposes and particulate organic carbon measurements (e.g. Bishop, 1986; McCave et al., 2001; Gardner et al., 2003).

Measured in weight per volume (e.g. mg L^{-1} or µg L^{-1}) calibrations are carried out by filtration and gravimetric analysis of dried filters. Fine suspended particles (i.e. <53 um) tend to give precise and accurate values relative to the true

concentration. However the presence of coarser particles and filtration of subsamples can introduce errors due to rapid settling. According to Gibbs (1974) both Nucelopore and Millipore filters give satisfactory results. However, Nucelopore are more commonly used and are superior in open ocean environments where there are lower concentrations of particles (e.g. Feely, 1975; Spinard et al., 1989; McCave et al., 2001). These thin plastic membranes with punched holes are lighter, with less loss of weight due to wetting agents being removed by the water and the smoother surface allowing for easier microscopic work. Furthermore, they give lower chemical blanks for a number of elements. Millipore filters on the other hand, are thicker and resemble an intricate cellular network, with higher sustained flow rates and higher retention. After internal corrections are applied, the gravimetric weight of the material is correlated using linear regression with the output of the particularsensor (e.g. Gardner et al. 1985; Bishop, 1986; WetLabs Inc 2008).

Optical data from natural suspension is very complex and a function of the size index of refraction and the shape of the particles and therefore calibrations can be a great source of error. Previously substitute material in a standard solution (e.g. Formazin-a colloidal suspension is relatively stable and reproducibly prepared) was commonly used for calibrating shallow water transmissometer or nephelometers. However, Gibbs (1974) reported that Polymer formazin and Formazin Turbidity Units can give errors up to 1000% and that these methods should be abandoned. These methods are now considered obsolete in favour of turbidity instruments calibrated with gravimetric samples.

There is no single way to establish an accurate relationship between beam attenuation/scattering and concentration due to relative changes in the biological and mineral material concentration (i.e. size, shape, refractive index; Durrieu de Madron et al., 1990; Azetsu-Scott et al., 1993; McCave et al. 2001; McCave and Hall, 2002). This has long been established. For example Biscaye and Eittreim, (1977) reported variation of more than a factor of 70 in SPM concentrations in the North Atlantic, while Gardner and Sullivan (1981) reported smaller variations (factor of 20) and they also reported daily changes of between a factor of 2 and 10. Therefore studies generally apply their own calibration or one of a representative area.

2.5 Context of nepheloid layers along the NE Atlantic margin

As reviewed above, there are many processes that can trigger sediment transport processes-particularly at the continental margin. Boundary currents at the margin can transport significant amounts of material (e.g. Ewing et al., 1971; Biscaye and Eittreim, 1977; McCave, 1986; Anderson et al., 1994; McCave and Carter, 1997). The steep bathymetry at margins traps and induces the downslope transport of material and the formation of other processes that increase particle fluxes and sediment exchange (e.g. turbidity currents, slumps and slides). The steep gradients (density, topography etc) also promote the reflection and intensification of energy (e.g. Cacchione and Wunsch, 1974). Thus, continental margins are "hotspots" for nepheloid layer formation. The NE Atlantic is no exception with many previous studies reporting the presence of both benthic and intermediate nepheloid layers (e.g. Dickson and McCave, 1986; Thorpe and White, 1988; Ruch et al., 1993; Duineveld et al., 1997; de Stigter et al., 2007; Mienis et al., 2007).

2.5.2 Regional oceanography: The Celtic Margin, NE Atlantic

The general surface oceanography of the NE Atlantic is characterised by the northward transport of warm subtropical water by the NAC towards the European Margin and southward transport by the Azores Current (AC) towards the African Margin (Fig. 2.10). The Gulf Stream (western boundary current) and Canary currents (continuation of the AC; eastern boundary current) connect to the NAC (north) and North Equatorial Current (south) to complete the anticyclonic subtropical gyre. The NAC also splits into two (main) branches; cyclonic in the north entering the Norwegian-Greenland Sea and anticyclonic in the south flowing into the Bay of Biscay linking in with the subtropical gyre (e.g. Xu et al., 2015). Eddies are common, induced by bottom topography and flow instabilities (e.g. Woodward and Rees, 2001; Xu et al., 2015). These are very important in the mixing and dispersion of material, including organic material (Pollard et al., 1996; Koutsikopoulos and Le Cann, 1996; Dullo et al., 2008).

The Celtic Sea Shelf is a wide and productive area, with a steep sloping margin (mean gradient of 11°) incised with many submarine canyons that act as funnels for material from the shelf into the deep abyss. Surface waters are modified by atmospheric interactions and the seasonal thermocline usually

develops between 50 m to 100 m (Pollard et al., 1996). Most of the water masses in the Bay of Biscay and at the Celtic Margin have their origin in the Northern Atlantic Ocean and belong to the north-eastern Atlantic circulatory system or are the result of interactions between North Atlantic and Mediterranean waters (Dullo et al., 2008; Pollard et al., 1996; van Aken, 2000). Residual currents over the shelf are mainly formed by the wind, tides and the differences in water density (e.g. Pingree et al., 1982 and Fig. 2.10). During the summer months winds are directed south, resulting in offshore Ekman transport of the surface waters that induces upwelling and southward surface circulation (Pingree and LeCann, 1990). During the winter, the winds are mainly directly to the NW and induce stronger mainly north-easterly surface circulation (Pingree and LeCann, 1990).

Below the surface, slope currents dominate the flow in the upper 1000 m. At the continental margin, the Shelf Edge Current (SEC) flows as a light, warm, saline boundary current along the upper continental slope between 300–600 m (White and Bowyer, 1997). The SEC flows in a predominantly poleward direction (NW; Pingree and Le Cann, 1990; Xu et al., 2015) with a generally northward increase in the mean slope current speed and transport (Pingree et al., 1999). Mean flows at 500 m are reported to be 6 cm s^{-1}, although this slope current displays strong seasonality with a minimum in the principal driving mechanism during the summer months and can display reversal of flow (Pingree et al., 1999; Xu et al., 2015). Near the seabed, flow is mainly tidally induced with mean speeds of 15 cm s^{-1} observed in the downslope current (Pingree and LeCann, 1989).

Barotropic tides are proportional to the width of the continental shelf and large amounts of tidal energy are present at the shelf-edge of the Celtic Sea (Huthnance, 1995; 2001). Strong baroclinic currents also result from suitable conditions and the Celtic Shelf is globally considered as a hotspot for tidal energy dissipation with dominant semi-diurnal currents (Baines, 1982). Internal waves at the continental slope also serve to reinforce bottom current velocities.

The Celtic Sea is a highly productive area with the energetic oceanography re-fuelling nutrients and promoting annual phytoplankton blooms and good fishing in the area (Sharples et al., 2007; 2013). At the margin, primary production is estimated to be between 100 – 250 g C m^{-2} yr^{-1} (Joint et al., 1986; Rees et al., 1999; Wollast and Chou, 2001).

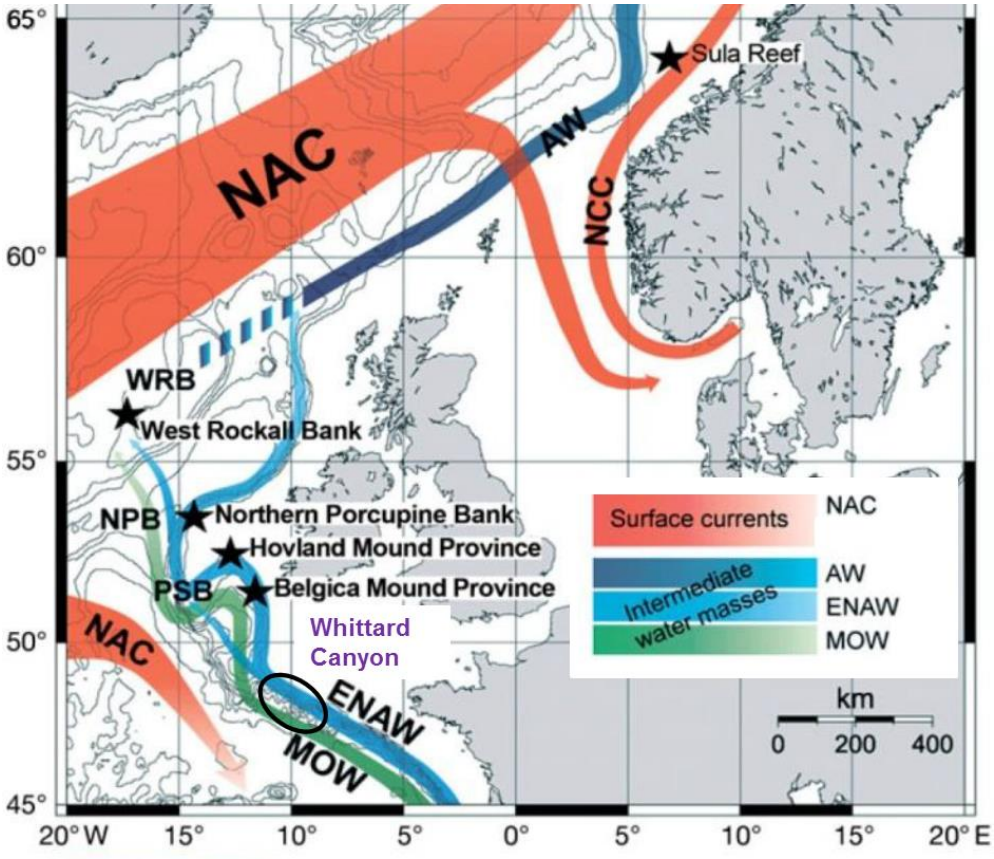

Fig. 2.10 Regional oceanography and prevailing currents at the Celtic Margin, North Atlantic. Red arrows indicate surface currents, blue and green arrows indicate intermediate water masses (Mediterranean Outflow Water (MOW); Eastern North Atlantic Water (ENAW) and Atlantic Water (AW) (From Dullo et al., 2008).

2.5.3 The Whittard Canyon

The Whittard Canyon has recently been reviewed in Amaro et al. (2016; Appendix B). Heavily influenced by the local oceanography (Bay of Biscay and the Celtic Margin), the Whittard Canyon (47 ° – 49 ° N and 9 ° 30’ – 11 ° 30’ W) is situated on the Irish continental margin, connected to the shelf at 200 m water depth and extends to the continental rise at 4000 m (Fig. 2.11). It is bound by the Goban Spur (west) and the Berthois spur (east). Four main branches extend more than 100 km and the whole system is approximately 100 km wide. The complex branching and valleys are influenced by the existing NNW-SSE trending fault system and by an old buried canyon (Cunningham et al., 2005). Scars, scarps, gullies and interfluves of the canyon are formed by; (hemi-) pelagic sedimentation; deposition and remobilisation in response to hydrodynamic conditions (tidal and wave currents); slope deposits (contourites and sediment

waves) and gravity-driven deposits (slides, debris flows and turbidity currents (Bourillet et al. 2003).

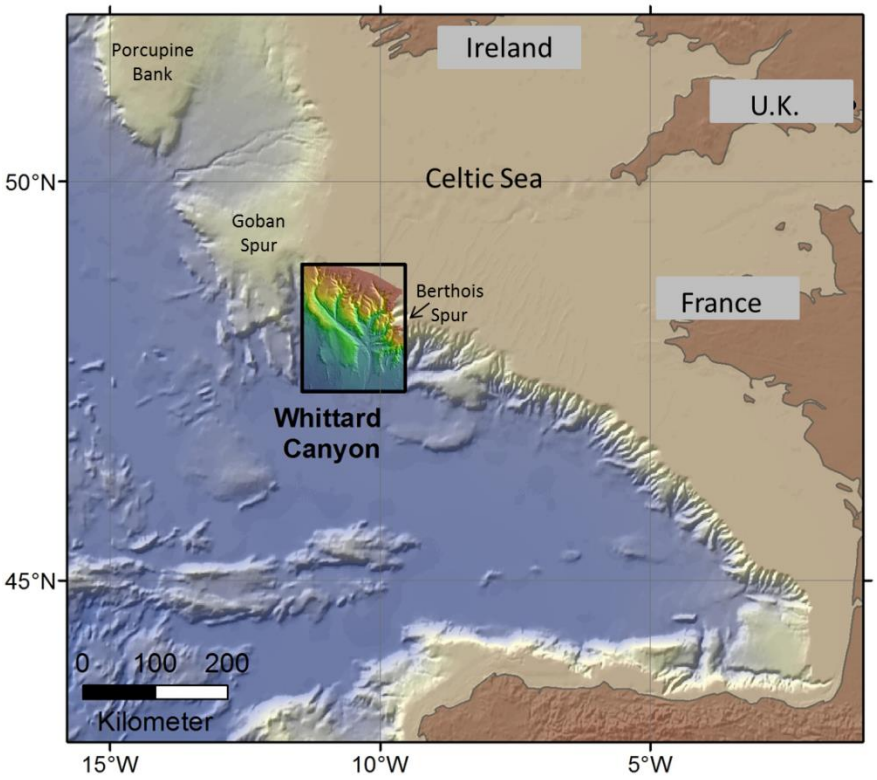

Fig. 2.11 The Whittard Canyon (Source: https://codemap2015.wordpress.com/about/science/).

The Whittard Canyon is an important site of biological, geological and oceanographic research and has been the centre of much submarine canyon research in the last decade. The location of the canyon and the complex shelf-incising and varied topography (vertical walls and steep slopes) give rise to a broad range of processes (e.g. internal waves, small-scale slope failures, sediment gravity flows, lateral transport; Allen & Durrieu de Madron, 2009; Puig et al., 2014). Whittard canyon is also a refuge for rich, varied and unique biological communities (Huvenne et al., 2011; Johnson et al., 2013; Appendix A). In terms of nepheloid layers, Huvenne et al., (2011) have previously identified a BNL in the middle and upper canyon branches from 1200 m to 200 m water depth and showed that the material within it was of high quality, rich in labile organic matter. However, their study only showed a snap shot of the potential extent and importance of NLs in the Whittard Canyon.

The Whittard Canyon provides an ideal location for the study of SPM and NLs. Firstly, because it is a submarine canyon, it is typified by enhanced sediment transport and interesting oceanography. Secondly, the adjacent Celtic Sea and

margin likely supplies high quality organic material. Thirdly, the system is now known to host rich communities of fauna (benthic, meio and macro fauna).

2.6 Conclusion

Many processes contribute to the formation, composition and nature of material transported in NLs. From the literature it appears that both the processes generating NLs and influencing the quality of material, are site specific. Understanding the mechanisms generating these layers and the interaction between the physical and biogeochemical components will aid our understanding of bio-physical coupling regimes. Each system is unique but similarities between well explored systems may aid our understanding of the unknown. The Whittard Canyon and Celtic margin are well established as important areas for the shelf-edge exchange of material. Understanding the transport of organic material and functioning of this system will aid proper utilisation and protection of this canyon and its resources.

References

Agrawal, Y. 2004. Science box: Bottom nepheloid layer. Oceanography, 17, 79, http://dx.doi.org/10.5670/oceanog.2004.51.

Alldredge, A.L. and Gotschalk, C.C., 1989. Direct observations of the mass flocculation of diatom blooms: characteristics, settling velocities and formation of diatom aggregates. Deep Sea Research Part A. Oceanographic Research Papers, 36, 159-171.

Alldredge, A.L. and Silver, M.W., 1988. Characteristics, dynamics and significance of marine snow. Progress in oceanography, 20, 41-82.

Allen, S.E. and Durrieu de Madron, X., 2009. A review of the role of submarine canyons in deep-ocean exchange with the shelf. Ocean Science, 5, 607-620.

Amaro, T., Huvenne, V.A.I., Allcock, A.L., Aslam, T., Davies, J.S., Danovaro, R., de Stigter, H.C., Duineveld, G.C.A., Gambi, C., Gooday, A.J., Gunton, L.M., Hall, R., Howell, K.L., Ingels, J., Kiriakoulakis, K., Kershaw, C.E., Lavaleye, M.S.S., Robert, K., Stewart, H., Van Rooij, D., White, M., Wilson, A.M., (2016) The Whittard Canyon-a case study of submarine canyon processes, Progress in Oceanography, 146, 38-57.

AML, 2016. http://www.amloceanographic.com/Technical-Demo/Turbidity/ Nephelometric - Sensors-Backscatter-Sensors-and-Transmissometers (Accessed 7/5/2016).

Anderson, R.F., Rowe, G.T., Kemp, P.F., Trumbores, S. and Biscaye, P.E., 1994. Carbon budget for the mid-slope depocenter of the Middle Atlantic Bight. Deep Sea Research Part II: Topical Studies in Oceanography, 41, 669-703.

Apel, J.R., 2000. Solitons near Gibraltar: views from the European remote sensing satellites. Report GOA, 1.

Apel, J.R., 2004. Oceanic internal waves and solitons. In: Jackson, C.R., Apel, J.R. (Eds.), Synthetic Aperture Radar Marine User's Manual. US Department of Commerce, National Oceanic and Atmospheric Administration, Silver Spring, pp. 189 – 206.

Armstrong, R.A., Lee, C., Hedges, J.I., Honjo, S. and Wakeham, S.G., 2001. A new, mechanistic model for organic carbon fluxes in the ocean based on the quantitative association of POC with ballast minerals. Deep Sea Research Part II: Topical Studies in Oceanography, 49, 219-236.

Arthur, M.A., Dean, W.E. and Laarkamp, K., 1998. Organic carbon accumulation and preservation in surface sediments on the Peru margin. Chemical Geology, 152, 273-286.

Asper, V.L., 1987. Measuring the flux and sinking speed of marine snow aggregates. Deep Sea Research Part A. Oceanographic Research Papers, 34, 1-17.

Azetsu-Scott, K., Johnson, B.D. and Petrie, B., 1995. An intermittent, intermediate nepheloid layer in Emerald Basin, Scotian Shelf. Continental Shelf Research, 15, 281-293.

Baines, P.G., 1982. On internal tide generation models. Deep Sea Research Part A. Oceanographic Research Papers, 29, 307-338.

Baker, E.T. and Hickey, B.M., 1986. Contemporary sedimentation processes in and around an active west coast submarine canyon. Marine Geology, 71, 15-34.

Béthoux, J.P., Durrieu de Madron, X., Nyffeler, F. and Tailliez, D., 2002. Deep water in the western Mediterranean: peculiar 1999 and 2000 characteristics, shelf formation hypothesis, variability since 1970 and geochemical inferences. Journal of Marine Systems, 33, 117-131.

Billett, D.S.M., Lampitt, R.S., Rice, A.L. and Mantoura, R.F.C., 1983. Seasonal sedimentation of phytoplankton to the deep-sea benthos. Nature, 302, 520-522.

Biscaye, P.E. and Eittreim, S.L., 1974. Variations in benthic boundary layer phenomena: nepheloid layer in the North American Basin. (Eds.) Gibbs, R.J., Springer, New York, USA (1974). pp. 227-260

Biscaye, P.E. and Eittreim, S.L., 1977. Suspended particulate loads and transports in the nepheloid layer of the abyssal Atlantic Ocean. Developments in Sedimentology, 23, 155-172.

Bishop, J.K., 1986. The correction and suspended particulate matter calibration of Sea Tech transmissometer data. Deep Sea Research Part A. Oceanographic Research Papers, 33, 121-134.

Bloesch, J., 1994. A review of methods used to measure sediment resuspension. Hydrobiologia, 284, 13-18.

Boetius, A., Springer, B. and Petry, C., 2000. Microbial activity and particulate matter in the benthic nepheloid layer (BNL) of the deep Arabian Sea. Deep Sea Research Part II: Topical Studies in Oceanography, 47, 2687-2706.

Borenäs, K. and Wåhlin, A., 2000. Limitations of the streamtube model. Deep Sea Research Part I: Oceanographic Research Papers, 47, 1333-1350.

Boucher, J., Ibanex, F., Prieur, L., 1987 Daily and Seasonal variation in the spatial distribution of zooplankton populations in relation to physical structure in the Ligurian Sea Front. Journal of Marine Research, 45, 133 - 173.

Bourillet, J.F., Reynaud, J.Y., Baltzer, A. and Zaragosi, S., 2003. The 'Fleuve Manche': the submarine sedimentary features from the outer shelf to the deep-sea fans. Journal of Quaternary Science, 18, 261-282.

Bout-Roumazeilles, V., Cortijo, E., Labeyrie, L. and Debrabant, P., 1999. Clay mineral evidence of nepheloid layer contributions to the Heinrich layers in the northwest Atlantic. Palaeogeography, Palaeoclimatology, Palaeoecology, 146, 211-228.

Cacchione, D. and Wunsch, C., 1974. Experimental study of internal waves over a slope. Journal of Fluid Mechanics, 66, 23-239.

Cacchione, D.A. and Drake, D.E., 1986. Nepheloid layers and internal waves over continental shelves and slopes. Geo-Marine Letters, 6 , 147-152.

Cacchione, D.A., Pratson, L.F. and Ogston, A.S., 2002. The shaping of continental slopes by internal tides. Science, 296, 724-727.

Canals, M., Danovaro, R., Heussner, S., Lykousis, V., Puig, P., Trincardi, F., Calafat, A., Durrieu de Madron, X., Palanques, A. and Sanchez-Vidal, A., 2009. Cascades in Mediterranean submarine grand canyons. Oceanography, 22, 26-43.

Canals, M., Puig, P., Durrieu de Madron, X., Heussner, S., Palanques, A. and Fabres, J., 2006. Flushing submarine canyons. Nature, 444, 354-357.

Cenedese, C., Whitehead, J.A., Ascarelli, T.A. and Ohiwa, M., 2004. A dense current flowing down a sloping bottom in a rotating fluid. Journal of Physical Oceanography, 34, 188-203.

Chambers, R.L. and Eadie, B.J., 1981. Nepheloid and suspended particulate matter in south-eastern Lake Michigan. Sedimentology, 28, 439-447.

Chronis, G., Lykousis, V., Georgopoulos, D., Zervakis, V., Stavrakakis, S. and Poulos, S., 2000. Suspended particulate matter and nepheloid layers over the southern margin of the Cretan Sea

(NE Mediterranean): seasonal distribution and dynamics. Progress in Oceanography, 46, 163-185.

Connary, S.D. and Ewing, M.A.U.R.I.C.E., 1972. The nepheloid layer and bottom circulation in the Guinea and Angola Basins. Studies in Physical Oceanography, 2, 169-184.

Cunningham, M.J., Hodgson, S., Masson, D.G., Parson, L.M. 2005. An evaluation of along- and down-slope sediment transport processes between Goban Spur and Brenot Spur on the Celtic Margin of the Bay of Biscay. Sedimentary Geology, 179, 99-116.

De Silva, I.P.D., Imberger, J. and Ivey, G.N., 1997. Localized mixing due to a breaking internal wave ray at a sloping bottom. Journal of Fluid Mechanics, 350, 1-27.

De Stigter, H.C., Boer, W., de Jesus Mendes, P.A., Jesus, C.C., Thomsen, L., van den Bergh, G.D. and van Weering, T.C., 2007. Recent sediment transport and deposition in the Nazaré Canyon, Portuguese continental margin. Marine Geology, 246, 144-164.

Dean, W.E. and Gardner, J.V., 1998. Pleistocene to Holocene contrasts in organic matter production and preservation on the California continental margin. Geological Society of America Bulletin, 110, 888-899.

Dickson, R.R. and McCave, I.N., 1986. Nepheloid layers on the continental slope west of Porcupine Bank. Deep Sea Research Part A. Oceanographic Research Papers, 33, 791-818.

Drake, D.E. and Gorsline, D.S., 1973. Distribution and transport of suspended particulate matter in Hueneme, Redondo, Newport, and La Jolla submarine canyons, California. Geological Society of America Bulletin, 84, 3949-3968.

Duineveld, G.C.A., Lavaleye, M.S.S., Berghuis, E.M., De Wilde, P.A.W.J., Van Der Weele, J., Kok, A., Batten, S.D. and De Leeuw, J.W., 1997. Patterns of benthic fauna and benthic respiration on the Celtic continental margin in relation to the distribution of phytodetritus. Internationale Revue der gesamten Hydrobiologie und Hydrographie, 82, 395-424.

Dullo, W.-C., S. Flögel, and A. Rüggeberg (2008). Cold-water coral growth in relation to the hydrography of the Celtic and Nordic European continental margin. Marine Ecology Progress Series, 165-176.

Durrieu de Madron, X., Nyffeler, F. and Godet, C.H., 1990. Hydrographic structure and nepheloid spatial distribution in the Gulf of Lions continental margin. Continental Shelf Research, 10, 915-929.

Durrieu de Madron, X., 1994. Hydrography and nepheloid structures in the Grand-Rhône canyon. Continental Shelf Research, 14, 457-477.

Durrieu de Madron, X., Ferré, B., Le Corre, G., Grenz, C., Conan, P., Pujo-Pay, M., Buscail, R., Bodiot, O., 2005. Trawling-induced resuspension and dispersal of muddy sediments and dissolved elements in the Gulf of Lion (NW Mediterranean). Continental Shelf Research, 25, 2387-2409.

Durrieu de Madron, X., Wiberg, P.L. and Puig, P., 2008. Sediment dynamics in the Gulf of Lions: the impact of extreme events. Continental Shelf Research, 28, 1867-1876.

Eittreim, S., Gordon, A.L., Ewing, M.A.U.R.I.C.E., Thorndike, E.M. and Bruchhausen, P.E.T.E.R., 1972. The nepheloid layer and observed bottom currents in the Indian-Pacific Antarctic Sea. Studies in Physical Oceanography, 2, 19-35.

Eittreim, S., Thorndike, E.M. and Sullivan, L., 1976. Turbidity distribution in the Atlantic Ocean. Deep Sea Research and Oceanographic, 23, 1115-1127.

Epping, E., van der Zee, C., Soetaert, K. and Helder, W., 2002. On the oxidation and burial of organic carbon in sediments of the Iberian margin and Nazaré Canyon (NE Atlantic). Progress in Oceanography, 52, 399-431.

Ewing, M. and Thorndike, E.M., 1965. Suspended matter in deep ocean water. Science, 14, 1291-1294.

Ewing, M., Eittreim, S.L., Ewing, J.I. and Le Pichon, X., 1971. Sediment transport and distribution in the Argentine Basin. Nepheloid layer and processes of sedimentation. Physics and Chemistry of the Earth, 8, 49-77.

Feely, R.A., 1975. Major-element composition of the particulate matter in the near-bottom nepheloid layer of the Gulf of Mexico. Marine Chemistry, 3, 121-156.

Frederiksen, R., Jensen, A. and Westerberg, H., 1992. The distribution of the scleractinian coral Lophelia pertusa around the Faroe Islands and the relation to internal tidal mixing. Sarsia, 77, 157-171.

Gardner, W.D. and Sullivan, L.G., 1981. Benthic storms: temporal variability in a deep-ocean nepheloid layer. Science, 213, 329-331.

Gardner, W.D. and Walsh, I.D., 1990. Distribution of macroaggregates and fine-grained particles across a continental margin and their potential role in fluxes. Deep Sea Research Part A. Oceanographic Research Papers, 37, 401-411.

Gardner, W.D., 1989a. Baltimore Canyon as a modern conduit of sediment to the deep sea. Deep Sea Research Part A. Oceanographic Research Papers, 36, 323-35

Gardner, W.D., 1989b. Periodic resuspension in Baltimore Canyon by focusing of internal waves. Journal of Geophysical Research: Oceans, 94, 18185-18194.

Gardner, W.D., Biscaye, P.E., Zaneveld, J.R.V. and Richardson, M.J., 1985. Calibration and comparison of the LDGO nephelometer and the OSU transmissometer on the Nova Scotian Rise. Marine Geology, 66, 323-344.

Gardner, W.D., Richardson, M.J., Carlson, C.A., Hansell, D. and Mishonov, A.V., 2003. Determining true particulate organic carbon: bottles, pumps and methodologies. Deep Sea Research Part II: Topical Studies in Oceanography, 50, 655-674.

Gardner, W.D., Walsh, I.D. and Richardson, M.J., 1993. Biophysical forcing of particle production and distribution during a spring bloom in the North Atlantic. Deep Sea Research Part II: Topical Studies in Oceanography, 40, 171-195.

Gaudin, M., Berné, S., Jouanneau, J.M., Palanques, A., Puig, P., Mulder, T., Cirac, P., Rabineau, M. and Imbert, P., 2006. Massive sand beds attributed to deposition by dense water cascades in the Bourcart canyon head, Gulf of Lions (northwestern Mediterranean Sea). Marine Geology, 234, 111-128.

Gibbs, R.J., 1974. Principles of studying suspended materials in water. In Suspended Solids in Water. (Eds.) Gibbs, R.J., Springer, New York, USA (1974). pp. 3-15.

Gonzalez, E.A. and Hill, P.S., 1998. A method for estimating the flocculation time of monodispersed sediment suspensions. Deep-Sea Research Part I, 45, 1931-1954.

Gooday, A.J., Turley, C.M. and Allen, J.A., 1990. Responses by Benthic Organisms to Inputs of Organic Material to the Ocean Floor: A Review [and Discussion}. Philosophical Transactions of the Royal Society of London A: Mathematical, Physical and Engineering Sciences, 331, 119-138.

Graf, G. and Rosenberg, R., 1997. Bioresuspension and biodeposition: a review. Journal of Marine Systems, 11, 269-278.

Graf, G., 1989. Benthic-pelagic coupling in a deep-sea benthic community. Nature, 341, 437-439.

Guillén, J., Palanques, A., Puig, P., Durrieu de Madron, X. and Nyffeler, F., 2000. Field calibration of optical sensors for measuring suspended sediment concentration in the western Mediterranean. Scientia Marina, 64, 427-435.

Hall, I.R., Schmidt, S., McCave, I.N. and Reyss, J.L., 2000. Particulate matter distribution and disequilibrium along the Northern Iberian Margin: implications for particulate organic carbon export. Deep Sea Research Part I: Oceanographic Research Papers, 47, 557-582.

Hickey, B., Baker, E. and Kachel, N., 1986. Suspended particle movement in and around Quinault submarine canyon. Marine Geology, 71, 35-83.

Hickey, B.M., 1995. Coastal submarine canyons. Topographic effects in the ocean, In Proceedings of Hawaiian Winter Workshop, January 1995. pp.95-110.

Hill, P.S., Nowell, A.R.M. and McCave, I.N., 1990. The Potential Role of Large, Fast-Sinking Particles in Clearing Nepheloid Layers [and Discussion].Philosophical Transactions of the Royal Society of London A: Mathematical, Physical and Engineering Sciences, 331, 103-117.

Hill, P.S., Boss, E., Newgard, J.P., Law, B.A. and Milligan, T.G., 2011. Observations of the sensitivity of beam attenuation to particle size in a coastal bottom boundary layer. Journal of Geophysical Research: Oceans, 116, C02023, DOI:10.1029/2010JC006539.

Holdaway, G.P., Thorne, P.D., Flatt, D., Jones, S.E. and Prandle, D., 1999. Comparison between ADCP and transmissometer measurements of suspended sediment concentration. Continental shelf research, 19, 421-441.

Hollister, C.D. and McCave, I.N., 1984. Sedimentation under deep-sea storms. Nature, 309, 220-225.

Hotchkiss, F.S. and Wunsch, C., 1982. Internal waves in Hudson Canyon with possible geological implications. Deep Sea Research Part A. Oceanographic Research Papers, 29, 415-442.

Holt, J., Wakelin, S. and Huthnance, J., 2009. Down-welling circulation of the northwest European continental shelf: A driving mechanism for the continental shelf carbon pump. Geophysical Research Letters, 36, L14602, DOI:10.1029/2009GL038997.

Hunkin, K., Thorndike, E.M. and Mathieu, G., 1969. Nepheloid Layers and Bottom Currents in the Arctic Ocean. Journal of Geophysical Research, 74, 6695-7008.

Huthnance, J.M., 1981. Waves and currents near the continental shelf edge. Progress in Oceanography, 10, 193-226.

Huthnance, J.M., 1995. Circulation, exchange and water masses at the ocean margin: the role of physical processes at the shelf edge. Progress in Oceanography, 35, 353-431.

Huthnance, J.M., Coelho, H., Griffiths, C.R., Knight, P.J., Rees, A.P., Sinha, B., Vangriesheim, A., White, M. and Chatwin, P.G., 2001. Physical structures, advection and mixing in the region of Goban spur. Deep Sea Research Part II: Topical Studies in Oceanography, 48, 2979-3021.

Huvenne, V.A., Tyler, P.A., Masson, D.G., Fisher, E.H., Hauton, C., Hühnerbach, V., Le Bas, T.P. and Wolff, G.A., 2011. A picture on the wall: innovative mapping reveals cold-water coral refuge in submarine canyon. PLoS ONE, 6, e28755.

Inthorn, M. 2006 Lateral particle transport in nepheloid layers – a key factor for organic matter distribution and quality in the Benguela high-productivity area. Berichte, Fachbereich Geowissenschaften, Universität Bremen, No. 244, 124 pages, Bremen, 2006. ISSN 0931-0800.

Inthorn, M., Mohrholz, V. and Zabel, M., 2006. Nepheloid layer distribution in the Benguela upwelling area offshore Namibia. Deep Sea Research Part I: Oceanographic Research Papers, 53, 1423-1438.

Inthorn, M., Wagner, T., Scheeder, G. and Zabel, M., 2006. Lateral transport controls distribution, quality, and burial of organic matter along continental slopes in high-productivity areas. Geology, 34, 205-208.

Jerlov, N.G., 1959. Maxima in the vertical distribution of particles in the sea. Deep Sea Research (1953), 5, 173-184.

Jerlov, N.G., 1968. Optical oceanography, 5, Elsevier, pp.194

Johnson, M.P., White, M., Wilson, A., Würzberg, L., Schwabe, E., Folch, H. and Allcock, A.L., 2013. A vertical wall dominated by Acesta excavata and Neopycnodonte zibrowii, part of an undersampled group of deep-sea habitats. PLoS ONE, 8, e79917.

Joint, I.R., Owens, N.J.P. and Pomroy, A.J., 1986. Seasonal production of photosynthetic picoplankton and nanoplankton in the Celtic Sea. Marine Ecology Progress Series, 28, 251 -258.

Kalle, K., 1937. Nährstoff-Untersuchungen als hydrographisches Hilfsmittel zur Unterscheidung von Wasserkörpern. Annalen der Hydrographie und Maritimen Meteorologie, 65, 1-18.

Karageorgis, A.P., Georgopoulos, D., Kanellopoulos, T.D., Mikkelsen, O.A., Pagou, K., Kontoyiannis, H., Pavlidou, A. and Anagnostou, C., 2012. Spatial and seasonal variability of particulate matter optical and size properties in the Eastern Mediterranean Sea. Journal of Marine Systems, 105, 123-134.

Keil, R.G., Tsamakis, E., Fuh, C.B., Giddings, J.C., Hedges, J.I., 1994. Mineralogical and textural controls on the organic composition of coastal marine-sediments—hydrodynamic separation using splitt-fractionation. Geochimica Et Cosmochimica Acta, 58, 879–893.

Kemker, C. 2014 Measuring Turbidity, TSS, and Water Clarity. Fundamentals of Environmental Measurements. Fondriest Environmental, Inc. 5 Sep. 2014. http://www.fondriest.com/environmental-measurements/equipment/measuring-water-quality/turbidity-sensors-meters-and-methods/. (Accessed 20/05/2016).

Kennett, J.P., 1982. Marine Geology, Prentice-Hall, Englewood, pp. 813.

Kiriakoulakis, K., Bett, B.J., White, M. and Wolff, G.A., 2004. Organic biogeochemistry of the Darwin Mounds, a deep-water coral ecosystem, of the NE Atlantic. Deep Sea Research Part I: Oceanographic Research Papers, 51, 1937-1954.

Kiriakoulakis, K., Blackbird, S., Ingels, J., Vanreusel, A. and Wolff, G.A., 2011. Organic geochemistry of submarine canyons: the Portuguese Margin. Deep Sea Research Part II: Topical Studies in Oceanography, 58, 2477-2488.

Kiriakoulakis, K., Freiwald, A., Fisher, E. and Wolff, G.A., 2007. Organic matter quality and supply to deep-water coral/mound systems of the NW European Continental Margin. International Journal of Earth Sciences, 96, 159-170.

Koutsikopoulos, C. and Le Cann, B., 1996. Physical processes and hydrological structures related to the Bay of Biscay anchovy. Scientia Marina, 60, 9-19.

Lampitt, R.S., 1985. Evidence for the seasonal deposition of detritus to the deep-sea floor and its subsequent resuspension. Deep Sea Research Part A. Oceanographic Research Papers, 32, 885-897.

Lampitt, R.S., Raine, R.C.T., Billett, D.S.M. and Rice, A.L., 1995. Material supply to the European continental slope: A budget based on benthic oxygen demand and organic supply. Deep Sea Research Part I: Oceanographic Research Papers, 42, 1865-1880.

Legg, S., Ezer, T., Jackson, L., Briegleb, B.P., Danabasoglu, G., Large, W.G., Wu, W., Chang, Y., Ozgokmen, T.M., Peters, H. and Xu, X., 2009. Improving oceanic overflow representation in climate models: the gravity current entrainment climate process team. Bulletin of the American Meteorological Society, 90, 657-670, DOI:10.1175/2008BAMS2667.1

Liu, J.T., Wang, Y.H., Lee, I.H. and Hsu, R.T., 2010. Quantifying tidal signatures of the benthic nepheloid layer in Gaoping Submarine Canyon in Southern Taiwan. Marine Geology, 271, 119-130.

Lorenzoni, L., Thunell, R.C., Benitez-Nelson, C.R., Hollander, D., Martinez, N., Tappa, E., Varela, R., Astor, Y. and Muller-Karger, F.E., 2009. The importance of subsurface nepheloid layers in transport and delivery of sediments to the eastern Cariaco Basin, Venezuela. Deep Sea Research Part I: Oceanographic Research Papers, 56, 2249-2262.

Martín, J., Palanques, A. and Puig, P., 2006. Composition and variability of downward particulate matter fluxes in the Palamós submarine canyon (NW Mediterranean). Journal of Marine Systems, 60, 75-97.

Martín, J., Palanques, A., Vitorino, J., Oliveira, A. and de Stigter, H.C., 2011. Near-bottom particulate matter dynamics in the Nazaré submarine canyon under calm and stormy conditions. Deep Sea Research Part II: Topical Studies in Oceanography, 58, 2388-2400.

Martín, J., Puig, P., Palanques, A. and Ribó, M., 2014. Trawling-induced daily sediment resuspension in the flank of a Mediterranean submarine canyon. Deep Sea Research Part II: Topical Studies in Oceanography, 104, 174-183.

Masson, D.G., Huvenne, V.A.I., de Stigter, H.C., Arzola, R.G. and LeBas, T.P., 2011. Sedimentary processes in the middle Nazaré Canyon. Deep Sea Research Part II: Topical Studies in Oceanography, 58, 2369-2387.

McCave, I.N., 1984. Size spectra and aggregation of suspended particles in the deep ocean. Deep Sea Research Part A. Oceanographic Research Papers, 31, 329-352.

McCave, I.N., 1986. Local and global aspects of the bottom nepheloid layers in the world ocean. Netherlands Journal of Sea Research, 20, 167-181.

McCave, I.N. and Carter, L., 1997. Recent sedimentation beneath the deep Western Boundary Current off northern New Zealand. Deep Sea Research Part I: Oceanographic Research Papers, 44, 1203-1237.

McCave, I.N., Hall, I.R., Antia, A.N., Chou, L., Dehairs, F., Lampitt, R.S., Thomsen, L., van Weering, T.C.E. and Wollast, R., 2001. Distribution, composition and flux of particulate material over the European margin at 47–50 N. Deep Sea Research Part II: Topical Studies in Oceanography, 48, 3107-3139.

McCave, I.N. and Hall, I.R., 2002. Turbidity of waters over the Northwest Iberian continental margin. Progress in Oceanography, 52, 299-313.

McPhee-Shaw, E.E. and Kunze, E., 2002. Boundary layer intrusions from a sloping bottom: A mechanism for generating intermediate nepheloid layers. Journal of Geophysical Research: Oceans, 107, C6 3050, DOI: 10.1029/2001JC000801

McPhee-Shaw, E., 2006. Boundary–interior exchange: reviewing the idea that internal-wave mixing enhances lateral dispersal near continental margins. Deep Sea Research Part II: Topical Studies in Oceanography, 53, 42-59.

McPhee-Shaw, E.E., Sternberg, R.W., Mullenbach, B. and Ogston, A.S., 2004. Observations of intermediate nepheloid layers on the northern California continental margin. Continental Shelf Research, 24, 693-720.

Mienis, F., de Stigter, H.C., White, M., Duineveld, G., de Haas, H. and van Weering, T.C.E., 2007. Hydrodynamic controls on cold-water coral growth and carbonate-mound development at the SW and SE Rockall Trough Margin, NE Atlantic Ocean. Deep Sea Research Part I: Oceanographic Research Papers, 54, 1655-1674.

Mienis, F., de Stigter, H.C., de Haas, H. and van Weering, T.C.E., 2009. Near-bed particle deposition and resuspension in a cold-water coral mound area at the Southwest Rockall Trough margin, NE Atlantic. Deep Sea Research Part I: Oceanographic Research Papers, 56, 1026-1038

Milligan, T.G., Hill, P.S. and Law, B.A., 2007. Flocculation and the loss of sediment from the Po River plume. Continental Shelf Research, 27, 309-321.

Mudroch, A. and Mudroch, P., 1992. Geochemical composition of the nepheloid layer in Lake Ontario. Journal of Great Lakes Research, 18, 132-153.

Munk, W. and Wunsch, C., 1998. Abyssal recipes II: Energetics of tidal and wind mixing. Deep Sea Research Part I: Oceanographic Research Papers, 45, 1977-2010.

Nash, J.D., Kunze, E., Toole, J.M. and Schmitt, R.W., 2004. Internal tide reflection and turbulent mixing on the continental slope. Journal of Physical Oceanography, 34, 1117-1134.

Naudin, J.J. and Cauwet, G., 1997. Transfer mechanisms and biogeochemical implications in the bottom nepheloid layer. A case study of the coastal zone off the Rhone River (France). Deep Sea Research Part II: Topical Studies in Oceanography, 44, 551-575.

Oliveira, A., Rodrigues, A., Jouanneau, J.M., Weber, O., Alveirinho-Dias, J.M. and Vitorino, J., 1999. Suspended particulate matter distribution and composition on the northern Portuguese margin. Boletin Intituto Español de Oceanografia, 15, 101-110.

Oliveira, A., Vitorino, J., Rodrigues, A., Jouanneau, J.M., Dias, J.A. and Weber, O., 2002. Nepheloid layer dynamics in the northern Portuguese shelf. Progress in Oceanography, 52, 195-213.

Orr, M.H. and Hess, F.R., 1978. Remote acoustic monitoring of natural suspensate distributions, active suspensate resuspension, and slope/shelf water intrusions. Journal of Geophysical Research: Oceans, 83, 4062-4068.

Pak, H., Codispoti, L.A. and Zaneveld, J.R.V., 1980. On the intermediate particle maxima associated with oxygen-poor water off western South America. Deep Sea Research Part A. Oceanographic Research Papers, 27, 783-797.

Palanques, A. and Drake, D.E., 1990. Distribution and dispersal of suspended particulate matter on the Ebro continental shelf, northwestern Mediterranean Sea. Marine Geology, 95, 193-206.

Palanques, A., Guillén, J., Puig, P. and Durrieu de Madron, X., 2008. Storm-driven shelf-to-canyon suspended sediment transport at the southwestern Gulf of Lions. Continental Shelf Research, 28, 1947-1956.

Palanques, A., Puig, P., Durrieu de Madron, X., Sanchez-Vidal, A., Pasqual, C., Martín, J., Calafat, A., Heussner, S. and Canals, M., 2012. Sediment transport to the deep canyons and open-slope of the western Gulf of Lions during the 2006 intense cascading and open-sea convection period. Progress in Oceanography, 106, 1-15.

Pingree, R.D. and Le Cann, B., 1989. Celtic and Armorican slope and shelf residual currents. Progress in Oceanography, 23, 303-338.

Pingree, R.D. and Le Cann, B., 1990. Structure, strength and seasonality of the slope currents in the Bay of Biscay region. Journal of the Marine Biological Association of the United Kingdom, 70, 857-885.

Pingree, R.D., Mardell, G.T., Holligan, P.M., Griffiths, D.K. and Smithers, J., 1982. Celtic Sea and Armorican current structure and the vertical distributions of temperature and chlorophyll. Continental Shelf Research, 1, 99-116.

Pingree, R.D., Sinha, B. and Griffiths, C.R., 1999. Seasonality of the European slope current (Goban Spur) and ocean margin exchange. Continental Shelf Research, 19, 929-975.

Pollard, R.T., Griffttths, M.J., Cunningham, S.A., Read, J.F., Pérez, F.F. and Ríos, A.F., 1996. Vivaldi 1991-A study of the formation, circulation and ventilation of Eastern North Atlantic Central Water. Progress in Oceanography, 37, 167-192.

Pomar, L., Morsilli, M., Hallock, P. and Bádenas, B., 2012. Internal waves, an under-explored source of turbulence events in the sedimentary record. Earth-Science Reviews, 111, 56-81.

Puig, P. and Palanques, A., 1998a. Nepheloid structure and hydrographic control on the Barcelona continental margin, northwestern Mediterranean. Marine Geology, 149, 39-54.

Puig, P. and Palanques, A., 1998b. Temporal variability and composition of settling particle fluxes on the Barcelona continental margin (Northwestern Mediterranean). Journal of Marine Research, 56, 639-654.

Puig, P., Palanques, A., Sanchez-Cabeza, J.A. and Masqué, P., 1999. Heavy metals in particulate matter and sediments in the southern Barcelona sedimentation system (North-western Mediterranean). Marine Chemistry, 63, 311-329.

Puig, P., Palanques, A. and Guillén, J., 2001a. Near-bottom suspended sediment variability caused by storms and near-inertial internal waves on the Ebro mid continental shelf (NW Mediterranean). Marine Geology, 178, 81-93.

Puig, P., Company, J.B., Sardà, F. and Palanques, A., 2001b. Responses of deep-water shrimp populations to intermediate nepheloid layer detachments on the Northwestern Mediterranean continental margin. Deep Sea Research Part I: Oceanographic Research Papers, 48, 2195-2207.

Puig, P., Ogston, A.S., Mullenbach, B.L., Nittrouer, C.A., Parsons, J.D. and Sternberg, R.W., 2004a. Storm-induced sediment gravity flows at the head of the Eel submarine canyon, northern California margin. Journal of Geophysical Research: Oceans, 109, C03019, DOI: 10.1029/2003JC001918.

Puig, P., Palanques, A., Guillén, J. and El Khatab, M., 2004b. Role of internal waves in the generation of nepheloid layers on the northwestern Alboran slope: implications for continental margin shaping. Journal of Geophysical Research: Oceans, 109, C09011 DOI: 10.1029/2004JC002394.

Puig, P., Palanques, A., Orange, D.L., Lastras, G. and Canals, M., 2008. Dense shelf water cascades and sedimentary furrow formation in the Cap de Creus Canyon, northwestern Mediterranean Sea. Continental Shelf Research, 28, 2017-2030.

Puig, P., Durrieu de Madron, X., Salat, J., Schroeder, K., Martín, J., Karageorgis, A.P., Palanques, A., Roullier, F., Lopez-Jurado, J.L., Emelianov, M. and Moutin, T., 2013a. Thick bottom nepheloid layers in the western Mediterranean generated by deep dense shelf water cascading. Progress in Oceanography, 111, 1-23.

Puig, P., Greenan, B.J., Li, M.Z., Prescott, R.H. and Piper, D.J., 2013b. Sediment transport processes at the head of Halibut Canyon, eastern Canada margin: An interplay between internal tides and dense shelf-water cascading. Marine Geology, 341, 14-28.

Puig, P., Palanques, A. and Martín, J., 2014. Contemporary sediment-transport processes in submarine canyons. Annual review of marine science, 6, 53-77.

Pusceddu, A., Mea, M., Gambi, C., Bianchelli, S., Canals, M., Sanchez-Vidal, A., Calafat, A., Heussner, S., Durrieu de Madron, X., Avril, J. and Thomsen, L., 2010. Ecosystem effects of dense water formation on deep Mediterranean Sea ecosystems: an overview. Advances in Oceanography and Limnology, 1, 67-83.

Qaker, J.E., Eisenreich, S.J., Johnson, T.C. and Halfman, B.M., 1985. Chlorinated hydrocarbon cycling in the benthic nepheloid layer of Lake Superior. Environmental science & technology, 19, 854-861.

Ransom, B., Shea, K.F., Burkett, P.J., Bennett, R.H. and Baerwald, R., 1998. Comparison of pelagic and nepheloid layer marine snow: implications for carbon cycling. Marine Geology, 150, 39-50.

Ransom, B.B.R.H., Bennett, R.H., Baerwald, R. and Shea, K., 1997. TEM study of in situ organic matter on continental margins: occurrence and the “monolayer” hypothesis. Marine Geology, 138, 1-9.

Rebesco, M., Hernández-Molina, F.J., Van Rooij, D. and Wåhlin, A., 2014. Contourites and associated sediments controlled by deep-water circulation processes: state-of-the-art and future considerations. Marine Geology, 352, 111-154.

Rees, A.P., Joint, I. and Donald, K.M., 1999. Early spring bloom phytoplankton-nutrient dynamics at the Celtic Sea Shelf Edge. Deep Sea Research Part I: Oceanographic Research Papers, 46, 483-510.

Rhines, P.B., 1970. Edge-, bottom- and Rossby waves. Geophysical Fluid Dynamics, 1, 273–302.

Ribó, M., Puig, P., Salat, J. and Palanques, A., 2013. Nepheloid layer distribution in the Gulf of Valencia, northwestern Mediterranean. Journal of Marine Systems, 111, 130-138.

Richardson, M.J., Weatherly, G.L. and Gardner, W.D., 1993. Benthic storms in the Argentine Basin. Deep Sea Research Part II: Topical Studies in Oceanography, 40, 975-987.

Ritzrau, W., 1996. Microbial activity in the benthic boundary layer: small-scale distribution and its relationship to the hydrodynamic regime. Journal of Sea Research, 36, 171-180.

Ruch, P., Mirmand, M., Jouanneau, J.M. and Latouche, C., 1993. Sediment budget and transfer of suspended sediment from the Gironde estuary to Cap Ferret Canyon. Marine Geology, 111, 109-119.

Sanchez-Vidal, A., Canals, M., Calafat, A.M., Lastras, G., Pedrosa-Pàmies, R., Menéndez, M., Medina, R., Hereu, B., Romero, J. and Alcoverro, T., 2012. Impacts on the deep-sea ecosystem by a severe coastal storm. PLoS ONE, 7, e30395.

Sandilands, R.G. and Mudroch, A., 1983. Nepheloid layer in lake Ontario. Journal of Great Lakes Research, 9, 190-200.

Shanmugam, G., 2006. Deep-Water Processes and Facies Models: Implications for Sandstone Petroleum Reservoirs: Implications for Sandstone Petroleum Reservoirs (Vol. 5). Elsevier. ISBN: 1567-8032.

Shapiro, G.I., Huthnance, J.M. and Ivanov, V.V., 2003. Dense water cascading off the continental shelf. Journal of Geophysical Research: Oceans, 108, C12, 3390, DOI: 10.1029/2002JC001610

Sharples, J., Tweddle, J.F., Mattias Green, J.A., Palmer, M.R., Kim, Y.N., Hickman, A.E., Holligan, P.M., Moore, C., Rippeth, T.P., Simpson, J.H. and Krivtsov, V., 2007. Spring-neap modulation of internal tide mixing and vertical nitrate fluxes at a shelf edge in summer. Limnology and Oceanography, 52, 1735-1747.

Sharples, J., Tweddle, J.F., Mattias Green, J.A., Palmer, M.R., Kim, Y.N., Hickman, A.E., Holligan, P.M., Moore, C., Rippeth, T.P., Simpson, J.H. and Krivtsov, V., 2007. Spring-neap modulation of internal tide mixing and vertical nitrate fluxes at a shelf edge in summer. Limnology and Oceanography, 52, 1735-1747.

Shatova, O. 2008. Understanding Intermediate Nepheloid Layers: A Multi-platform Approach. DOI: 10.1.1.502.7280

Shepard, F.P., 1976. Tidal components of currents in submarine canyons. The Journal of Geology, 84, 343-350.

Shepard, F.P., Marshall, N.F. and McLoughlin, P.A., 1974. Currents in submarine canyons. Deep sea research and Oceanographic Abstracts, 21, 691-706.

Spinrad, R.W., Glover, H., Ward, B.B., Codispoti, L.A. and Kullenberg, G., 1989. Suspended particle and bacterial maxima in Peruvian coastal waters during a cold water anomaly. Deep Sea Research Part A. Oceanographic Research Papers, 36, 715-733.

Thomsen, L. and Graf, G., 1994. Boundary-layer characteristics of the continental-margin of the Western Barents Sea. Oceanologica Acta, 17, 597-607.

Thomsen, L. and Gust, G., 2000. Sediment erosion thresholds and characteristics of resuspended aggregates on the western European continental margin. Deep Sea Research Part I: Oceanographic Research Papers, 47, 1881-1897.

Thomsen, L. and van Weering, T.C., 1998. Spatial and temporal variability of particulate matter in the benthic boundary layer at the NW European Continental Margin (Goban Spur). Progress in Oceanography, 42, 61-76.

Thomsen, L., 2003. The Benthic Boundary Layer. In Ocean Margin Systems (Eds) Wefer, G., Billet, D., Hebbeln, D., Jorgensen, B.B., Schlüter, M., Weering, T.C.E.V., Springer, Berlin (2003), pp. 143-155.

Thomsen, L., Graf, G., Martens, V. and Steen, E., 1994. An instrument for sampling water from the benthic boundary layer. Continental Shelf Research, 14, 871-882.

Thorndike, E.M., 1975. A deep sea, photographic nephelometer. Ocean Engineering, 3, 1-15.

Thorpe, S.A., 1987. On the reflection of a train of finite-amplitude internal waves from a uniform slope (with appendix by S.A. Thorpe and A.P. Haines). Journal of Fluid Mechanics, 178, 279–302.

Thorpe, S.A. and White, M., 1988. A deep intermediate nepheloid layer.Deep Sea Research Part A. Oceanographic Research Papers, 35, 1665-1671.

Thorpe, S.A., 2005. The turbulent ocean. Cambridge University Press. (2005).ISBN-100-521-83543-7

Turner, J.T., 2002. Zooplankton fecal pellets, marine snow and sinking phytoplankton blooms. Aquatic Microbial Ecology, 27, 57-102.

Tyler, P.A., 1988. Seasonality in the deep sea. Oceanography and Marine Biology, An Annual Review, 26, 227-258.

Van Aken, H.M., 2000. The hydrography of the mid-latitude northeast Atlantic Ocean: I: The deep water masses. Deep Sea Research Part I: Oceanographic Research Papers, 47, 757-788.

Van Weering, T.C.E., Thomsen, L., Heerwaarden, J., Koster, B. and Viergutz, T., 2000. A seabed lander and new techniques for long term in situ study of deep-sea near bed dynamics. Sea Technology, 41, 17-27.

Van Weering, T.C., de Stigter, H.C., Balzer, W., Epping, E.H., Graf, G., Hall, I.R., Helder, W., Khripounoff, A., Lohse, L., McCave, I.N. and Thomsen, L., 2001. Benthic dynamics and carbon fluxes on the NW European continental margin. Deep Sea Research Part II: Topical Studies in Oceanography, 48, 3191-3221.

Vangriesheim, A., 1988. Deep layer variability in the Eastern North Atlantic: the EDYLOC experiment. Oceanologica acta, 11, 149-158.

Von Lom-Keil, H., Spieß, V. and Hopfauf, V., 2002. Fine-grained sediment waves on the western flank of the Zapiola Drift, Argentine Basin: evidence for variations in Late Quaternary bottom flow activity. Marine Geology, 192, 239-258.

Wells, L.E. and Deming, J.W., 2003. Abundance of Bacteria, the Cytophaga-Flavobacterium cluster and Archaea in cold oligotrophic waters and nepheloid layers of the Northwest Passage, Canadian Archipelago. Aquatic Microbial Ecology, 31, 19-31.

WET Labs, 2008. Sea-Bird Electronics Inc., WET Labs C-star Transmissometer manual.

WET Labs, 2011. Sea-Bird Electronics Inc., Transmissometer C-Star User's Guide Revision V Dec. 2011.

White, M. and Bowyer, P., 1997. The shelf-edge current north-west of Ireland. Annales Geophysicae, 15, 1076-1083

White, M., and Dorschel, B., 2010. The importance of the permanent thermocline to the cold water coral carbonate mound distribution in the NE Atlantic. Earth and Planetary Science Letters, 296, 395-402.

White, M.G., 1990. The temperature and current structure on the sloping benthic boundary layer (Doctoral dissertation, University of Southampton).

Wolanski, E., Marshall, K. and Spagnol, S., 2003. Nepheloid layer dynamics in coastal waters of the Great Barrier Reef, Australia. Journal of Coastal Research,19, 748-752.

Wollast, R. and Chou, L., 2001. The carbon cycle at the ocean margin in the northern Gulf of Biscay. Deep Sea Research Part II: Topical Studies in Oceanography, 48,3265-3293.

Wollast, R., 1998. Evaluation and comparison of the global carbon cycle in the coastal zone and in the open ocean. In -The Sea, Chapter 9, (Eds) Brink, K.H. and Robinson, A.R., University of Brussels (1998), pp.213-252.

Woodward, E.M.S. and Rees, A.P., 2001. Nutrient distributions in an anticyclonic eddy in the northeast Atlantic Ocean, with reference to nanomolar ammonium concentrations. Deep Sea Research Part II: Topical Studies in Oceanography, 48, 775-793.

Wright, S.G. and Rathje, E.M., 2003. Triggering mechanisms of slope instability and their relationship to earthquakes and tsunamis. Pure and Applied Geophysics, 160, 1865-1877.

Wunsch, C., 1969. Progressive internal waves on slopes. Journal of Fluid Mechanics, 35, 131-144.

Xu, W., Miller, P.I., Quartly, G.D. and Pingree, R.D., 2015. Seasonality and interannual variability of the European Slope Current from 20years of altimeter data compared with in situ measurements. Remote Sensing of Environment, 162, 96-207.

Yanagi, T., Takahashi, S., Hoshika, A. and Tanimoto, T., 1996. Seasonal variation in the transport of suspended matter in the East China Sea. Journal of Oceanography, 52, 539-552.

Chapter 3
Methods

3.1 Survey details

The data and samples presented in this thesis were collected during three research surveys to the Whittard Canyon by NUI Galway under the Sea Change strategy with the support of the Marine Institute and the Marine Research Sub-Programme of the National Development Plan 2007–2013. All three surveys were carried out on the *RV Celtic Explorer* and the survey details are given in Table 3.1 (see supplementary information also S3.7-3.9). The station positions for each of the surveys are shown in Fig. 3.1–3.3 (note only stations related to research discussed in this thesis are shown). All three surveys were explorative, under the heading of bio-discovery and deep-sea and canyon ecosystem functioning. The research presented in this thesis contributed to the oceanographic (bio-geo-chemical) component of these surveys under the umbrella of ecosystem functioning.

Table 3.1 Details of the surveys described in this thesis.

Cruise code	Date	Cruise title
CE11006	22/04/2011–29/04/2011	Biodiscovery and deep-ocean ecosystems
CE12006	12/04/2012–29/04/2012	Biodiscovery and deep-ocean ecosystems
CE13006	30/05/2013–21/06/2013	Biodiscovery and ecosystem function of canyons

CE11006

Survey CE11006 was the first of three studies under the title "Biodiscovery and ecosystem function" carried out in April 2011. The multidisciplinary research conducted combined components of zoology, biochemistry and oceanography, with the aim of furthering the understanding of ecosystem functioning and with the aspiration of discovering novel compounds from the deep-sea with medical and pharmaceutical use.

In terms of the research for this thesis, the primary objectives of this survey were: (i) to examine the mechanisms whereby biogenic material, essentially derived from the spring diatom bloom and deposited on the continental shelf, is advected into layers in the water column from whence it sinks to the sea bed; (ii) delineate the advective extent of these nepheloid layers of biogenic material derived from the continental shelf.

Although the weather was calm and permitted the successful deployment of all gear, survey CE11006 was cut short due to an engine malfunction. 19

stations were sampled including eight CTD casts that formed one transect of a western branch (WC2 in Fig. 3.1) and Table 3.1.

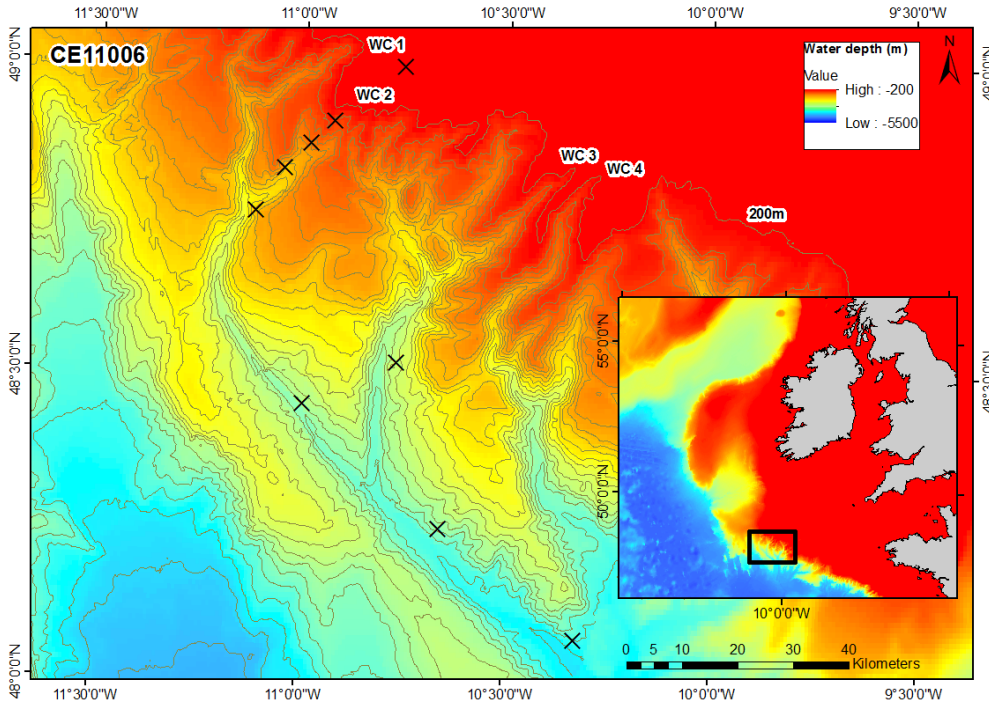

Fig. 3.1. CE11006 station positions.

CE12006

Survey CE12006 was a continuation of the postponed CE11006 survey. Aims and objectives from all disciplines were similar to those of the year previous, with an additional objective for this study to; (iii) Characterise and determine the origins, lability and recycling of organic matter supporting the heterotrophic nature of deep sea communities.

Severe weather conditions for the duration of the survey limited the deployment of the ROV required for the zoological and biodiscovery component of the survey and therefore ship-time was handed over to the deployment of more robust instruments. From an oceanographic point of view survey CE12006 was very successful with data from 65 CTD casts collected along two branches of the canyon (western branch, WC2 and eastern branch, WC3; Fig. 3.2). Measurements of the water column were made both before and after two significant storms. Problems with the battery charger of a Stand Alone Pump System (on-loan from University of Liverpool) did not permit material in nepheloid layers to be sampled. However, a makeshift system was put in place and large

quantities of water collected from the rosette was filtered through the head of the Stand Alone Pump System. These samples are not dealt with in this thesis.

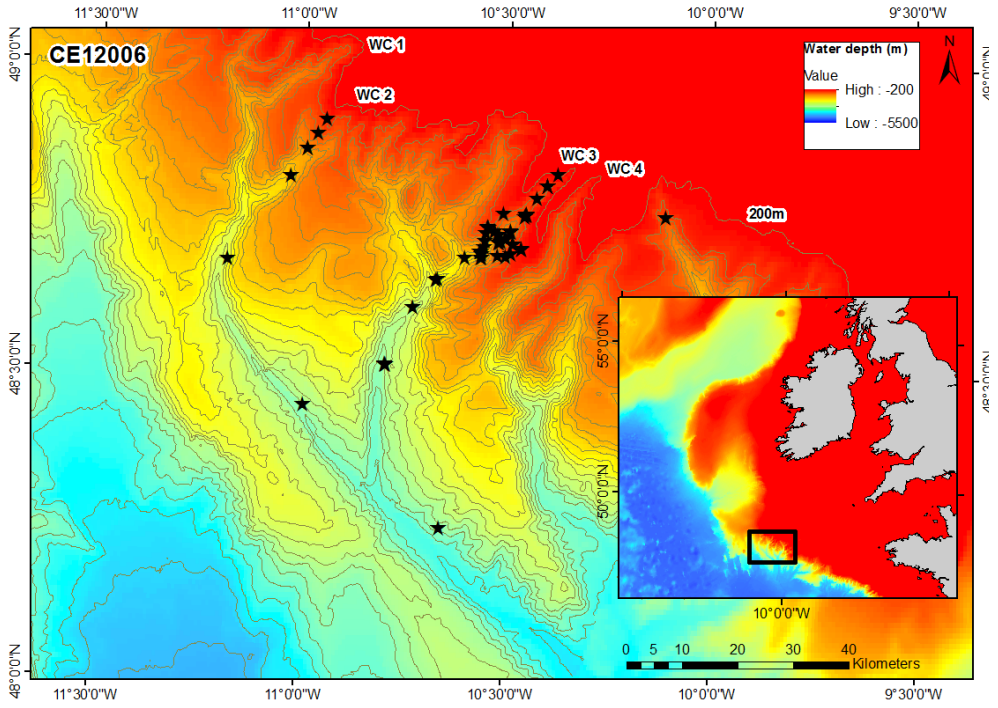

Fig. 3.2. CE12006 station positions.

CE13006

Survey CE13008 was a further continuation of CE12006, with particular emphasis on the canyon communities. A site on the Northern Porcupine Bank was also surveyed but will not be dealt with herein.

The (survey) objectives for this PhD study remained the same with a particular prominence given to objectives (iii) investigating the content and origin of nepheloid layers by filtering the particulate matter within them and (iv) obtaining greater temporal cover of hydrographic data through the deployment of a lander.

The weather for the duration of the cruise was calm and allowed for operations to proceed as planned including 40 CTD casts along four branches of the canyon (WC1–WC4; Fig. 3.3). The battery and charger of the Stand Alone pump System operated without fail and allowed for 23 successful deployments (14 in Whittard Canyon). Unfortunately due to problems with the acoustic releases and deck unit the lander could not be deployed. With no other opportunities to redeploy the lander, this component of the study was abandoned.

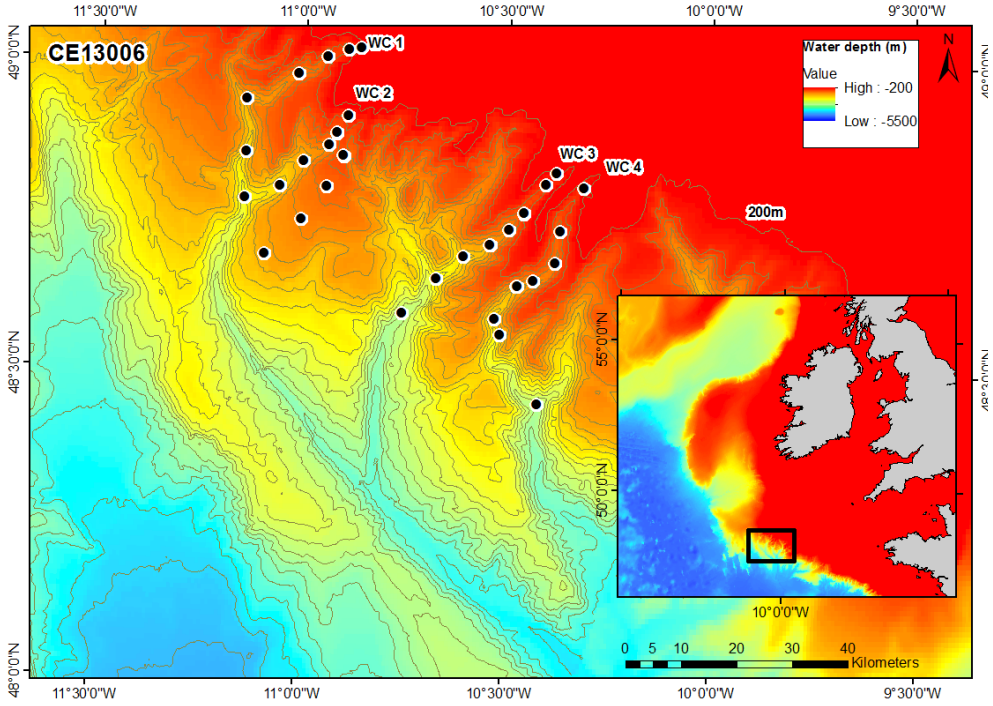

Fig. 3.3. CE13008 station positions.

3.2 Sample and data collection

A summary of the data collected and samples taken during each survey are detailed in Table 3.2. CTD transects were made along and across the canyon branches WC1–4 (Table 3.2), as shown in Fig. 3.1–3.3. Station details for each individual station can be found in the supplementary information (S3.7-3.9). Repeat vertical profiles were made at selected stations. Hydrographic observations; temperature, salinity, pressure, density and transmission were carried out using a Seabird SBE911 CTD and SBE32 Rosette system. Fluorescence and oxygen measurements were carried out intermittently but are not dealt with here. Turbidity measurements were made by a 0.25 m path-length transmissometer (C-star, WET Labs) operating at 650 nm. Before deployment, the transmissometer pathway was cleaned with distilled water and lint free wipes. On recovery, the conductivity cell was flushed with distilled water using a plastic syringe, which remained attached to the conductivity cell with tubing until the next deployment.

Water samples for calibration and biogeochemical analysis were collected in 10 L Niskin bottles mounted on the CTD rosette frame. All equipment used for collecting and measuring water was acid-washed (10% HCl) before the survey and rinsed with deionised water and sample water before the sample was taken.

Bottles were remotely triggered and closed at chosen depths. Samples were collected from near surface (0–20 m), at intermediate depths within intermediate nepheloid layers and at the bottom within the bottom nepheloid layer. Mid-water depths were chosen usually at turbidity maxima, at the top and bottom boundaries of Mediterranean Outflow Water and based on the water structure of CTD profiles. Samples in the clear water turbidity minima were also collected for calibration purposes. Samples were collected in the following order to avoid contamination/degradation (every effort was made to do this); pigment, molecular and elemental samples, followed by SPM and salinity samples. Gear choice and sample parameters were dependant on the features observed in the individual CTD profiles, availability and time between stations. A Stand Alone Pumps System (SAPS; Challenger Oceanic) was used to filter large volumes of water for suspended particle analysis. Where the SAPS was not available due to battery charging or samples from numerous depths were desired, an alternative small scale method termed mini SAPS was used (see below).

Table 3.2. Summary of data and samples collected at Whittard Canyon during three research surveys presented in this thesis (see supplementary data for additional details and survey station logs).

Survey	**Data**						**Samples collected**				
	# CTD casts	Transects covered				ADCP	SPM	Sal	SAPS	Mini SAPS	Chl-a Phaeo
		WC1	WC2	WC3	WC4						
CE11006	9		✓			NA	2	NA	NA	NA	NA
CE12006	65		✓	✓		Hull	20	✓	*14	NA	NA
CE13008	40	✓	✓	✓	✓	NA	15	✓	14	36	49

*Due to malfunction of the SAPS during C12006, water from the CTD rosette was filtered manually through the SAPS. These samples are not dealt with in this thesis.

3.2.1 Suspended particulate matter (SPM) samples

Samples of SPM for calibration of the transmissometer were collected during the three surveys accordingly to the methods of McCave et al. (2001). Sea-water was collected in jerry cans from the CTD rosette. Collection vessels were inverted before filtering a sub-sample of the contents. Volumes were measured using plastic volumetric cylinders and 1.7–10 L of water was filtered through, 47 mm, 0.4 μm pore size pre weighted Nuclepore filters. Filters were rinsed well with deionised water and very gently dried with the vacuum of the pump (ensuring no

rips or tears) before storing in labelled petri dishes. Samples were stored in the dark at ~4 °C for the duration of the survey and transferred to desiccators on return to the laboratory.

3.2.2 Salinity

Salinity samples were collected in clear glass salinity bottles with plastic inserts and screw caps. The bottles were first rinsed three times with the sample water before filling up to the shoulder of the bottle. The top of the bottle was dried with Kim wipes, to prevent salt crystals forming on the top of the bottle, before inserting a plastic insert to make a tight seal and prevent evaporation. The bottles were closed with a screw cap and stored upright at room temperature until analysis.

3.2.3 SAPS

SAPS was deployed on a wire winch or attached to the CTD rosette. 163–1443 L of water was mechanically filtered through two stacked pre-combusted (400 °C; >6 hrs) glass fibre GF/F filters (293 mm diameter), (Kiriakoulakis et al., 2011). SAPS operated for 1–2 h depending on depth and particle loading as estimated by the turbidity sensors of the CTD. Depth from the seabed was determined by an altimeter on the CTD. Delay times were programmed to ensure that the SAPS started pumping when it had reached the seabed. On recovery the filters were folded into quarters and wrapped in pre-combusted foil and stored at -80 °C for the duration of the cruise. Filters were freeze-dried and subsequently stored at -20 °C until analysis.

3.2.4 Mini SAPS

The small scale alternative method to the SAPS for molecular and elemental analysis consisted of two stacked 47 mm glass fibre GF/F filters, pre-combusted (400 °C; >6 hrs) and stored wrapped in (combusted) foil. Sea-water was collected from the CTD rosette in jerry cans and sub-samples taken. Volumes were carefully measured using plastic measuring cylinders before being filtered (5–10 L) in glass filtration units. Filters were folded in half onto themselves and re-wrapped in the foil. Samples were treated and stored as per the SAPS filters detailed above.

3.2.3 Pigments

Samples for pigment analysis were collected from various water depths on separate 47 mm GF/F (0.7 μm nominal pore size) filters. Volume filtered (1.6–6 L) was measured carefully and was dependent on particle loading with smaller volumes required from surface samples. Filters were folded onto themselves and into quarters before storing in plastic 15 ml centrifuge tubes at -80 °C or -20 °C (depending on what was available) until laboratory analysis.

3.3 Hydrographic data

3.3.1 CTD data processing

Post processing of CTD data from all three surveys was carried out following the methods of Dr. Jenny Ullgren (see White et al., 2008). CTD data was processed using Seabird software, SBE data processing. Firstly, data was converted to engineering units using the data conversion function. The data was then filtered using a low pass filter (0.75 s) to eliminate any high frequency fluctuations. Secondary variables i.e. salinity, density, σ_θ and potential temperature were then derived from the primary variables (conductivity, temperature, pressure). The derive function was run after the first filter to ensure more consistent salinity values. A loop edit was applied to remove effects of the CTD moving up and down the water column with the pitch, roll and heave of the ship. Any negative pressure changes on the downcast or positive pressure changes on the upcast were flagged as 'bad' here and were excluded. Data recorded when the CTD was slowing down to less than 0.5 m s^{-1} was removed. Surface soak and any other looping in the pressure signal was discarded. A second low pass filter (0.75 s) was applied to clean up the derived data. Finally, data was binned to averages of 1 m depth intervals. The sensor package is on the bottom of the CTD rosette and therefore the downcast data were converted to .txt to be analysed using MATLAB R2011a.

3.3.2 Salinity calibrations

Temperature, conductivity and pressure sensors on the SBE 911 CTD (system 1) on-board the *RV Celtic Explorer* are regularly calibrated by the manufacturer. The calibration dates for the primary sensors with regard to each of the cruises are shown in Table 3.3.

Table 3.3. List of calibration dates for sensors used during the three surveys.

Sensor	CE11006	CE12006	CE13009
Temperature & conductivity	18/05/2010	15/09/2011	29/09/2012
Pressure	11/09/2008	19/09/2008	19/09/2008

The initial accuracy of the conductivity sensor is +/- 0.0003 S/m per month and the typical stability for conductivity sensor is 0.0003 S/m per month (WET Labs, 2014).

Discrete water samples for salinity calibration were collected during the 2012 and 2013 surveys. Salinity samples collected during survey CE12006 were analysed at NUI Galway but unfortunately due to malfunction of the Autosal salinometer the data was void. Salinity samples from survey CE13008 were analysed on a Portasal Salinometer (Ocean Scientifiic International Ltd, (OSIL)) at the Marine Institute, Rinville, Oranmore. To measure the conductivity of a sample, four electrode conductivity cells are suspended in a temperature-controlled bath. According to standard operating procedure; samples are allowed to reach room temperature before being read. Samples are inverted, and the head of the bottle wiped before inserting into the Portasal. The four conductivity cells were allowed to fill and were flushed three times before taking a reading. Two consecutive conductivity readings within 0.00002 units of each other weretaken before the salinity can be recorded. The temperature of the salinometer water bath is set and stabilized to ~1–2 °C above the ambient room temperature (19.6 – 21.2 °C during analysis carried out (20/11/13)). The instrument must be flushed with distilled water before and after use. The conductivity is related to salinity by calibration with a known standard (IAPSO seawater standard, OSIL). At the beginning of each batch of samples, a high and low standard, an IAPSO standard Sal ~10 and Sal ~38 and DI water (Sal ~0) must be tested and a |z| score <2 must be obtained. Unfortunately IAPSO high and low standards were not available during the run and therefore an error cannot be calculated. The data from the CE13008 was used to perform a linear regression in order to assess the reliability of the data (Fig. 3.4). A strong relationship was found with R^2 = 0.723. Unfortunately triplicate samples were not available to carry out further statistical analysis. Due to the issues encountered with the salinity samples and the accuracy

and frequent calibrations of the sensors, in addition to the good match here, it was found to be acceptable to use the CTD data without a correction as it was likely more reliable.

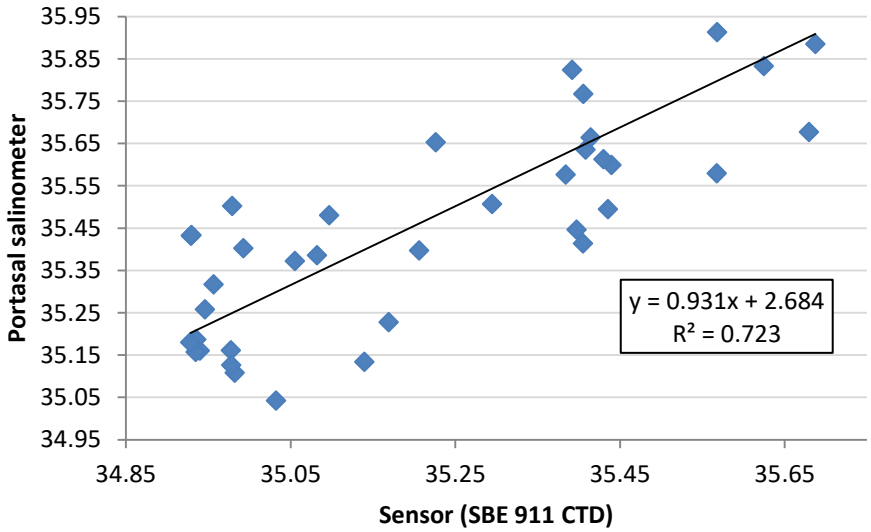

Figure 3.4. Linear regression of salinity data collected during CE13008. Salinity values from discrete seawater samples measured using Portasal salinometer and values from conductivity sensor on SBE 911 CTD.

3.3.3 Transmissometer calibration

Filters for measurement of SPM were dried by desiccation and weighed gravimetrically using a 10^{-6} g balance with static reduction, following the methods of McCave et al. (2000). Filters were weighted until three consecutive readings with four decimal places identical were obtained (Table 3.4). Calibration of the WET Labs C-star transmissometer was then carried out according to the manufacturer's instructions (WET Labs, 2008; 2011; 2014) and raw voltage values were related to the concentration of suspended particles express in µg L^{-1}, following the methods of Gardner et al. (1985); Bishop, (1986); McCave et al. (2001). Parameters used in the calculations are listed in Table 3.4. Raw transmissometer values were converted to beam attenuation (c) by;

$$c = -(1/\mathrm{x}) * \mathrm{LN}\,(\mathrm{Tr(dec)}) \qquad (3.1)$$

where x is the path length (0.25 m) of the transmissometer and Tr is the transmittance output of light at 660 nm from the instrument expressed in decimal. The percentage light transmission $(\%)$ is expressed as;

$$\mathbf{Tr}\ (\%)\ =\ ((\mathrm{M} * (\text{Raw voltage signal})\ +\ (\mathrm{B})) \tag{3.2}$$

where, M and B are calibration coefficients WET Labs, 2008; 2011; 2014). Here, M = 19.253 and B = -1.08144, were calculated using the following equations;

$$\mathrm{M}\ =\ (\mathbf{Tr}\ (\%)/[\mathbf{V_{W0}} - \mathbf{V_{D0}}])\ *\ (\mathbf{V_{A0}} - \mathbf{V_{D0}})/(\mathbf{V_{A1}} - \mathbf{V_{D1}}) \tag{3.3}$$

$$\mathrm{B}\ =\ -\mathrm{M} * (\mathbf{V_{D1}}) \tag{3.4}$$

$\mathbf{V_{A1}}$ and $\mathbf{V_{D1}}$ all values recorded during CE13008 were averaged and used to calculate the beam attenuation values for all three cruises.

Beam attenuation values (c) were correlated by linear regression with the mass of SPM obtained from 37 filtered water samples collected during the three surveys. The relationship;

$$SPM = 0.00048 * BAC + 0.3893 \tag{3.5}$$

was found with a strong correlation of $R^2 = 0.8306$ (see Fig. 4.2, Chapter 4; Wilson et al., 2015). BAC values were converted to the concentration of SPM µg L^{-1} for all three surveys (Table 3.5) following the calculation shown below.

Table 3.4 List of parameters used to calculate percentage transmission (see WET Labs, 2008; 2011; 2014).

Parameter	Desciption	Value
**Tr (%)	% transmission in pure water	100
V_{W0}	Voltage Pure water(factory output):factory calibration of voltage of pure water	5.25
V_{D0}	Voltage Dark value (factory output): factory calibration from manufacturer, dark values when light path is blocked	0.056
*V_{A0}	Voltage Air (factory output): factory calibration of voltage in air	4.743
*V_{A1}	Voltage Air (in field): voltage output in air in the field	4.7377
V_{D1}	Voltage output when path is blocked in field	0.0562

*The voltage air is used as a reference to track instrument drift over time.

**Tr (%) the transmission of pure water is taken here as 100% (for transmission relative to water). As of 2004, Sea-bird has calculated M and B relative to water and indicated these values on their calibration sheets. Tw relative to air are subject to change therefore it is the preference of optical oceanographers to report the transmissometer measurements relative to water rather than air. At 660 nm using a 25 cm path length transmissometer, % transmission in pure water relative to air is 90.2–91.3% (Pope and Fry 1997; Smith and Baker, 1998), However these values are subject to change.

Calculations:

$$Y = 0.0005x + 0.3893$$

$$BAC = 0.00048\,(SPM) + 0.3893$$

$$0.00048\,(SPM) = BAC - 0.3893$$

$$SPM = \left[BAC - \left(\frac{0.3893}{0.0005}\right)\right]$$

$$SPM = \left(\frac{1}{0.0005}\right)c - \left(\frac{0.3893}{0.0005}\right)$$

$$SPM = 2000c - 778.6$$

Table 3.5. Mass of SPM obtained from SPM samples obtained from filtered water samples for calibration curve

	Event	CTD	S. Depth (m)	Vol. (L)	Ave. (g)	SPM (µg L^{-1})	Raw Volts	Tr (%)	Tr (dec)	BAC (c)
CE13008	41	22	7	1.7	0.00078	458.82	4.31	81.92	0.82	0.797672
	44	24	674	8	0.00201	250.83	4.68	88.99	0.89	0.466421
	46	25	1318	10	0.00526	526.00	4.56	86.79	0.87	0.566575
	47	26	1752	10	0.01699	1699.25	4.00	75.95	0.76	1.100393
	48	27	1017	10	0.00251	250.50	4.78	91.01	0.91	0.376701
	54	32	303	6	0.00051	84.44	4.75	90.29	0.90	0.408701
	59	37	998	10	0.00170	170.33	4.78	90.97	0.91	0.378754
	60	38	885	10	0.00046	45.67	4.79	91.21	0.91	0.368206
	61	39	1358	10	0.00811	811.33	4.14	78.65	0.79	0.960465
	64	41	1972	5.5	0.00969	1777.37	4.32	82.07	0.82	0.790498
	79	54	1856	10	0.00413	412.67	4.63	88.06	0.88	0.508578
	80	55	1017	10	0.00029	28.67	4.80	91.25	0.91	0.366377
	81	56	2859	5	0.02520	5040.50	2.56	48.15	0.48	2.923114
	83	58	864	10	0.00582	582.00	4.57	86.95	0.87	0.559439
	84	59	1331	10	0.00271	271.00	4.65	88.54	0.89	0.486867
CE12006	14		5	3	0.00053	177.78	4.56	86.68	0.87	0.571691
	9		900	10	0.00067	67.00	4.73	89.90	0.90	0.43
	4		191	2.5	0.00061	244.00	4.70	89.44	0.89	0.446294
	3		367	5	0.00101	202.67	4.71	89.59	0.90	0.439536

	8		3	3	0.00136	453.33	4.62	87.92	0.88	0.515018
	15		1231	5	0.00051	102.00	4.72	89.87	0.90	0.42702
	15		1826	5	0.00150	299.00	4.69	89.15	0.89	0.459237
	14		749	5	0.00103	206.67	4.60	87.53	0.88	0.532729
	9		1314	5	0.0006	120.00	4.70	89.45	0.89	0.446072
	32		991	8.9	0.002287	256.93	4.66	88.69	0.89	0.479961
	16		1600	5	0.001273	254.67	4.69	89.15	0.89	0.459247
	14		550	6	0.001133	188.89	4.64	88.23	0.88	0.500935
	79		60	4.5	0.001347	299.26	4.68	88.93	0.89	0.469248
	77		2956	8.1	0.000697	86.01	4.74	90.17	0.90	0.413854
	26		348	5	0.000643	128.67	4.74	90.18	0.90	0.413364
	78		2494	4.5	0.0053033	1178.52	3.99	75.68	0.76	1.114552
	80		892	10	0.0004833	48.33	4.70	89.37	0.89	0.449384
	84		180	5	0.0008833	176.67	4.72	89.76	0.90	0.432258
	18		600	5	0.000817	163.33	4.72	89.73	0.90	0.433251
	17		1552	5	0.00075	150.00	4.71	89.68	0.90	0.435539
CE11006	5		12	10	0.0017	170.00	3.73	70.73	0.71	1.385078
	18		996	9	0.0013	144.44	4.72	89.79	0.90	0.430668

3.4 Analytical analysis

3.4.1 Elemental: sPOC and sPN

After freeze-drying, punched circles (7.07–113 mm) were taken from the top SAPS filters to measure suspended particulate organic carbon and nitrogen (sPOC, sPN). Care was taken to avoid areas of the filter that appeared to be heterogeneous (i.e. large darker/lighter or coloured spots were avoided). POC values were obtained after de-carbonation of the top filters (by HCl vapor method; Yamamouro and Kayanne, 1995) and PN values were determined before decarbonation on separate circles. The analyses were carried out using a CEInstruments NC 2500 CHN analyzer in duplicate and the mean value was taken. The bottom filters of the stacks were used as 'DOM blanks' to correct for overestimations of POC and PN due to adsorption of dissolved organic matter (ad-DOM) onto the filters (see Turnewitsch et al., 2007). The measurements were carried out as for sPOC and sPN. All values of sPOC and sPN were corrected for ad-DOM. Consistent variability between circles from the edge and middle of the filter, a filtration artifact, were observed and mean values were therefore taken to give a better approximation of the true value of the filter (for both POC and PN). OC and N values of the top filters that were close to the analytical detection limit were often lower than adsorbed values and in these cases sPOC and sPN values were considered nil.

3.4.2 Molecular: lipid biomarkers

Lipid extractions

Material was extracted from portions (1/4) of the SAPS filters following the methods of Kiriakoulakis et al. (2001) and Wolff et al. (1995). All equipment (glassware, tools etc) was cleaned in Decon90 reagent for 24 hours, rinsed with tap water, followed by deionised water and dried in an oven before use. Bench space was cleaned and covered in muffled (400 °C; 6 + h) foil and wiped with DCM:MeOH (9:1), before carrying out the extractions.

The filters were cut into pieces and submerged in a minimum amount (~20 ml) of DCM:MeOH (9:1) in a glass centrifuge tube. The extract was spiked with 20 µl of internal standard (100 ng/µl 5α(H)-Cholestane; Sigma). The material on the filter was extracted by sonication in a water bath (30 min; 30 °C; x 3). The

solvent was decanted into a round bottom flask and evaporated to dryness under a vacuum on a rotary evaporator. The residual was taken up in a minimum amount of solvent (100% DCM) using a (muffled) Pasteur pipette and passed through (muffled) anhydrous sodium sulphate ($NaSO_4$) and into a clean vial to further dry the extract. Columns were prepared by plugging a Pasteur pipette with (muffled) glass wool using a tweezers and filling ¾ of the pipette with $NaSO_4$. The solvent was then removed by evaporation under a nitrogen stream and extracts were stored at -20 ^{o}C until GC-MS analysis.

Before GC-MS analysis, the extracts were transmethylated with methanolic Acetyl chloride (MeOH:Acetyl Chloride 30:1). The extracts were redissolved in solvent (100% DCM) and transferred to a reaction vial using a Pasteur pipette and blown down to dryness. 1 ml of methanolic acetyl was added and the vials closed, wrapped in foil and left to react (40 ° C; 24 hours). Methanolic acetyl chloride was then removed completely under a stream of nitrogen, before re-dissolving the samples in solvent (100% DCM) and passing through a (muffled) potassium carbonate column (K_2CO_3), into a clean vial, to clean up the extracts. The columns were prepared as described above. The solvent was evaporated by nitrogen gas again and the extracts were stored at -20 °C.

Immediately before running in the GC-MS, the extracts were derivatised by adding 50 µl of *bis*-trimethylsilyltrifluoroacetamide (BSFTA, 1% trimethylsilylchloride; Sigma) was added to each sample using a glass syringe. Samples were incubated for 30 minutes at 40 °C. The extracts were blown down with nitrogen gas. Extracts were re-dissolved in 100 µl of solvent (100% DCM) measured using a glass syringe and transferred to clean GC-MS vials using clean (muffled) pipettes. Lids were crimped and wrapped in Parafilm before storing at -20 °C until analysis.

Gas Chromatography-Mass Spectrometry analysis

GC-MS analyses were carried out on aliquots of the transmethylated and derivatised total extracts out using a Varian 450 Gas Chromatographyer Mass Spectrometer (GC-MS). A CP8400 autosampler was used with a CP-1177 split/splitless injector to load the samples onto an Agilent VF-MS column (30 m x 0.25 mm, 0.25 µm). Helium was used as the carrier gas at a rate of 1 mL min^{-1}, set and controlled at a constant flow using an electron flow controller. The oven

temperature was programmed from 60 to 170 °C at 6 °C min^{-1} after 1 min, and then to 315 °C at 2.5 °C min^{-1} and held for 5 minutes to give a total run time of 82 minutes. The column was fed directly into the electron (EI) source of a Saturn 220 mass spectrometer (ionisation potential 70 eV; source temperature 220 °C; trap current 300 μA. The instrument was operated in Full Data Acquisition mode (50-600 Thompsons cycled every second). Data were collected on a VAX 3500 Workstation.

Quantification and identification of lipids

Chromatograms were reviewed and processed using Varian Data Review software. An example is shown in Fig. 3.5. Compounds were identified by comparison of their mass spectra and relative retention times with authentic standards (Supelco TM37 FAME mix; 47085-U; 47015-U; 47033 Sigma-Aldrich) using the total ion current (TIC) chromatogram. Compound concentrations were calculated by comparison of the peak areas with that of the internal standard (5α(H)-cholestane spiked into samples before extraction) using the software. The relative response factors of the analytes were determined individually for 40 – 44 representative fatty acids, sterols and alcohols from the authentic standards (see Fig. 3.5 and Table 3.6). Where exact response factors were not available, the response factors for similar compounds of the same class and/or similar structure were used. Reproducibility of similar lipid analyses was determined to be < ± 15% by Kiriakoulakis et al. (2000). Organic contamination in procedural blanks extracted with each sample batch was subtracted from the sample values.

Excessive storage time of some samples between the derivatisation step and GC-MS analysis caused the sterols to elute in the non-derivatised form. Sterols were therefore omitted and fatty acids and alcohols only were assessed. Lipid concentrations were normalised to the amount of water filtered and to the amount of organic carbon estimated by elemental analysis. Individual lipids were grouped into classes i.e. Saturated Fatty Acids (SFA), Monounsaturated Fatty Acids (MUFA), Polyunsaturated Fatty Acids (PUFA) and Fatty Alcohols.

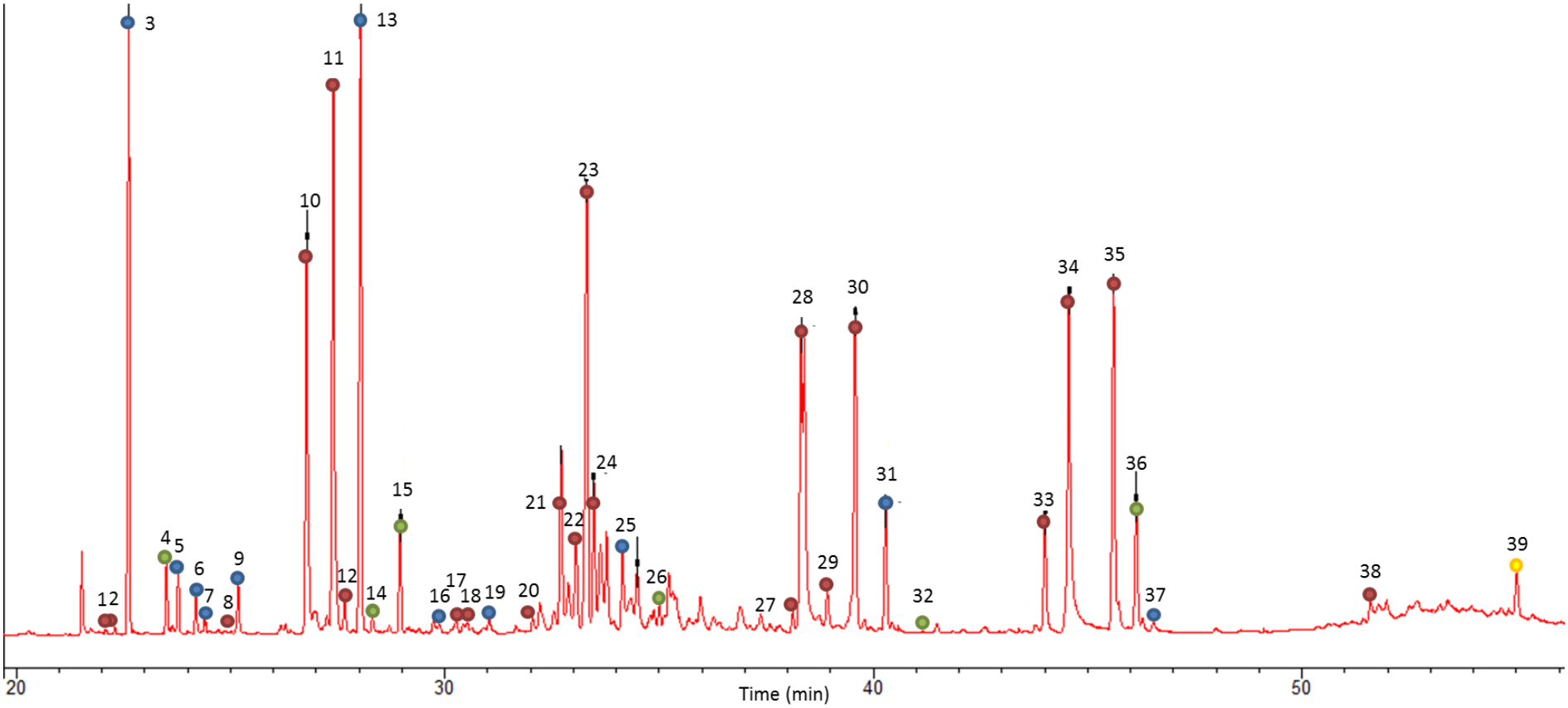

Fig. 3.5. Example of lipid chromatography. Blue circles are saturated fatty acids (FAMEs); Red circles are unsaturated fatty acids (MUFAs & PUFAs); Green circles are fatty alcohols; yellow circle is Cholestane-the internal standard.

Table 3.6. List of compounds identified in chromatogram shown in Fig. 3.5 with retention times and molecular ion. Compound names are colour coded corresponding to dots in fig. 3.5 and the principal classes i.e. blue for Saturated Fatty Acids (SFA), red for unsaturated fatty acids (monounsaturated (MUFA) and polyunsaturated (PUFA)) and green for fatty alcohols.

	RT (elution time)	Compound	Group	M/Z (molecular ion)
1	22.082	i-C14:1	MUFA	240
2	22.304	a-C14:1	MUFA	240
3	22.625	C14:0	FAME	242
4	23.504	C14:0	Alcohol	286
5	23.781	i-C15:0	FAME	256
6	24.191	a-C15:0	FAME	256
7	24.402	C15:0	FAME	256
8	24.875	C15:1	MUFA	254
9	25.18	C15:0	FAME	256
10	26.773	C16:4 (tentatively)	PUFA	262
11	27.396	br-C16:1	MUFA	268
12	27.66	st-C16:1	MUFA	268
13	28.03	C16:0	FAME	270
14	28.307	C16:1	unsatAlcohol	312
15	28.958	C16:0	Alcohol	314
16	29.87	C17:0	FAME	284
17	30.264	br-C17:1	MUFA	282
18	30.527	st-C17:1	MUFA	282
19	31.032	C17:0	FAME	284
20	32.041	C18:5 (tentatively)	PUFA	288
21	32.709	C18:3	PUFA	292
22	33.06	C18:2	PUFA	294
23	33.313	C18:1	MUFA	296
24	33.473	C18:1	MUFA	296
25	34.138	C18:0	FAME	298
26	35.007	C18:0	Alcohol	342
27	38.121	C20:4 or C20:6	PUFA	/
28	38.319	C20:5	PUFA	316
29	38.937	C20:4 (tentatively)	PUFA	318
30	39.576	C20:3	PUFA	320
31	40.29	C20:0	FAME	326
32	41.151	C20:0	Alcohol	370
33	44.004	C22:6	MUFA	342
34	44.565	C22:5 (tentatively)	MUFA	344
35	45.6	C22:1	MUFA	352
36	46.138	C22:1	unsatAlcohol	396
37	46.534	C22:0	FAME	354
38	51.593	C24:1	MUFA	380
39	55.017	Cholestane	Internal std.	372

3.4.3 Pigments

Chlorophyll and phaeopigment extractions

Chlorophyll a and phaeopigment concentrations were determined by fluorometry and based on the methods of Tett (1986) and Arar and Collins (1997). Filters were extracted in the 15 ml centrifuge tubes they were stored in using 90% acetone. The filter was initially submerged in 4 ml of the solvent and sonicated in a cold water bath for 7 min. Extracts were then made up to 10 ml, vortexed and stored in a fridge (4 °C) for 24 hours. The extracts were then shaken and centrifuged (5 min, 450 rpm) and stored in the fridge until analysis. Samples were kept in the dark and cold throughout analysis to limit the degradation of material.

Fluorometry

Before reading, samples were allowed to reach room temperature. Fluorescence before and after acidification (10% HCl) were measured using a Turner model 10 fluorometer. Cuvettes were rinsed with distilled water and acetone between samples and dried using Kim wipes before taking the reading. Data quality was checked with blanks (90% acetone) throughout the runs.

3.4.4 Scanning Electron Microscopy

Circle punches (~113 mm^2) of freeze-dried SAPS filters were mounted on aluminium stubs using carbon pads and allowed to air dry. The stubs were sputter coated with a thin layer of 100% palladium to electrically insulate the samples. Specimens were viewed using an Oxford INCA x-act XT Microscope Control scanning electron microscope at accelerating voltages of 5–20 kV. Analysis was carried with qualitative objectives rather than quantitative as the filters were not specifically prepared for quantitative analysis. Phytoplankton, zooplankton and detrital material were identified using published literature.

References

Arar, E.J. and Collins, G.B., 1997. Method 445:0 In vitro determination of chlorophyll a and Pheophytin a in Marine and Freshwater Algae by Fluorescence, U.S. Environmental Protection, Office of Research and Development, Agency National Exposure Research Laboratory, 1997.

Bishop, J.K.B., 1986. The correction and suspended particulate matter calibration of Sea Tech transmissometer data. Deep-Sea Research, 33, 121 – 134.

Gardner, W.D., Biscaye, P.E., Zaneveld, J.R.V., Richardson, M.J., 1985. Calibration and comparison of the LDGO nephelometer and the OSU transmissometer on the Nova Scotian rise. Marine Geology, 66, 323-344.

Kiriakoulakis, K., Marshall, J.D., Wolff, G.A., 2000. Biomarkers in a Lower Jurassic concretion from Dorset (UK). Journal of the Geological Society, 157, 207-220.

Kiriakoulakis, K., Stutt, E., Rowland, S. J., Vangriesheim, A., Lampitt, R. S., Wolff, G. A., 2001. Controls on the organic chemical composition of settling particles in the Northeast Atlantic Ocean. Progress in Oceanography, 50, 65-87.

Kiriakoulakis K., Blackbird S., Ingels J., Vanreusel A., Wolff G.A., 2011. Organic geochemistry of submarine canyons: The Portuguese margin, Deep Sea Research Part II, 58, 2477-2488.

McCave, I.N., Hall, I.R., Antia, A.N., Chou, L., Dehairs, F., Lampitt, R.S., Thomsen, L., van Weering, T.C.E., Wollast, R., 2001. Distribution, composition and flux of particulate material over the European margin at 47°–50°N. Deep-Sea Research II, 48, 3107–3139.

Pope, R.M. and Fry, E.S., 1997. Absorption spectrum (380–700 nm) of pure water. II. Integrating cavity measurements. Applied Optics, 36, 8710-8723.

Smith, R.C. and K. S. Baker, K.S., 1981. Optical properties of the clearest natural waters, Applied Optics, 20, 177–184.

Tett, P.B., 1987. Plankton. In Biological Surveys of Estuaries and Coasts (eds.) Baker, J.M. and Wolff, J.W., Cambridge University Press, Cambridge (1987), pp. 280 – 341.

Turnewitsch, R., M. Springer, B.M., Kiriakoulakis, K., Vilas, J.C., Arístegui, J., Wolff, G., Peine, F., Werk, S., Graf, G., Waniek., J.J., 2007. Determination of particulate organic carbon (POC) in seawater: The relative methodological importance of artificial gains and losses in two glass-fiber-filter-based techniques. Marine Chemistry, 105, 208-228.

WET Labs, 2008. Sea-Bird Electronics Inc., WET Labs C-star Transmissometer manual.

WET Labs, 2011. Sea-Bird Electronics Inc., Transmissometer C-Star User's Guide Revision V Dec. 2011.

WET Labs, 2014. Sea-Bird Electronics Inc., SBE 911 CTD plus data sheet.

White, M., Ullgren, J., Goddijin, L., Mohn, C., 2008. Appendix I RV Celtic Voyage CTD User's Guide. Department of Earth and Ocean Sciences, NUI Galway.

Wilson, A.M., Raine, R., Mohn, C., White, M., 2015. Nepheloid layer distribution in the Whittard Canyon, NE Atlantic Margin. Marine Geology, 367, 130 – 142. DOI: 10.1016/j.margeo.2015.06.002.

Wolff, G.A., Boardman, D., Horsfall, I.M., Sutton, I., Davis, N., Chester, R., Ripley, M., Lewis, A.C., Rowland, S.J., Patching, J., Ferrero, T., Lambshead, P.J.D., Rice, A.L., 1995. The biogeochemistry

of sediments from the Madeira Abyssal Plain-preliminary results. Internationale Revue der gestamen, Hydrobiologie, 80, 333-349.

Yamamouro, M., Kayanne, H., 1995. Rapid direct determination of organic carbon and nitrogen in carbonate-bearing sediments with a Yanaco MT-5 CHN analyser. Limnology and Oceanography, 40, 1001-1005.

Supplementary information

Table S3.7. CE11006 Station log

Event_#	Latitude	Longitude	Water depth (m)	Date_Time (UTC)	Gear deployed
1	48.83075	-11.0497	1512	24/04/2011 10:20	CTD
2	48.83045	-11.0488	1380	24/04/2011 13:40	ROV
3	48.8305	-11.0489	1380	24/04/2011 14:35	Plankton net
4	48.83045	-11.0487	1380	24/04/2011 15:20	ROV
5	48.99828	-10.7595	152	24/04/2011 22:46	CTD
6	48.99833	-10.7594	152	24/04/2011 23:10	Box core
7	48.99829	-10.7595	152	24/04/2011 23:52	Box core
8	48.90813	-10.9309	420	25/04/2011 01:20	Box core
9	48.9082	-10.9308	420	25/04/2011 01:38	CTD
10	48.87191	-10.9879	890	25/04/2011 02:47	CTD
11	48.76046	-11.1179	1620	25/04/2011 04:35	CTD
12	48.83879	-11.0473	1380	25/04/2011 07:55	ROV
13	48.82599	-11.0568	1240	25/04/2011 13:55	Phytoplankton net
14	48.82605	-11.0568	1300	25/04/2011 15:15	ROV
15	48.44866	-10.9934	2920	25/04/2011 23:42	Box core
16	48.4487	-10.9934	2920	26/04/2011 01:11	CTD
17	48.25065	-10.6566	3200	26/04/2011 05:37	CTD
18	48.51858	-10.7674	2500	26/04/2011 10:20	CTD
19	48.4911	-10.6923	2000	26/04/2011 13:40	ROV

Table S3.8. C12006 Station log

Event_#	Latitude	Longitude	Water depth (m)	Date_Time (UTC)	Gear deployed
1	48.8093	-10.4081	375	2012-04-15 15:35:00	CTD
2	48.8094	-10.4081	375	2012-04-15 16:25:00	ROV
3	48.8095	-10.4088	375	2012-04-15 19:16:00	CTD with SAPS
4	48.8281	-10.3821	196.6	2012-04-15 21:38:00	CTD
5	48.8281	-10.382	197	2012-04-15 22:00:00	Phytoplankton net
6	48.7344	-10.4969	1000	2012-04-15 23:12:00	CTD with SAPS
7	48.7344	-10.497	1000	2012-04-15 23:53:00	SAPS at 30m
8	48.7335	-10.4969	1000	2012-04-16 01:16:00	CTD
9	48.6907	-10.5676	1320	2012-04-16 02:57:00	CTD
10	48.761	-10.459	740	2012-04-16 00:00:00	CTD (Yoyo CTD)
11	48.761	-10.459	740	2012-04-16 07:15:00	SAPS at 20m
12	48.7607	-10.4608	750	2012-04-16 07:22:00	ROV
13	48.7631	-10.4588	740.9	2012-04-16 18:35:00	Box core

14	48.7606	-10.4606	750	2012-04-16 19:21:00	CTD
15	48.691	-10.6075	1820	2012-04-16 21:23:00	CTD
16	48.6558	-10.6732	2200	2012-04-16 23:49:00	CTD
17	48.6083	-10.7305	2758	2012-04-17 02:36:00	CTD
18	48.5156	-10.7961	3100	2012-04-17 05:47:00	CTD
19	48.7009	-10.5689	1350	2012-04-19 05:13:00	CTD
20	48.7164	-10.5248	1096	2012-04-19 06:57:00	CTD
21	48.6906	-10.5667	1290	2012-04-19 08:26:00	CTD
22	48.6964	-10.5669	1575	2012-04-19 09:45:00	CTD
23	48.7091	-10.56	1410	2012-04-19 11:31:00	CTD
24	48.7192	-10.558	860	2012-04-19 16:11:00	CTD
25	48.7192	-10.558	860	2012-04-19 17:00:00	Plankton net
26	48.7316	-10.5571	641	2012-04-19 17:40:00	CTD
27	48.7403	-10.5496	381	2012-04-19 18:30:00	CTD
28	48.763	-10.5151	275	2012-04-19 00:00:00	CTD
29	48.8091	-10.4077	380	2012-04-19 20:34:00	CTD
30	48.7886	-10.4326	493	2012-04-19 00:00:00	CTD
31	48.7627	-10.458	730	2012-04-19 22:40:00	CTD
32	48.733	-10.4968	1000	2012-04-19 23:52:00	CTD
33	48.7164	-10.525	1104	2012-04-20 01:10:00	CTD
34	48.694	-10.5276	957	2012-04-20 02:36:00	CTD
35	48.6938	-10.509	645	2012-04-20 03:37:00	CTD
36	48.6973	-10.4948	440	2012-04-20 04:30:00	CTD
37	48.7139	-10.5243	1100	2012-04-20 05:45:00	Box core
38	48.7016	-10.5698	1270	2012-04-19 16:11:00	CTD
39	48.7015	-10.5696	1310	2012-04-20 08:40:00	ROV
40	48.7015	-10.5699	1300	2012-04-20 13:30:00	ROV
41	48.741	-10.5526	345	2012-04-20 16:05:00	CTD
42	48.7342	-10.5361	554	2012-04-20 16:45:00	CTD
43	48.7288	-10.5295	720	2012-04-20 17:35:00	CTD
44	48.7219	-10.5077	990	2012-04-20 18:28:00	CTD
45	48.7141	-10.4905	600	2012-04-20 19:39:00	CTD
46	48.7053	-10.47	285	2012-04-20 21:05:00	CTD
47	48.7219	-10.5079	1025	2012-04-20 21:51:00	CTD
48	48.7406	-10.5523	361	2012-04-20 23:24:00	CTD
49	48.7342	-10.5355	580	2012-04-21 00:16:00	CTD
50	48.729	-10.5231	740	2012-04-21 01:17:00	CTD
51	48.7219	-10.508	1034	2012-04-21 02:27:00	CTD
52	48.7142	-10.49	615	2012-04-21 03:36:00	CTD
53	48.7061	-10.4703	298	2012-04-21 04:26:00	CTD
54	48.722	-10.508	1030	2012-04-21 04:55:00	CTD

55	48.7013	-10.5695	1350	2012-04-21 06:29:00	CTD (for ROV)
56	48.7106	-10.5399	1333	2012-04-21 08:18:00	Box core
57	48.7077	-10.5459	1380	2012-04-21 10:30:00	Box core
58	48.7078	-10.5457	1409.4	2012-04-21 12:17:00	Box core
59	48.5154	-10.7947	3028	2012-04-21 17:35:00	CTD
60	48.6547	-10.6761	2220	2012-04-21 22:22:00	CTD
61	48.7012	-10.5692	1333	2012-04-22 02:08:00	CTD
62	48.5154	-10.7947	50	2012-04-21 20:15:00	Phytoplankton net
63	48.7627	-10.4584	745	2012-04-22 03:30:00	CTD with SAPS
64	48.7014	-10.5697	1335	2012-04-22 05:50:00	ROV
65	48.6639	-10.6537	2047	2012-04-22 15:47:00	Box core
66	48.7015	-10.5692	1346	2012-04-22 19:19:00	CTD
67	48.7015	-10.569	1284	2012-04-22 05:17:00	CTD
68	48.719	-10.555	999	2012-04-24 07:00:00	SAPS
69	48.759	-10.4619	745	2012-04-24 08:52:00	CTD
70	48.8094	-10.4075	376	2012-04-24 10:22:00	CTD
71	48.7591	-10.4619	750	2012-04-24 13:20:00	ROV
72	48.7169	-10.5193	1070	2012-04-24 15:09:00	CTD
73	48.7016	-10.5698	1330	2012-04-24 17:33:00	CTD
74	48.7016	-10.5698	1330	2012-04-24 19:00:00	SAPS
75	48.5163	-10.796	3090	2012-04-24 23:55:00	CTD
76	48.2518	-10.6575	3150	2012-04-25 04:37:00	CTD
77	48.4472	-10.9935	2911	2012-04-25 22:48:00	CTD
78	48.6806	-11.1866	2536	2012-04-26 05:18:00	CTD
79	48.7601	-10.1172	1570	2012-04-26 10:19:00	CTD
80	48.8177	-11.0373	1449	2012-04-26 12:52:00	CTD
81	48.8624	-10.9969	1020	2012-04-26 00:00:00	CTD
82	48.8624	-10.9971	1009	2012-04-26 14:33:00	CTD
83	48.8873	-10.9725	680	2012-04-26 16:09:00	CTD
84	48.9114	-10.9509	334	2012-04-26 17:05:00	CTD
85	51.5918	-10.8355	157	2012-04-26 19:00:00	CTD
86	52.5082	-10.2492	96	2012-04-26 19:00:00	CTD
87	53.2153	-9.14682	16.3	2012-04-28 07:16:00	CTD

Table S3.9. C13008 Station log

Event_#	**Latitude**	**Longitude**	**Water depth (m)**	**Date_Time (UTC)**	**Gear deployed & CTD #**
1	53.1951	-9.55634	44	01/06/2013 15:15	ROV
2	53.1951	-9.55634	44	01/06/2013 16:17	ROV
3	53.1951	-9.55634	44	01/06/2013 17:30	CTD_1
4	53.9926	-12.6219	907	02/06/2013 08:00	Lander

					deployment
5	53.9862	-12.6099	759	02/06/2013 10:20	SAPS
6	53.9862	-12.61	760	02/06/2013 10:30	CTD_2
7	53.9738	-12.6227	763	02/06/2013 12:00	ROV
8	53.9307	-12.5743	426	03/06/2013 00:05	CTD_3 & SAPS
9	54.0036	-12.6209	1007	03/06/2013 02:25	CTD_4
10	54.0125	-12.6327	1445	03/06/2013 03:55	CTD_5 & SAPS
11	54.0118	-12.6368	1480	03/06/2013 07:50	ROV
12	54.0471	-12.6365	1800	03/06/2013 21:00	CTD_6
13	54.0605	-12.5558	1421	03/06/2013 23:20	CTD_7 &SAPS
14	54.0572	-12.5531	1202	04/06/2013 03:35	ROV
15	54.056	-12.5548	1401	04/06/2013 12:00	ROV
16	53.9687	-12.6174	750	04/06/2013 21:00	Box core
17	53.9845	-12.7553	750	04/06/2013 22:35	Box core
18	53.9845	-12.7552	740.9	04/06/2013 23:00	CTD_8 &SAPS
19	53.9266	-12.7556	431	05/06/2013 02:25	CTD_9 &SAPS
20	54.0269	-12.7552	1009	05/06/2013 03:40	CTD_10
21	54.1304	-12.7553	1500	05/06/2013 05:40	CTD_11 & SAPS
22	54.1765	-12.7553	1800	05/06/2013 08:53	CTD_12
23	53.9274	-12.7549	428	05/06/2013 12:10	SAPS
24	53.9274	-12.7549	428	05/06/2013 12:10	CTD_13
25	54.0283	-12.7554	1023	05/06/2013 13:40	CTD_14 &SAPS
26	54.0599	-12.5493	1350	05/06/2013 20:25	ROV
27	54.0599	-12.5493	1350	05/06/2013 23:28	ROV
28	54.1433	-12.5946	2400	06/06/2013 07:55	CTD_15 & SAPS
29	54.1433	-12.5946	2400	06/06/2013 12:25	Box core
30	54.2219	-12.7567	2377.3	06/06/2013 15:10	CTD_16 & SAPS
31	54.0537	-12.5963	1579	06/06/2013 20:25	CTD_17
32	54.0537	-12.5963	1579	06/06/2013 22:11	ROV
33	54.0052	-12.6281	1168.3	07/06/2013 12:25	Box core
34	54.0052	-12.6281	1168	07/06/2013 13:55	CTD_18
35	54.0052	-12.628	1168	07/06/2013 14:55	Box core
36	54.0552	-12.5457	1361	07/06/2013 16:55	ROV
37	53.9861	-12.61	751	08/06/2013 08:30	CTD_19
38	49.0098	-10.9489	655	09/06/2013 14:10	CTD_20
39	49.0098	-10.9488	666	09/06/2013 18:43	ROV
40	49.0098	-10.9488	670	10/06/2013 09:07	CTD_21 & SAPS
41	49.021	-10.8973	390	10/06/2013 11:20	CTD_22
42	49.0246	-10.8668	197	10/06/2013 12:15	CTD_23 & SAPS
43	49.0246	-10.8668	197	10/06/2013 13:45	SAPS
44	48.9817	-11.0203	914	10/06/2013 15:30	CTD_24

45	49.0101	-10.9449	654	10/06/2013 17:00	ROV
46	48.9392	-11.1451	1300	11/06/2013 11:55	CTD_25 & SAPS
47	48.8526	-11.1451	1732	11/06/2013 15:15	CTD_26
48	48.6784	-11.1462	2063	11/06/2013 18:30	CTD_27 & SAPS
49	48.7984	-11.0608	1686.41	11/06/2013 21:43	CTD_28
50	48.8408	-11.0258	1355	11/06/2013 23:45	CTD_29 & SAPS
51	48.8859	-10.9227	775	12/06/2013 03:05	CTD_30
52	48.8856	-10.9229	780	12/06/2013 04:42	ROV
53	48.9152	-10.8954	393	12/06/2013 10:00	CTD_31
54	48.8867	-10.9227	650	12/06/2013 11:16	CTD_32 & SAPS
55	48.8673	-10.9339	964	12/06/2013 12:20	CTD_33
56	48.8494	-10.904	550	12/06/2013 14:05	CTD_34 &SAPS
57	48.8501	-10.9059	562	13/06/2013 00:10	CTD_35 & SAPS
58	48.7992	-10.9462	745	13/06/2013 02:45	CTD_36
59	48.7465	-11.0054	1000	13/06/2013 04:30	CTD_37
60	48.6885	-11.0938	1302	13/06/2013 07:29	CTD_38 & SAPS
61	48.6441	-10.4757	1379	13/06/2013 11:55	CTD_39
62	48.644	-10.4758	1360	13/06/2013 17:00	ROV
63	48.6439	-10.4736	1383	14/06/2013 08:46	CTD_40 & SAPS
64	48.5649	-10.5151	1977	14/06/2013 13:50	CTD_41
65	48.6545	-10.6736	2251	14/06/2013 17:30	CTD_42
66	48.7101	-10.5417	1285	14/06/2013 21:27	CTD_43 & SAPS
67	48.7345	-10.4954	986.4	15/06/2013 00:25	CTD_44
68	48.7613	-10.4595	749	15/06/2013 02:10	CTD_45 &SAPS
69	48.8096	-10.4074	375	15/06/2013 04:45	CTD_46
70	48.8282	-10.3814	197	15/06/2013 06:00	SAPS
71	48.8282	-10.3814	197	15/06/2013 07:13	CTD_47
72	48.8041	-10.3145	310	15/06/2013 08:45	CTD_48
73	48.7344	-10.3709	640	15/06/2013 09:30	CTD_49
74	48.6826	-10.3826	880	15/06/2013 10:09	CTD_50
75	48.6533	-10.4356	1042	15/06/2013 11:50	CTD_51
76	48.7632	-10.4599	745	15/06/2013 14:28	ROV
77	48.7631	-10.4599	745	16/06/2013 01:45	CTD_52
78	48.7103	-10.5417	1387	16/06/2013 04:10	CTD_53
79	48.6909	-10.6072	1828	16/06/2013 06:55	CTD_79
80	48.5967	-10.7555	2777	16/06/2013 10:45	CTD_55
81	48.4532	-10.4209	2814	16/06/2013 14:45	CTD_56
82	48.591	-10.5282	1786	16/06/2013 19:30	CTD_57
83	48.644	-10.4748	1376	16/06/2013 22:00	CTD_58
84	48.7102	-10.5421	1363	17/06/2013 00:35	CTD_59
85	48.6258	-10.7069	2560	17/06/2013 03:53	ROV

86	48.6857	-10.6178	1880	17/06/2013 18:00	Box core
87	48.7109	-10.5334	1214	17/06/2013 20:00	Box core
88	48.6441	-10.4709	1350	17/06/2013 22:00	Box core
89	48.6563	-10.4124	1031	18/06/2013 00:30	ROV
90	48.5872	-10.5304	1801	18/06/2013 14:25	Box core
91	48.6375	-10.6839	2400	18/06/2013 16:15	ROV

Chapter 4
Nepheloid layer distribution in the Whittard Canyon, NE Atlantic Margin

Annette M. Wilson*[a], Robin Raine[a], Christian Mohn[b] and Martin White[a]

[a]Earth and Ocean Sciences, Ryan Institute and School of Natural Sciences, National University of Ireland Galway, University Road, Galway, Ireland.

[b]Department of Bioscience, Aarhus University, 4000, Roskilde, Denmark .

Published: Marine Geology 367 (2015) 130–142.

***Role:** Lead author, responsible for overall sampling, data collection, processing and analysis. Responsible for the generation of figures and writing of manuscript. Martin White provided training and support in oceanographic data processing, conception and design of the sampling regime and analysis. Martin White and Robin Raine contributed to the interpretation of the data, discussion of results and guided the writing of the manuscript. Christian Mohn was responsible for processing and assisted with the interpretation of ADCP data.

Abstract

The dynamics and distribution of nepheloid layers in multiple branches of the Whittard Canyon were observed during three hydrographic surveys carried out between 2011 and 2013. The sources of permanent and temporal variation of the layers were investigated. Seasonal variations in primary production at the surface were reflected in the nepheloid layers extending down in the water column, particularly in the upper reaches of the canyon. Benthic nepheloid layers were observed along the canyon axes to depths greater than 2500 m, a distance of ~30 km. Intermediate nepheloid layer were detected as lateral extensions of the benthic nepheloid layer, centred at ~550 m, 850 m, 1150 m and 1600 m and stretching ~20–25 km off slope. Critical and supercritical conditions for semidiurnal tide reflection were identified coinciding with the occurrence of intermediate nepheloid layers, with other hotspots found at the boundaries of the permanent thermocline and Mediterranean Outflow Water. Weak seasonal stratification during the survey in 2012 appeared to permit storm induced mixing at deeper water depths than expected, altering the distribution of material in the nepheloid layers. The dynamic conditions of the canyon encourage nepheloid layer formation with implications for deposition rates and food supply to the unique communities that are found in the Whittard Canyon and likely other similar canyon systems.

Keywords: Nepheloid layers; Whittard Canyon; Baroclinic motions; Permanent thermocline; Mediterranean Outflow Water

4.1 Introduction

Nepheloid layers (NLs) are significant contributors to the shelf edge exchange of sediment, serving as a link in the transport of material from shallow productive environments to the abyss (Amin and Huthnance, 1999; Puig and Palanques, 1998). They are primarily defined as elevated concentrations of suspended particulate matter (SPM) recognised by increased light scattering and absorption in comparison to the surrounding clear water (McCave, 1986; Dickson and McCave, 1986; Puig et al., 2014). Driven by local hydrodynamics and energetic flows, deep benthic (BNLs) are commonly found along slopes and in deep basins (e.g. McCave, 1986). Lateral transport of material from intense regions in BNLs, due to the interaction of processes that increase mixing in a stratified environment, can result in the formation of intermediate nepheloid layers (INLs) along isopycnal surfaces (Thorpe and White, 1988; van Weering et al., 2002). Sediment transport processes across continental margins are constrained by hydrodynamic energy, morphology and time (Palanques et al., 2008). Submarine canyons incising continental margins and characterised by steep sloping topography, act as preferential pathways for material escaping from the continental shelf to the abyss (Gardner, 1989a; Durrieu de Madron, 1994; Puig et al., 2014). Canyons are noted for their dynamic hydrographic interaction and enhanced energy (Boyer et al., 2004; Allen and Durrieu de Madron, 2009; Canals et al., 2013); increasing particle fluxes and accumulation rates (van Weering et al., 2002; de Stigter et al., 2007).

Contemporary sediment transport processes within canyons have recently been reviewed by Puig et al. (2014) and can be classified as; gravity-driven processes and flow-driven events. Rapidly moving turbulent and sediment laden water driven by large density contrasts, often referred to as gravity flows; regularly result from flood, slope and mud failures (Puig et al., 2014), while, flow-driven transport events result from the resuspension and advection by storms, tidal motions, internal waves and the inflow of slope water onto continental shelves. Both benthic and seasonal storms can induce turbidity currents (de Stigter et al., 2000) or cold water bores (Gardner, 1989b), often self-accelerating processes that are controlled by local slope gradients and modulated by internal tides (Puig et al., 2014). Tidal rectification of barotropic flows and the generation and reflection of small scale internal motions are associated with

complex topography and can generate enhanced velocities (Hotchkiss and Wunsch, 1982; Cacchione and Drake, 1986; Holt and Thorpe, 1997; Thorpe, 1999; Kunze et al., 2002; Allen and Durrieu de Madron, 2009). Other flows related to frontal features and surges of cooled dense shelf waters in cascading events can also encourage the resuspension of sediments particularly in canyons (Palanques et al., 2006; Puig et al., 2008).

Resuspension, infill prevention and erosion by these processes play a role in the shaping of continental margins and maintain high concentrations of material in suspension for BNL and INL formation (Cacchione and Wunsch, 1974; Gardner, 1989a; Cacchione et al., 2002; Canals et al., 2006). The conduit nature of canyons combined with enhanced transport processes induced by their setting ensues higher concentrations of SPM within the canyon channel, creating quantitatively important pathways of organic matter in comparison to their adjacent slopes (Durrieu de Madron, 1994; van Weering et al., 2002; Kiriakoulakis et al., 2011; Canals et al., 2013). This is often reflected in the enhanced biomass present in canyons and forms important habitats for many species (e.g. De Leo et al., 2010).

Climate-change driven extreme weather events are predicted to increase cascading and sediment slumping events (Canals et al., 2006) and recently resuspension by bottom trawling on continental shelves has been suggested as a significant sediment transport process in its own right (Martín et al., 2015). Thus there is a requirement to understand the competing processes involved in sediment transport that lead to the complex picture present at submarine canyons. Whittard Canyon has been noted as an important refuge for faunal communities (Huvenne et al., 2011; Morris et al., 2013). Recently, Amaro et al. (2015) suggested that elevated concentrations of labile organic matter co-occurring with holothurians in Whittard Channel are linked with advection and redistribution by bottom currents rather than down-canyon transport. They suggest that an additional mechanism concentrating phytodetritus deposits in the channel is required. In the upper reaches of the canyon it has been hypothesized that a key factor in explaining the distribution of suspension feeding fauna is the concentrating of food supplies in NLs (Johnson et al., 2013; Appendix A). This study describes the distribution of NLs and the dominant hydrodynamic processes affecting their structure in Whittard Canyon. Applicable elsewhere, the

identification of such processes broadens our understanding of the exchange of material from the productive Celtic Sea Shelf to the deep Atlantic Ocean.

4.2 Setting

The Whittard Canyon is a dendritic submarine canyon located on the wide Celtic continental margin in the northern Bay of Biscay (Fig. 4.1). It lies ~300 km from nearest coasts (Ireland, UK and France), with prominent branches that extend over 100 km from the shelf edge (~200 m) to abyssal depths (>3000 m). The deeply incised branches extend from the upper slope, where the walls are steep sided (Hunter et al., 2013; Johnson et al., 2013; Appendix A), and converge into one large channel at ~3800 m water depth, before opening out into the Porcupine Abyssal Plain and contributing to the formation of the Celtic deep-sea turbidite (clastic) system at ~4000 to 4900 m (Zaragosi et al., 2000).

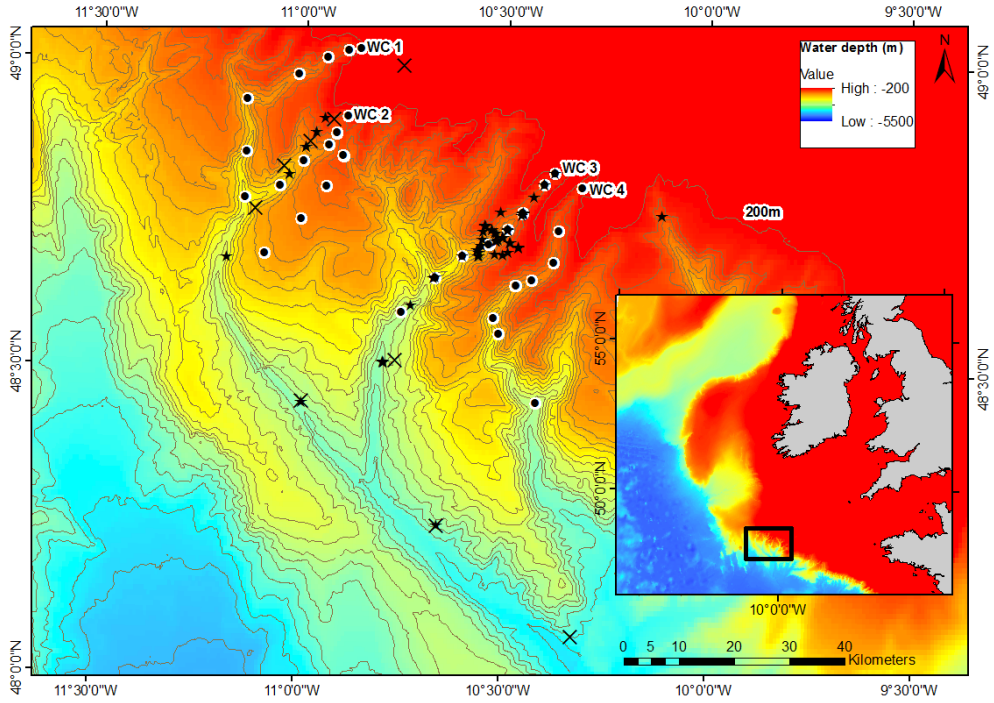

Fig. 4.1 Bathymetry of Whittard Canyon with station and transect location of the 2011 (✕), 2012 (★) and 2013 (⦿) surveys. Contour interval is 200 m. Branches surveyed labelled WC1, WC2, WC3, WC4. Background bathymetry was sourced from the Irish National Seabed Survey, Geological Survey of Ireland and Integrated Mapping for the Sustainable Development of Ireland's Marine Resource (INFOMAR) and the General Bathymetric Chart of the Oceans (GEBCO) operating under the International Oceanographic Commission (IOC) and the International Hydrographic Organization (IHO). Data was combined using ArcGIS software.

The central water masses of the Whittard Canyon comprise Eastern North Atlantic Water (ENAW), Mediterranean Outflow Water (MOW), and Labrador Sea Water (LSW) and are underlain by North Atlantic Deep Water (NADW) (Pollard et al., 1996; van Aken, 2000). ENAW is the most prominent water mass found below the seasonal thermocline (~100 m) down to ~600 m where it is separated from the underlying MOW by the permanent thermocline, typically observed in the NE Atlantic at 600–1000 m. MOW extends down to 1200 m, before mixing with the underlying Labrador Sea Water marked by a salinity minimum at ~1800 m.

The Celtic Sea shelf break is an energetic "hotspot" for tidal energy conversion and a significant contributor to global internal tidal energy flux (Vlasenko et al., 2014). The region is defined by high barotropic tidal energy, which is subsequently converted to baroclinic internal tides where internal waves are generated by the residual flow across the bathymetry of the slope (Baines, 1982; Hotchkiss and Wunsch, 1982; New, 1988; Holt and Thorpe, 1997; Allen and Durrieu de Madron, 2009). The upper hydrography of the area is characterised by a north-westerly flowing European Slope current with typical mean flows of 5–10 cm s^{-1} (Pingree and Le Cann, 1990; Xu et al., 2015). This typically poleward flow displays seasonal variability with a weakening during the spring and summer months and/or reversal in the mean direction flow (Pingree et al., 1999; Xu et al., 2015). Boundary flows at intermediate depths are associated with MOW (van Rooij et al., 2010). Bottom currents in the boundary layer display tidal frequencies with maximum velocities of 16 cm s^{-1} (3752 m) recorded by Reid and Hamilton (1990) but maximum speeds in excess of 25–40 cm s^{-1} at 1000 m and 20 cm s^{-1} at 2000 m have been recorded (Duros et al., 2011). Deeper in the channel (4166 m) bottom currents also display weak semi-diurnal frequencies with velocities $\leq$10 cm s^{-1} (van Weering et al., 2000; Amaro et al., 2015).

Strongly influenced by the oceanographic setting, surface water above the upper reaches of the canyon supports high fluxes of organic matter, associated with high primary production (~160 g C m^{-2} yr^{-1}) at the ocean margin in the Bay of Biscay (Lampitt et al., 1995; Wollast and Chou, 2001). Sediments at the Whittard Canyon and Channel are characterised by distinct layers (Duros et al., 2011; Amaro et al., 2015) and consist of pelagic material and sediment reworked from the outer shelf and canyon edges (Duros et al., 2011). The upper canyon is dominated by coarse sediments while the lower canyon is covered in finer

material, implying downward transport within the canyon, with vertical alterations in grain size attributed to episodic gravity flows deeper in the canyon (Duros et al., 2011; Hunter et al., 2013; Amaro et al., 2015). The canyon and channel floors are locally enriched in comparison to the adjacent slope, with elevated organic matter mineralisation rates and sediments enriched with particulate organic carbon and labile material (Duineveld et al., 2001; Duros et al., 2011; Amaro et al., 2015). Benthic community assemblages are suggested to reflect differing oceanographic and disturbance regimes in the eastern and western branches, with baroclinic motions, gravity and benthic flows and nepheloid layers suggested as the governing sedimentary processes in submarine canyons (Zaragosi et al., 2000; de Stigter et al., 2007, 2011; Duros et al., 2011).

4.3 Methods

Four branches within the Whittard system (WC1–WC4) were surveyed between 2011 and 2013 on the RV *Celtic Explorer* as part of an Irish biodiscovery and ecosystem functioning research initiative (Fig 4.1 and table 4.1). Hydrographic and nephelometric measurements were performed in varying seasonal conditions. Two storms with significant wave heights of 8–9m took place during the 2012 survey in April. Stable meteorological conditions persisted for the majority of the 2011 and 2013 surveys, both carried out post phytoplankton spring bloom.

Table 4.1. Survey details and branches covered by CTD transects during three surveys to the Whittard Canyon (results here focus on WC2 and WC3).

Year	Cruise code	Sample dates	# CTD casts	WC1	WC2	WC3	WC4
2011	CE11006	24-26 April	9		X		
2012	CE12006	15-26 April	65		X	X	
	Storms	~17-18th & 23rd April					
2013	CE13008	9-17 June	40	X	X	X	X

Hydrographic observations (temperature, salinity, pressure, density and transmission) were carried out in transects using a Seabird SBE 911 CTD and SBE32 Rosette system. Repeat vertical profiles were performed at selected locations. Salinity was calibrated by analysing discrete water samples on a Guildline Portasal salinometer (Model 8410A). Turbidity measurements were

determined by a 0.25 m path-length transmissometer (C-star, WET Labs) operating at 650 nm. Raw transmission values were adjusted according to the clear and dark water values and converted to beam attenuation coefficient (BAC) according to Bishop (1986) and data were averaged to 1 m vertical bins.

Seawater samples were collected in Niskin bottles (10 L) from the CTD rosette for the determination of SPM concentration (µg L^{-1}), assuming that BAC is linearly related to SPM for particles with a small range in grain size (e.g. Gardner et al., 1985; Bishop, 1986). Here, water was sampled during the three surveys in layers of optical turbidity maxima and minima and filtered through pre-weighted Nuclepore polycarbonate filters (0.4 µm pore size, 47 mm diameter) according to the methods of McCave et al. (2001). BAC was correlated by linear regression with the mass of SPM obtained from filtered water samples (n = 37) and the relationship;

$$SPM = 0.00048 * BAC + 0.3893 \quad (4.1)$$

was found with a strong correlation of $R^2 = 0.83$ (Fig. 4.2).

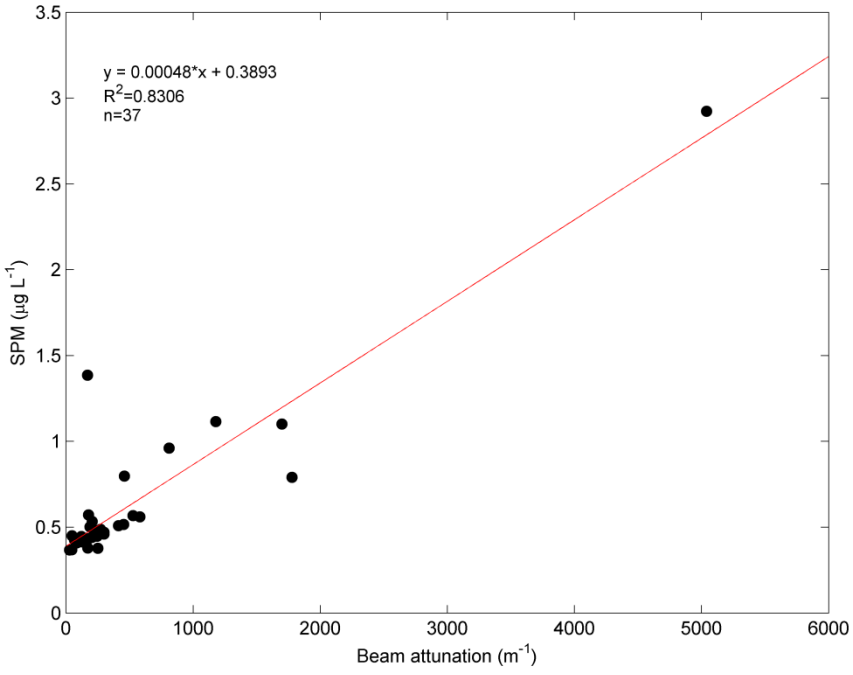

Fig. 4.2. Suspended particulate matter (SPM) versus beam attenuation (BAC) for 37 samples from CE11006, CE12006 and CE13008.

On-station and underway ADCP data were collected intermittently throughout the three surveys. On-station velocities were collected with a 75-kHz Ocean Surveyor (RDI 4869/50) in 16 m bins down to a maximum 800 m water depth. Processing was carried out using the Common Oceanographic Data Access System (CODAS, Firing et al., 1995) as described in Mohn et al. (2013). Data were gridded at 10 m resolution, starting at 20 m with 99 depth levels and the data were reduced to 5 min ensembles. Quality control and transducer misalignment adjustments were made accordingly.

4.4 Results

4.4.1 Hydrography

4.4.1.1 General oceanographic setting

The water masses present at the Whittard Canyon were identified using T-S (temperature-salinity) profiles (>2000 m) combined from data sets from 2011, 2012 and 2013 (Fig. 4.3). Water masses displayed consistency over the three surveys. Below the seasonally warmed surface layer (~150 m) ENAW; $27.1<\sigma_\theta<27.25$ dominates the upper water column. The permanent thermocline (~600–900 m) was identified between ENAW and saline MOW (700–1100 m); 9<T<11 °C, S>35.6 with a MOW core centred between σ_θ = 27.5 to 27.6 kg m^{-3}. The influence of the MOW in shallower profiles was observed in discrete patches extending into the canyon branches. Below the MOW, ENAW mixes with LSW which displayed inter-annual variability at ~1600 m with a gradually decreasing salinity extending down into deeper water. The distinct LSW salinity minimum usually observed between 1800 and 2000 m was very weak. The upper levels of Northeast Atlantic Deep Water (NEADW); T<2.5 °C were observed below this.

4.4.1.2 Seasonal and storm variation

During the 2012 survey, the hydrographic regime was significantly affected by storm activity (Fig. 4.4). Before and after CTD profiles show evidence of the previous winter mixed layer down to ~400 m, after which there is a significant increase in density with depth (i.e. the permanent thermocline). Early seasonal warming is evident in the upper 240 m before the storm, resulting in weak seasonal stratification, which is subsequently eroded by the storm, deepening the upper homogenous layer by ~40 m post-storm. An overall

sharpening in the gradient of the permanent thermocline at ~450 m was observed after the storm cessation. Vessel mounted ADCP data recorded during the storm revealed a corresponding 2-layer flow, predominantly in a south easterly (SE) direction (Fig. 4.5). In the upper 200 m, flow speeds reached 0.1 m s^{-1} and were likely much higher in the upper 20 m not covered by the ADCP. Below this, a change in the flow pattern to a south westerly (SW) direction was observed down to ~400 m matching with the new mixed layer, before returning to the dominating SE flow down to the deepest observations, with a lower magnitude of ~0.05 m s^{-1}.

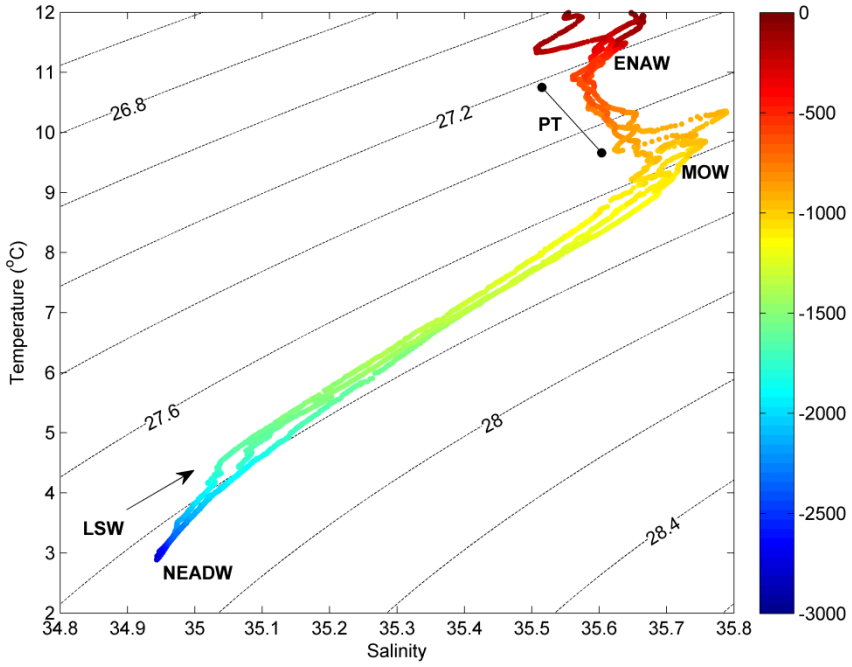

Fig. 4.3. Temperature-Salinity diagram for selected CTD profiles in >2000 m water depth from CE11006, CE12006, CE13008. Colour coding indicates depth (m) and dashed lines show isopycnals (σ_θ, kg m^{-3}) with contour interval at 0.2. Water masses are labelled; Eastern North Atlantic Water (ENAW), Mediterranean Outflow Water (MOW), Labrador Sea Water (LSW) and North Eastern Atlantic Deep Water (NEADW). The permanent thermocline is marked PT.

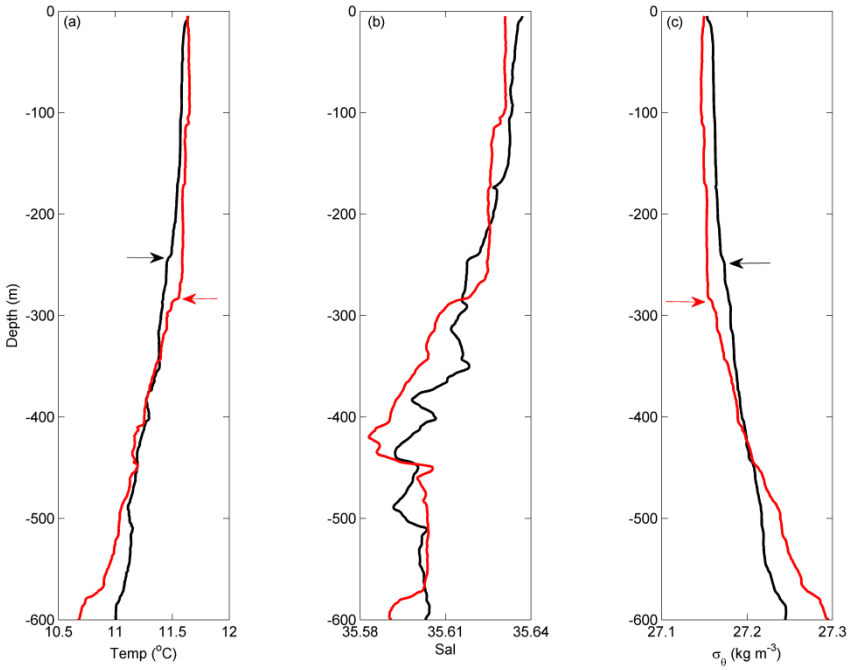

Fig. 4.4. Vertical profiles of (a) Temperature (°C), (b) salinity and (c) density (σ_θ, kg m^{-3}) in ~1000 m water depth, before (–) and after (–) the storm in WC3. Only the top 600 m is shown to emphasis the effects of storm activity on seasonal stratification. Black arrows indicate depth of seasonal stratification before storm and red arrows show after.

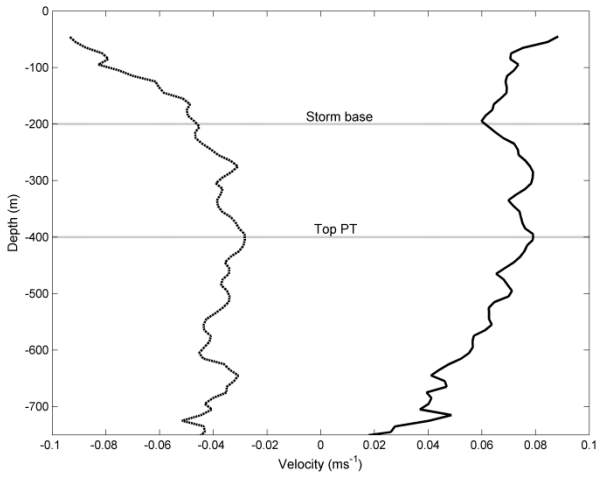

Fig. 4.5. Averaged residual current vectors measured during storm (CE12006) over 25 hours by vessel-mounted ADCP displayed as vertical profiles of north velocity (v --) and the east velocity (u–), expressed in (m s^{-1}). Thin dashed lines indicate approximate the depth of the storm base and top of the permanent thermocline (PT).

4.4.2 Nepheloid layers and SPM distribution

4.4.2.1 General overview of SPM concentrations and nepheloid layers

Permanent and ephemeral NLs were observed in all four branches during the three surveys. Here, we focus on the results from two branches: WC2 and WC3 where repeat transects and observation were made (Figs. 4.6–4.9; Table 4.1). SPM values ranged from 25 to 1100 µg L^{-1} with some higher values > 8000 µg L^{-1}. These values are consistent with other studies in the NE Atlantic and in other canyon systems, notwithstanding difference in setting and sediment composition; e.g. Goban Spur (50–130 mg m^{-3} (McCave et al., 2001); NW Iberian margin nephel study 25–1000 mg m^{-3} (McCave and Hall, 2002); Nazaré Canyon and Portuguese shelf 1000–4000 µg L^{-1} (Oliveira et al., 2007).

High SPM concentrations, typically ≳300 µg L^{-1}, were observed in the surface waters above all branches during the three surveys (Fig. 4.6). Generally higher concentrations of SPM were observed at the surface in 2011 and 2013, while, throughout the canyon, background values in 2011 and 2012 were higher relative to 2013. Surface concentrations were generally reflected at depth in the benthic and intermediate layers. INLs manifested as mid-water lateral extensions from the BNLs at the seabed (Fig. 4.7). INL detachments extended up to ~20–25 km off slope about two to three times the internal Rossby radius, (NH/πƒ), where H is the mean water depth (taken here as 1200 m), ƒ the Coriolis parameter, N the buoyancy frequency, expressed by;

$$N^2 = -(g/\rho_0) * d\rho/dz \qquad (4.2)$$

and g is gravity, ρ is the density and z is the vertical coordinate, such that $d\rho/dz$ represents the gradient in density.

4.4.2.2 Permanent nepheloid layers

Observations during all surveys detected extensive BNLs extending down to >2500 m in the branches (WC1–3) covering the entire surveyed axis up to 40 km distance (Fig. 4.6 and 4.7). In WC2 and WC3 the BNLs displayed consistency in character, with thicknesses of ~150–200 m and concentrations typically ranging between ~150–400 µg L^{-1} (Fig. 4.6 and 4.7). In the upper reaches of the WC2, below the sub-surface minimum in SPM, concentrations generally increased

towards the bottom to ~1600 m with values in the BNL ~200–400 μg L^{-1} (Fig. 4.6). Below this in the lower reaches of the canyon, SPM values were much lower ranging between 75–170 μg L^{-1} (Fig. 4.6a–b). This is evident in profiles from both 2011 and 2012, however 2013, unusually high SPM values ranging between 900 and 1100 μg L^{-1} were observed in the lower reaches (i.e. >1600 m, Fig. 4.6c).

Well defined INLs were sourced from areas of highest BNL SPM concentration at depths; e.g. 550 m, 850 m, 1150 m and 1600 m, in both WC2 (Fig. 4.6) and WC3 (Fig. 4.7). Thickness typically ranged between 50 and 200 m and concentrations of SPM between 75 and 300 μg L^{-1}. INLs observed along the branches were traced back to BNLs at shallower reaches further up the branch. INLs displayed lateral continuity, with high concentration extensions (~200 μg L^{-1}) typically stretching ~5 km off slope (Fig. 4.7). Concentrations decreased with extension down the canyon axis with weaker INLs (~100 μg L^{-1}) continuing typically for ~20 km. After the storm in 2012, INLs continued to emanate from source regions in WC3 (Fig. 4.7a and b). INLs were largely observed in the upper reaches of the canyon above ~1600 m, however in 2013 an INL with high concentrations (> 500 μg L^{-1}) was observed at ~2200 m (Fig. 4.7c). Similarly high values were detected in the lower reaches of WC2 during this survey (Fig. 4.6c).

A transect across the upper reaches of WC3 in 2012 also showed a general trend of SPM increasing towards the bottom of the canyon (Fig. 4.8). The BNLs with values of SPM ~200 μg L^{-1}, stretched from the northern to southern wall and a strong INL centred at ~550 m was repeatedly observed in profiles at the middle station (~1000 m, Fig. 4.8b).

4.4.2.3 Temporal variation

Localised peaks in turbidity were detected during the 2013 survey particularly in WC4 (not shown here) and in the lower reaches of WC2 (Fig. 4.6c) and WC3 (Fig. 4.7c). Concentrations of SPM in the peaks in WC4 exceeded general observations at comparable locations by at least an order of magnitude. In WC3, an unusual peak at ~2200 m was observed at the seabed with SPM concentrations ~800 μg L^{-1} and a thick (~200 m) layer extending ~6.5 km off slope with SPM >500 μg L^{-1} (Fig. 4.7c). Dissimilar to observations below 1600 m in 2011 and 2012 in WC2, high SPM values (900–1100 μg L^{-1}) were detected at ~1700 m and ~ 2000 m (Fig. 4.6c). The role of bottom trawling in sediment transport has recently been highlighted in Mediterranean canyons (e.g. Martín et al., 2014) and previous

studies have suggested that bottom trawling may also contribute to turbidity peaks and other sediment gravity flows observed in this area (van Weering et al., 2000; Amaro et al., 2015). The occurrence of these events will be further discussed in another paper (see Chapter 5).

A link between the turbid surface layer and water within the upper reaches (i.e. < 500 m) of both WC2 and WC3 was observed 2011 and 2012 (Fig. 4.6 and 4.7). This feature was less obvious in 2013 (Fig. 4.7c), perhaps reflective of the time elapsed since initiation of the spring bloom and the generally lower background values detected in 2013. Pre and post storm transects of WC3 showed a decrease in SPM from ~500 μg L^{-1} to 375 μg L^{-1} at the surface (Fig. 4.7a and b). The link observed ~5–12 km down the branch before the storm, withdrew to ~0–7 km after the event (Fig. 4.7a and b). During the storm, the BNLs remained extending along the axis with a reduction of SPM of ~100 μg L^{-1}. Weaker INLs emanated at INL core depths centred at; 550 m, 850 m, 1150 m and 1600 m, mirroring the reduced SPM concentrations in the BNLs (Fig. 4.7a and b).

A thick layer of SPM (~200 μg L^{-1}) was observed down to ~200–300m across the upper reaches of WC3, coinciding with development of a homogenous layer to ~200–300 m (Fig. 4.8). Repeat profiles in the middle of the axis of WC3 at ~1300 m capture the development and decay of this layer (Fig. 4.9). At the onset of the storm, this layer is most prominent with a bulge between 200–300 m and INL cores at 550 m and 850 m also initially increasing to thickness of ~100 m with SPM values ~200 μg L^{-1} (Fig. 4.9; T + 0). After this initial increase, INL cores moved vertically off central locations presenting as many weak, thin layers in preference to thicker layers of material particularly between 1000–1200 m (Fig. 4.9; T + 48 to T + 107). These repeat profiles at the central location in WC3 showed the continued presence of INLs throughout the progression of the storm with the breakup of thicker layers, possibly as a result of storm effects and/or the exhaustion of SPM.

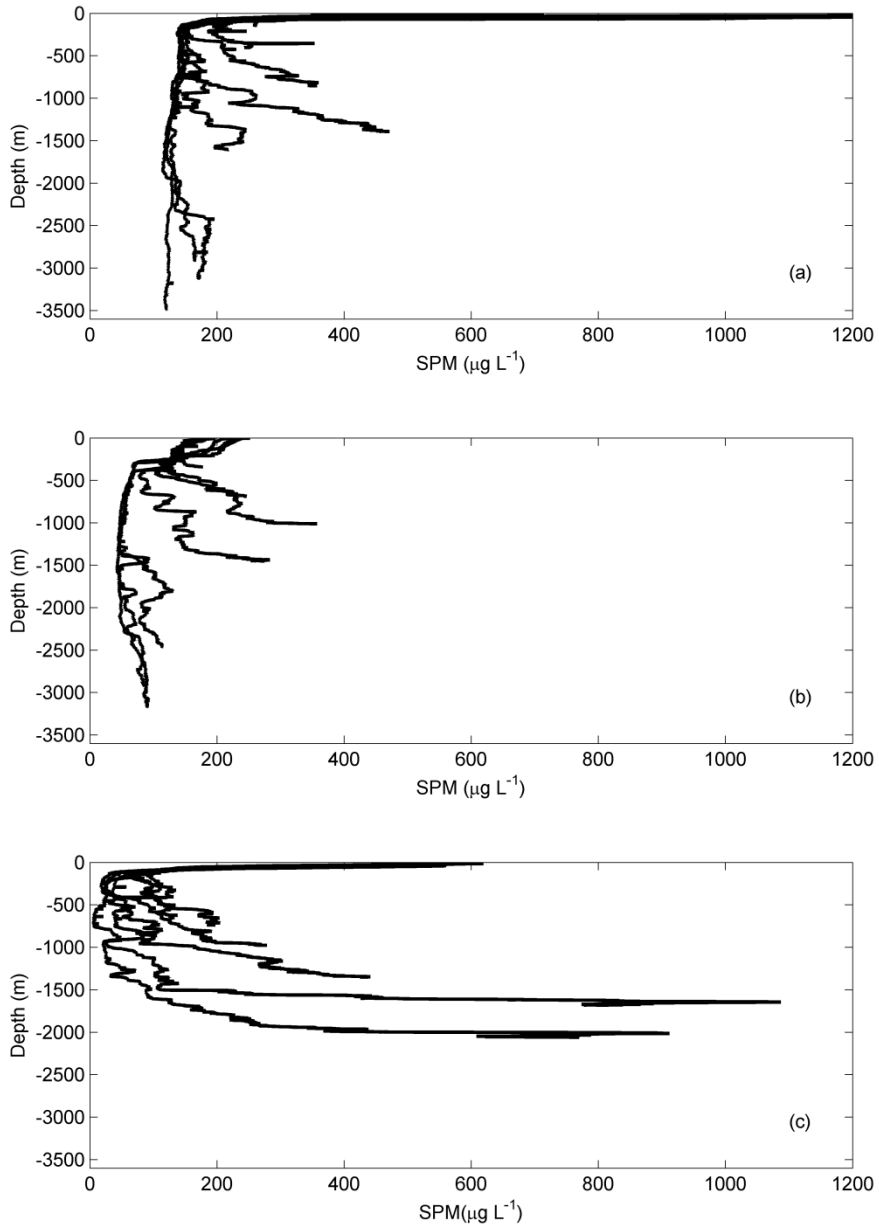

Fig. 4.6. Vertical profiles of SPM (μg L^{-1}) along axis of WC2 in (a) April 2011, (b) April 2012, (c) June 2013.

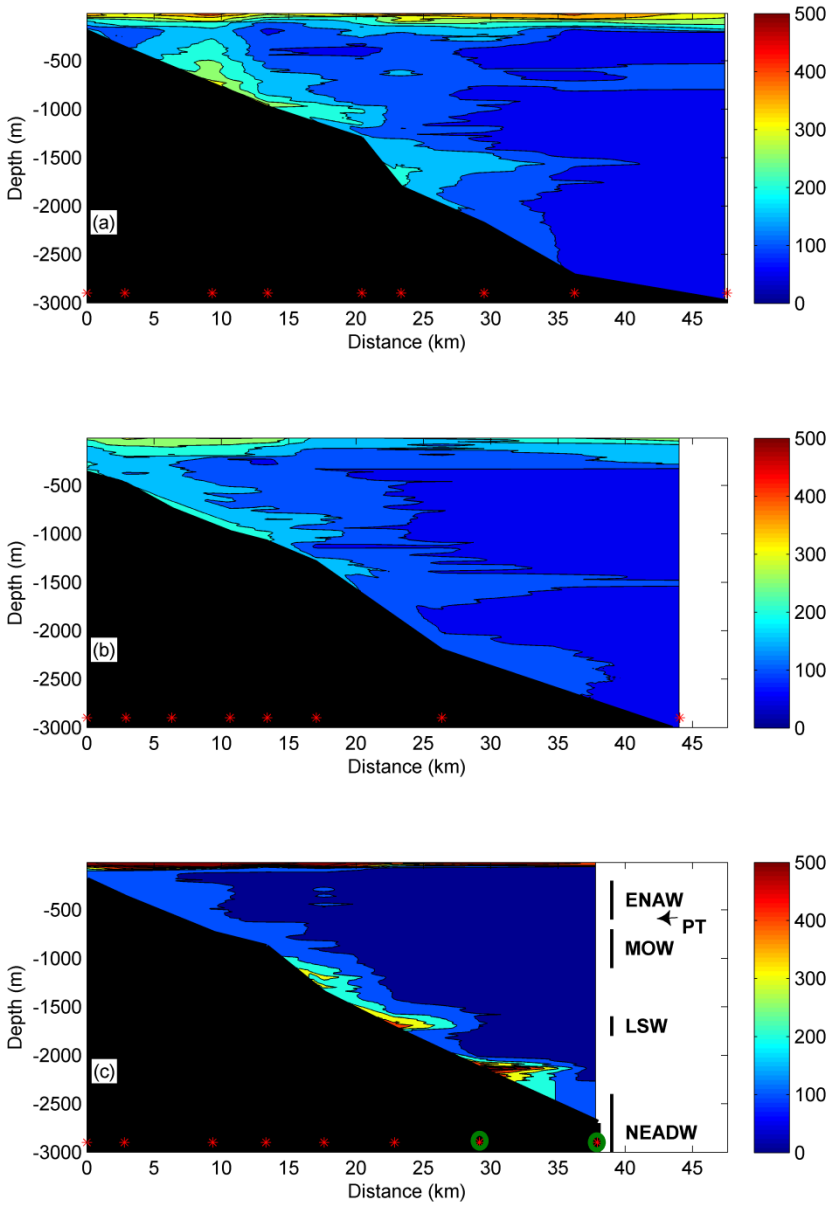

Fig. 4.7. Nepheloid layer distribution along axis of WC3 (a) pre storm, 2012 (b) post storm, 2012 and (c) 2013. Colour bar indicates concentration of SPM (μg L^{-1}). Station locations are indicated with a red star. Green circle indicates location of possible anthropogenic influence from WC4. Water masses; Eastern North Atlantic Water (ENAW), Mediterranean Outflow Water (MOW), Labrador Sea Water (LSW), North Eastern Atlantic Deep Water (NEADW) and the permanent thermocline (PT) are labelled.

4.5 Discussion

4.5.1 Seasonal and temporal influences

Variations in concentrations of SPM at the surface and the presence and absence of a turbid link from the surface to ~500 m can be accounted for by the survey timing relative to the phytoplankton spring bloom. Both the 2011 and 2012 surveys were carried out in April likely coinciding with the initialisation of the spring bloom (Garcia-Soto and Pingree, 2009), characterised by increased rapid sinking and settling of phytodetritus (settling velocities: 430–1380 m d^{-1}). Small delays in this seasonal phenomenon can have marked influences and lower surface values in 2012 can be accounted for by the slightly later launch of this survey before the intensification of this feature (NASA Earth Observations, 2014). An extensive coccolithophore bloom was observed on the passage from the Celtic Sea shelf to Whittard Canyon during the 2013 survey. This phytoplankton group indicates the progression of the spring bloom, thus combined with the timing of the survey in early June allowing sufficient time for the sinking of material, explaining the absence of this feature.

4.5.2 Storm effects during 2012 survey

Winds changed from north-easterly to a north-westerly direction (WNW–NW) reaching speeds of ~30 m s^{-1} during the storm activity in 2012. The currents measured during the storm showed an upper layer of higher flow that corresponded to the deeper mixed layer created by the storm. A change in the easterly component observed at ~400 m matched the depth of the previous winter mixed layer and the permanent thermocline. The slope current along this margin with a typically poleward flow (Huthnance, 1986) appears to have been reversed to a south-ward drift here (e.g. Pingree et al., 1999). The flow characteristics measured are likely caused by the combination of the general storm generated upper layer and the seasonal weakening of the slope flow (the SOMA response, Pingree and Le Cann, 1990). The increased mixing further down the water column, combined with the net flow of water up canyon (Amaro et al., 2015) maybe causing the INLs to break up into numerous weak, thinner layers observed during the storm. The reduced stratification could also induce better matching or transmissive reflection of internal waves with energy propagating

upslope during the storm causing the dissipation of INLs. Gardner et al. (1989b) postulated that mixing in layers (decreasing stratification and N) could create a feedback mechanism where internal waves are more likely to be focused where mixed layers are established and intercept the slope, which may explain the increased number of layers during the storm.

The accumulation of material in a shelf break-like INL was observed in the upper ~200–300 m. The development of a shelf-break INL during storms where the thermocline intersects the seabed has been documented elsewhere (Puig & Palanques, 1998). Although too shallow for influence of the permanent thermocline, the depth range coincides with the base of mixing by the storm, suggesting that this gradient constituted an interface to retain material resuspended during the storm. Significant wave heights of 8 –9 m were observed during the storm which would certainly induce bottom orbital currents sufficient to resuspend fine bottom material in the upper reaches of the canyon and onto the shelf (Oliveira et al., 2002). Resuspended material potentially flows then as a turbid plume into the head of the canyon, restricted by the base of the storm (McCave and Hall, 2002). Emphasis of the surface to ~500 m link in WC2 turbidity provided further evidence of material at the surface coming in from the shelf. Decreased surface concentrations indicate down-ward mixing by the storm which holds important implications for temporal nutrient fluxes with the rapid transport and mixing of fresh material renewing nutrients at the surface.

The effect of storms on SPM distribution contrasts between canyons (e.g. Durrieu de Madron, 1994; Puig et al., 2004). Water column stratification and the density field are closely related in the development of NLs (Oliveira et al., 2002) and effects on these appear key to the influence of storms. At the highly stratified Guadiaro Canyon, the distribution of material was not directly affected by the occurrence of storms but rather the well-established seasonal stratification and density fronts present during the summer time (May) survey that restricted the storm effects (Puig et al., 2004). The absence of strong stratification during the onset of the storm here appears to have allowed for greater storm influence, and combined with other seasonal phenomena in the typical currents observed, affects the distribution of SPM in the canyon.

4.5.3 The recurrent generation of INLs

Reports on of NLs in the Whittard Canyon are limited but observations in the mid-lower reaches of the branch adjacent to WC4 showed a BNL present from 1200 – 2000 m (Huvenne et al., 2011). Here, BNLs were observed extending to > 2500 m in all branches (WC1–3). Repeated observations of INLs at approximately the same depth range suggest recurrent processes interacting at the seabed. INL offshore extensions (~20–25 km) twice the Rossby radius are greater than typical extensions observed at open slope locations (Thorpe and White, 1988), probably owing to the intensification of processes due to the canyon topography.

4.5.3.1 Baroclinic motions

Numerous studies have linked the focusing of internal wave energy within submarine canyons to benthic resuspension and INL formation (e.g. Shepard, 1975; Cacchione and Drake, 1986; Gardner, 1989b; Puig et al., 2004). Further north along the slope at the Porcupine Bank, internal waves have also been suggested as physical drivers for enhanced resuspension and INL generation (Dickson and McCave, 1986; Thorpe and White; 1988). Tidally transformed barotropic flows and locally generated baroclinic motions can take two forms; (i) bottom trapped baroclinic waves of period $> 2\pi/f$ or (ii) freely propagating internal waves that can be focused (Hotchkiss and Wunsch, 1982). The extent of amplification of bottom trapped waves suggests matching of the forcing diurnal frequency, and the natural oscillation period within the water column, determined by N and slope of the seabed slope (α), such that;

$$N * \sin(\alpha) = maximum \qquad (4.3)$$

Rhines (1970) and Huthnance (1981). The permanent thermocline is characterised by large N values and promotes large fluxes of resuspended material along and across slopes at mid-water depths (White, 2007; White and Dorschel, 2010). Bottom current enhancement might therefore be expected from baroclinic motions driven by tidal forcing at intersects of the permanent thermocline with the seabed (Cacchione and Drake, 1986; Thorpe, 1999). Indeed, White and Dorschel (2010) have shown that strong baroclinic tidal motions and residual currents are apparent at the permanent thermocline, resulting in maximum

residual flows that exceed the threshold for the resuspension of fresh organic material (15 cm s^{-1}) >50% of the time (Thomsen and Gust, 2000).

Maxima in N were detected between 575–975 m (575 m, 875 m, 975m) in WC2 and (725 and 875 m) in WC3 coinciding with the depth range of the permanent thermocline (600–900 m), corresponding to the occurrence of INLs centred at ~ 550 and 850 m. The permanent thermocline can trap diurnal currents causing enhanced velocities at the intersection, however, there was no evidence of diurnal tides here and it is more likely that it acts as a preferential guide for propagating internal waves focusing energy at the seabed and/or as a surface for the extension of advected and resuspended material (Puig & Palanques, 1998).

The reflection of freely propagating internal waves can lead to the focusing of energy. The characteristics and breaking of the internal wave ray slope and angle of energy propagation (β) is dependent on N, f and the wave frequency (σ), where;

$$\tan(\beta) = [(\sigma^2 - f^2)]/(N^2 - \sigma^2)]^{1/2} \quad (4.4)$$

β is maintained by wave reflection, such that the wave number of the internal waves, changes on reflection from a sloping seabed (Thorpe, 1987; White and Dorschel, 2010). Where critical conditions are found (α/β = 1); energy is focused at the boundary resulting in enhanced current velocities and turbulent mixing that inhibits the settlement of SPM. In canyons, reflective supercritical conditions (α/β>1) are common with steep vertical walls focusing waves towards the canyon floor (Hotchkiss and Wunsch, 1982). Where transmissive or subcritical conditions (α/β<1) are met energy from further offshore can be propagated upslope into the canyon head.

To assess the type of reflection in WC2 and WC3, the resonance of internal waves were calculated over mean profiles of N at 50 m intervals, from CTD density profiles, with α determined from the INFOMAR bathymetry data set projected in ArcGIS. Critical conditions were identified between 400–500 m, 925–1575 m and 1725–1825 m (Fig. 4.10), corresponding to approximately the same depths of INL occurrence. Supercritical conditions were noted between the depths of critical reflection with peaks at 575 m, 675 m, 875 m, 975 m, 1125 m, 1275 m, 1775 m. Steep vertical walls in Whittard potentially reflect the internal

wave angle of propagation at right angles, altering the wavelength and focusing the wave into the lower reaches of the canyon (Hotchkiss and Wunsch, 1982; Gardner, 1989b) and thus resuspending material at the seabed where deeper INLs were observed (e.g. WC3 ~2300 m Fig. 4.7c). It seems likely that the high density displacements concentrated on the southern side of WC3 observed by Johnson et al. (2013; their Fig. 7; Appendix A) are a result of this focusing. In highly complex corrugated environments, the propagation of internal waves is 3-dimensional and highly varied (Holt and Thorpe, 1997) and it is also likely to be occurring across the branches here as seen in models of other canyons (e.g. Hall and Carter, 2011). Whether the turbulent energy transport in INL extensions continues to resuspend material, contributing to the source of other layers by reflection or is dissipated as the layer decays away from the seabed is unclear.

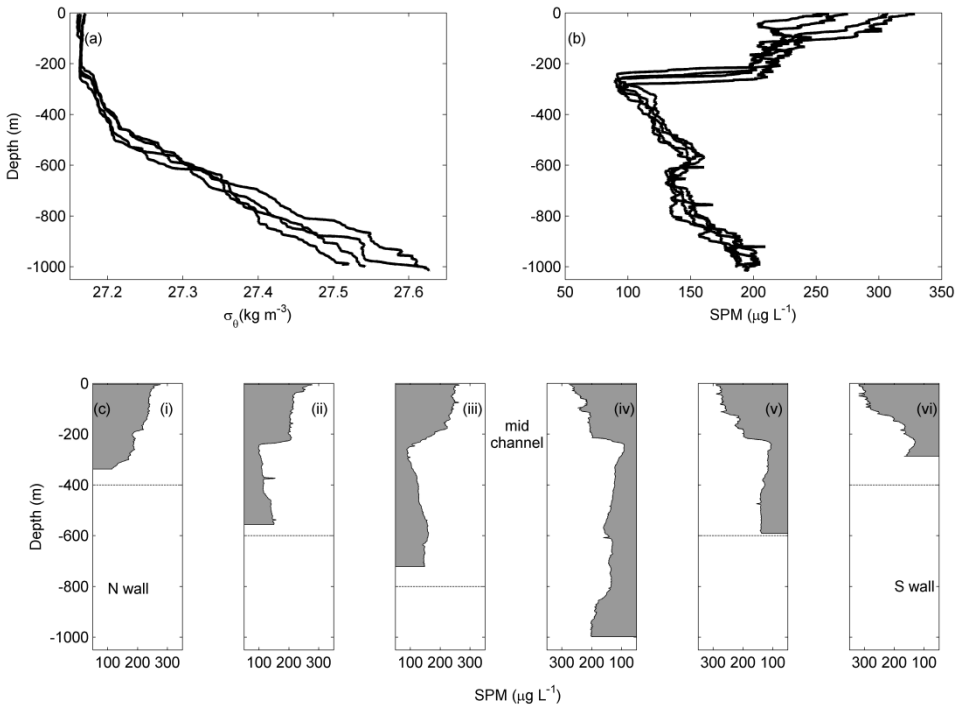

Fig. 4.8. Across transect at upper WC3 in 2012 (over 6–7 h). Vertical profiles of (a) density (σ_θ, kg m^{-3}), (b) SPM (μg L^{-1}) taken at the middle station and (c) distribution of nepheloid layers extending from west to east canyon walls. Last three profiles (iv-vi) are reversed to demonstrate the extension of the layers from the sloping "V-shaped" canyon walls.

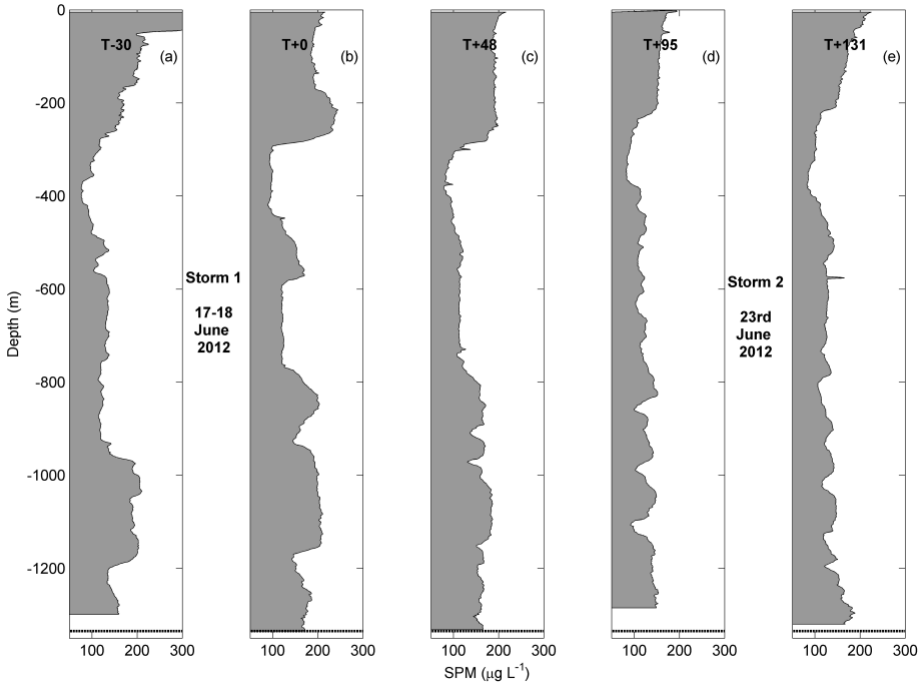

Fig. 4.9. Time-series of repeat vertical profiles at ~1300 m in WC3 over ~6 days period at (a) Storm (T = 0) - 30hrs, (b) storm onset T = 0, (c) Post storm T + 48 hrs, (c) T + 95 hrs, (d) T + 131hrs. Onset of storm 1 is at T + 0 and storm 2 is at T + 114. Thin dashed lines show the seabed.

4.5.3.2 Influence of Mediterranean Outflow Water

The importance of MOW as an erosional and depositing contourite has emerged in recent years with observations of increased turbidity at the boundaries caused by enhanced velocities (van Rooij et al., 2010; Rebesco et al., 2014). NLs have been associated with intensified internal tidal motions at the intersection of the upper boundary of the MOW vein in Nazaré canyon (41–43 °N) further south on the Portuguese shelf (Oliveira, et al., 2007). MOW flowing north of Nazaré has significantly reduced in turbidity (<25 mg m^{-3}) and salinity with a core reduced from 36.7 in the Gulf of Cadiz to ~36.2 (McCave and Hall, 2002). Further north at Whittard (48–49 °N) further particle fall out and dilution of salinity can be assumed with salinities observed here between 35.6–35.8.

MOW between 700–1100 m coincides with observation of large BNL and INL extensions at reccurring depths (e.g. Fig. 4.7). Fig. 4.11 shows a T–S diagram

colour coded to the concentration of SPM for profiles made in water depths (a) <1400 m and (b) >1400 m. The presence of MOW in the canyon appears to present two different scenarios. At shallower water depths (i.e. <1400 m), MOW flows like a boundary current close to the continental slope. High SPM values were often observed at the lower boundary of the core (i.e. ~1000–1100m) which is less saline (35.625) than counterparts further offshore. In deeper waters (i.e. >1400 m) MOW is flowing further offshore and maintains its integrity due to minimum interactions and mixing (35.75). These boundaries and the strong highly saline core are characterised by relatively clear water suggesting that increased SPM at mid-water depths are not directly related to MOW presence.

McCave and Hall (2002) similarly detected increased turbidity with spatial and temporal variability due to MOW, with INL decay in MOW from SW Portugal to NW Spain due to particle fall out and mixing with underlying LSW. The results here would suggest that MOW flowing at shallower depths (i.e. at the margin) interacts with the sloping seabed and induces INL extension from turbulent mixing in the BNLs. The mixing zone at lower boundary of MOW provides a pycnocline for the extension of resuspended material or maybe a preferential level for propagation of internal waves at a localised maximum of N (McCave and Hall, 2002).

Maxima in N in both WC2 and WC3, coincides with the MOW core at ~900 m (35.6–35.8). Peaks in N were also detected at 725 m and 975 m with critical conditions between 925–1225 m and supercritical reflection at 975 m, 1125 m and 1275 m related to MOW (Fig. 4.10). The upper boundary of MOW also coincides with the lower boundary of the permanent thermocline (600–900 m). Thus local maxima in N induced by the steep density gradients of these boundaries appears to encourage baroclinic reflection between ~600–1200 m aiding the resuspension that derives INLs, rather than the mixing zones of these boundaries being solely responsible (McCave and Hall, 2002). Differentiation between the effects of the permanent thermocline and MOW are difficult here, but likely contribute to varying degrees.

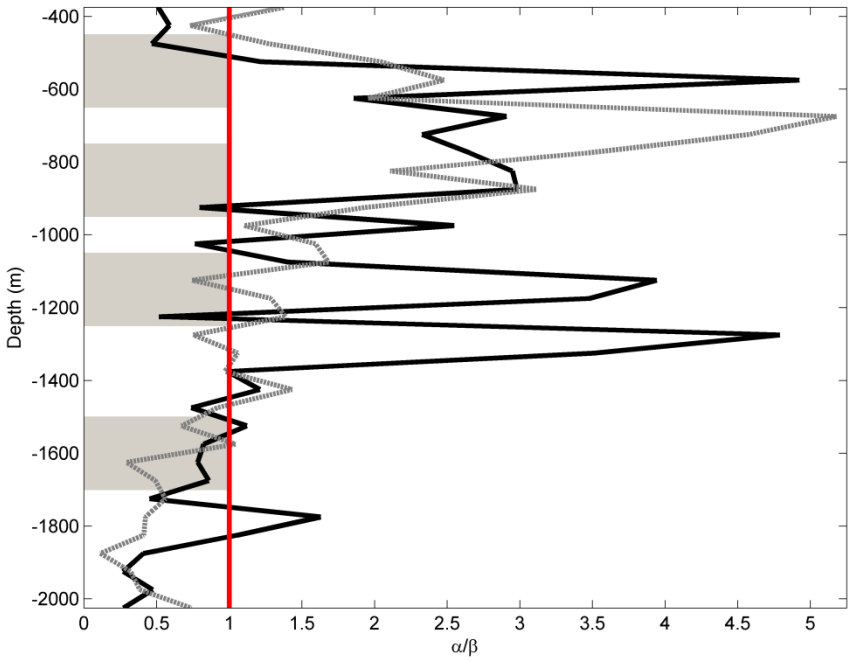

Fig. 4.10. Vertical profile of α/β for WC2 (–) and WC3 (---). Red line shows critical condition (α/β = 1). Shaded grey areas show depth ranges of repeated nepheloid layer occurrence.

4.6 Conclusions

In Whittard Canyon the distribution of SPM in NLs, extending the depth of the water column, is driven by local hydrodynamics and topographic interactions and is closely related to variations in the density stratification, attributed to a naturally varying N. Material is transported through Whittard in extensive BNLs and laterally advected distances of ~25 km in INLs. The presence of BNLs and INLs at similar depth ranges during three surveys suggests that these are permanent features generated by recurrent processes. Major resuspension areas were found in association with (i) baroclinic motions (400–500 m, 900–1600 m & 1700–1800 m) and baroclinic motions propagating at the intersection of (ii) the permanent thermocline (600–900 m) and (iii) boundaries of MOW (700–1100 m). Variation in the vertical stratification particularly through storm activity, emphasised by weak seasonal stratification, transferred to temporal variation in the distribution of NLs. The results emphasise the tandem effects of seasonal, episodic and persistent processes and responding hydrographic patterns with varying spatial importance. Whittard Canyon has been the focus of much recent research. NLs are likely aiding the advection and transport of fresh biogenic and resuspended, decayed or lithogenic material through the canyon. The description and identification of the

locations and processes involved in generating these layers is likely to aid future explorations and extend our general understanding of submarine canyons and sediment transport process. We anticipate that hydrodynamic modelling of tidal and baroclinic energy fluxes would prove valuable in furthering our understanding of these processes and predicting the occurrence of NLs.

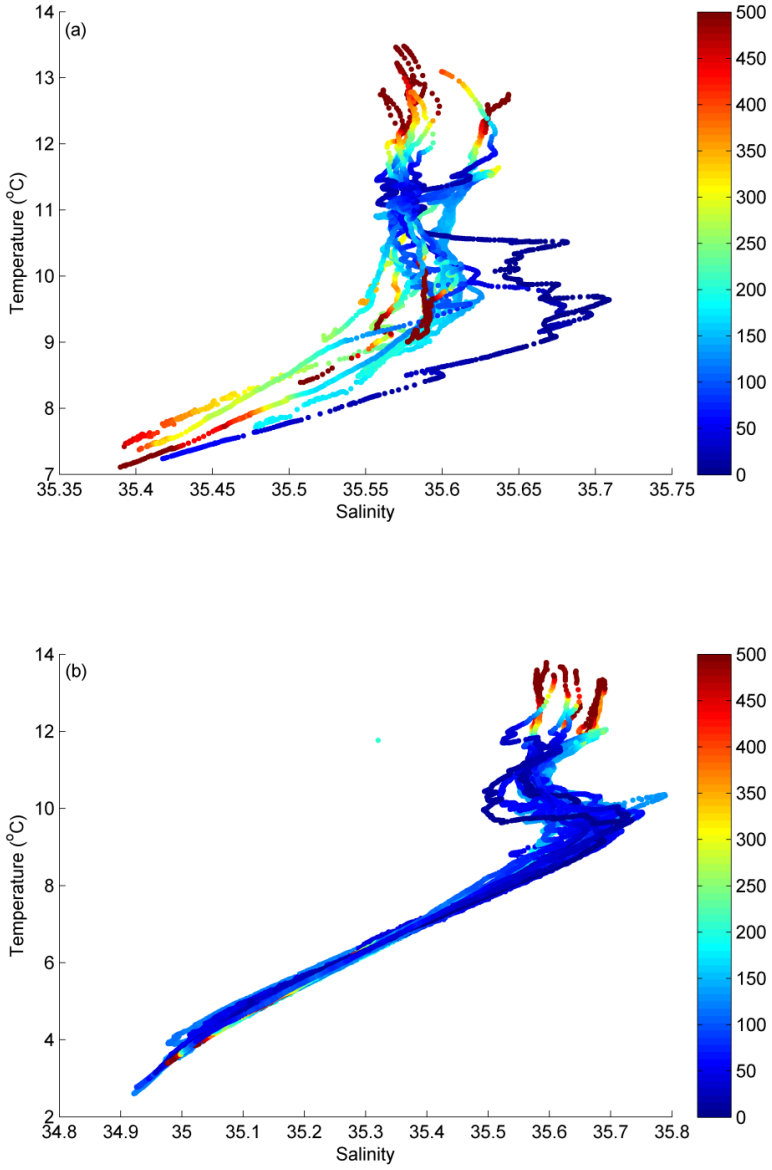

Fig. 4.11. Temperature-Salinity profiles colour coded to concentration of SPM (µg L^{-1}). Colour bar indicates concentration 0 to ≥500 µg L^{-1}. Depth range of profiles are from (a) 900–1400 m and (b) >1400 m.

Acknowledgements

This research was carried out under the Sea Change strategy with the support of the Marine Institute and the Marine Research Sub-Programme of the National Development Plan 2007–2013. We are very grateful to the captain, crew and scientists involved in; CE11006, CE12006 and CE13008, particularly chief scientist Louise Allcock and Mark Johnson as PI. Annette M. Wilson is funded by the Hardiman Research Scholarship, NUI Galway. We thank two anonymous reviewers whose comments and critiques have greatly improved this paper.

References

Allen, S. and Durrieu de Madron, X. 2009. A review of the role of submarine canyons in deep-ocean exchange with the shelf. Ocean Science, 5, 607 – 620.

Amaro, T., de Stigter, H., Lavaleye, M., Duineveld, G. 2015. Organic matter enrichment in the Whittard Channel (northern Bay of Biscay margin, NE Atlantic); its origin and possible effects on benthic megafauna. Deep Sea Research Part I: Oceanographic Research Papers, 102, 90 – 100.

Amin, M. and Huthnance, J.M., 1999. The pattern of cross-slope depositional fluxes. Deep Sea Research Part I: Oceanographic Research Papers, 46, 1565 – 1591.

Baines, P.G., 1982. On internal tide generation models. Deep Sea Research Part A. Oceanographic Research Papers, 29, 307 – 338.

Bishop, J.K.B., 1986. The correction and suspended particulate matter calibration of Sea Tech transmissometer data. Deep-Sea Research, 33, 121 – 134.

Boyer, D.L., Haidvogel, D.B. and Pérenne, N., 2004. Laboratory-numerical model comparisons of canyon flows: A parameter study. Journal of Physical Oceanography, 34, 1588 – 1609.

Cacchione, D., and Wunsch, C., 1974. Experimental study of internal waves over a slope. Journal of Fluid Mechanics, 66, 223 – 239.

Cacchione, D.A. and Drake, D.E., 1986. Nepheloid layers and internal waves over continental shelves and slopes. Geo-Marine Letters, 6, 147 – 152.

Canals, M., Puig, P., Durrieu de Madron, X., Heussner, S., Palanques, A., Fabres, J., 2006. Flushing submarine canyons. Nature, 444, 354 – 7.

Canals, M., Company, J. B., Martín, D., Sanchez-Vidal, A., Ramirez-Llodra, E., 2013. Integrated study of Mediterranean deep canyons: Novel results and future challenges. Progress in Oceanography, 118, 1 – 27.

De Leo, F.C., Smith, C.R., Rowden, A.A., Bowden, D.A., Clark, M.R., 2010. Submarine canyons: hotspots of benthic biomass and productivity in the deep sea. Proceedings of the Royal Society B: Biological Sciences, 277, 2783 – 2792 (rspb20100462).

De Stigter, H.C., Boer, W., de Jesus Mendes, P. A. Jesus, C. C. Thomsen, L., van den Bergh, van Weering, T.C.E., 2007. Recent sediment transport and deposition in the Nazaré Canyon, Portuguese continental margin. Marine Geology, 246, 144 – 164.

De Stigter, H.C., Jesus, C.C., Boer, W., Richter, T.O., Costa, A., van Weering, T.C.E., 2011. Recent sediment transport and deposition in the Lisbon–Setúbal and Cascais submarine canyons, Portuguese continental margin. Deep Sea Research Part II: Topical Studies in Oceanography, 58, 2321 – 2344.

Dickson, R.R. and McCave, I.N., 1986. Nepheloid layers on the continental slope west of Porcupine Bank Deep Sea Research Part A. Oceanographic Research Papers, 33, 791 – 818.

Duineveld, G., Lavaleye, M., Berghuis, E., de Wilde, P., 2001. Activity and composition of the benthic fauna in the Whittard Canyon and the adjacent continental slope (NE Atlantic). Oceanologica acta, 24, 69 – 83.

Duros, P., Fontanier, C., Metzger, E., Pusceddu, A., Cesbron, F., de Stigter, H.C., Bianchelli, S., Danovaro, R., Jorissen F. J., 2011. Live (stained) benthic foraminifera in the Whittard Canyon,

Celtic margin (NE Atlantic). Deep Sea Research Part I: Oceanographic Research Papers, 58, 128 – 146.

Durrieu de Madron, X., 1994. Hydrography and nepheloid structures in the Grand-Rhône canyon. Continental Shelf Research, 14, 457 – 477.

Firing, E., Ranada, J., Caldwell, P., 1995. Processing ADCP Data with the CODAS Software System Version 3.1. User's Manual. Joint Institute for Marine and Atmospheric Research, University of Hawaii, USA.

Garcia-Soto, C., and Pingree., R.D., 2009. Spring and summer blooms of phytoplankton (SeaWiFS/MODIS) along a ferry line in the Bay of Biscay and western English Channel. Continental Shelf Research, 29, 1111 – 1122.

Gardner, W.D., Biscaye, P.E., Zaneveld, J.R.V., Richardson, M.J., 1985. Calibration and comparison of the LDGO nephelometer and the OSU transmissometer on the Nova Scotian rise. Marine Geology, 66, 323-344.

Gardner, W.D., 1989a. Baltimore Canyon as a modern conduit of sediment to the deep sea. Deep-Sea Research, 36, 323 – 358.

Gardner, W.D., 1989b. Periodic Resuspension in Baltimore Canyon by focusing of internal waves. Journal of Geophysical Research, 94, 18185 – 18194.

Hall, R.A., Carter, G.S., 2011. Internal tides in Monterey submarine canyon. Journal of Physical Oceanography, 41, 186 – 204.

Holt, J.T., and Thorpe, S.A., 1997. The propagation of high frequency internal waves in the Celtic Sea. Deep Sea Research Part I: Oceanographic Research Papers, 44, 2087 – 2116.

Hotchkiss, F.S. and Wunsch, C., 1982. Internal waves in Hudson Canyon with possible geological implications. Deep Sea Research Part A. Oceanographic Research Papers, 29, 415 – 442.

Hunter, W. R., Jamieson, A., Huvenne, V. A. I., Witte, U. 2013. Sediment community responses to marine vs. terrigenous organic matter in a submarine canyon. Biogeosciences, 10, 67 – 80.

Huthnance, J.M., 1981. Waves and currents near the continental shelf edge. Progress in Oceanography, 10, 193 – 226.

Huthnance, J.M., 1986. The Rockall slope current and shelf-edge processes. Proceedings of the Royal Society of Edinburgh. Section B. Biological Sciences, 88, 83 – 101.

Huvenne, V.A.I., Tyler, P.A., Masson, D.G., Fisher, E.H., Hauton, C., Hühnerbach, V., Le Bas, T.P., Wolff, G.A., 2011. A Picture on the Wall: Innovative Mapping Reveals Cold-Water Coral Refuge in Submarine Canyon. PLoS ONE, 6, e28755.

Johnson, M.P., White, M., Wilson, A., Würzberg, L., Schwabe, E., Folch, H., Allcock, A.L., 2013. A Vertical Wall Dominated by Acesta excavata and Neopycnodonte zibrowii, Part of an Undersampled Group of Deep-Sea Habitats. PLoS ONE, 8, e79917.

Kiriakoulakis, K., Blackbird, S., Ingels, J., Vanreusel, A., Wolff, G.A., 2011. Organic geochemistry of submarine canyons: The Portuguese Margin. Deep Sea Research Part II: Topical Studies in Oceanography, 58, 2477 – 2488.

Kunze, E., Rosenfeld, L.K., Carter, G.S., Gregg, M.C., 2002. Internal Waves in Monterey Submarine Canyon. Journal of Physical Oceanography, 32, 1890 – 1913.

Lampitt, R. S., Raine, R. C. T., Billett, D. S. M., Rice, A. L. 1995. Material supply to the European continental slope: A budget based on benthic oxygen demand and organic supply. Deep Sea Research Part I: Oceanographic Research Papers, 42, 1865 – 1880.

Martín, J., Puig, P., Palanques, A., Ribó, M., 2014. Trawling-induced daily sediment resuspension in the flank of a Mediterranean submarine canyon. Deep Sea Research Part II: Topical Studies in Oceanography, 104, 174 – 183.

Martín, J., Puig, P., Palanques, A., Giamportone, A., 2015. Commercial bottom trawling as a driver of sediment dynamics and deep seascape evolution in the Anthropocene. Anthropocene. doi:10.1016/j.ancene.2015.01.002.

McCave, I.N., 1986. Local and global aspects of the bottom nepheloid layers in the world ocean. Netherlands Journal of Sea Research, 20, 167 – 181.

McCave, I.N., Hall, I.R., 2002. Turbidity of waters over the northwest Iberian continental margin. Progress in Oceanography, 52, 299 – 314.

McCave, I.N., Hall, I.R., Antia, A.N., Chou, L., Dehairs, F., Lampitt, R.S., Thomsen, L., van Weering, T.C.E., Wollast, R., 2001. Distribution, composition and flux of particulate material over the European margin at 47 ° –50 °N. Deep-Sea Research II, 48, 3107 – 3139.

Mohn, C., Erofeeva, S., Turnewitsch, R., Christiansen, B., White, M. 2013. Tidal and residual currents over abrupt deep-sea topography based on shipboard ADCP data and tidal model solutions for three popular bathymetry grids. Ocean Dynamics, 63, 195 – 208.

Morris, K. J., Tyler, P. A., Masson, D. G., Huvenne, V. I., Rogers, A. D. 2013. Distribution of cold-water corals in the Whittard Canyon, NE Atlantic Ocean. Deep Sea Research Part II: Topical Studies in Oceanography, 92, 136 – 144.

NASA Earth Observations, 2014. Available at: http://neo.sci.gsfc.nasa.gov/analysis/configure.php (Accessed: December 2014).

New, A.L., 1988. Internal tidal mixing in the Bay of Biscay. Deep Sea Research Part A. Oceanographic Research Papers, 35, 691 – 709.

Oliveira, A., Vitorino, J., Rodrigues, A., Jouanneau, J. M., Dias, J. A., Weber, O., 2002. Nepheloid layer dynamics in the northern Portuguese shelf. Progress in Oceanography, 52, 195 – 213.

Oliveira, A., Santos, A. I., Rodrigues, A., Vitorino, J., 2007. Sedimentary particle distribution and dynamics on the Nazaré canyon system and adjacent shelf (Portugal). Marine Geology, 246, 105 – 122.

Palanques, A., Durrieu de Madron, X., Puig, P., Fabres, J., Guillén, J., Calafat, A., Bonnin, J., 2006. Suspended sediment fluxes and transport processes in the Gulf of Lions submarine canyons. The role of storms and dense water cascading. Marine Geology, 234, 43 – 61.

Palanques, A., Guillén, J., Puig, P., Durrieu de Madron, X., 2008. Storm-driven shelf-to-canyon suspended sediment transport at the southwestern Gulf of Lions. Continental Shelf Research, 28, 1947 – 1956.

Pingree, R.D. and Le Cann, B., 1990. Structure, strength and seasonality of the slope currents in the Bay of Biscay region. Journal of the Marine Biological Association of the United Kingdom, 70, 857 – 885.

Pingree, R.D., Sinha, B., Griffiths, C.R., 1999. Seasonality of the European slope current (Goban Spur) and ocean margin exchange. Continental Shelf Research, 19, 929 – 975.

Pollard, R.T., Griffiths, M.J., Cunningham, S.A., Read, J.F., Pérez, F.F., Ríos, A.F., 1996. Vivaldi 1991-A study of the formation, circulation and ventilation of Eastern North Atlantic Central Water. Progress in Oceanography, 37,167 – 192.

Puig, P., Palanques, A. 1998. Nepheloid structure and hydrographic control on the Barcelona continental margin, northwestern Mediterranean. Marine Geology, 149, 39 – 54.

Puig, P., Palanques, A., Guillén, J., El Khatab, M., 2004. Role of internal waves in the generation of nepheloid layers on the northwestern Alboran slope: Implications for continental margin shaping. Journal of Geophysical Research, 109, C09011.

Puig, P., Palanques, A., Orange, D.L., Lastras, G., Canals, M., 2008. Dense shelf water cascades and sedimentary furrow formation in the Cap de Creus Canyon, northwestern Mediterranean Sea. Continental Shelf Research, 28, 2017 – 2030.

Puig, P., Palanques, A., Martín, J. 2014. Contemporary sediment-transport processes in submarine canyons. Annual Review of Marine Science, 6, 53 – 77.

Rebesco, M., Hernández-Molina, F.J., van Rooij, D., Wåhlin, A., 2014. Contourites and associated sediments controlled by deep-water circulation processes: State-of-the-art and future considerations. Marine Geology, 352, 111 – 154.

Reid, G.S., Hamilton, D., 1990. A reconnaissance survey of the Whittard Sea Fan, Southwestern Approaches, British Isles. Marine geology, 92, 69 – 86.

Rhines, P.B., 1970. Edge-, bottom- and Rossby waves. Geophysical Fluid Dynamics, 1, 273 – 302.

Shepard, F.P., 1975. Progress of internal waves along submarine canyons. Marine Geology, 19, 131 – 138.

Thomsen, L., and Gust, G., 2000. Sediment erosion thresholds and characteristics of resuspended aggregates on the western European continental margin. Deep Sea Research Part I: Oceanographic Research Papers, 47, 1881 – 1897.

Thorpe, S.A., 1987. On the reflection of a train of finite-amplitude internal waves from a uniform slope (with appendix by S.A. Thorpe and A.P. Haines). Journal of Fluid Mechanics, 178, 279–302.

Thorpe, S.A., 1999. The generation of along slope currents by breaking internal waves. Journal of Physical Oceanography, 29, 29 – 38.

Thorpe, S. A., and White, M., 1988. A deep intermediate nepheloid layer. Deep Sea Research Part A. Oceanographic Research Papers, 35, 1665 – 1671.

Van Aken, H.M., 2000. The hydrography of the mid-latitude Northeast Atlantic Ocean: II: The intermediate water masses. Deep Sea Research Part I: Oceanographic Research Papers, 47, 789 – 824.

Van Rooij, D., Iglesias, J., Hernández-Molina, F.J., Ercilla, G., Gomez-Ballesteros, M., Casas, D. Llave, E., De Hauwere, A., Garcia-Gil, S., Acosta, J., Henriet, J.P., 2010. The Le Danois Contourite Depositional System: interactions between the Mediterranean outflow water and the upper Cantabrian slope (North Iberian margin). Marine Geology, 274, 1 – 20.

Van Weering, T.C.E., Thomsen, L., van Heerwaarden, J., Koster, B., Viergutz, T., 2000. A seabed lander and new techniques for long term in situ study of deep-sea near bed dynamics. Sea Technology, 41, 17 – 27.

Van Weering, T.C.E., de Stigter, H.C., Boer, W., de Haas, H., 2002. Recent sediment transport and accumulation on the NW Iberian margin. Progress in Oceanography, 52, 349 – 371.

Vlasenko, V., Stashchuk, N., Inall, M.E. Hopkins, J.E., 2014. Tidal energy conversion in a global hotspot: On the 3-D dynamics of baroclinic tides at the Celtic Sea shelf break, Journal Geophysical Research Oceans, 119, 3249–3265, doi:10.1002/2013JC009708.

White, M., 2007. Benthic dynamics at the carbonate mound regions of the Porcupine Sea Bight continental margin. International Journal of Earth Sciences, 96, 1 – 9.

White, M., and Dorschel, B., 2010. The importance of the permanent thermocline to the cold water coral carbonate mound distribution in the NE Atlantic. Earth and Planetary Science Letters, 296, 395 – 402.

Wollast, R., and Chou, L., 2001. The carbon cycle at the ocean margin in the northern Gulf of Biscay. Deep Sea Research Part II: Topical Studies in Oceanography, 48, 3265 – 3293.

Xu, W., Miller, P.I., Quartly, G.D., Pingree R.D., 2015. Seasonality and interannual variability of the European Slope Current from 20 years of altimeter data compared with in situ measurements. Remote Sensing of the Environment, 162, 196 – 207.

Zaragosi, S., Auffret, G. A., Faugères, J.C., Garlan, T., Pujol, C., Cortijo, E., 2000. Physiography and recent sediment distribution of the Celtic Deep-Sea Fan, Bay of Biscay. Marine Geology, 169, 207 – 237.

Chapter 5

Anthropogenic influence on sediment transport in the Whittard Canyon, NE Atlantic.

Annette M. Wilson*[a], Konstadinos Kiriakoulakis[b], Robin Raine[a], Hans D. Gerritsen[c], Sabena Blackbird[d], A. Louise Allcock[a] and Martin White[a]

[a]School of Natural Sciences and Ryan Institute, National University of Ireland Galway, University Road, Galway, Ireland.

[b]School of Natural Sciences and Psychology, Liverpool John Moores University, Liverpool L3 3AF, UK.

[c]Marine Institute, Rinville, Oranmore, Co. Galway, Ireland.

[d]School of Environmental Sciences, University of Liverpool, Liverpool L69 3BX, UK.

***Published: Marine Pollution Bulletin 101 (2015) 320–329.**

Role: Lead author, responsible for overall sampling (preparation and collection), data processing, analysis, figures and writing of manuscript. Martin White assisted with the conception of the paper and design of the sampling regime, analysis and interpretation of the data. Kostas Kiriakoulakis and Robin Raine contributed to the interpretation of the elemental data and in the discussion of results. Louise Allcock was chief scientist on board during the survey and assisted with the design of the sampling regime, sample processing on board, and editing of the manuscript. Sabena Blackbird ran CHN analyser (elemental analysis). Hans Gerritsen sourced and provided the VMS data.

Abstract

Unusual peaks in turbidity were detected in two branches of the Whittard Canyon in June 2013. Enhanced Nepheloid Layers (ENLs) were defined as layers with concentrations of suspended particulate matter exceeding those of nepheloid layers typically observed in a given region. Here, ENLs had peaks in turbidity and elevated suspended particulate matter concentrations exceeding ~1 mg L^{-1} with the largest ENLs measuring between ~2–8 mg L^{-1}. The ENLs measured ~100–260 m in vertical height and were detected in water depths of between 640–2880 m. Vessel Monitoring System data showed that high spatial and temporal activity of potential bottom trawling vessels coincided with the occurrence of the ENLs. Molar C/N ratios of the suspended organic material from the ENLs showed a high degree of degradation. Regular occurrences of such events are likely to have implications for increased sediment fluxes, burial of organic carbon and alteration of benthic and canyon ecosystems.

Keywords: Trawling; Suspended particulate matter; Resuspension; Turbidity; Enhanced nepheloid layers; Whittard Canyon

5.1 Introduction

The steep sloping topography of submarine canyons promotes complex hydrographic and sedimentary conditions and provides a preferential pathway for the transport of material from continental shelves to the deep sea (Canals et al., 2013). The conduit nature of canyons causes greater food availability, attracting a wealth of benthic species and enhancing the burial of organic carbon (Masson et al., 2010). Sediment gravity flows and other disturbance events can resuspend and transport material to great depths (e.g. Hotchkiss and Wunsch, 1982; Gardner, 1989; Puig et al., 2008; 2014; de Stigter et al., 2007). Nepheloid layers, containing higher concentrations of suspended particulate matter (SPM) than the surrounding clear-water minimum (Dickson and McCave, 1986), are products of such resuspension processes and are significant contributors to the shelf edge exchange of sediment (Amin and Huthnance, 1999; Puig et al., 2014). The generation of these cloud-like benthic (BNL) and intermediate nepheloid layers (INL) is supported by the amplification of energetic processes in submarine canyons (Wilson et al., 2015; Chapter 4).

The worlds' continental margins are constantly undergoing natural evolutionary change. There is now evidence that fishing and bottom trawling significantly modify the ocean over large spatial scales (e.g. Sheppard, 2006). The capture of bottom-dwelling animals by trawling involves towing large nets that are kept open by otter trawl boards (OTBs) or rigid metal bars and blades that dig into the seabed mobilising soft sediment and crushing harder substrates. Extensive reports on the physical disturbance of the seabed by towed bottom gear conclude that trawling has negative effects on benthic fauna as well as the physical structure of the seabed and on sediment dynamics (see Gray et al., 2006). Continental shelves and deep seafloors have been homogenized, altering benthic habitats (e.g. Jennings and Kaiser, 1998; Watling and Norse, 1998; Roberts et al., 2006), smoothing topography (Puig et al., 2012) and impacting continental margin sediment transport dynamics (Martín et al. 2008; 2014a). Primarily resuspension by bottom trawling is caused directly by the weight (~10-ton) and mechanical dragging of gear (by ~1000 hp engines) along the bottom (e.g. Watling and Norse, 1998). The interaction of towed fishing gear with the seabed and surrounding ambient water can also produce high velocity bed shear stress and turbulence that entrain sediment, which disperses as a veil of SPM settling out with turbulent

decay (O'Neill and Summerbell, 2011). The excess material created in this manner can feed thick nepheloid layers (Pilskaln et al., 1998; Palanques et al., 2001; Durrieu de Madron et al., 2005) or provide additional dense elements to trigger sediment gravity flows (Palanques et al., 2006a; Puig et al., 2012; Martín et al., 2014b). Accurate estimates of the quantity of material being introduced to the water column are needed to better our understanding of the broader environmental and ecological impacts of bottom trawling (O'Neill and Summerbell, 2011). The elevated sediment transport rates and consequent impacts reported in the NW Mediterranean during trawling periods (e.g. Palanques et al., 2014) are likely to be occurring in other intensively trawled areas like the Celtic Sea. Since the 1980s the NE Atlantic and central European margin have been heavily trawled due to the increase in fishing and industrialization of fleets (Puig et al., 2012). In the northern Celtic Sea over two-thirds of the bottom area is impacted by trawling at least once per year and some areas are impacted more than ten times per year (Gerristen et al., 2013). At the edge of the continental shelf in the Celtic Sea, the Whittard Canyon has been the focus of much research in this area. Although there have been no direct studies of trawling activity in the water column at Whittard, ROV footage and side scan sonar have shown trawl marks on the spurs of the upper part of the canyon (Huvenne et al., 2011), while other studies have detected inexplicably high peaks in turbidity deeper in the Whittard Channel (Amaro et al., 2015).

In this paper we report unusual peaks in turbidity detected in two tributaries of the Whittard Canyon. We investigate the possibility that these plumes are induced by bottom trawling and discuss the effect on sediment transport dynamics at the Whittard Canyon.

5.2 Methods

5.2.1 Study area

The Whittard Canyon is a dendritic submarine canyon located at the edge of the continental shelf approximately 300 km off southwest Ireland with Goban spur to the west and Meriadzek Terrace to the south-east (Fig. 5.1). The system cuts the continental margin with the head of the canyon connected to the Celtic Sea shelf at ~200 m water depth. The branches extend (100 km) from the upper slope and are characterized by steep vertical walls. Incised by numerous gullies,

the branches converge into one deep channel at ~3800 m. The principal water masses comprise; Eastern North Atlantic Water (ENAW), Mediterranean Outflow Water (MOW), Labrador Sea Water (LSW) and North Atlantic Deep Water (NADW) (Pollard et al., 1996; van Aken, 2000). The upper water column (150–700 m) is characterized by the boundary slope or Shelf Edge Current (SEC), with mean flows of 5–10 cm s^{-1} (Pingree and Le Cann, 1990; Xu et al., 2015). Bottom currents display tidal frequencies with reports of maximum velocities varying between 16 and 40 cm s^{-1} (Reid and Hamilton, 1990; van Weering et al., 2000; Duros et al., 2011; Amaro et al., 2015). Nepheloid layers are commonly observed throughout the water column along the NE Atlantic continental margin (e.g. Thorpe and White, 1988; McCave et al., 2001) and dominate distribution patterns of SPM in the Whittard Canyon (Wilson et al., 2015; Chapter 4).

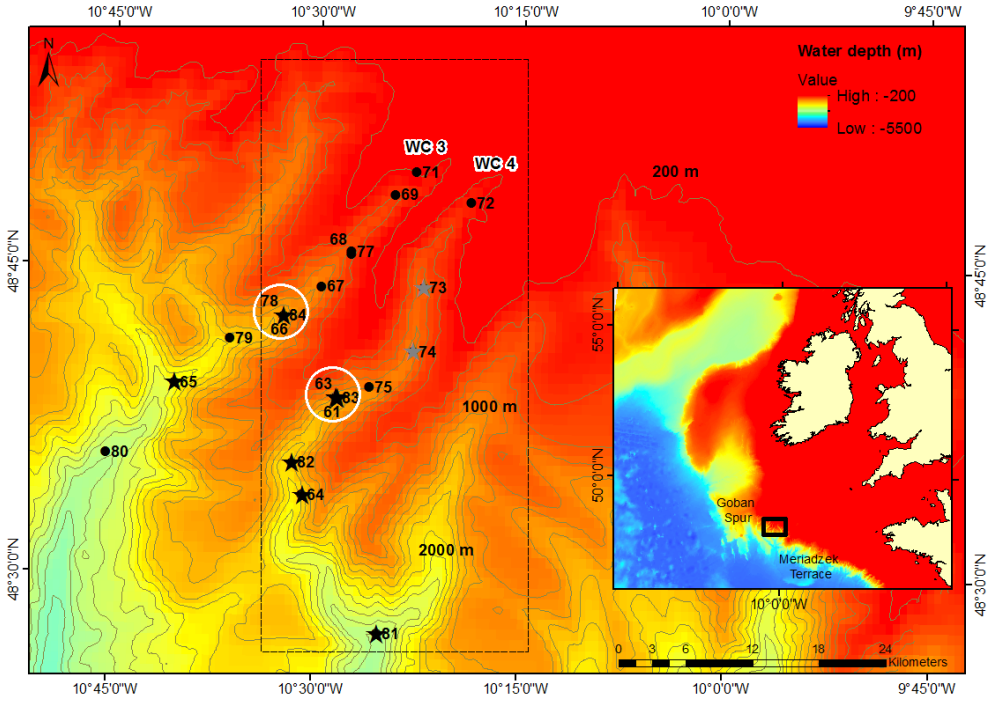

Fig. 5.1. Location and bathymetry of Whittard Canyon on the Celtic Sea Shelf, NE Atlantic. CTD stations during survey CE13008 in branches WC3 and WC4 are shown as black dots (●) and labeled with cast numbers. Locations of enhanced nepheloid layers (ENLs) are shown as black (★; high concentration) and grey (★; dilute) stars. Central stations where repeat profiles were made are marked with a white circle. Contour interval is 200 m. VMS quadrangle (48 ° 30’ – 48 ° 55’ N, 10 ° 35’ – 10 ° 15’ W) is marked with (--) box. Background bathymetry sourced from the Geological Survey of Ireland (GSI), Integrated Mapping for the Sustainable Development of Ireland’s Marine Resource (INFOMAR) and the General Bathymetric Chart of the Ocean (GEBCO).

Pelagic material and reworked sediments from the outer shelf and canyon edges tend to be coarse in the upper canyon in contrast to the alternations of coarse and fine material found in the lower reaches (Duros et al., 2011). The Celtic Sea shelf break is characterized by high internal tidal energy fluxes (Vlasenko et al., 2014) that drive nutrient fluxes and fuel enhanced primary productivity (Sharples, 2007) in surface waters along the margin and in the Bay of Biscay (100–250 g C m^{-2} yr^{-1}, Wollast and Chou, 2001). High primary production promotes good fishing (Sharples et al., 2010; 2013) and the Celtic Sea shelf break is heavily fished by various fleets mainly from Spain, France and Ireland using bottom trawls, pelagic trawls and longlines (Gerritsen and Lordan, 2014).

5.2.2 Sampling and analytical methods

Four branches of the Whittard Canyon system were surveyed between 2011 and 2013 on the RV *Celtic Explorer* with BNLs and INLs observed in all four surveyed branches (see their Fig. 1 and Table 1; Wilson et al., 2015; Chapter 4 Fig. 4.1 and Table 4.1). Here we focus on unusual observations from two of those branches, WC3 and WC4 (Fig. 5.1), during the 2013 survey (CE13008; 9–17th June), where highly turbid layers were observed repeatedly during a five day period (13–17th June). Transects and locations of sampling stations where these layers were detected are shown in Fig. 5.1 and details of water samples used in this study are shown in Table 5.1.

Hydrographic measurements were carried out using a Seabird SBE 911 CTD and SBE32 rosette system in transects along the branches with repeat profiles taken at key stations (Fig. 5.1). Vertical profiles of water turbidity were recorded by a 0.25 m path-length transmissometer attached to the CTD (C-star, WET Labs) operating at 650 nm. Transmission values were converted to beam attenuation coefficient (BAC) which was correlated by linear regression with the SPM (expressed herein mg L^{-1}) obtained from filtered water samples collected during three surveys 2011–2013 as described in Wilson et al. (2015); see their Fig. 2; Chapter 4 Fig. 4.2.

Samples for qualitative analysis (organic carbon and total nitrogen) of the SPM were collected on two stacked pre-combusted (400 °C, 4 hrs) 47 mm GF/F filters, using water samples (2–10 L) collected from the CTD rosette. On recovery, each filter was folded in half (onto itself) and then into quarters before wrapping

in combusted foil and storing at –80 °C for the duration of the cruise. Samples were analyzed according to the methods of Kiriakoulakis et al. (2009). Briefly, after freeze-drying, punched circles (~7 mm^2) were taken from homogenous areas on the top filters of the stacks (at the middle and edge of the filters) for measurement of particulate organic carbon and nitrogen (POC, PN). POC values were obtained after de-carbonation of the filters (by HCl vapor method; Yamamouro and Kayanne, 1995) and PN values were determined before decarbonation on separate circles. The analyses were carried out using a CEInstruments NC 2500 CHN analyzer in duplicate and the mean value was taken. Consistent variability between circles from the edge and middle of the filter, a filtration artifact, was observed and mean values were therefore taken to give a better approximation of the true value of the filter. The bottom filters of the stacks were used to correct for overestimations of POC and PN due to adsorption of dissolved organic matter (DOM) onto the filters (see Turnewitsch et al., 2007).

Data on the activity of fishing vessels are remotely collected by the Irish Naval Service through Vessel Monitoring Systems (VMS). These systems transmit a vessel's position and speed at intervals of 2 h or less. VMS data for the study area quadrangle (48 ° 30'–48 ° 55' N, 10 ° 35 –10 ° 15' W) for the month of June 2013 were extracted. The total records for the month of June (589) were reduced to those fitting the criteria for trawling activity and recorded during the operational survey period to Whittard Canyon (9–17th June 2013). To fit the criteria for (likely) trawling activity, vessels must be reporting the use of bottom trawling gear and be operating at ≤5 knots, a suitable threshold to denote fishing activity (Gerritsen and Lordan, 2011). Vessels meeting these criteria were selected and plotted using ArcGIS 10.2 (ESRI). Data outside these criteria were discarded.

Table 5.1. Geochemical data; date, time (UTC), co-ordinates, location, elemental; particulate nitrogen (PN), particulate organic carbon (POC) and suspended particulate matter concentrations (SPM) of samples from enhanced nepheloid layers (ENLs), dilute ENLs and water samples where no ENL was present.

	Date (June 13)	Time (UTC)	Branch WC	Cast #	Latitude N	Longitude W	Sample depth (m)	Bottom depth (m)	PN ($\mu g\ L^{-1}$)	POC ($\mu g\ L^{-1}$)	C/N (molar)	SPM ($mg\ L^{-1}$)
ENLs	14	13:50	4	64	48.5649	-10.5151	1972	1992	28.69	236.21	10	1.94
	16	14:45	4	81	48.4532	-10.4209	2758	2875	62.81	365.37	7	2.47
	16	14:45	4	81	48.4532	-10.4209	2858	2875	87.08	689.80	9	5.32
	16	19:30	4	82	48.591	-10.5282	1831	1856	104.67	625.23	7	7.48
	16	22:00	4	83	48.644	-10.4748	1148	1376	42.76	279.72	8	2.27
	16	22:00	4	83	48.644	-10.4748	1380	1377	38.77	289.83	9	8.14
	17	00:35	3	84	48.7102	-10.5421	1331	1363	NA	NA	NA	NA
Dilute	13	11:55	4	61	48.6441	-10.4757	1356	1371	47.08	190.98	5	1.20
ENLs	13	11:55	4	61	48.6411	-10.4757	1356	1371	41.25	196.83	6	1.20
	14	17:30	3	65	48.6545	-10.6736	2293	2304	49.69	271.29	6	1.00
	15	09:30	4	73	48.7344	-10.3709	635	640	22.30	199.04	10	1.14
	15	10:09	4	74	48.6826	-10.3826	860	922	14.43	337.94	27	0.73
No ENLs	15	00:25	3	67	48.7345	-10.4954	647	990	62.50	175.56	3	0.14
	15	08:45	4	72	48.8041	-10.3145	296	310	38.30	146.13	4	0.41
	16	06:55	3	79	48.6909	-10.6072	1708	1871	56.75	47.73	1	0.47
	16	10:45	3	80	48.5967	-10.7555	2583	2797	27.40	106.13	5	0.09
	16	10:45	3	80	48.5967	-10.7555	2800	2797	69.85	172.51	3	0.07
	15	04:45	3	69	48.8096	-10.4074	12	378	128.47	601.89	5	0.75

5.3 Results

5.3.1 Distribution of SPM in the water column and peaks in turbidity

The distributions of SPM and nepheloid layers under normal conditions at the Whittard Canyon are described by Wilson et al. (2015); Chapter 4. Increased SPM concentrations were commonly observed at benthic and various intermediate mid-water depths with concentrations ranging between ~ 0.28–0.6 mg L^{-1} (Fig. 5.2a and b and Wilson et al., 2015; Chapter 4). In 2013, vertical profiles in WC3 (Fig. 5.2a, c, e) and WC4 (Fig. 5.2b, d, f) showed a general increase in SPM concentration towards the seabed in significant BNLs. Similarities in thickness and depth ranges of occurrence were observed in both branches in comparison to the observations in these and other branches (WC1 and WC2) during this and previous surveys (2011, 2012, see Wilson et al., 2015; Chapter 4). BNL thicknesses of 150 – 200 m were detected with INLs extending from the BNL at 250 m, 850 m, 1150 m and 1600 m (Fig. 5.2a and b).

Unusual peaks in turbidity were observed in a number of profiles from the mid-lower reaches (i.e. >~1150m) of WC3 and WC4 (Fig. 5.2c and d) during the 2013 survey. These observations were unexpected and therefore measurements were restricted to a small number of isolated profiles. The term Enhanced Nepheloid Layer (ENL) was used to describe these layers and can be defined as nepheloid layers with SPM concentrations significantly higher (typically an order of magnitude) than the mean maximum in a given region. Concentrations of SPM in ENLs here ranged from ~1–8 mg L^{-1}; exceeding the normal range of ~0.075–0.5 mg L^{-1} for nepheloid layers in the Whittard Canyon (see Wilson et al., 2015; Chapter 4). Typical BNL concentrations were observed up to ~400 m above the seabed (Fig. 5.2e and f) with maximum SPM in the ENL just above the seabed with comparable thicknesses of normal BNLs, ranging from ~100–260 m. The ENLs were detected in the upper reaches of WC4 at ~640 m and all along the axis down to ~2875 m, a distance of ~24 km, with two observations in the middle of WC3 at 1363–2304 m.

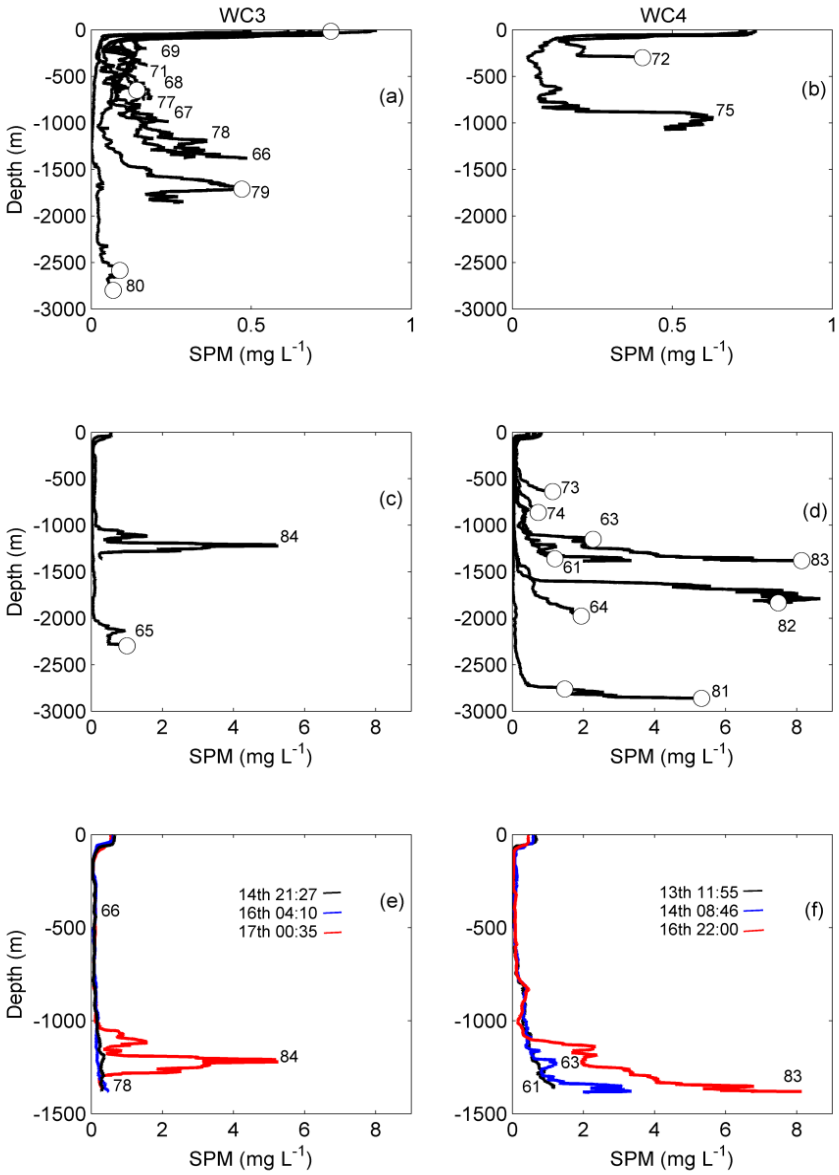

Fig. 5.2. Vertical profiles of suspended particulate material expressed in mg L^{-1} along the axis of WC3 (a, c, e) and WC4 (b, d, f). Panels show normal profiles (a, b); enhanced nepheloid layers (ENLs) (c, d); and repeat profiles at central location ~1350 m (e, f). Profiles are labelled by cast numbers. Note change in scale between normal and ENLs profiles. Depths of water samples in table 5.1 are indicated with open circles (○).

The ENLs were first observed in the middle of branch WC4 (central station indicated with white circle in Fig. 5.1) at ~1370 m (Fig. 5.2d and f; cast 61) on June 13th with concentrations of ~1.2 mg L^{-1}. This relatively low value in comparison to what was to follow was still more than twice typical maximum values (~0.5 mg L^{-1})

observed in BNLs and INLs in eastern and western branches during this and previous surveys (Wilson et al., 2015; Chapter 4). Repeat measurements at this station less than 24 hours later, revealed ENLs with SPM concentrations reaching ~3 mg L^{-1} (cast 63). On June 16th SPM concentrations exceeded 8 mg L^{-1} (Fig. 5.2f; cast 83). In the upper reaches of the branch (i.e. <1370 m) dilute ENLs (SPM values of ~1–2 mg L^{-1}) were also detected (Fig. 5.2d; cast 73, 74) on June 15th. In the lower reaches (i.e. >1370 m) conspicuous ENLs were detected at 1856 m (cast 81) and again at 2875 m (cast 82) on June 16th, with maximum concentrations at both locations exceeding 4 mg L^{-1} and matching the highest observations at the central station (white circle, Fig. 5.1) of ≥8 mg L^{-1}, 24 km further up the branch. A diluted ENL between these two locations at 1992 m was observed on 14th June with maximum concentrations of ~1.9 mg L^{-1}.

On the same day, 8.9 km to the west in the adjacent branch, WC3, a more dilute intermediate ENL (iENL) was observed with values of ~1 mg L^{-1} at 2200 m (Fig. 5.2c; cast 65). Further up the branch at ~1370 m, no evidence of enhanced turbidity was detected until June 17th at 00:35 (Fig. 5.2e). At 00:35, concentrations exceeded 5 mg L^{-1}, with a thick iENL (~110 m) observed lying between 1180–1290 m ~70 m above the seabed (cast 84). Repeat vertical profiles at this station, ~1370 m in WC3 (central station indicated with a white circle in Fig. 5.1), captured the appearance of an ENL during a ~20 h period, while profiles in WC4 show the ongoing appearance of the ENLs (Fig. 5.2f). In WC4, concentrations increased by ~2 mg L^{-1} within 21 h. iENLs were observed with peaks of the order of ~1.2 mg L^{-1} between 1100–1250 m. SPM concentrations in these layers doubled (≥2.4 mg L^{-1}) within 61 h with iENLs detected at similar depth ranges and thicknesses of ~125 m presenting as a continuum into the benthic ENL.

5.3.2 ENL categorization and molar C/N analysis of suspended particulate organic matter (sPOM)

ENLs were detected on June 13th, 14th, 15th, 16th and 17th 2013 in two tributaries of the canyon at eight locations (Table 5.1). Measurements from June 13–15th inclusive had concentrations greater than or equal to ~1 mg L^{-1} and were categorized as diluted or remnant ENLs (light grey in Table 5.1). Measurements exceeding ~2 mg L^{-1} were classified as highly turbid ENLs (dark grey Table 5.1) and were observed mainly on June 16th and 17th, in water depths of ≥1150 m.

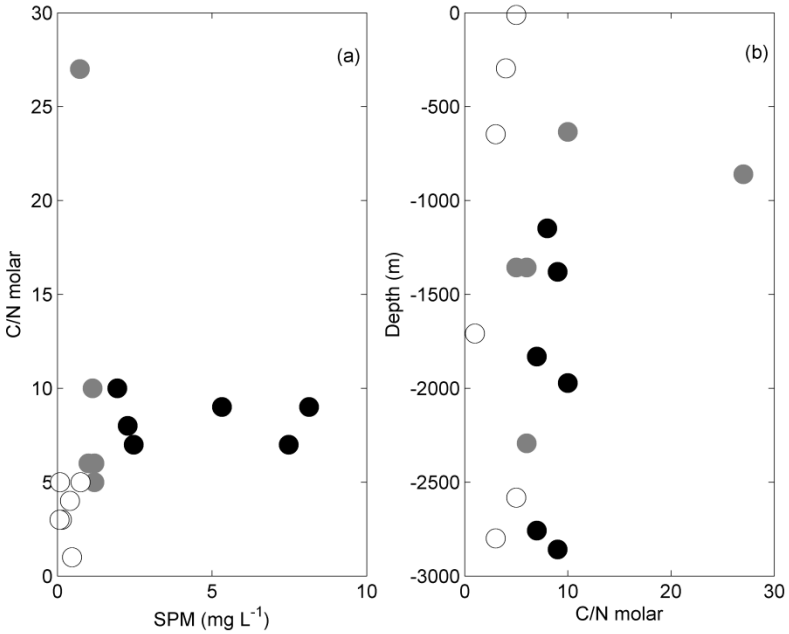

Fig. 5.3. (a) Molar C/N versus concentration of suspended particulate material (SPM) measured in mg L-1 and (b) Molar C/N versus depth (m). Data from concentrated enhanced nepheloid layers (ENLs) are shown with black circles (●); grey circles show dilute ENLs (●) and open circles (○) show data from samples where there were no ENLs. Corresponding geochemical data is shown in table 5.1.

Water samples for elemental analysis of the organic components of SPM were collected at a range of water depths, from normal profiles and profiles indicating ENLs (Fig. 5.2 and Table 5.1). Two distinct groupings were observed in the dataset corresponding to samples from ENLs and other samples from typical to small BNLs and INLs and the surface (Fig. 5.3). Generally, molar C/N ratios of sPOM increase with water depth, with ratios of 6–9 in surface waters generally indicating that the organic material is mainly sourced from phytoplankton with higher values implying that sPOM may have terrestrial contributions (unlikely thus far from land) or is more likely degraded (Kiriakoulakis et al., 2011 and references therein). A general trend of increasing molar C/N ratios with concentration of sPOM was seen in all samples (Fig. 5.3 and Table 5.1) with values within the range of those reported in other studies (e.g. Kiriakoulakis et al., 2011; Huvenne et al., 2011). Molar C/N of surface waters had a value of 5 (cast 69; SPM = 0.75 mg L^{-1}). A sample in the upper reaches of the canyon (cast 72; ~300 m) had a similar value of 4. Samples from typical to small nepheloid layers were taken from a range of depths (650–2800 m) and C/N ratios ranged between 1 and 4 (SPM ≈ 0.1–0.5 mg

L^{-1}). Samples from the largest ENLs (i.e. exceeding ~2 mg L^{-1}) had high molar C/N ratios ranging from 7–10 (SPM = 1.94–8.14 mg L^{-1}), while samples from more diluted ENLs with lower SPM concentrations (i.e. <2 mg L^{-1}) had C/N ratios ranging from 5 to 27 (SPM = ~0.73–1.2 mg L^{-1}).

5.3.3 Trawling activity on the spurs

VMS data showed 428 data points fitting the criteria for trawling activity in June 2013 and 126 during the survey period (June 9–17th) for the quadrangle studied (Fig. 5.4). The highest number of recordings for vessels that fitted the criteria during the survey period occurred on June 15th (43 data points) and June 16th (38 data points; Fig. 5.4). Vessel positions recorded by VMS were linked to the bathymetry of the area and indicated that the majority of the activity took place in 200–300 m water depths (Table 5.2). The data revealed that trawling took place day and night regardless of time, with the shallowest recording at 122 m on June 16th and the deepest on June 15th at 492 m.

The temporal activity of trawling vessels in lines or fishing tracks along the two spurs adjacent to WC3 and WC4 was revealed by VMS data (Fig. 5.5 and Table 5.2). On June 13th, one trawler was identified (based on nationality origin code and times), towing down and up the spur (146–216 m water depth) bounded by WC3 and WC4 between 2:24 and 11:24 (Fig. 5.5a). An ENL was detected in ~1370 m water depth during a CTD cast at 11:55. On June 14th at least four trawlers were identified in the area (individual trawlers were identified only where national code and times clearly showed a track), towing across the shelf at the heads of the canyon branches and down the spur between WC3 and WC4 in water depths of 144–326 m (Fig. 5.5b). Highly turbid benthic ENLs were detected in WC4 at 1387 m (8:46) and 1992 m (13:50). A less concentrated benthic and intermediate ENL was also detected in WC3 at 2304 m (17:30). Recordings for June 15th and June 16th particularly (Fig. 5.5c and d), emphasized the close proximity of trawling activity to locations where ENLs were observed. On June 15th (Fig. 5.5c), the date of highest trawling activity, at least four trawlers were active between 00:24–22:09 in water depths of 142–492 m. Time marks indicated trawling activity up and down the spur between WC3 and WC4 and to the west of WC3 including on the shelf around the head of the branches. Only two CTD casts were made in the upper reaches of the WC4 but both revealed dilute benthic ENLs at 640 m (9:30)

and 922 m (10:09). Similarly on June 16th (Fig. 5.5d), tows up and down both spurs were identified throughout a 24 h period (00:03–23:30). At least three vessels were active in water depths of 122–284 m. Benthic ENLs were detected in WC4 at three locations in water depths >1370 m at 14:45, 19:30 and 22:00. In WC3 a benthic and intermediate ENL was detected at ~1360 m at 00:35 on June 17th, approximately one hour after the last VMS recording on June 16th.

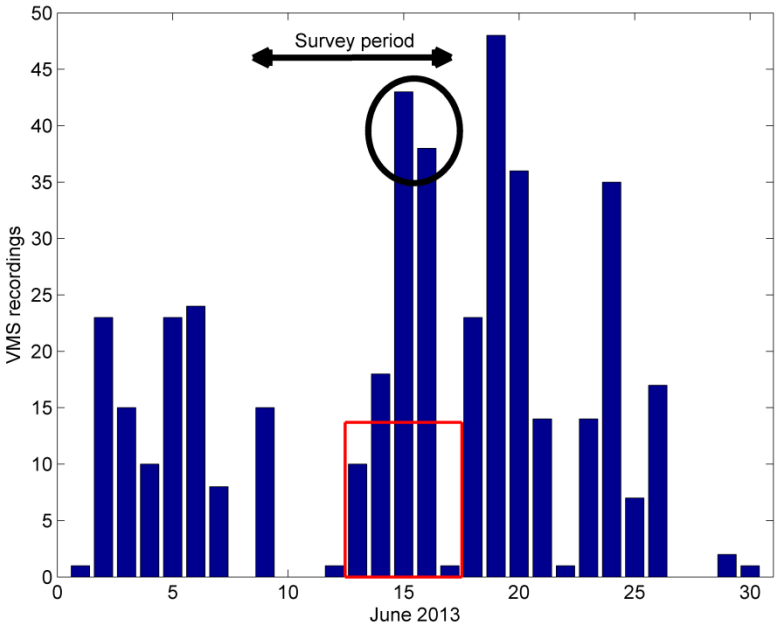

Fig. 5.4. Vessel Monitoring System (VMS) recordings of bottom trawlers in the study area (48 ° 30' – 48 ° 55' N, 10 ° 35' – 10 ° 15' W) in June 2013. Survey period is marked with an arrow and the dates when enhanced nepheloid layers (ENLs) were detected are marked with a red box. The black circle highlights the highest frequency in VMS recordings and the dates when maximum turbidity was detected.

Table 5.2. Timeline of trawling activity and enhanced nepheloid layers (ENL) occurrence. Date, number of VMS recordings for bottom trawlers, number of vessels (based on country of origin and time (UTC)), water depth range fished (based on position and local bathymetry) and fishing tracks with corresponding ENLs details.

Date (June 2013)	**# recordings**	**# vessels**	**Water depth range (m) (max-min)**	**Track period (UTC)**	**Track description & details**	**ENLs (Time)**	**Location**	**Bottom depth (m)**	**Cast #**	**ENL details**
13th	10	1	216-146	**02:24-11:24**	Down and up spur between WC3&4	**11:55**	WC4	1371	61	Small ENL (benthic)
14th	18	4	326-144	**06:24-23:24** (Blue)	Shelf edge around head and down spur to E of WC3	**08:46**	WC4	1387	63	ENL (benthic)
				11:35-21:13 (Brown)	Down spur between WC3&4	**13:50**	WC4	1992	64	Small ENL (benthic)
				15:28-17:21 (Yellow)	Across heads of WC3&4 on shelf edge	**17:30**	WC3	2304	65	Small ENL (benthic and intermediate)
				19:06-23:06 (Green)	Across heads of WC3&4 on shelf edge					
15th	43	4	492-142	**00:24** (Green)	Spur W of WC4					
				0:06-21:06 (Brown)	Shelf edge at head and spur E of WC3; down and up spur x3					

				0:24-23:23 (Blue)	Shelf edge at head of WC3 and down spur between WC3&4	**09:30**	WC4	640	73	Small ENL (benthic)
				01:01-22:09 (Yellow)	Spur between WC3&4; down and up x3	**10:09**	WC4	922	74	Small ENL (benthic)
16th	38	3	284-122	**00:03-23:30** (Green)	Spur between WC3&4; down and up x3	**14:45**	WC4	2875	81	ENL (benthic)
				00:06-06:06 (Blue)	Shelf edge at head and spur E of WC3; down and up spur x1.5	**19:30**	WC4	1856	82	ENL (benthic)
				0:23-06:23 (Yellow)	Spur between WC3&4; down and up to shelf edge	**22:00**	WC4	1376	83	ENL (benthic)
17th						**00:35**	WC3	1363	84	ENL (benthic & intermediate)

5.4. Discussion

5.4.1 Evidence for trawl-induced ENLs

The results presented here suggest that trawling activity is likely responsible for the ENLs detected at the Whittard Canyon. The times of the trawls and spatial distribution of the track lines, present a clear indication that this activity is causing increased turbidity in the water column. All of the observed ENLs were detected during a period or immediately after a period of trawling activity along the adjacent spurs or on the shelf edge at the head of the branch. Clear track lines on June 13th, 15th (yellow track) and 16th (green track), coincided both temporally and spatially with the observed ENLs. On June 14th, 18 VMS data records were clustered at the heads of both branches with time marks suggesting tows across the shelf edge. Although the activity was not directly adjacent to where the ENLs were observed, the conduit nature of the canyon is likely to have transported the material to >1300 m, where the ENLs were detected. The highest number of trawl recordings on June 15th and 16th coincided with the largest peaks in turbidity occurring on June 16th and 17th. The buildup of material with the increase in activity to this peak in fishing activity (during the study period) likely explains why the ENLs detected on June 16th and 17th were the most concentrated. Material suspended by fishing activity at the head of the canyon branches on June 14th and 15th is likely to have been transported down the canyon by this time and contributed to these concentrations.

The dislodgment and mobilization of SPM in the concentrations detected here could be induced by meteorologically driven events (e.g. storms or dense shelf water cascading (Gardner, 1989; Palanques et al., 2006b). However, the weather during the 2013 survey was calm, relative to previous surveys here (see Wilson et al., 2015; Chapter 4) and to typical conditions in the NE Atlantic. Tectonic activity is another possibility for the natural mobilization and resuspension of material in the water column detected here. However, USGS public seismic records confirmed that no there were no earthquakes (with magnitudes >2) within a 500 km radius of Whittard during the 2013 survey period (British Geological Survey earthquake database, 2015; U.S. Geological Survey, 2015). Therefore such natural processes as the generation mechanism for the ENLs observed can be disregarded here.

As a control, VMS data from the same area of the Whittard Canyon for the periods surveyed in (24–26th April) 2011 and (15–26th April) 2012 were also examined. Hydrographic data from both surveys do not show any evidence of ENLs. VMS recordings fitting the criteria for fishing were limited to 14 recordings in 2011 and were randomly scattered in the quadrangle during the survey period. There were no evident trawl lines down spurs and the low activity was possibly insufficient to induce ENLs. During the 2012 survey, 43 recordings were measured with indications of fishing tracks along the spur between WC3 and WC4 and one to the west of WC4. The hydrographic data coinciding with these tracks however was limited to mid-lower reaches of WC3. If ENLs were present, it is likely that they were missed. The increased trawling activity on the spurs during the 2013 survey period in comparison to 2011 and 2012 and advantageous CTD deployments in branches adjacent to these spurs during this time frame, allowed for the detection of these events.

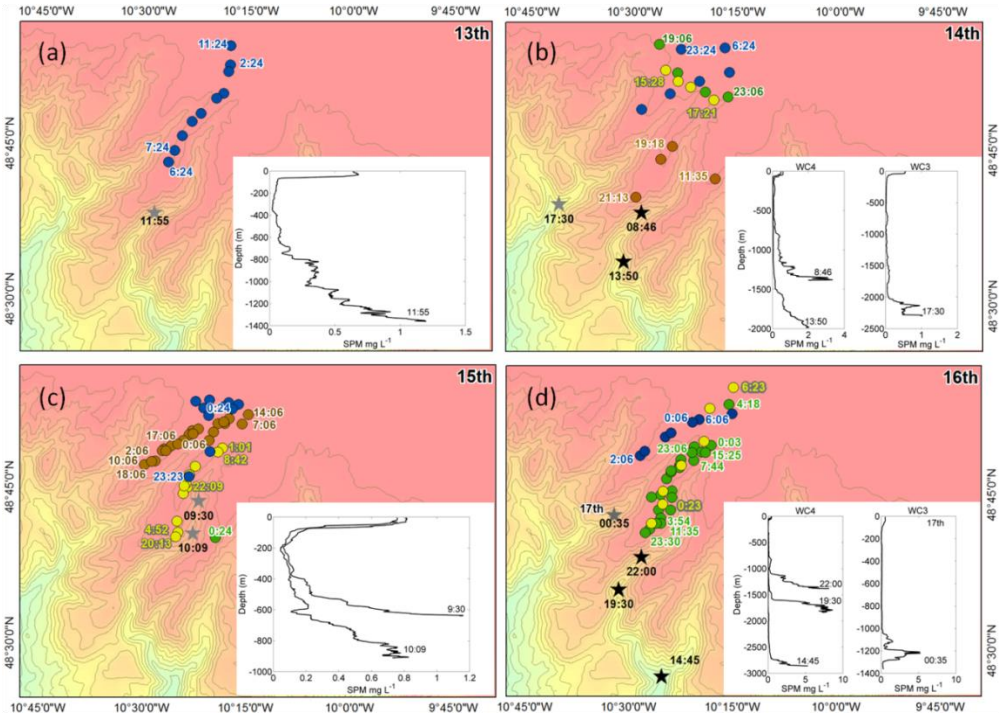

Figure 5.5. Vessel Monitoring System (VMS) recordings in study area (48 ° 30’ – 48 ° 55’ N, 10 ° 35’ – 10 ° 15’ W) on the dates enhanced nepheloid layers (ENLs) were detected; June (a) 13th; (b) 14th; (c) 15th and (d) 16th 2013. Different vessels can be identified by the colours of the dots with corresponding time marks. Locations of ENLs are shown as black (★; high concentration) and grey (★; dilute) stars. Inset on each map shows vertical profiles of ENLs expressed in suspended particulate matter (mg L^{-1}) with time (UTC) of CTD cast.

5.4.2 Concentrated deep V dilute shallow ENLs and reccurring events

The branches of the Whittard Canyon are incised with many tributaries that run from the top of the walls on the spurs into the canyon axis, providing ducts for trawl induced resuspended material. Many other studies have reported similar observations of material from sediment gravity flows or resuspension events induced by trawling being incorporated into nepheloid layers (e.g. Pilskaln et al., 1998; Palanques et al., 2001, 2014; Durrieu de Madron et al., 2005; Martín et al., 2014b). At La Fonera Canyon, the occurrence of gravity flows in the canyon axis matched with the timing of local fisherman passing a tributary of the canyon (Palanques et al., 2006a). Similarly here, ENLs were observed during a period of fishing activity or immediately after a tow. Concentrated ENLs were restricted to water depths >1300 m, although spatially the locations where dilute ENLs were detected were closer in proximity to the fishing activity. Slope analysis of bathymetry data from GSI and INFOMAR using ArcGIS (Fig.5.6), revealed steeper canyon walls in the mid-lower canyon branches (water depths >1300 m) where the most turbid ENLs were detected. In comparison, where dilute ENLs were observed in the upper reaches, the walls are lower grade. Fishing activity was restricted to the smooth spurs however, the down slope propagation of material in sediment gravity flows is more likely to occur at the steep rims of the canyon and down the steeper walls in the lower reaches (i.e. >1300 m) (Martín et al., 2014b). The bigger slopes at these locations in the canyon will cause a bigger driving force and thus explain the observations of the most turbid ENLs here.

Sediment composition may also be a factor. Sediments in upper Whittard Canyon are coarse, while those in the lower reaches are fine (e.g. Duros et al., 2011). The deeper sites where high turbidity ENLs were detected are likely lined with finer sediments that are easier to resuspend, accounting for higher concentrations of material. Coarse material in the upper reaches where dilute ENLs were detected would be more difficult to resuspend. Sediment gravity flows generated on the smooth spurs propagating down the steep canyon walls are also likely to encourage more resuspension in transit. Thus the higher concentration ENLs further offshore at deeper sites are likely a combination of both steeper sloping walls and finer underlying sediment.

It is also possible that the dilute ENLs are remnants of more turbid ENLs from previous events. The dilute ENLs may be composed of lighter material that

has remained in suspension for longer rather than heavy, coarse material. Similarly iENLs observed in WC3 between 2000–2150m (cast 65) and 1055–1290 m (cast 84), are likely to be density induced detachments. Other studies have observed the detachment of nepheloid layers from canyon spurs at the depth ranges exploited by trawling (Martín et al., 2014b) but VMS data here revealed that trawling activity was limited to water depths <500 m. The hydrographic data showed the ENLs dominated the SPM distribution of the water column, diminishing any natural nepheloid structure in the water column. Material suspended by critical internal waves that generate the nepheloid layers here (Wilson et al., 2015; Chapter 4) is presumably mixed with the newly introduced sediment. When the plume settles out after a number of hours (Martín et al., 2014b), lighter material may form intermediate nepheloid layers at another resuspension point.

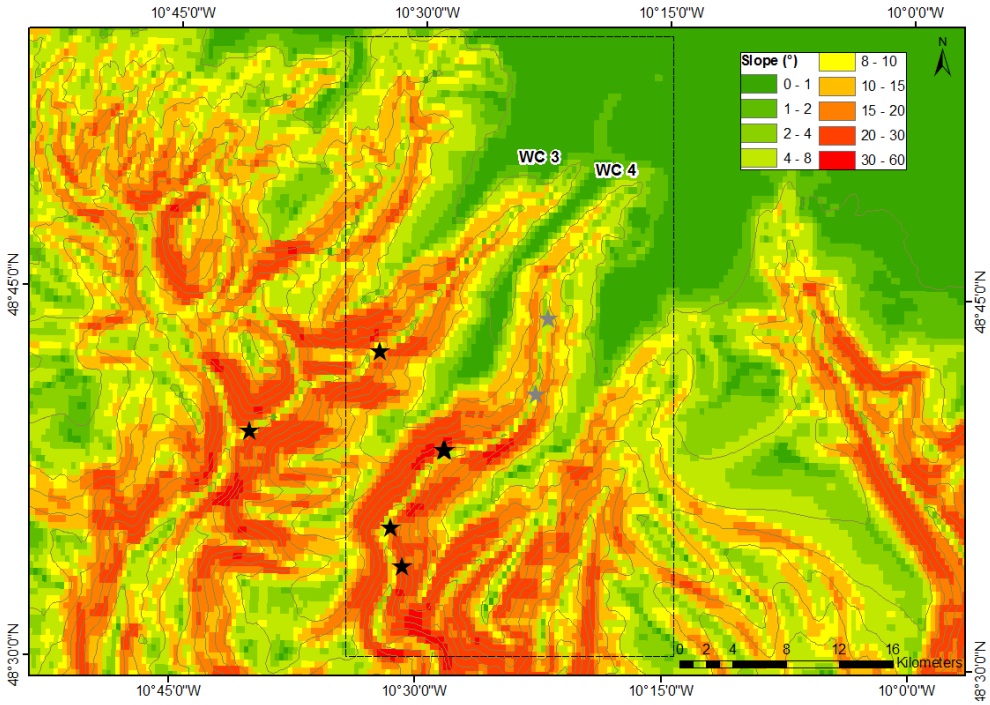

Fig. 5.6. Slope analysis of bathymetry (sourced from GSI and INFOMAR) of canyon branches (WC3 and WC4) illustrating smooth spurs and shelf at the head of the branches (<8 °) and steep canyon rims and walls (> 30°) where highly turbid ENLs (★) were detected and lower gradient (15–20 °) where dilute ENLs (★) were detected. VMS quadrangle (48 ° 30′ – 48 ° 55′ N, 10 ° 35′ – 10 ° 15′ W) is marked with (--) box.

The dilute ENLs may also be the product of smaller events prior to the larger events with the highest turbidity coinciding with the peak in fishing activity.

The amalgamation of numerous smaller events may be the cause of the high concentration ENLs. However, due to the limited data set it is not possible to conclude whether the ENLs were sourced by one event or a number of recurring events, with varying distance from the source before they were detected suggesting dilute or concentrated events. Dilute benthic and iENLs were detected in WC3 (cast 84), only two and a half hours after a highly turbid benthic ENL was observed in WC4. Although the time stamps may suggest that these events are related, with changing tides advecting material from WC4 to the adjacent branch, the VMS data shows activity on both spurs adjacent to both branches. Therefore, it is more reasonable to assume that these are recurring events. The sporadic sampling regime may be responsible for the detection of the plume in WC3 shortly after the event in WC4, while this event may have been happening instantaneously as has been reported in other studies (Palanques et al., 2006a). It seems most likely that material is coming down as sedimentary gravity flows from the sides of both canyon branches.

5.4.3 C/N ratios of sPOM in ENLs

The categorization of SPM based on molar C/N ratios of sPOM showed that material from the ENLs was degraded in comparison to material taken from areas where there were no ENLs. As expected, a general trend of increasing C/N ratios from the surface to depth was observed due to the natural break down of sinking organic matter. C/N ratios higher than the Redfield ratio (~6), often reflect the preferential loss of nitrogen-rich organic compounds (e.g. amino acids) during transport (Redfield et al., 1963; Kiriakoulakis et al., 2001). Samples from ENLs had higher C/N values than samples not from ENLs (i.e. typical nepheloid layers; see Fig. 5.5c) within the same depth range, indicating that sPOM from ENLs have undergone further degradation than that which is naturally observed with depth (see also Kiriakoulakis et al., 2001). These results would suggest trawling activity was resuspending degraded superficial sediment and lithogenic material from the shelf that had been in the system for some time.

sPOM from diluted ENLs also showed high C/N ratios, but with generally higher values observed in conjunction with higher SPM concentrations. Greater amounts of material in suspension were detected primarily on the dates of highest trawling activity, indicating that perhaps greater fishing effort mobilized

and entrained deeper sub-surface sediment. The very dilute ENL (cast 74) had a very high C/N ratio which may suggest that this is a remnant of a larger event. Lighter material from the initial event may have remained in suspension for a longer time and thus allowed for degradation of this order, which is indicative of microbial activity. Sampling procedure errors due to filter rinsing and heterogeneous subsamples of water from the CTD rosette are likely responsible for the scatter of values observed between repeat samples (cast 61).

Surface samples had high SPM and corresponding C/N ratios of 5 (cast 69) indicating fresh phytoplankton-rich material. Samples from normal nepheloid layers showed considerable variability with ratios ranging between 1 and 5. Kiriakoulakis et al. (2011) similarly reported highly variable C/N values in Portuguese submarine canyons, particularly in samples collected near the seafloor and were attributed to the heterogeneity of sinking sources and heterotrophic reworking of sPOM. Variable contributions of oxidized suspended material by diagenetic processes may explain lower C/N values (Cowie et al., 1995) or nitrogen-enriched fine grained material (Keil et al., 1994) may be responsible for very low C/N values (1 – 3) detected in some of these samples (cast 79, 67, 80).

5.4.4 Impacts and implications of bottom trawling transporting sediment

Trawling is now widely recognised as a significant driver of sediment transport dynamics (Palanques et al., 2014; Puig et al., 2012; 2014; Martín al., 2014a; 2014b). The effects of trawling vary widely with physical impacts ranging from changes in sediment characteristics, water quality and sediment transport dynamics to alterations in seabed morphology (e.g. Martín et al., 2008; Puig et al., 2012). In the Mediterranean, the industrialisation of the fishing fleet has been held accountable for accelerated sedimentation and accumulation rates in sediment cores there (Martín et al., 2008) and it is likely that intensive fishing at the Celtic margin is having a similar affect. One third of the sediment exported from the Gulf of Lions shelf is estimated to be brought about by trawling induced resuspension (Ferré et al., 2008), while export at the shelf of Ebro increased by 5–9 times during trawling periods (Palanques et al., 2014) and 5.4 x 10^3 tons of sediment was estimated to be exported from fishing grounds in 136 days at La Fonera Canyon (Puig et al., 2012). The ENLs observed here incorporate any naturally occurring nepheloid layers present before the event, into one large

gravity flow after the trigger, as similarly observed by e.g. Palanques et al. (2014) and, with concentrations of SPM at typically an order of magnitude higher than previously observed in normal nepheloid layers, are likely to have similar effects on sediment transport rates, deposition and transfer fluxes.

The physical changes made to grain sizes and deposition rates by trawling activity are also likely to influence carbon fluxes and sequestration. As discussed by Martín et al. (2014a), if bottom trawling influences, and in most cases enhances, lateral transport of sediments, then local and regional carbon budgets will be affected as will the export of material to the deep ocean. Excess turbidity can clog the respiratory surfaces of fauna, while smoothing of topographic features may disturb larval settlement and affect the unique canyon ecosystems (e.g. Jones, 1992 and references therein; Watling and Norse, 1998). The vertical walls of Whittard Canyon harbor unique assemblages (Johnson et al., 2013; Appendix A). Although the ENLs were not detected in the upper water column where these walls are found, these density laden flows are likely to impinge on the lower parts of the wall and with repeated activity could alter the morphology and habitats found on this feature. It would be reasonable to presume that trawling is causing more resuspension events that those reported here. Previous studies have also found evidence of trawling marks at the Whittard Canyon (Huvenne et al., 2011); while others have suggested the possibility that trawling causes large peaks in turbidity (Amaro et al., 2015).

Most studies on trawling resuspension have taken place in coastal and continental shelf environments but the effects of trawling are likely to be more profound at slope depths (Martín et al., 2014a). High steep slopes trigger sediment gravity flows more easily, thus promoting the down slope propagation of material (Martín et al., 2014b). Therefore, the steep slope characteristic of submarine canyon rims and bathymetry likely increases their vulnerability to the impacts of trawl induced resuspension. Background values of trawl-induced suspended sediment return after a number of hours (e.g. Martín et al., 2014b), however the processes induced by the repeated action of trawling appear to pose the greatest threat to the ocean/benthic ecosystems and margin shaping (Puig et al., 2012). The frequency of these events could not be assessed as a consequence of the nature of the study however this is a vital component and should be addressed in future studies.

5.5 Conclusions

Through a dedicated hydrographic and nephelometric study in Whittard Canyon we have detected unusual peaks in turbidity with high concentrations of SPM over a five day period. Although concentrated nepheloid layers are commonly observed in Whittard, the layers detected here had concentrations of SPM typically an order of magnitude higher than maximum values normally found in nepheloid layers at this site. The locations and presence of bottom trawlers in the area provides persuasive evidence for the relationship between trawling activity on the adjacent spurs and the occurrence of ENLs. The ENLs appear to be induced by the excess density of the additional sediment. The molar C/N ratios of sPOM were highly heterogeneous and suggested that material from the ENLs is degraded more than passively sinking or recently deposited particles on the sea floor, indicating its long residence times in the system. VMS logs and the data presented here would suggest that these are recurring events, with sufficient activity inducing dilute and concentrated plumes. Our study only provides a snapshot of the full story and more extensive study is required to fully explain these and other unusual peaks that have been detected in this region (Amaro et al., 2015). Sediment dating and knowledge of the sedimentation and accumulations rates would greatly increase our understanding. The deep sea is a fragile environment vulnerable to alterations and takes a long time to recover from negative impacts. It is likely that recurrence of plumes like those described here would have similar effects on sediment transport rates and dynamics to those reported in the Mediterranean.

Acknowledgments

This research was carried out under the Sea Change strategy with the support of the Marine Institute and the Marine Research Sub-Programme of the National Development Plan 2007–2013. We are very grateful to the captain, crew and scientists involved in RV Celtic Explorer cruises CE11006, CE12006 and CE13008. Annette M. Wilson is funded by the Hardiman Research Scholarship, NUI Galway and also received funding from the Thomas Crawford Hayes Award Trust and the Marine Institute Travel grant scheme to carry out this work. Technical support from Dave Williams and Hazel Clark and Helka Folch is gratefully acknowledged. We thank two anonymous reviewers whose suggestions and comments have greatly improved the clarity of this manuscript.

References

Amaro, T., de Stigter, H., Lavaleye, M., Duineveld, G., 2015. Organic matter enrichment in the Whittard Channel (northern Bay of Biscay margin, NE Atlantic); its origin and possible effects on benthic megafauna. Deep Sea Research Part I: Oceanographic Research Papers, 102, 90 –100.

Amin, M., Huthnance, J.M., 1999. The pattern of cross-slope depositional fluxes. Deep Sea Research Part I: Oceanographic Research Papers, 46, 1565 – 1591.

British Geological Survey earthquake database, 2014. Available at: http:// earthquakes. bgs. ac.uk/ earthquakes /dataSearch.html (Accessed on 12/9/2014 & 09/6/2014).

Canals, M., Company, J. B., Martín, D., Sanchez-Vidal, A., Ramirez-Llodra, E., 2013. Integrated study of Mediterranean deep canyons: Novel results and future challenges. Progress in Oceanography, 118, 1 – 27.

Cowie, G.l., Hedges, J.I., Prahl, F.G., Delange, G.J., 1995. Elemental and major biochemical-changes across on oxidation front in a relict turbidite-an oxygen effect. Geochimica et Cosmochimica Acta, 59, 33 – 46.

De Stigter, H.C., Boer, W., de Jesus Mendes, P.A., Jesus, C.C., Thomsen, L., van den Bergh, G.D., van Weering, T.C.E., 2007. Recent sediment transport and deposition in the Nazaré Canyon, Portuguese continental margin. Marine Geology, 246, 144 –164.

Dickson, R.R., McCave, I.N., 1986. Nepheloid layers on the continental slope west of Porcupine Bank. Deep Sea Research Part A: Oceanographic Research Papers, 33, 791 – 818.

Duros, P., Fontanier, C., Metzger, E., Pusceddu, A., Cesbron, A., de Stigter, H.C., Bianchelli, A., Danovaro, R., Jorissen, F.J., 2011. Live (stained) benthic foraminifera in the Whittard Canyon, Celtic margin (NE Atlantic). Deep Sea Research Part I: Oceanographic Research Papers, 58, 128 – 146.

Durrieu de Madron, X., Ferré, B., Le Corre, G., Grenz, C., Conan, P., Pujo-Pay, M., Buscail, R., Bodiot, O., 2005. Trawling-induced resuspension and dispersal of muddy sediments and dissolved elements in the Gulf of Lion (NW Mediterranean). Continental Shelf Research, 25, 2387 – 2409.

Ferré, B., Durrieu de Madron, X., Estournel, C., Ulses, C., Le Corré, G., 2008. Impact of natural (waves and currents) and anthropogenic (trawl) resuspension on the export of particulate matter to the open ocean: application to the Gulf of Lion (NW Mediterranean). Continental Shelf Research, 28, 2071 – 2091.

Gardner, W.D., 1989. Periodic Resuspension in Baltimore Canyon by Focusing of Internal Waves. Journal of Geophysical Research, 94, 18185 – 18194.

Gerritsen, H.D. Lordan C., 2011. Integrating Vessel Monitoring Systems (VMS) data with daily catch data from logbooks to explore the spatial distribution of catch and effort at high resolution. ICES Journal of Marine Science, 68, 245 – 252.

Gerritsen, H.D., Lordan, C. 2014. Atlas of Commercial Fisheries around Ireland. Marine Institute, Ireland.

Gerritsen, H.D., Minto, C., Lordan, C., 2013. How much of the seabed is impacted by mobile fishing gear? Absolute estimates from Vessel Monitoring System (VMS) point data. ICES Journal of Marine Science, 70, 532 – 539.

Gray, J.S., Dayton, P., Thrush, S., Kaiser, M.J., 2006. On effects of trawling, benthos and sampling design. Marine Pollution Bulletin, 52, 840 – 843.

Hotchkiss, F.S., Wunsch, C., 1982. Internal waves in Hudson Canyon with possible geological implications. Deep Sea Research Part A. Oceanographic Research Papers, 29, 415 – 442.

Huvenne, V.A.I., Tyler, P.A., Masson, D.G., Fisher, E.H., Hauton, C., Hühnerbach, V., Le Bas, T.P., Wolff, G.A., 2011. A Picture on the Wall: Innovative Mapping Reveals Cold-Water Coral Refuge in Submarine Canyon. PLoS ONE, 6, e28755.

Jennings, S., Kaiser, M.J., 1998. The effects of fishing on marine ecosystems. Advances in Marine Biology, 34, 201 – 352.

Johnson, M.P., White, M., Wilson, A., Würzberg, L., Schwabe, E., Folch, H., Allcock, A.L., 2013. A Vertical Wall Dominated by Acesta excavata and Neopycnodonte zibrowii, Part of an Undersampled Group of Deep-Sea Habitats. PLoS ONE, 8, e79917.

Jones, J.B., 1992. Environmental impact of trawling on the seabed: a review. New Zealand Journal of Marine Freshwater Research, 26, 59 – 67.

Keil, R.G., Tsamakis, E., Fuh, C.B., Giddings, J.C., Hedges, J.I., 1994. Mineralogical and textural controls on the organic composition of coastal marine-sediments—hydrodynamic separation using splitt-fractionation. Geochimica Et Cosmochimica Acta, 58, 879 – 893.

Kiriakoulakis, K., Blackbird, S., Ingels, J., Vanreusel, A., Wolff, G. A., 2011. Organic geochemistry of submarine canyons: the Portuguese Margin. Deep Sea Research Part II: Topical Studies in Oceanography, 58, 2477 – 2488.

Kiriakoulakis, K., Stutt, E., Rowland, S. J., Vangriesheim, A., Lampitt, R. S., Wolff, G. A., 2001. Controls on the organic chemical composition of settling particles in the Northeast Atlantic Ocean. Progress in Oceanography, 50, 65 – 87.

Kiriakoulakis, K., Vilas, J.C., Blackbird, S.J., Arístegui, J., Wolff, G.A., 2009. Seamounts and organic matter-Is there an effect? The case of Sedlo and Seine seamounts, Part 2. Composition of suspended particulate matter. Deep-Sea Research II, 56, 2631 – 2645.

Martín J., Puig, P., Palanques, A., Giamportone, A., 2014a. Commercial bottom trawling as a driver of sediment dynamics and deep seascape evolution in the Anthropocene. Anthropocene, 7, 1 – 15. http://dx.doi.org/10.1016/j.ancene.2015.01.002.

Martín, J., Puig, P., Palanques, A., Masqué, P., García-Orellana, J., 2008. Effect of commercial trawling on the deep sedimentation in a Mediterranean submarine canyon. Marine Geology, 252, 150 – 155.

Martín, J., Puig, P., Palanques, A., Ribó, M., 2014b. Trawling-induced daily sediment resuspension in the flank of a Mediterranean submarine canyon. Deep Sea Research Part II: Topical Studies in Oceanography, 104, 174 – 183.

Masson, D.G., Huvenne, V.A.I., de Stigter, H.C., Wolff. G.A., Kiriakoulakis, K., Arzola, R.G., Blackbird, S., 2010. Efficient burial of carbon in a submarine canyon. Geology, 38, 831 – 834.

McCave, I.N., Hall, I.R., Antia, A.N., Chou, L., Dehairs, F., Lampitt, R.S., Thomsen, L., van Weering, T.C.E., Wollast, R., 2001. Distribution, composition and flux of particulate material over the European margin at 47° – 50°N. Deep-Sea Research II, 48, 3107 – 3139.

O'Neill, F.G., Summerbell, K., 2011. The mobilisation of sediment by demersal otter trawls. Marine Pollution Bulletin, 62, 1088 – 1097.

Palanques, A., Martín, J., Puig, P., Guillén, J., Company, J.B., Sardà, F., 2006a. Evidence of sediment gravity flows induced by trawling in the Palamós (Fonera) submarine canyon (northwestern Mediterranean). Deep Sea Research Part I: Oceanographic Research Papers, 53, 201 – 214.

Palanques, A., Durrieu de Madron, X., Puig, P., Fabres, J., Guillén, J., Calafat, A., Bonnin, J., 2006b. Suspended sediment fluxes and transport processes in the Gulf of Lions submarine canyons. The role of storms and dense water cascading. Marine Geology, 234, 43 – 61.

Palanques, A., Guillén, J., Puig, P., 2001. Impact of bottom trawling on water turbidity and muddy sediment of an unfished continental shelf. Limnology and Oceanography, 46, 1100 – 1110.

Palanques, A., Puig, P., Guillén, J., Demestre, M., Martín, J., 2014. Effects of bottom trawling on the Ebro continental shelf sedimentary system (NW Mediterranean). Continental Shelf Research, 72, 83 – 98.

Pilskaln, C. H., Churchill, J. H., Mayer, L. M., 1998. Resuspension of sediment by bottom trawling in the Gulf of Maine and potential geochemical consequences. Conservation Biology, 12, 1223 – 1229.

Pingree, R.D., Le Cann, B., 1990. Structure, strength and seasonality of the slope currents in the Bay of Biscay region. Journal of the Marine Biological Association of the United Kingdom, 70, 857 – 885.

Pollard, R. T., Griffttths, M. J., Cunningham, S. A., Read, J. F., Pérez, F. F., Ríos, A. F., 1996. Vivaldi 1991-A study of the formation, circulation and ventilation of Eastern North Atlantic Central Water. Progress in Oceanography, 37, 167 – 192.

Puig, P., Canals, M., Company, J.B., Martín, J., Amblas, D., Lastras, G., Palanques, A., Calafat, A., 2012. Ploughing the deep sea floor. Nature, 489, 286 – 289.

Puig, P., Palanques, A., Martín, J., 2014. Contemporary sediment-transport processes in submarine canyons. Annual review of marine science, 6, 53 – 77.

Puig, P., Palanques, A., Orange, D.L., Lastras, G., Canals, M., 2008. Dense shelf water cascades and sedimentary furrow formation in the Cap de Creus Canyon, northwestern Mediterranean Sea. Continental Shelf Research, 28, 2017 – 2030.

Redfield, A. C., Ketchum, B. H., Richards, F. A., 1963. The influence of organisms on the composition of sea-water. In M. N. Hill, The sea, 2 (pp. 26 – 77). New York: Interscience.

Reid, G.S., Hamilton, D., 1990. A reconnaissance survey of the Whittard Sea Fan, Southwestern Approaches, British Isles. Marine Geology, 92, 69 – 86.

Roberts, J. M., Wheeler, A. J., Freiwald, A., 2006. Reefs of the deep: the biology and geology of cold-water coral ecosystems. Science, 312, 543 – 547.

Sharples, J., 2010. From physics to fish: at the shelf edge. Ocean Challenge, 17, 23 – 28.

Sharples, J., Scott, B.E., Inall, M.E., 2013. From physics to fishing over a shelf sea bank, Progress in Oceanography, 117, 1 – 8.

Sharples, J., Tweddle, J.F., Green, J.A.M., Palmer, M.R., Kim, Y-N., Hickman, A.E., Holligan, P.M., Moore, C.M., Rippeth, T.P., Simpson, J.H. Krivtsov, V., 2007. Spring-neap modulation of internal tide mixing and vertical nitrate fluxes at a shelf edge in summer. Limnology and Oceanography, 52, 1735 – 1747.

Sheppard, C., 2006. Trawling the sea bed. Marine Pollution Bulletin, 52, 831 – 835.

Thorpe, S. A., White, M., 1988. A deep intermediate nepheloid layer. Deep Sea Research Part A. Oceanographic Research Papers, 35, 1665 – 1671.

Turnewitsch, R., M. Springer, B.M., Kiriakoulakis, K., Vilas, J.C., Arístegui, J., Wolff, G., Peine, F., Werk, S., Graf, G., Waniek., J.J., 2007. Determination of particulate organic carbon (POC) in seawater: The relative methodological importance of artificial gains and losses in two glass-fiber-filter-based techniques. Marine Chemistry, 105, 208 – 228.

U.S. Geological Survey, 2015. Available at: http://earthquake.usgs.gov/earthquakes/map (Accessed on 09/6/2014).

Van Aken, H.M., 2000. The hydrography of the mid-latitude Northeast Atlantic Ocean: II: The intermediate water masses. Deep Sea Research Part I: Oceanographic Research Papers, 47, 789 – 824.

Van Weering, T.C.E., Thomsen, L., van Heerwaarden, J., Koster, B., Viergutz, T., 2000. A seabed lander and new techniques for long term in situ study of deep-sea near bed dynamics. Sea Technology, 41, 17 – 27.

Vlasenko, V., Stashchuk, N., Inall, M.E., Hopkins, J.E., 2014. Tidal energy conversion in a global hotspot: On the 3-D dynamics of baroclinic tides at the Celtic Sea shelf break, Journal Geophysical Research Oceans, 119, 3249 – 3265, doi:10.1002/2013JC009708.

Watling, L., Norse, E.A., 1998. Disturbance of the seabed by mobile fishing gear: a comparison to forest clearcutting. Conservation Biology, 12, 1180 – 1197.

Wilson, A.M., Raine, R., Mohn, C., White, M., 2015. Nepheloid layer distribution in the Whittard Canyon, NE Atlantic Margin. Marine Geology, 367, 130 – 142. doi: 10.1016/j.margeo.2015.06.002.

Wollast, R., Chou, L., 2001. The carbon cycle at the ocean margin in the northern Gulf of Biscay. Deep Sea Research Part II: Topical Studies in Oceanography, 48, 3265 – 3293.

Xu, W., Miller, P.I., Quartly, G.D., Pingree R.D., 2015. Seasonality and interannual variability of the European Slope Current from 20 years of altimeter data compared with in situ measurements. Remote Sensing of the Environment, 162, 196 – 207.

Yamamouro, M., Kayanne, H., 1995. Rapid direct determination of organic carbon and nitrogen in carbonate-bearing sediments with a Yanaco MT-5 CHN analyser. Limnology and Oceanography, 40, 1001 – 1005.

Chapter 6

The composition of suspended particulate matter transported in nepheloid layers in the Whittard Canyon.

Annette M. Wilson*[a], Martin White[a], Robin Raine[a], Sabena Blackbird[b], Nicola Dempster[c], Kostas Kiriakoulakis[c].

[a]Earth and Ocean Sciences, Ryan Institute and School of Natural Sciences, National University of Ireland Galway, University Road, Galway, Ireland.

[b]School of Environmental Sciences, University of Liverpool, Liverpool L69 3BX, UK.

[c]School of Natural Sciences and Psychology, Liverpool John Moores University, Liverpool L3 3AF, UK.

Planned submission: Progress in Oceanography

Role: Lead author, responsible for overall sampling (preparation and collection), data analysis and writing of manuscript. Martin White, Robin Raine and Kostas Kiriakoulakis contributed to the conception and design of the sampling regime, method development, analysis and interpretation of the data. Robin Raine and Kostas Kiriakoulakis provided training in lipid biomarker and pigment analysis and phytoplankton identification. Sabena Blackbird ran CHN analyser (elemental analysis) and Nicola Dempster operated the GC-MS (lipid biomarker analysis).

Abstract

The biogeochemical composition of suspended particulate material within benthic and intermediate nepheloid layers was examined from four branches of the Whittard Canyon, NE Atlantic. Material from the surface waters above the canyon had high contributions of chlorophyll *a* and other compounds derived from phytoplankton. Enrichment with fresh particulate organic matter was detected at depth, in both benthic and intermediate nepheloid layers, however spatial heterogeneity was observed. Enrichment of labile lipid compounds (mono and poly unsaturated fatty acids respectively) were higher in suspended particulate organic matter from benthic nepheloid layers at ~650–750 m than that at the surface, due to an apparent accumulation of freshly settled material. Benthic nepheloid layers at ~1300–1400 m were also characterised by their labile organic matter content but to a much lesser degree, with higher molar C/N values and bacterial signatures; suggesting reworking and formation by resuspension processes. An apparent distinction between eastern and western branches may be due to the influence of trawl induced resuspension events, at areas adjacent to the eastern branches, which seem to be altering the composition of naturally generated nepheloid layers. Heterogeneity between the various canyon branches likely reflects localised variation in energy and the differing degree of trawl activity adjacent to individual canyon branches. Distribution patterns of unique communities in the Whittard Canyon that are associated with nepheloid layers may be affected by subsequent changes in the delivery of the high-quality organic material that is utilised as a rich food source.

Keywords: Whittard Canyon; nepheloid layers; suspended particulate organic matter; organic carbon; fatty acids.

6.1 Introduction

The deep sea is generally a food limited environment and is ultimately fuelled by sinking and laterally advected particles (Antia et al., 2001). Continental margins are now recognised as important zones for the exchange and export of organic matter between productive shelf seas and the deep abyss (e.g. Walsh, 1991; van Weering et al., 1998; Wollast and Chou, 2001; Inthorn et al., 2006a). Organic matter (OM) in the ocean occurs as both dissolved and particulate material (suspended and sinking); marine snow, detritus, faecal material, phytoplankton, clays and bacteria (Volkman & Tanoue, 2002). Particulate organic carbon (POC) production throughout the water column is directly related to surface production, with typically ~5–15% of organic matter from fresh algae produced at the surface exported to the deep sea (Giering et al., 2014). In comparison to other pools of carbon, POC is relatively small. However, given the large volume of the deep ocean, POC forms a considerable reservoir of carbon and sinking particles play a crucial role in the transport of carbon from the surface to the deep sea and sediments and, in marine and global carbon cycles (Prentice et al., 2001; Turnewitsch et al. 2007).

Submarine canyons incise continental shelves and slopes; increasing the export of organic and inorganic particles, sediments and pollutants across margins (Puig et al., 2014). Canyons can act as important traps and pathways for organic matter (Masson et al., 2010; Kiriakoulakis et al., 2011), often with increased food availability in comparison to adjacent slope areas (Vetter and Dayton, 1998). Greater hydrodynamic activity in canyons due to the interaction of local flows with the variable topography enhances energy fluxes and primary production and promotes localised areas of enrichment (Bosley et al., 2004; de Stigter et al., 2007; Allen and Durrieu de Madron, 2009).

Nepheloid layers (NLs) are significant contributors to the shelf edge exchange of material. Defined by their enhanced suspended particulate matter content in comparison to surrounding clear waters, NLs are important lateral transporters of particles and OM in the pelagic to benthic coupling of material (Amin and Huthnance, 1999; Inthorn et al., 2006a). These layers of increased turbidity are often generated by baroclinic motions at the shelf edge (e.g. Dickson and McCave, 1986; Cacchione and Drake, 1986; White, 2007; Johnson et al., 2001; Puig et al., 2004). Studies on particulate organic matter (POM) have indicated that

material transported in NLs can be fresh and rich in labile components (e.g. Boetius et al., 2000; Antia et al., 2001). Spatial and temporal changes to POC and its delivery can influence (benthic) community structure (e.g. The 'Amperima Event' at the Porcupine Abyssal Plain; Billet et al., 2010). Many canyon and margin studies have also suggested that heterogenetic delivery of OM through NLs is responsible for the zonal distributions of suspension feeding fauna, organic carbon (OC) accumulation and higher preservation at margins in deep deposits (i.e. depocenters), (Puig et al., 2001; Inthorn et al., 2006a; Johnson et al., 2013; Appendix A; Kiriakoulakis et al., 2011).

The Whittard Canyon is situated on the edge of the Celtic Sea shelf – a region that is recognised as a 'hotspot' for barotropic tidal energy conversion to baroclinic motions, contributing to global internal energy fluxes (Holt and Thorpe, 1997; Allen and Durrieu de Madron, 2009; Vlasenko et al., 2014). The energetic oceanography induces intense mixing and drives nutrient fluxes that fuel rich phytoplankton communities (Joint et al., 2001; Sharples, 2007). High primary production in the area is reflected in the annual estimatesof 140 - 200 g C m^{-2} yr^{-1} for the surface waters above the canyon (Wollast and Chou, 2001). Sediments in the head of the canyon are also enriched with labile phytodetrital OM and higher concentrations of POC (Duineveld et al., 2001). Benthic nepheloid layers (BNLs) are a permanent feature in the Whittard Canyon, with extensions of intermediate nepheloid layers (INLs) at generation hotspots throughout the water column (Wilson et al. 2015a; Chapter 4). INLs between 500 and 750 m were found in association with a dense assemblage of limid bivalves and deep-sea oysters on a vertical wall (Johnson et al., 2013; Appendix A). Refuge sites for cold water corals have also been found at deeper depths associated with high turbidity and the presence of BNLs (Huvenne et al., 2011). Factors leading to enhanced POC inputs in the Whittard Canyon give rise to greater variability in coral populations and abundance in comparison to nutrient poorer areas (Morris et al., 2013). It has been suggest that fresh OM found in the Whittard Canyon is mainly brought from vertical deposition and lateral transport of phytoplankton blooms with occasional gravity flows carrying large amounts of material downslope (Duineveld et al., 2001; Duros et al., 2011; Amaro et al., 2015). NLs potentially provide pathways for the rapid transport and accumulation of rich OM, acting as a mechanism for lateral transport. This study investigates the composition of NLs through

qualitative and quantitative assessments of the organic components in order to evaluate the role of NLs as vehicles of OM supply to communities in the Whittard Canyon.

6.2 Regional Setting

The Whittard Canyon (~49 – 47 °N, 9 – 11 °W) is located ~300 km from land and, is the most westerly located of a series of 35 submarine canyons, beginning in the Bay of Biscay, that incise the slope along the Celtic Sea on the European continental margin beginning in the Bay of Biscay. The geology, sedimentology and oceanographic setting of the Whittard Canyon are heavily influenced by the Celtic Sea shelf and have recently been reviewed by Amaro et al. (2016). The dendritic morphology of the canyon with four prominent branches that extend for ~100 km, are connected to the broad (~1000 km wide) heavily fished Celtic Sea shelf at approximately 200 m water depth (Reid and Hamilton, 1990; Gerritsen and Lordan, 2014). The branches lead into deep channels with water depths of ~4000 m, before converging together into one channel in the Porcupine Abyssal Plain (~4500 m). Together the mouths of the Whittard Canyon system (west) and the Shamrock Canyon system (east) contribute to the formation of the Celtic Deep-Sea Fan (Zaragosi et al., 2000). The steep upper canyon branches (average slope 8°) are characterised by overhangs, vertical walls and cliffs that provide habitats and refuge for faunal communities (Huvenne et al., 2011; Johnson et al., 2013; Appendix A).

A significant proportion of the sediment found in the Whittard Canyon originates on the Celtic Sea shelf, consisting of pelagic material and also sediment reworked from the outer shelf and canyon edges (Reid and Hamilton, 1990; Cunningham et al. 2005; Duros et al., 2011). Sediments in the upper reaches are coarse, while deeper in the canyon along the thalwegs sediments are much finer, softer and the area is flatter (Roberts et al., 2014). Distinct layers between fine and coarse material are found deeper in the canyon and channel (Duros et al., 2011). In terms of OM enrichment, higher concentrations of POC and phytodetritus are reported in the canyon in comparison to the adjacent slope areas, particularly in the head of the system (Duineveld et al., 2001). Net sediment transport and OM fluxes from a BOBO lander in the channel (3913 m) were reported to be 0.38 and 0.01 g m^{-2} d^{-1}, respectively (Amaro et al., 2015).

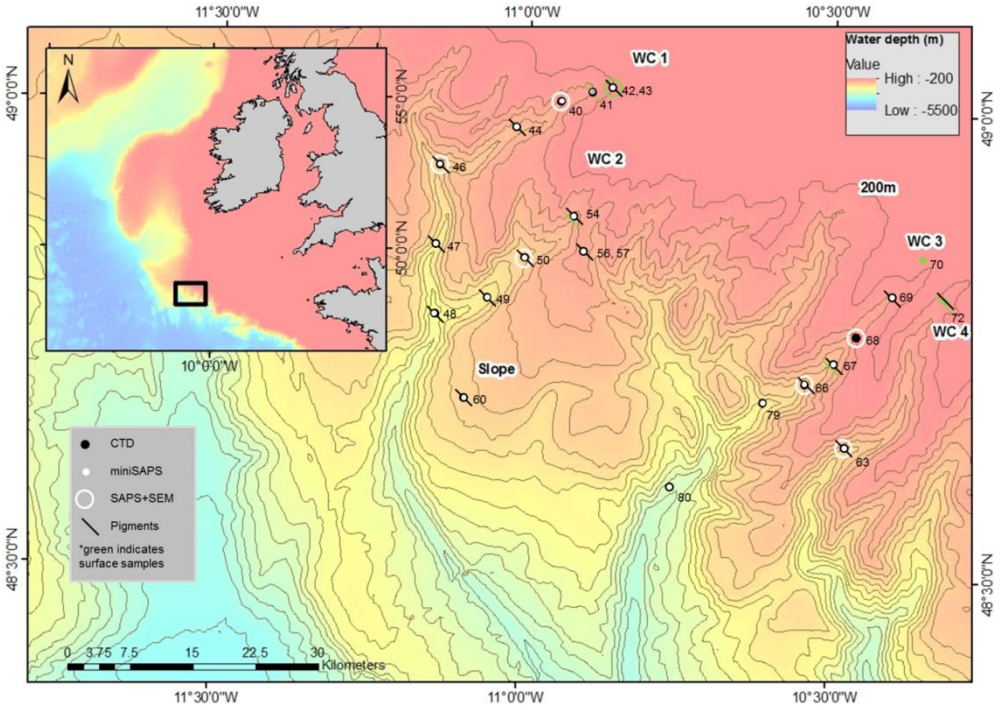

Figure 6.1. Location map showing the edge of the Celtic Sea shelf and the location of the Whittard Canyon on the continental margin. Bathymetric map shows the station locations and samples taken along the four branches (WC1–WC4) and slope in June 2013. Stations are labelled with event numbers corresponding to data in Table 6.1.

Central and intermediate water masses of Eastern North Atlantic Water, Mediterranean Outflow Water (MOW) and Labrador Sea Water comprise the upper 2000 m of the water column. The permanent thermocline lies above MOW at ~600–900 m (Pollard et al., 1996). Flow in the upper water column is dominated by boundary flows that are associated with MOW (van Rooji et al., 2010) and the European Slope current (ESC) with mean speeds of 0.5–0.1 m s^{-1} (Pingree and Le Cann et al., 1990; Xu et al., 2015). The slope current, typically flowing poleward, is known to display seasonality and often exhibits flow reversals (see September-October-March-April "SOMA" response; Pingree et al., 1999). Unusual meteorological conditions combined with the effects of seasonal stratification are also known to cause changes in the flow regime of the upper water column (down to ~400 m) with storm activity impacting baroclinic waves and energy fluxes (Stephenson et al., 2015; Wilson et al., 2015a; Chapter 4). At the margin and within the canyon, flow near the seabed displays tidal frequencies (Pingree and LeCann, 1989). Reports on the maximum speed of bottom currents

within the canyon vary between 0.16–0.4 m s^{-1} (Reid and Hamilton, 1990; Duros et al., 2011; Amaro et al., 2015), with recent modelling showing elevated baroclinic energy >0.4 m s^{-1} within some branches (Amaro et al. (2016); their Fig. 3). These tidal flows can entrain sediment and likely maintain extensive BNLs that cover the axis of the canyon down to water depths >2500 m (Wilson et al., 2015a; Chapter 4). INLs immerge from the BNLs, migrating >25 km off the slope, and are associated with the boundaries of the permanent thermocline, MOW and near-critical internal wave reflection within certain depth ranges (Wilson et al., 2015a; Chapter 4).

Differences in faunal community compositions and abundances, environmental parameters (see e.g. Gunton et al., 2015 and their table S1) and sediment characteristics (Duros et al., 2011; 2012; Hunter et al., 2013) have been observed between the eastern and western branches of the canyon and, are suggested to be related to the physical dynamics. Episodic events of down-canyon transport attributed to turbidity currents, mud-flows and sediment gravity flows have been detected in the channel (Amaro et al., 2015; 2016), while anthropogenically induced resuspension has been observed in some of the canyon branches in the eastern part of the system (Wilson et al., 2015b; Chapter 5).

Table 6.1. Station details and elemental (POC & PN), suspended particulate material (SPM), lipid (fatty acids & alcohols) and total pigments & chlorophyll *a* data used in this study. Values shaded in grey are measured from SAPS filters. Notes lipids are expressed in ng L^{-1}. POC, PN, SPM, Total. Pigments and chlorophyll *a* are in µg L^{-1}.

Station (Ev #)	CTD (#)	Location (branch)	Date June'13	Latitude (N)	Longitude (W)	Depth (m)	Sample depth (m)	POC (µg L^{-1})	PN (µg L^{-1})	SPM (µg L^{-1})	T. FA & alcohols (ng L^{-1})	T. Pigments (µg L^{-1})	Chlorophyll *a* (µg L^{-1})
40	21	WC1	10	49.0098	-10.9488	670	650	12.90	4.86	183.09	196.07	-	-
41	22	WC1	10	49.021	-10.8973	381	378	280.97	20.94	144.49	-	-	-
41	22	WC1	10	49.021	-10.8973	380	7	-	-	846.13	-	1.660	1.310
42	23	WC1	10	49.0246	-10.8668	197	~187	21.25	2.53	~75.67	-	0.093	0.015
43	-	WC1	10	49.0246	-10.8668	197	12	205.94	40.94	-	163.22	-	-
44	24	WC1	15	48.9817	-11.0203	933	930	116.17	39.17	1001.90	-	0.211	0.000
44	24	WC1	10	48.9817	-11.0203	933	859	71.14	45.45	524.58	-	0.086	0.000
46	25	WC1	11	48.9392	-11.1451	1330	~1308	34.15	2.64	1179.20	51.17	0.087	0.004
47	26	WC1	11	48.8526	-11.1415	1752	1751	258.13	57.23	1483.30	-	0.552	0.012
49	28	WC2	11	48.7984	-11.0608	1686	1677	207.22	60.54	815.78	-	0.197	0.000
48	27	WC1	11	48.6784	-11.1462	2063	~2031	34.50	4.55	754.49	-	0.161	0.000
50[x]	29	WC2	11	48.8408	-11.0258	1360	1355	23.46	2.75	425.14	18.54	-	-
50	29	WC2	11	48.8408	-11.0258	1360	1327	-	-	378.44	-	0.128	0.000
54[x]	32	WC2	12	48.8867	-10.9227	653	~642	46.31	1.90	~130.75	-	0.025	0.007
54	32	WC2	12	48.8867	-10.9227	653	8	-	-	449.03	-	0.896	0.747
66	43	WC3	10	48.7101	-10.5417	1377	421	67.07	82.33	86.24	-	0.032	0.011
66	43	WC3	10	48.7101	-10.5417	1377	1187	128.87	19.66	359.52	-	0.025	0.002
66[x]^	43	WC3	14	48.7101	-10.5417	1377	~1370	15.31	0.51	~294.26	130.21	0.094	0.000
67	44	WC3	15	48.7345	-10.4954	990	6	-	-	761.18	-	1.607	1.263
67	44	WC3	15	48.7345	-10.4954	990	647	175.56	62.50	142.60	-	0.017	0.000
67	44	WC3	15	48.7345	-10.4954	990	986	-	-	242.05	-	0.011	0.002
68	45	WC3	15	48.7613	-10.4595	753	664	157.78	33.03	140.19	-	0.023	0.007
68[x]	45	WC3	15	48.7613	-10.4595	753	739	19.93	1.35	171.87	245.44	0.014	0.003
69	46	WC3	15	48.8096	-10.4074	380	12	601.89	128.47	748.74	-	1.792	1.493
69	46	WC3	15	48.8096	-10.4074	380	378	194.87	37.27	171.87	-	0.049	0.007
70	-	WC3	15	48.8282	-10.3814	197	12	67.07	12.71	-	-	-	-
79	54	WC3	16	48.6909	-10.6072	1871	1708	47.73	56.75	470.67	-	-	-
79	54	WC3	16	48.6909	-10.6072	1871	1854	216.56	17.78	275.54	-	0.122	0.000
80	55	WC3	16	48.5967	-10.7555	2800	2583	106.13	27.40	89.49	-	0.011	0.000
80	55	WC3	16	48.5967	-10.7555	2800	2797	172.51	69.85	68.85	-	0.003	0.000
72	48	WC4	15	48.8041	-10.3145	310	10	-	-	755.61	-	0.077	0.009
72	48	WC4	15	48.8041	-10.3145	310	296	146.13	38.30	406.82	-	0.100	0.012

63*^	40	WC4	14	48.6439	-10.4736	1368	1383	44.75	6.79	2159.20	79.77	-	-
56	34	Slope	12	48.8494	-10.904	555	542	30.69	6.72	130.57	-	-	-
57	35	Slope	13	48.8501	-10.9059	562	545	11.30	2.41	123.54	-	0.023	0.007
60	38	Slope	13	48.6885	-11.0938	1302	1302	3.37	0.57	61.02	-	0.017	0.00

Exact depths of some stations varied during deployments due to steep bathymetry and swell that caused drift of the vessel particularly during SAPS pumping time (1-2 hrs). This did not affect interpretation of results.

[X]Torn SAPS filters

*Data not corrected for adsorption of DOM as there was no bottom filter. Elemental data is not included in figures.

^Data possibly affected by trawling.

6.3 Material and methods

6.3.1 Sampling

Four branches of the Whittard Canyon were surveyed during summer 2013 (CE130009: 9–17th June 2013) on the *RV Celtic Explorer* (Fig. 6.1). BNLs and INLs were detected by a 0.25 m path-length transmissometer (C-star, WET labs) operating at 650 nm in conjunction with hydrographic measurements made with a CTD (Seabird SBE 911) and SBE32 rosette system. Transmissometer data was calibrated according to the manufacturer's manual and using the calibration curve presented in Wilson et al. (2015a; see their Fig. 2; Chapter 4 Fig. 4.2) from which estimates of the concentration of suspended particulate material (SPM) at sample depths were derived (Table 6.1).

POM was collected on filters using large-volume filtration by a Stand Alone Pump System (SAPS; Challenger Oceanic) and by filtering smaller volumes of water collected from Niskin bottles by the CTD rosette (hereafter miniSAPS). Different sampling apparatus may sample different pools of organic carbon (Turnewitsch et al. 2007; Kiriakoulakis et al., 2009). While SAPS collects mainly fresh suspended POM (i.e. sPOM and sPOC), miniSAPS collects the total sinking and suspended POM (i.e. POM and POC). Accordingly, and for ease of identification between the sampling data, data collected by SAPS is referred to as sPOM and sPOC while data collected by miniSAPS is referred to as POM and POC.

Samples were collected from surface, intermediate (miniSAPS only) and near bottom depths (<32 m above bottom) by SAPS and miniSAPS. The sampling method chosen was dependant on the availability of equipment and number of required sampling depths based on the hydrographic structure and turbidity maxima observed in the CTD profiles. The SAPS was deployed by a winch on the CTD wire or was attached to the CTD rosette. Height above the seabed was determined by an altimeter on the CTD. SAPS operated for 1–2 h depending on the depth and particle loading as estimated by the transmissometer on the CTD and was programmed for sampling water just above the seabed (5–32 m). Total volumes of 163–1443 L of water were filtered through two stacked pre-combusted (400 °C; >6 hrs) glass fibre GF/F (Whatman, 293 mm diameter) filters. For the miniSAPS method; 5–10 L of seawater was filtered through two stacked pre-combusted (400 °C; >6 hrs) glass fibre GF/F (Whatman, 47 mm diameter)

using glass filtration units. On recovery, all filters were treated the same, folded into quarters, wrapped in pre-combusted aluminium foil and stored at -80 °C for the duration of the cruise. Filters were subsequently freeze-dried and stored at -20 °C until analysis.

Samples for pigment analysis were also collected from various depths. Sub-samples (1.6–6 L) of the water collected by the CTD rosette were filtered on separate GF/F (Whatman, 47 mm) filters. The filters were folded into quarters and stored in 15 ml centrifuge tubes at -80 °C or -20°C until laboratory analysis by fluorometry.

6.3.2. Analytical methods

6.3.2.1. Elemental analysis (POC and PN)

Filters for elemental carbon and nitrogen analysis were freeze-dried and particulate organic carbon (POC) and particulate nitrogen (PN) were measured on sub-samples of the top filter of the SAPS and miniSAPS stacks. Punched circles (7.07–113 mm^2) were made using a metal puncher, in homogeneous areas at the middle and edge of the filter. Analyses were carried out using a CEInstruments NC 2500 CHN analyser in duplicates and the mean value was taken. POC values were obtained after de-carbonation (HCl vapour method; Yamamuro and Kayanne, 1995) of the filters whereas PN values were determined without de-carbonation. The bottom filters of the stacks were used to correct for the adsorption of dissolved organic matter (DOM) onto GF/F filters which can lead to an overestimate of POC and PN concentrations, particularly when these are low (Liu et al., 2005; Turnewitsch et al., 2007). Values were therefore corrected for DOM adsorption and are presented in Table 6.1. Variability between circles from the middle and edge of the filters was consistently observed. Mean values were therefore taken to eliminate this filtration artefact and to give a better approximation of the true value of the filter. Concentrations below the limit of detection (<0.01) were considered nil. In cases where the top filter was torn on recovery (SAPS filters only); the average of the top and bottom filters was taken and corrected with the average DOM value from all the bottom filters (marked ^{x} in Table 6.1).

Variability between the POC data sets was observed, however regardless of the carbon pool sampled, data collected by both methods were agreeable.

When comparable material was analysed by both methods the miniSAPS, whose C/N ratio reproducibility was determined to be <± 15% with an SD of 1.2 (see Wilson et al., 2015b; Chapter 5; Table 5.1), and an additional sample from SAPS (EV63 Table 6.6) gave a result within 94% of the miniSAPS values.

6.3.2.2 Molecular analysis (Lipids: Total fatty acids and alcohols)

Lipids analyses were carried out on sPOM from a section of the SAPS filters. Extractions and analyses were carried out according to the methods of Kiriakoulakis et al. (2011). Portions (1/4) of the SAPS filter (~6.21–7.75 g) were spiked with 20 µl of internal standard (100 ng/µl 5α(H)-Cholestane; Sigma) and extracted by sonication (30 min @ 30 °C; x 3) in ~20 ml dichloromethane:methanol (9:1). Extracts were transmethylated in the dark (24 hrs; 40 °C) with 1 ml methanolic acetyl chloride (30:1) and derivatised with 50 µl of *bis*-trimethylsilyltrifluoroacetamide (BSFTA, 1% trimethylsilylchloride; Stigma; 30 min @ 40 °C). Extracts were stored (-20 °C) until GC-MS analysis using a Varian 450 Gas Chromatographer Mass Spectrometer (GC-MS).

A CP8400 autosampler was used with a CP-1177 split/splitless injector to load the extracts onto an Agilent VF-MS column (30 m x 0.25 mm, 0.25 µm). Helium was used as the carrier gas at a rate of 1 mL min^{-1} set and controlled at a constant flow using an electron flow controller. The oven temperature was programmed from 60 to 170 °C at 6 °C min^{-1} after 1 min, and then to 315 °C at 2.5 °C min^{-1} and held for 5 minutes to give a total run time of 82 minutes. The column was fed directly into the electron (EI) source of a Saturn 220 mass spectrometer (ionisation potential 70 eV; source temperature 220 °C; trap current 300 µA). The instrument was operated in Full Data Acquisition mode (50–600 Thompsons) cycled every second.

Chromatograms were reviewed and processed using Varian MS Workstation software (version 6.9.1). Compounds were identified by comparison of their mass spectra and relative retention times with authentic standards (Supelco TM37 FAME mix; 47085-U; 47015-U; 47033 Sigma-Aldrich) using the total ion current (TIC) chromatogram. Compound concentrations were calculated by comparison of their peak areas with that of the internal standard. The relative response factors of the analytes were determined individually and/or for similar compounds. Organic contamination in procedural blanks extracted with each

sample batch was subtracted from the sample values. Reproducibility of similar lipid analyses was determined to be <± 15% by Kiriakoulakis et al. (2000).

Lipids (fatty acids and alcohols) were normalised to the amount of water filtered in sPOM samples and to the amount of OC and individual compounds were grouped into classes. Diagnostic lipid biomarkers (i.e. the organic compounds with a known biological origin) and their indices (e.g. Duineveld et al. 2012) were used to assess the quality of sPOM (see Table 6.2).

6.3.2.3 Scanning electron microscopy

Punched circles of the freeze-dried SAPS filters (~113 mm^2) were glued to stubs and sputter coated with palladium. Samples were viewed using an Oxford INCA x-act XT microscope control scanning electron microscope at accelerating voltages of 5–20 kV. Analysis was carried out with qualitative objectives as the filters were not specifically prepared for quantitative analysis.

6.3.2.4 Pigment analysis

Chlorophyll *a* and phaeopigment concentrations were determined using a Turner fluorometer (model 10) based on the fluorometric and extraction methods described in Tett (1986) and Arar and Collins (1997). Filters were extracted in the 15 ml centrifuge tubes used for storage. Initially the filters were submerged in 4 ml of 90% acetone and sonicated (7 min) in a cold water bath. Extracts were then made up to 10 ml, vortexed and stored in the dark at 4 °C overnight. After 24 hrs, extracts were centrifuged (5 min; @ 450 rpm) and stored in the fridge until analysis. Before reading, samples were allowed to reach room temperature. Fluorescence before and after acidification (with 10% HCl), were measured in order to estimate the proportion of chlorophyll *a* and phaeopigment (Table 6.1).

Table 6.2. Primary lipid biomarker and diagnostic indices used in this study; sources and literature references.

Lipid biomarker/index	**Sources/indicator for**	**Reference**
Lability Index: Unsaturated : SFA	Lability of organic fraction of SPM (unsaturated are more labile than SFAs)	Hayakawa et al. (1996) Kiriakoulakis et al. (2004) Duineveld et al. (2012)
Lability Index: (%) PUFA/total	Lability of organic fraction of SPM (PUFAs are more labile than MUFAs)	Wakeham et al. (1997) Kiriakoulakis et al. (2005; 2011)
Phytoplankton Index: (%) $C_{20:5(n-5)} + C_{22:6(n-3)}$ /total lipids	Lability and contribution of phytoplankton in organic fraction of SPM	Duineveld et al. (2012)
$C_{20:5(n-5)}$ Eicosapentaenoic acid (EPA)	Indicates diatoms (or herbivorous mesozooplankton)	Harwood & Russell (1984) Dodds et al. (2009) Parish, (2013)
$C_{22:6(n-3)}$ Docosahexaenoic acid (DHA)	Indicates dinoflagellates	Harwood & Russell (1984) Dodds et al. (2009) Parish, (2013)
$C_{22:6(n-3)}$ / $C_{20:5(n-5)}$ > 1 indicate a dominance of dinoflagellates, < 1 reflect a dominance of diatoms	Ratio of DHA:EPA can be used as an indicator of the predominant phytoplankton class	Budge & Parish, (1998)
Zooplankton Index: (%) $C_{20:1}$ $C_{22:1}$ $C_{24:1}$ fatty acids and alcohols/total lipids	Contribution of zooplankton in organic fraction of SPM	Dalsgaard et al. (2003) Duineveld et al. (2012)
$C_{20:1(n-9)}$, $C_{22:1(n-11)}$ & $C_{24:1}$ *Monounsaturated fatty acids and their alcohols	Degraded wax esters of zooplankton and indicators of zooplankton, mainly herbivorous species *Indicators of Calanoid copepods	Parish, (2013) Berge & Barnathan, (2005) Mudge, (2005) *Tolosa et al. (2003) *Dodds et al. (2009) *Dalsgaard et al. (2003)
$C_{14:0}$, $C_{16:0}$ fatty alcohols & $C_{18:1(n-9)}$ fatty acid	Indicate zooplankton: omnivorous or carnivorous non-calanoid copepods	Kattner et al. (2003) Berge & Barnathan, (2005) Dodds et al. (2009)
Bacteria Index: (%) Odd numbered saturated and branched FA & $C_{18:1(n-7)}$ /total lipids	Contribution of bacteria to the organic fraction of SPM	Volkman & Johns, (1977) Duineveld et al. (2012)
Degradation Index: $C_{18:1(n-9)}/C_{18:1(n-7)}$	$C_{18:1(n-7)}$ is synthesised from $C_{16:1(n-7)}$ which is of bacterial or algal origin. High ratio indicates bacterial degradation. Ratio can also imply carnivorous over herbivorous feeding modes.	Volkman and Johns, (1977) Graeve et al. (1997) Dodds et al. (2009)

6.4 Results

6.4.1 Suspended particulate matter (SPM) and nepheloid layers in Whittard Canyon

BNLs and INLs are commonly observed in the Whittard Canyon with concentrations of SPM ranging from ~75 to 600 µg L^{-1}, typically exceeding ~300 µg L^{-1} in the BNLs and lower concentration in the INLs (Wilson et al., 2015a; Chapter 4). BNLs and INLs were detected in the four surveyed branches (WC1 – WC4; see Fig. 6.1) in June 2013 (Fig. 6.2). BNLs, 150 - 200 m thick, were detected along the axes of the branches surveyed down to water depths of ~2500 m. INLs were observed as extensions up to 25 km off slope with thicknesses of ~50 m, decaying with distance from the benthic source and displaying similar characteristics to those observed during previous surveys (Wilson et al., 2015a; Chapter 4). INLs observed at distinct depth ranges are attributed to enhanced seabed currents and are typically associated with the presence of the permanent thermocline (750 m) and/or impingement of saline MOW cores (1150 m) on the slope and with near-critical internal wave reflection (at 450 m, 1250 m, 1750 m) as identified by Wilson et al., (2015a); Chapter 4.

Enhanced Nepheloid Layers (ENLs) related to bottom trawling were also observed in the two easterly branches (WC3 & WC4; see Fig. 6.1) during the survey (Wilson et al., 2015b; Chapter 5). Concentrations of SPM in the ENLs were typically an order of magnitude higher than the mean maximum of naturally generated NLs, with values of up to ~8000 µg L^{-1} detected. Vertical profiles affected by suspected trawling activity are presented in Wilson et al. (2015b); Chapter 5 and are not shown here. Higher SPM concentrations with values of 1850 µg L^{-1}, were also observed in WC1 (most westerly branch; see Fig. 6.1). This isolated observation is most likely related to variable energy fluxes within the canyon branches and has not been associated with bottom trawling activity.

A limited number of profiles from the open slope location (interfluve between WC2 and WC3; see Fig. 6.1), lacked the defined NL structure observed within the canyon. Increases in SPM near the sea-bed and in an INL ~180 m above the seabed were observed in one profile with maximum concentrations between 60–130 µg L^{-1}.

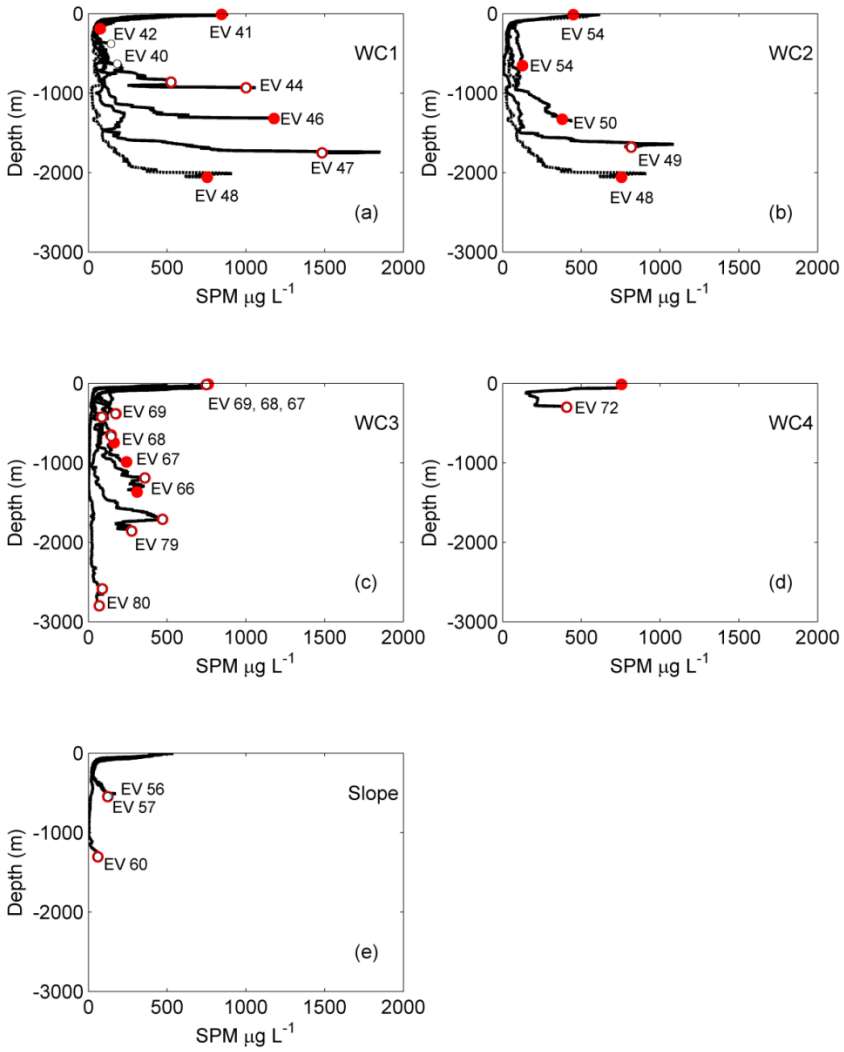

Figure 6.2. Vertical profiles of Suspended Particulate Matter (SPM) showing benthic and intermediate nepheloid layers in four channels and the open slope area (adjacent to WC2) of Whittard Canyon in June 2013. Depths of samples collected by the CTD rosette for pigment (●) and elemental (○) analysis are shown with corresponding event numbers (see Table 6.1). EV 48 is located at the junction of WC1&2 at 2063 m water depth. Note: Depth of SAPS samples with accompanying CTD profiles are shown in Fig. 6.6.

6.4.2 Particulate organic carbon content of SPM

Concentrations of sPOC and POC measured by both methods (i.e. SAPS and miniSAPS) ranged from ~3–602 µg L^{-1} (Fig. 6.3). Values and sampling method for each sample are detailed in Table 6.1. Generally, a trend of increasing SPM with water depth was apparent down to 2000 m, with lower values at deeper

depths (Fig. 6.3a). The highest sPOC and POC concentrations were observed in surface samples with values of ~67–602 μg L^{-1}. Surface values obtained by SAPS (67–205 μg L^{-1}) were more conservative in comparison to those from miniSAPS (602 μg L^{-1}). This appears to be the case for all the sPOC and POC data, with benthic samples measured by SAPS having lower values (3–46 μg L^{-1}) than those within the same depth range by miniSAPS (116–208 μg L^{-1}). A significant difference was observed between sPOC and POC data measured from SAPS and miniSAPS samples (Two-sample t-test assuming unequal variance, h = 1, $p<0.001$) and may be explained to related to the sampling of different pools of carbon (i.e suspended or particulate) depending on the apparatus employed.

sPOC and POC values from near-bottom samples (i.e. within 32 m of the seabed) were highly variable (red dots; Fig. 6.3b) and ranged from 3–280 μg L^{-1}. Mid-water samples were collected by miniSAPS only and the POC values were within the same range but were less variable (48–176 μg L^{-1}). POC concentrations relative to SPM (expressed as sPOC or POC/SPM ratio; Fig. 6.3c) were also highly variable (0.03–2.51; mean = 0.53 ± 0.62). Benthic and mid-water samples collected by miniSAPS at equivalent water depths (~400 m and ~1650 m), showed higher POC/SPM ratios in the BNLs. A significant positive correlation between POC and SPM was found for the miniSAPS data (Spearman's test; r = 0.66, p = 0.007). However, no correlation was found when sPOC measured from SAPS samples was included (Spearman's test; r = 0.30, p = 0.13). Both Pearson's and Spearman's correlations were carried out here (and for correlations described below). For non-parametric treatment of the influential outliers in the data sets Spearman's rho and p values are reported here, unless otherwise stated, but both tests agreed in all situations.

Benthic samples from within the canyon branches appeared to have higher sPOC and POC values (13–176 μg L^{-1}) than samples at equivalent depth ranges (~600 and 1300 m) on the open slope area of the spur adjacent to WC2 (3–31 μg L^{-1}). However, a statistical difference could not be distinguished between samples from the two locations (Two-sample t-test assuming unequal variance, h = 0, p = 0.37). SPM concentrations within the canyon (18–196 μg L^{-1}) and the open slope (61–130 μg L^{-1}) were also indistinguishable (h = 0, p = 0.21).

Spatially comparable benthic samples approximately 15 km and 40 km from the 200 m isobath from the open slope (~15 km: EV56, 57 and ~40km: EV60)

and within the canyon (~15 km: EV46 and ~40km: EV80), also showed higher sPOC, POC and SPM values within the canyon. Averaged sPOC or POC and SPM values within the canyon were 103.33 ± 69.18 µg L^{-1} and 624.03 ± 555.18 µg L^{-1} respectively while on the open slope concentrations were much lower with POC of 15.12 ± 11.48 µg L^{-1} and SPM of 105.04 ± 31.26 µg L^{-1}. However, again the data could not be distinguished statistically (Two-sample t-test assuming unequal variance, h = 0, p = 0.19 and p = 0.30). In order to eliminate possible distortion by sampling apparatus, sPOC values measured by SAPS only were considered (as there were no miniSAPS from the slope location), but they also showed no statistical difference (Two-sample t-test assuming unequal variance, h = 0, p = 0.36).

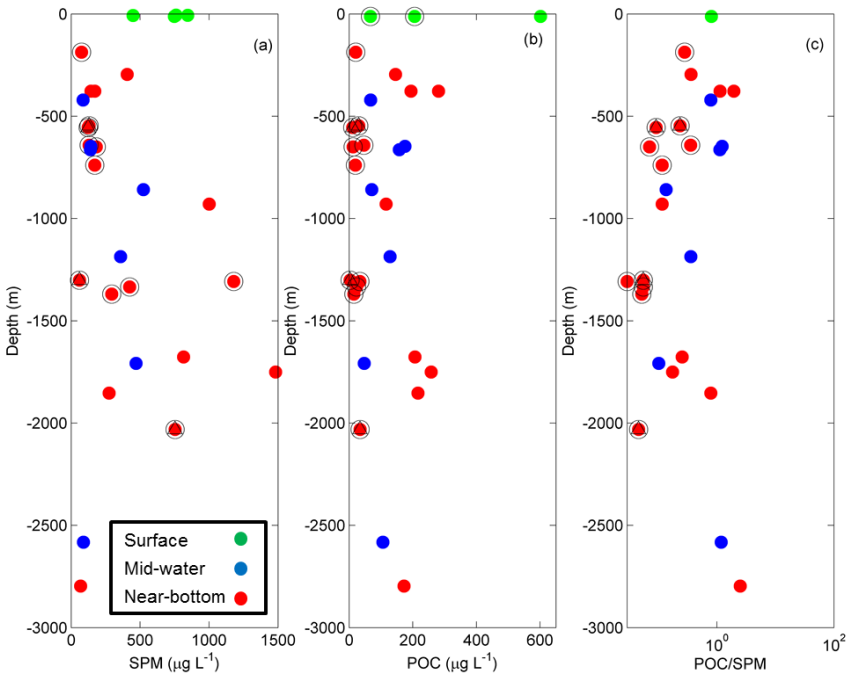

Figure 6.3. Concentrations of (a) suspended particulate matter (SPM); (b) particulate organic matter (from SAPS and miniSAPS); (c) particulate organic matter/suspended particulate matter (from SAPS and miniSAPS) at surface, mid-water and near-bottom depths of the Whittard Canyon. Note logarithmic scale of (c). Black halos indicate samples collected by SAPS i.e. sPOC (all others are miniSAPS). Slope samples are marked with black triangle. The surface sample with no CTD cast (EV 43) is not shown in (a) or (c).

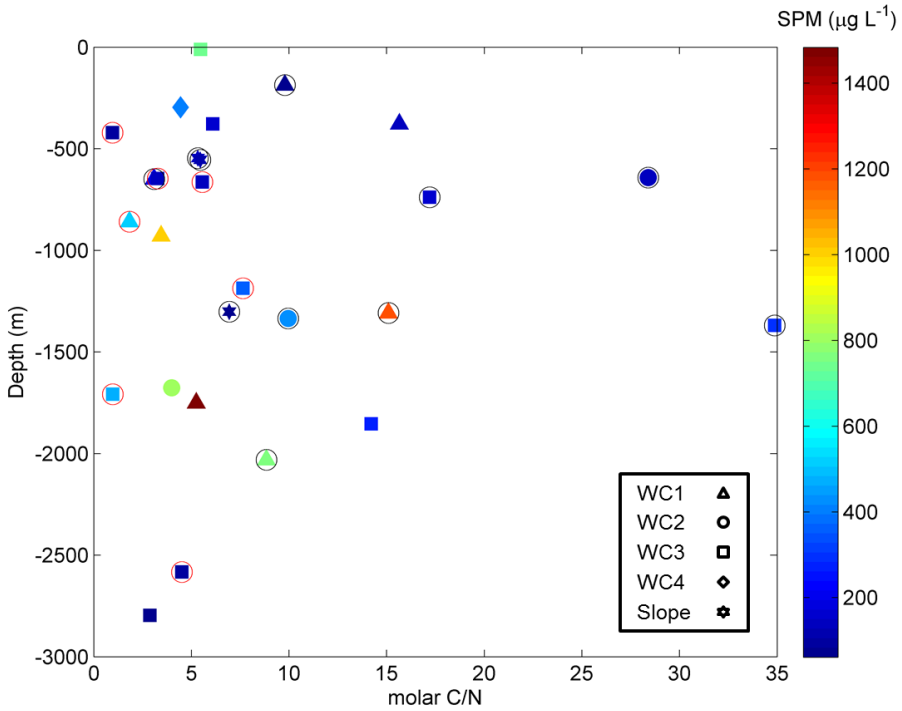

Figure 6.4. Molar C/N ratios of suspended particulate matter versus depth (m) at the Whittard Canyon. Colour bar indicates concentration of SPM in µg L^{-1}. Black halos indicate samples collected by SAPS (all others are miniSAPS). Red halos indicate mid-water samples i.e. INLs.

6.4.3 Molar C/N ratios

Molar C/N values of sPOM and POM from the surface, mid-water (INLs) and near-bottom (BNLs) samples down to ~2800 m ranged from 0.96–34.88 (Fig. 6.4, Table 6.1). C/N ratios of material influenced by trawling in concentrated ENLs ranged from 7–10 and are presented in Wilson et al. (2015b); Chapter 5.

Surface samples were tightly clustered and close to the Redfield ratio (i.e. 6.6) with values ranging from 5.5–6 (SD = 0.28), regardless of the sampling method. Apart from the surface, C/N values were highly variable and a significant difference between C/N ratios measured from SAPS and miniSAPS filters was confirmed by T-test (Two-sample t-test assuming unequal variance, h = 1, p = 0.01). However, all mid-water samples were collected by miniSAPS and this inherent variability appears to be natural rather than methodological as shown by the reproducibility of C/N ratios by miniSAPS and SAPS on comparable material (i.e. <± 15 %).

Values close to the Redfield ratio were found throughout the water column, but considerable variability was observed in both mid-water and benthic samples down to depths of >2000 m. The highest C/N values were detected in

BNLs in the upper reaches of the canyon branches (i.e. <1500 m) at ~650–730 and 1300–1400 m with values of 15–35. Although fewer samples were collected in the lower reaches (i.e. >1500 m), C/N values appeared to decrease with increasing depth from ~15 to 3. However, no relationship was found (Spearman's correlation r = 0.14, p = 0.78). C/N ratios of benthic samples increased with increasing concentration of SPM in some cases (data with red halos in Fig. 6.4), however this was not true for all benthic samples and there was no statistical significance (Spearman's correlation r = -0.06, p = 0.80). No correlations were found between C/N and SPM when all the data were considered (mid-water and benthic samples) indicating that C/N values were independent of SPM concentration (Spearman's correlation (for all C/N data) r = -0.004, p = 0.98).

C/N ratios in mid-water samples ranged from extremely low values of 0.96–0.98 to values near the Redfield ratio 5.6–7.6. Moderate to low concentrations of SPM (~130–290 μg L^{-1}), likely composed of material that had been in suspension longer, hosted the highest C/N values (28.4–34.8) while samples with the highest SPM mainly had C/N values (3.5–8.8) near the Redfield ratio. This apparent trend however was not confirmed by statistical analysis and no relationship was found with either SPM concentration or depth for the mid-water samples (Spearman's correlation r = 0.036, p = 0.96).

Regression analysis of PN and sPOC and POC showed a linear relationship where y = 0.1881x + 8.3298 (R^2 = 0.57, p < 0.001), indicating the presence of inorganic nitrogen in ~57% of the samples and thus providing an explanation for the very low C/N values due to the absorption of inorganic nitrogen to the particles (e.g. Müller, 1977).

C/N values from within the canyon were higher (18.32 $\pm$ 11.78) than those at comparable depths on the open slope (5.90 $\pm$ 0.71), however there was no significant difference between the groups (Two-sample t-test assuming unequal variance, h = 0, p = 0.15). C/N ratios within the canyon and from spatially comparable locations on the slope (i.e. distance from the 200 m isobath), also showed no statistically significant difference (Two-sample t-test assuming unequal variance, h = 0, p = 0.55).

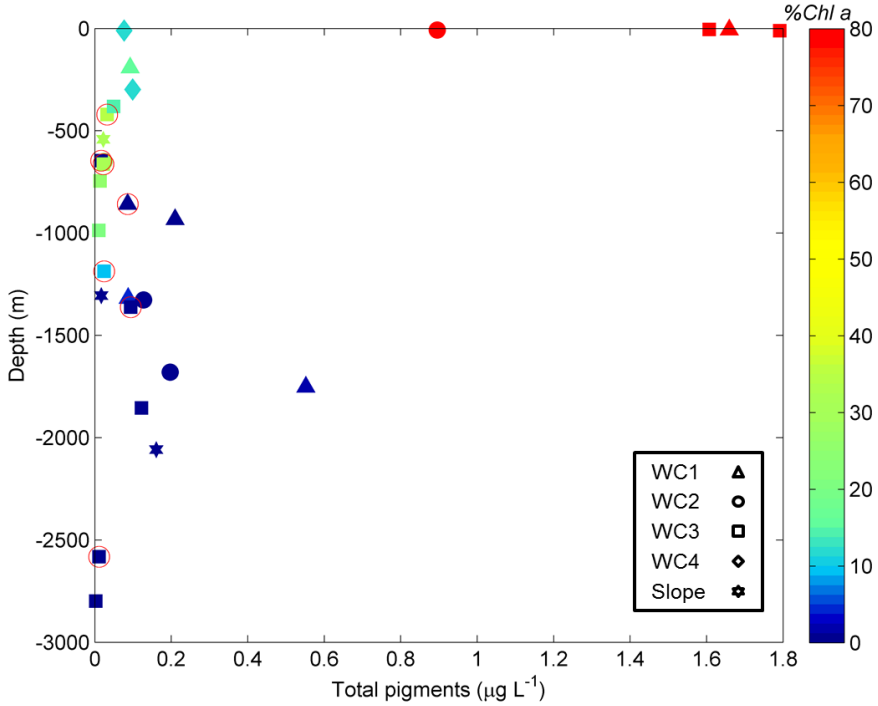

Figure 6.5. Pigment concentrations of near bottom and mid-water sPOM (µg L^{-1}) from the four branches and the slope location at Whittard Canyon. Colour bar indicates the % of Chlorophyll *a* contribution to the total pigments concentration. Red halos indicate mid water samples i.e. INLs.

6.4.4 Pigments: chlorophyll *a* and phaeopigments

Pigment concentrations generally decreased with depth with the highest pigment concentrations detected in the surface water (Fig. 6.5). Phaeopigment to chlorophyll *a* ratios increased with depth, primarily in benthic samples. Samples from the open slope location followed the general trends observed and were generally indistinguishable from the canyon samples.

Surface values ranged from 0.9 to 1.8 µg L^{-1} and were dominated by chlorophyll *a*, which contributed >80% of the total pigment content. Surface waters above WC 4 however showed much lower pigment concentrations of 0.07 µg L^{-1} with only ~20% contribution of chlorophyll *a,* suggesting old material possibility related to trawling activity in the area (Wilson et al., 2015b; Chapter 5).

Below 200 m, total pigment concentrations were much lower, generally <0.6 µg L^{-1}. A shift to phaeopigment dominance was observed in the composition, with chlorophyll *a* making up <25% of the total pigment concentrations, except between 420 m and 750 m where the chlorophyll *a* contribution increased to ~35%. A peak in total pigment concentration dominated by phaeopigments was observed between ~1500 and 2000 m water depth, with values of 0.1–0.6 µg L^{-1}.

Deeper samples with high concentrations of SPM were dominated by phaeopigments (Fig. 6.5 and Table 6.1).

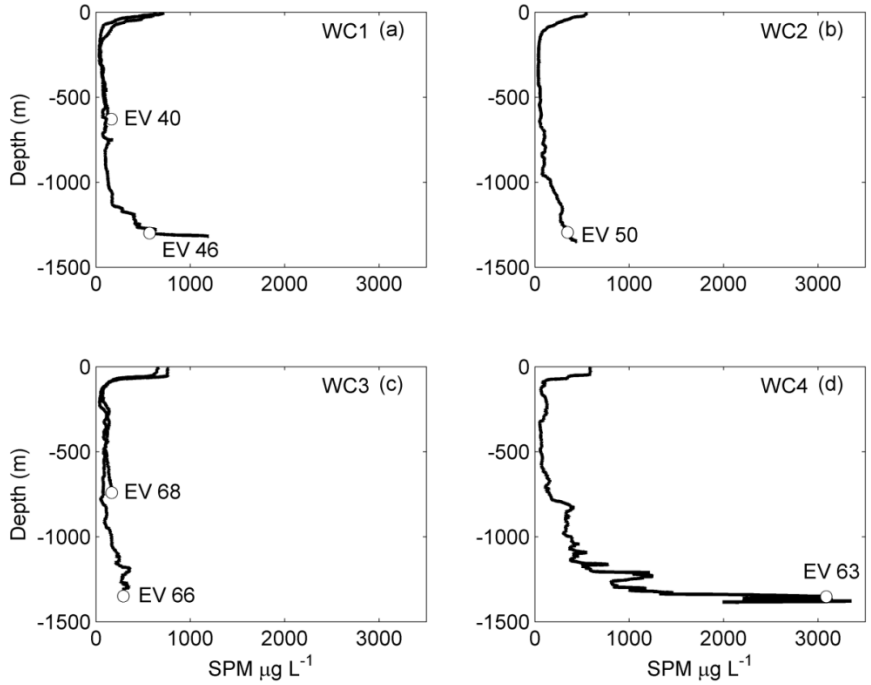

Figure 6.6 Vertical profiles of Suspended Particulate Matter in the four branches of Whittard Canyon in June 2013 showing depths of SAPS deployments (○) and corresponding event number (Table 6.1). Location of SAPS deployments are shown in Fig. 6.1. Note: SAPS deployment without CTD at the surface is not shown (EV 43).

6.4.5 Scanning electron microscopy

Punched circles of sPOM from SAPS filters collected in the surface and in benthic nepheloid layers (<25 m.a.b) were examined under SEM. Details of the sPOM analysed are detailed in Table 6.1 and profiles of where the samples (with accompanying lipid analysis) were collected are shown in Fig. 6.6. Random samples were selected to give an overview of the material found in different branches and at different depth ranges (Fig. 6.7). Clumps of detritus, phytoplankton fragments and remains ranging in size from ~20–30 µm were the abundant in the material observed. Mucus balls (probably of organic origin but not confirmed by X-ray) with diatoms frustules and coccolithophorids liths attached, were abundant in all samples.

Most intact phytoplanton were relatively small measuring ~5-10 µm. Species of diatoms, dinoflagellates, silicoflagellates and coccolithophores were identifded with the coccolithophores dominanting all samples. The

coccolithophores were found as coccospheres (~5–20 µm) and loose liths (~2 µm) often covering tintinnid loricas (40–50 µm). Often a mixture of plates from different coccolithophore species were found. *Emiliana huxleyi* was the most abundant but a variety of species were identified particulaly in the surface water sample including; *Acanthoica sp. (bicayenis*); *Coronosphaera* (*mediterranea*); *Calcidiscus leptoporus; Coccolithus pelagicus;* and tentatively; *Ophiaster sp. (formosus); Discosphaera sp. (tubifera); Calyptrosphaera sp.; Michaelsarsia sp.*

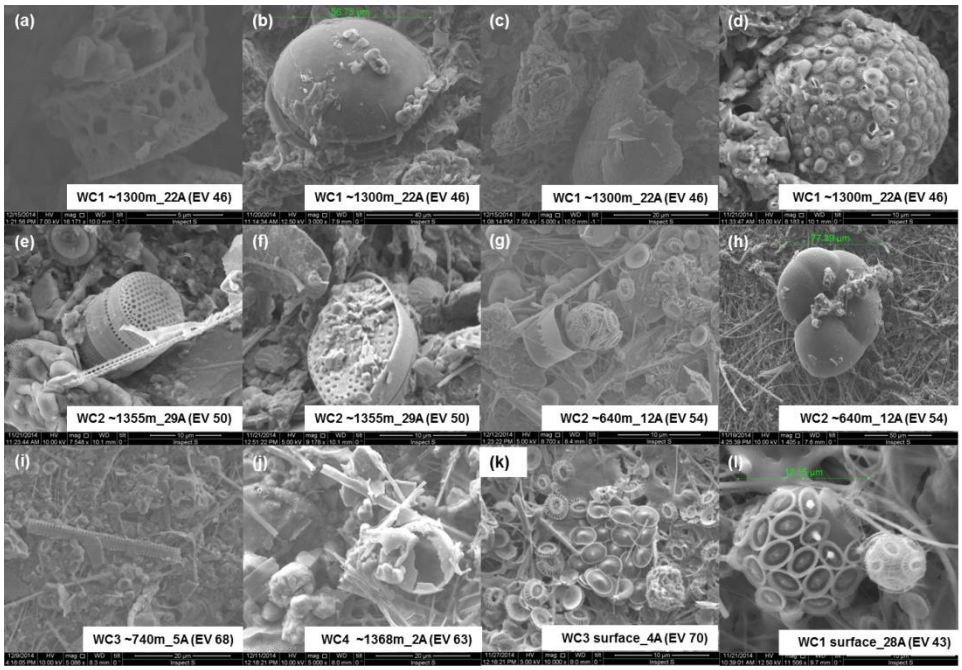

Figure 6.7. Selection of SEM photographs of sPOM collected in BNLs and at the surface at the Whittard Canyon in June 2013. (a) Diatom *Paralia sulcata* (scale: 5 µm); (b) unknown dinoflagellate (scale: 40 µm); (c) Faecal pellet (scale: 20 µm); (d) Tintinnid lorica covered with liths of coccolithophores, mainly *Emiliania huxleyi* (scale: 10 µm); (e) Diatom *Thalassiosira oestrupii* (scale: 10 µm); (f) Pennate Diatom with cocolithophore plates in the background (scale: 10 µm); (g) *Emiliania huxleyi* and other biogenic material and cells (scale: 10 µm); (h) Pelagic foram *Globigerina* (scale: 50 µm); (i) An example of the very common mixed debris seen on the filters at this depth (scale bar 20 µm); (j) Fragments of diatom frustules among other debris (scale: 20 µm); (k) Liths of *Acanthoica* sp. (*A. bicayenis*) & *Emiliana huxleyi* (scale: 10 µm); (l) *Coronosphaera mediterranea* & *Emiliana huxleyi* (scale: 10 µm).

Centric diatoms were also common in various sizes (10–40 µm) with many intact frustules in good condition found at depth. *Thalassiosira* spp. were mostly found and *Paralia sulcata* and some tentative identifications made of *Bacteriastrum* sp., *Coscinodiscus* sp., *Corethron* sp., *Porosira* sp., and a *Chaetoceros* resting spore. Broken frustules of these were abundant and only a

few pennate diatoms were found. Dinoflagellates were infrequent in all samples, ranging in size from 5 to ~60 µm, and were found mainly in the surface samples, WC1, WC2 and the slope.

The silicoflagellate, *Dictyocha speculum* (15–20 µm), was found at ~1300 m in a sample from WC1 and in a slope sample collected at ~2000 m. Micozooplankton and foraminifera were present occasionally. Pelagic forams (~30–80 µm) including *Globigerina* were observed in the upper reaches of WC2 (~640 m) and in a slope sample at a similar depth (~550 m). Faecal pellets (~20 µm) were observed but mainly in samples from the deeper depth range (>1300 m). Large zooplankton were not observed on the filters, but large copepods visible with naked eye were found on the SAPS filters during processing and removed before extraction of fatty acids and alcohols. Some fragmented material was observed and tentatively identified as parts of larger organisms e.g. copepod legs.

6.4.6 Lipids: Total fatty acids and alcohols

6.4.6.1 Total lipids

Lipid concentrations (total fatty acids and alcohols) of sPOM from the surface and BNLs from the four surveyed branches displayed complexity and heterogeneity in their compositions (Table 6.1). Vertical profiles of SPM show typical BNLs at two depth ranges (650–739 m and 1308–1383 m) that were sampled by SAPS (Fig. 6.6). The BNLs were within the ranges of typical NLs with SPM = 160–1300 µg L^{-1}, except in WC4 with SPM ≅ 3000 µg L^{-1} due to bottom trawl resuspension (Wilson et al., 2015b; Chapter 5).

Lipid concentrations were normalised to volume of water as a proxy for the overall food availability and ranged from 18.54 to 245.44 ng L^{-1} (Fig. 6.8a). In the surface, the total concentration of lipids was 163.22 ng L^{-1}. Concentrations in the upper reaches of the canyon exceeded that of the surface (650–739 m; 196.07–245.44 ng L^{-1}) and were at least 1.8 times higher than those at the deeper depth range in the lower reaches (1308–1383 m; 18.54–130.21 ng L^{-1}).

Within the two depth groups, variation in the concentrations were observed with generally higher values found in the more easterly branches (WC3 & WC4) compared to those in the west (WC1 & WC2). The highest lipid concentration was found in WC3 (east) with 245.44 ng L^{-1} at ~750 m. At a similar depth (~650 m) in WC1 (west), the concentration was lower with a value of 196.07 ng L^{-1} but still

higher than the surface and appreciably higher than the other samples. At the deeper depth range, lipid concentrations in the eastern branches were still higher than comparative samples in the west, the highest being in WC3 with values of 130 ng L^{-1} (1370 m). In WC4 (~1368 m) the lipid concentration remained relatively higher at 79.77 ng L^{-1}, in comparison to 51.77 ng L^{-1} in WC1 (1308 m) and only 18.54 ng L^{-1} in WC2 (1312 m).

Concentrations were also normalised to organic carbon as a proxy for the compositional quality of the material (Fig. 6.8b). Although there was some variation, the data showed similar trends with the highest values in the upper reaches of the canyon at the shallower depth range with 19.82 mg g^{-1} OC (WC 1) and 17.16 mg g^{-1} OC (WC3) respectively. Samples from the deeper depth generally had lower values, ranging from 0.81 to 3.43 mg g^{-1} C in WC1, WC2 and WC4. However at the deeper depth in WC3 a value of 5.89 mg g $^{-1}$ OC was measured, marginally higher than the surface value of 4.86 mg g^{-1} OC.

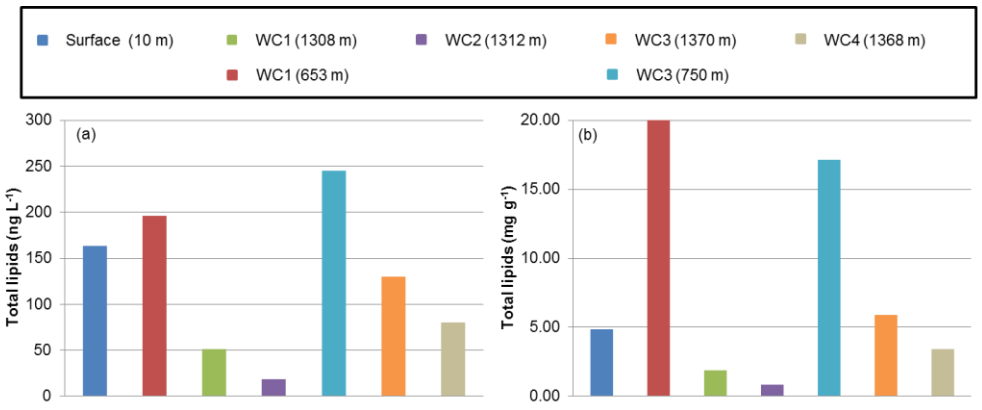

Figure 6.8. Concentrations of total lipids in sPOM from the surface and BNLs in the Whittard Canyon expressed in (a) ng of lipids per L of filtered water and (b) mg lipids per g of organic carbon.

6.4.6.2 Lipid class & functional groups

Individual lipids were grouped into the principal classes: saturated fatty acids (SFAs), branched fatty acids (BRFAs), monounsaturated fatty acids (MUFAs), polyunsaturated fatty acids (PUFAs) and (saturated, unsaturated and branched) fatty alcohols (Fig. 6.9). The general trends observed were the same whether the data was normalised to volume of water or weight of carbon. Data described hereon refer to the concentration of total lipid per L of water (ng L^{-1}). Variability in the principal lipid classes was observed across the seven samples. Both SFAs and MUFAs were well represented (32.28 $\pm$ 19.47 ng L^{-1} and 26.17 $\pm$ 13.22 ng L^{-1}

respectively). PUFAs dominated in samples from the surface and upper reaches of WC1 (west). All samples from the east (WC3 and WC4) were dominated by fatty alcohols (Fig. 6.9).

The composition of the surface sample had relatively even contributions of SFAs, MUFAs, PUFAs and only a small proportion of alcohols. In contrast to this, the samples at depth were more homogenous and dominated by one group or another. Some similarity was observed between the surface sample and the sample from the upper reaches of WC1, with comparable amounts of MUFAs and high contributions of PUFAs in both. The sample collected in the upper reaches of western branch (WC1) had the highest contribution of PUFAs, exceeding those in the surface. These characteristics were not observed in the other sample collected at this depth range on the eastern side of the system (WC3), which was dominated by fatty alcohols.

Fatty acids ranged from C_{14} to C_{24}. Saturated fatty acids, $C_{14:0}$, $C_{15:0}$, $C_{16:0}$ and $C_{18:0}$ were the most abundant compounds at all sites. BFAs were a minor constituent, represented by both isomers of $C_{15:0}$ (i-$C_{15:0}$ and a-$C_{15:0}$) and isomers of $C_{16:1}$. The monounsaturated fatty acid distribution also ranged from $C_{14:1}$ to $C_{24:1}$. The most abundant of these were, $C_{18:1(n-9)}$ and C $_{18:1(n-7)}$ homologues, which were found at all sites. The most common PUFAs detected were $C_{18:2}$ and $C_{20:5(n-5)}$ (Eicosapentaenoic acid, EPA). Important PUFAs, $C_{18:3}$, $C_{20:3}$, $C_{20:3}$, $C_{20:2}$, $C_{22:6(n-3)}$ (Docosahexenoic acid, DHA) and tentatively $C_{16:3}$ (tent.), $C_{18:5}$ (tent.) $C_{20:4/6}$ (tent.), $C_{22:5}$ (tent.), $C_{22:4/3}$ (tent.) were also identified and present in varying amounts. Alcohols ranged from C_{14} to C_{20} including branched $C_{15:0}$ fatty alcohols, mono unsaturated $C_{16:1}$, $C_{22:1}$, $C_{15:1}$, $C_{18:1}$, $C_{20:1}$ and poly unsaturated $C_{18:2}$ (tent.). Saturated alcohols $C_{14:0}$ and $C_{16:0}$ were abundant and detected at all sites.

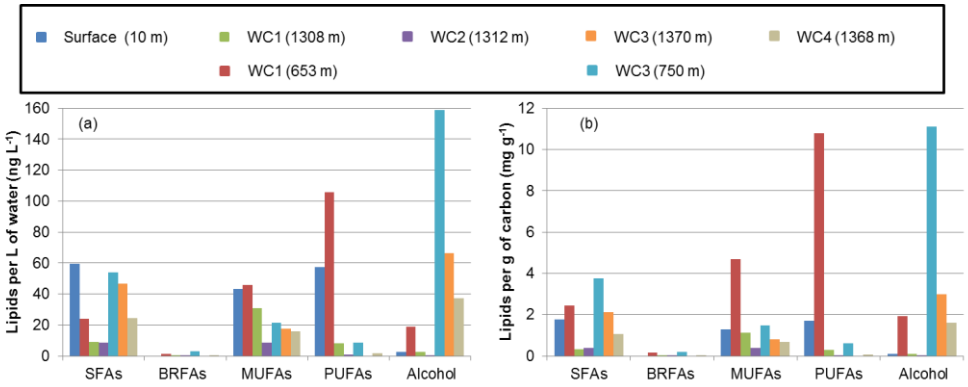

Figure 6.9. Principal lipid classes of sPOM in the Whittard Canyon expressed in (a) ng of lipids per L of filtered water and (b) mg lipids per g of organic carbon.

6.4.6.3 Lipid indices

Samples were compared with respect to diagnostic lipid biomarker indices based on their sources and reactivity described in the literature and as detailed in Table 6.2. Unsaturated fatty acids (i.e. MUFAs and PUFAs) are more labile than saturated and PUFAs are more labile than MUFAs (Hayakawa et al., 1997; Kiriakoulakis et al., 2004; Kiriakoulakis et al., 2005; Duineveld et al., 2012). Therefore lability was assessed based on the ratios of these groups; unsaturated fatty acids to SFAs and PUFAs to MUFAs (Fig. 10 a – b). According to these indices, all samples showed some level of lability. sPOM from the surface and in WC1 (at both depth ranges) showed the highest lability. All other samples particularly those from the eastern branches (WC3 and WC4) at the deeper depth range showed lower lability.

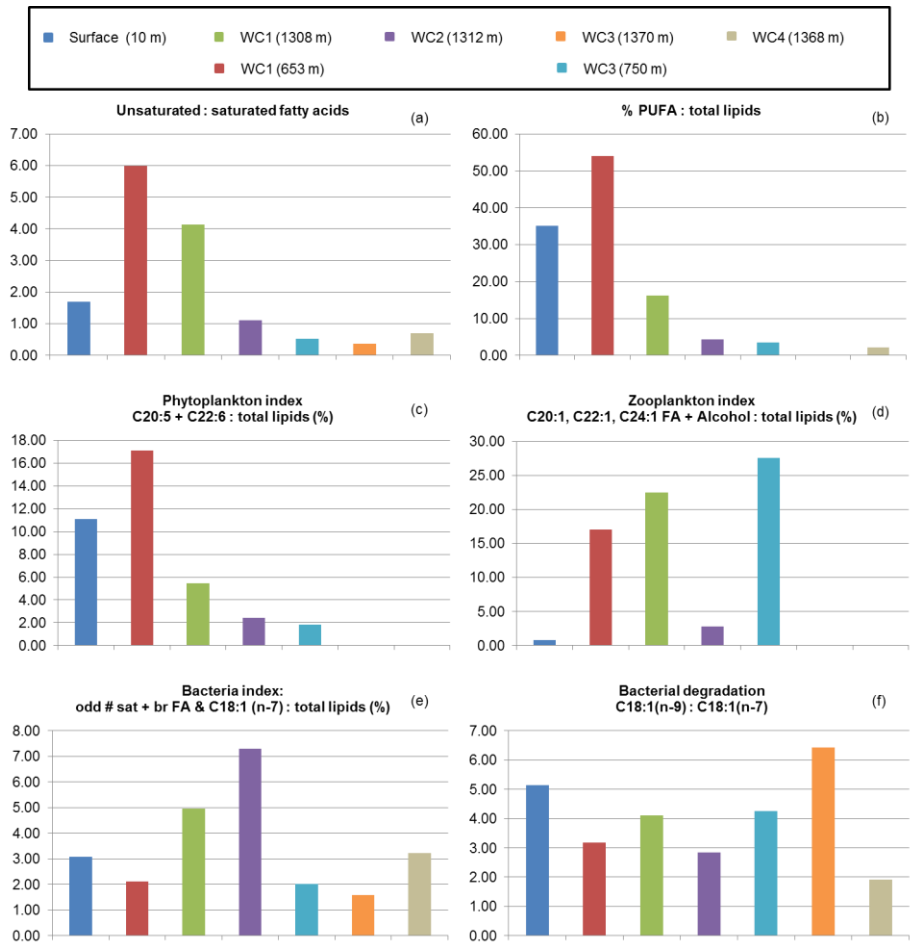

Figure 6.10. Diagnostic lipids indices of the sPOM indicating (a) & (b) lability; (c) contribution of phytoplankton lipid biomarkers; (d) zooplankton; (e) bacteria and (f) bacterial degradation. Based on indices of Duineveld et al. (2012) and literature detailed in Table 6.2.

$C_{20:5(n-5)}$ (EPA) and $C_{22:6(n-3),}$ (DHA) essential fatty acids are biosynthesised by phytoplankton, the former is abundant in diatoms while the latter is in dinoflagellates (Harwood and Russell; 1984; Parish, 2013). Based on this, Duineveld et al. (2012) defined a phytoplankton index as the concentration of these compounds as a percentage of the total lipids, and this was used here as an indicator of fresh sPOM mainly originating from phytoplankton (Fig 6.10c). The highest contributions of these biomarkers were observed in sPOM from the surface and upper reaches of WC1 whereas samples from the deeper depth range in the eastern branches (WC3 and WC4) completely lacked these compounds. The ratio of DHA to EPA was used as an indicator for the dominant phytoplankton group (Budge and Parish, 1998) and showed a high contribution of dinoflagellates in the surface sample.

The percentage of $C_{20:1}$, $C_{22:1}$, $C_{24:1}$ fatty acids and alcohols to the total lipids was defined by Duineveld et al. (2012) and used here as a zooplankton index, based on the observation that these compounds are abundant in zooplankton and copepods (Dalsgaard et al 2003; Tolosa et al., 2003; Bergé and Barnathan, 2005). Specifically, these compounds indicate herbivorous meso-zooplankton and Calanoid copepods (e.g. Tolsa et al., 2003; Bergé and Barnathan, 2005). sPOM from both depth ranges in WC1 and at the upper reaches of WC3 had high contributions of zooplankton (Fig. 6.10d). While sPOM from the lower depth range of WC2 had a slightly larger contribution than the surface, concentrations of compounds indicative of zooplankton were low in these samples and were completely absent in sPOM from the lower reaches of WC3 and WC4.

The concentration of odd numbered saturated and branched fatty acids and $C_{18:1(n-7)}$ as a percentage of the total lipids was used as an indicator of bacterial contributions in sPOM as per Duineveld et al. (2012). According to this index, all the samples had contributions of compounds indicative of bacterial activity (Fig. 6.10e). Samples from the lower depth range on the western side of the system (WC1 & WC2) had the highest bacterial signatures, followed by the surface and deeper sample from WC4. Bacterial compounds, although in relatively lower concentrations, were also detected in the deeper sample from WC3 and in both samples from the shallower depth range (650–750) on both sides of the system.

$C_{18:1(n-7)}$ is obtained from bacteria or is synthesised from $C_{16:1(n-7),}$ which is of bacterial or algal origin (Volkman and Johns, 1977). Based on this, Duineveld et al. (2012) used the ratio of $C_{18:1(n-9)}$ to $C_{18:1(n-7)}$ as an indicator of bacterial OM degradation. By this index, all samples showed degradation with the highest and lowest contributions of these compounds indicative of degradation at the lower depth range in the eastern branches of WC3 and the adjacent easterly branch WC4, respectively (Fig. 6.10f). Relatively high proportions of these compounds were also observed in the surface sample while they were relatively low in all other samples.

6.5 Discussion

6.5.1 POC sampling issues and limitations of methods

Discrepancies between different sampling apparatus are often related to the sampling of different pools of organic carbon and/or the adsorption of DOM, which can have variable influences depending on the area of the filter, filtered volume and sample depth (Gardner et al. 2003; Turnewisch et al. 2007; Liu et al., 2009; Vilas et al., 2009). A significant difference between sPOC and POC values measured by SAPS and miniSAPS was found. Such discrepancies are more prevalent in the deep than in the surface and may explain some of the variability, and apparent trends, in benthic and mid-water samples. Double stacks of GF/F filters with a nominal pore size of 0.7 µm were used for both methods and, although all the samples were corrected for DOM (except one; see Table 6.1), unavoidable higher pressure differentials, particularly across the larger SAPS filters, can cause POC and DOM to be pulled through the filters (Turnewisch et al. 2007). Some of the SAPS filters (marked in Table 1.6) were torn on recovery. Furthermore it has been suggested that pump-derived samples can underestimate POC and that large filters should be avoided (Gardner et al., 2003; Turnewisch et al. 2007). Other factors including wash out of particles during ascent, artificial particle formation, bias against zooplankton sampling and contamination cannot be neglected (Turnewisch et al. 2007; Liu et al., 2009; White et al., 2016). Accordingly, as these issues remain resolved, some caution must be exercised when considering POC values and the values presented here can only be taken as estimates.

However, although POC values were consistently lower by measurements from the SAPS, C/N values of POM from the surface sampled by both methods were remarkably similar (SD = 0.28). Furthermore, benthic samples of comparable material (i.e. affected by trawl-induced resuspension) by SAPS showed the same C/N ratios as those by miniSAPS presented in Wilson et al. (2015b); Chapter 5, (SD = 1.11 for SAPS and miniSAPS). Thus the inherent variance observed here is more likely to be natural rather than methodological. Furthermore, all mid-water samples were collected by miniSAPS and are therefore comparative with each other.

6.5.2 Quality and composition of POM at the Whittard Canyon

6.5.2.1 Surface water OM-the source of settling particles

The Celtic Sea shelf is a highly productive area. Semi-diurnal tides in the region have been observed to drive 28–48 W m^{-2} of energy on-shelf (Hopkins et al., 2014), increasing nutrient fluxes that support primary production and annual diatom blooms (e.g. Sharples et al., 2013). The spring bloom in the Celtic Sea (9 ° W 50 ° N) generally occurs in April with moderate chlorophyll *a* concentrations of between 4–6 mg m^{-3} (Gohin et al., 2015). Satellite images of the area showed chlorophyll *a* concentrations ranging from 0.6–5 mg m^{-3} and indicated high productivity at the surface during the survey period (Fig. 6.11). Molar C/N, POC and pigment analysis of the sPOM and POM here confirms the presence of fresh material in the surface waters above the canyon during the survey, with surface samples close to the Redfield ratio and contributions of chlorophyll *a* >80% of the total pigment concentration. As expected high concentrations of PUFAs were detected, further affirming that sPOM from the surface is fresh and rich in labile compounds originating from phytoplankton. SEMs of the sPOM showed the presence of phytoplankton in the surface. Coccolithophorids, primarily *Emiliana huxleyi,* dominated the community but pennate diatoms and, dinoflagellates - which would be more typically found during the summer months were also identified in the surface sample. A higher contribution of $C_{22:6}$ (DHA) over $C_{20:5}$ (EPA) was detected in the surface, indicating the dominance of dinoflagellates over diatoms, and was likely due to the sucession of dinoflagellates that occurs during the summer months in northern latitudes (Heinrich, 1962). Some caution must be exercised when considering with the ratio of DHA to EPA, as many classes

of phytoplankton produce significant amounts of DHA (Budge and Parrish, 1998). However, degradation of the spring (diatom) bloom is also indicated by the relatively high contributions of bacterial compounds measured in the surface sPOM. Although, neither techniques (biomaker or SEMS) employed in the manner here can give a fully quantitative assessment of the phytoplankton/zooplankton/bacterial biomass or their ecology, together they clearly indicate the presence of energy-rich organic matter mostly originating from phytoplankton.

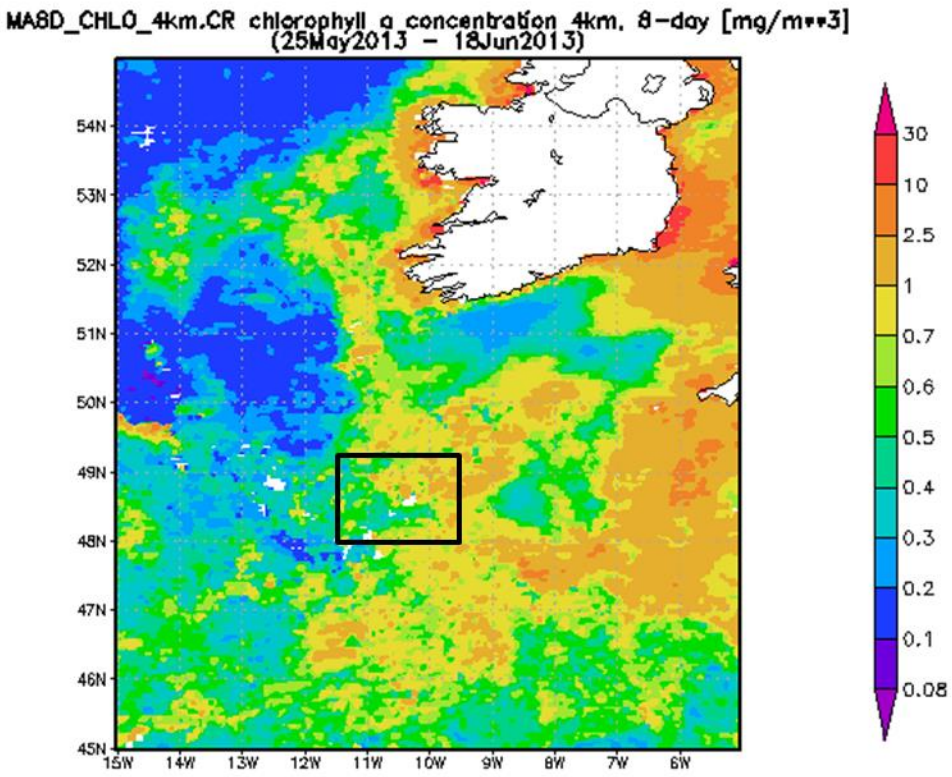

Figure 6.11. Chlorophyll *a* concentration (mg m^{-3}) from MODIS-Aqua satellite during the survey period (9–17th June 2013). Location of the Whittard Canyon is shown with a black box. Image produced by Giovanni online data system (NASA GES DISC).

6.5.2.2 Enrichment and composition of OM in benthic and intermediate nepheloid layers

From the productive surface waters, OM is generally transported to deeper depths by the gravitational settling of particles. However, rich labile OM from the surface can also be transported laterally via nepheloid layers (e.g. van Weering et al., 1998). Previous studies have also suggested that nepheloid layers

are responsible for nutritional enrichment within and along the axis of the Whittard Canyon (Masson, 2009; Duineveld et al., 2001; Huvenne et al., 2011). Sediments in the Whittard Channel are enriched in OC and C/N ratios show that the material is of marine origin and slightly degraded (Amaro et al. 2015). For fresh phytodetritus and labile OM to reach depths of 2000 m (Huvenne et al., 2011), other processes (i.e. lateral advection and internal energy fluxes) must be aiding vertical settling. The data presented here supports the idea that there is enrichment in BNLs, particularly in the upper reaches of the canyon (~650–750 m). INLs extend horizontally from the BNL source, using isopycnal boundaries as an interface for extension/detachment and supporting the accumulation of material including freshly settled phytodetritus (Mudroch and Mudroch, 1992), thus aiding suspension feeding fauna in the utilisation of this important food source (Johnson et al., 2013; Appendix A). Furthermore, INLs provide a mechanism for the dispersal, redistribution and modification of OM from the shelf and across the canyon. The data presented here clearly demonstrates that the NLs are composed of heterogeneously sourced particles, with indications of fresh rich OM derived from phytoplankton from the surface, degraded OM and mineral sediment grains by resuspension processes.

POC decreases rapidly with depth from the surface (e.g. Kiriakoulakis et al., 2011; Giering et al., 2014). However, the highest sPOC and POC concentrations, aside from the surface samples, were observed in near-bottom samples between 300–400 m and 1680–1850 m and thus indicating organic rich material. POC concentrations were fairly constant at mid-water depths throughout the water column contradicting general trends of decreasing POC with depth and together with high POC/SPM ratios suggesting enrichment of POM in INLs particularly at ~650 m and 1200 m. Furthermore, increased sPOC and POC concentrations observed in BNLs in water depths greater than 1500 m, suggest the resuspension of OC based sediments. The lack of correlation between SPM and POC concentrations may be due to the different stage of OM decomposition and/or variable lithogenic loading due to resuspension.

The heterogeneous C/N ratios measured in the sPOM from the BNL and INLs further demonstrate the range of sources, disaggregation and reworking of sinking POM, that are contributing to the composition of material (Kiriakoulakis et al., 2011). The highly varied benthic C/N ratios ranging from 3.5 to 34.9 indicated

both fresh phyto detrital and degraded material, supporting the idea of multiple sources of OM.

Weak BNLs with moderate to low concentrations of SPM (~130–290 μg L^{-1}) had the highest indications of degradation (28.4–34.4) and can be explained by the longer residence and suspension times of finer particles, allowing for greater degradation. Smaller grain sizes of sands and pure carbonates may also support higher C/N ratios, having increased specific surface for the adsorption of organic carbon on carbonate mineral surfaces (Suess, 1973; Müller, 1977; Mayer, 1994). Furthermore, the preferential decomposition of nitrogen compounds in POM generally shows increasing C/N values with depth and may explain higher C/N values in some of the deeper BNLs (Müller, 1977; Kiriakoulakis et al., 2001).

Samples from more turbid BNLs with high amounts of SPM (>500 μg L^{-1}) had lower C/N values (4–15), indicating high concentrations of fresher, less degraded OM. These values maybe accounted for by the formation and transport of large aggregates of fresh material from the surface. Large aggregates support higher settling velocities and a faster delivery of labile components to the deep (e.g. Alldredge and Gotschalk, 1989; Iverson and Ploug, 2010). sPOM from mid-water depth samples showed similar C/N values (3.2–7.6) for moderate INLs (~140–360 μg L^{-1}), indicative of fresh relatively unaltered material of marine (phytoplankton) origin (Meyers, 1997).

Some BNLs in water depths >1500 m showed very low C/N ratios and maybe related to particle sorting in the BNLs deeper in the canyon. Alternatively these values and similarly low C/N values (0.96–1.83) in INLs can be explained by the presence of inorganic nitrogen. Clay-rich SPM is preferential to the incorporation and protection of fixed ammonium (inorganic nitrogen) from the decomposition of OM (Müller, 1977). Regression analysis of PN and POC indicated that more than half of the samples were affected by the presence of inorganic nitrogen grains driving some of the variance and low C/N values observed and emphasising the heterogeneity found here.

Chlorophyll *a* and phaeopigments have previously been used to trace the amount of organic matter (and labile OC) and seasonal fluxes of phytodetritus produced by photosynthesis and as descriptors of the trophic state (e.g. Billett et al., 1983; Barlow et al., 1993; Stephens et al., 1997; Dell'Anno et al., 2002). Enrichment in pigment concentrations further supports the efficient transport of

organic matter via nepheloid layers and the presence of relatively fresh material at depth. Concentrations of total pigments were also elevated in BNLs (420 m, 660 m, 930 m, 1320 m, 1680–2060 m) and at mid-water depths (860 m and 1360 m), where INLs are known to occur (Wilson et al., 2015a; Chapter 4). Although phaeopigments contributed essentially 100% of the pigment content at the deeper depths, chlorophyll *a* degrades rapidly (~18–30 days, Graf et al., 1995; Bianchi et al., 2000). The high concentration of total pigments would suggest that although the material had undergone some degree of phyto-decay, which would be expected with the occurrence of the spring bloom in the Celtic Sea in late April 2013, it is still relatively fresh (Boon and Duineveld, 1996; Gohin et al., 2015).

SPM from BNLs and INLs in the upper reaches of the canyon (420–740 m) had higher proportions of chlorophyll *a* (25–35 %), thus indicating that this material is very fresh and must have been rapidly transported to these depths in the upper reaches of the canyon. The efficient transport of material from the surface via NLs is further supported by the presence of fully intact diatom frustules, cocolithophorides and some pelagic forams in SEMs of sPOM from BNLs down to depths of almost 1400 m. The generally good condition of some of the cells would suggest that at least a small amount of the material has escaped intensive modification during settling and has been protected in the turbid BNL.

The lipid results presented here further suggest that typical BNLs are composed of sPOM high in labile components, particularly in the upper reaches of the canyon (~650–750 m). These BNLs receive high inputs of OM from the productive overlying waters and, is likely transported further by enhanced energy at the seabed within this depth range (i.e. by internal waves reflection; Wilson et al., 2015a; Chapter 4). Concentrations of total lipids were within the range reported by Huvenne et al. (2011; 35.4–618.8 ng L^{-1}). Total lipids of the sPOM in moderate BNLs (SPM = 250–500 µg L^{-1}) in the upper reaches of WC1 and WC3 (~ 650–750 m) exceeded concentrations in the surface, both in terms of food availability and compositional quality. The fact that there are more lipids in the BNL than at the surface strongly suggests that the BNL is accumulating rich OM at the ~650–750 m depth range.

Both samples from the upper reaches of the canyon showed high contributions of labile compounds. sPOM from WC1 was characterised by PUFAs with similar contributions of phyto and zoo plankton markers. However, sPOM

from WC3 was dominated by monounsaturated fatty alcohols, suggestive of heterotrophic reworking of sPOM and compounds indicative of zooplankton, while contributions of phytoplankton biomarkers were low. Although Liu et al. (2009) have reported that zooplankton actively avoid SAPS, copepods were observed during the lipid extraction process. The monounsaturated alcohols ($C_{20:1}$ and $C_{22:1}$) detected are typically derived from Calanoid copepods or from the wax esters in their tissues (Dalsgaard et al., 2003). Furthermore SEM images of sPOM also showed likely zooplankton fragments. It has been suggested that zooplankton accumulate at the depth range of NLs and feed on the rich material (van Weering et al., 2001; Kiriakoulakis et al., 2011) and this appears to be the case here. BNLs (and INLs) are known to occur at this depth range, associated with the upper boundary of the MOW where it impinges on the slope and/or the permanent thermocline (Wilson et al., 2015a; Chapter 4). The evidence presented here would suggest that zooplankton were feeding on rich labile OM, and possibly PUFAs, that have accumulated in the BNL. Although low concentrations of PUFAs were detected, this does not exclude the possibility that they were present, and that feeding zooplankton had consumed these fresh highly labile compounds at the time of sampling. Zooplankton feeding on sPOM in WC1 may also be responsible for the high concentration of PUFAs detected, as these compounds can also be assimilated by zooplankton from their diet. Alternatively, some phytoplankton may not been consumed and/or there may be a constant supply of fresh material from the surface at this site which is possible at this time of the year (Gohin et al., 2015) and thus, demonstrating the spatial heterogeneity at the canyon.

6.5.3 Canyon processes and spatial heterogeneity

6.5.3.1 Canyon versus open slope

The mechanisms involved in transporting material from continental shelves to ocean basins vary from region to region (see Puig et al., 2014). Often nepheloid layers are the end product of many of these processes with turbidity currents, internal waves and/or triggered by storms causing lateral advection particularly at the shelf breaks (Oliveira et al., 2002; Martín et al., 2011; Johnson et al. 2013; Appendix A). The branches of the Whittard Canyon are steep with slopes of up to 40 ° along the rims (see Wilson et al., 2015b their Fig. 6; Chapter 5) and are more likely to trigger sediment transport processes and induce NL

formation than the flat open slope areas on the adjacent spurs (slope <8 °). Furthermore, submarine canyons are often described as preferential pathways for the transport of material from shelf environments to the deep abyss (e.g. Gardner, 1989; Lewis and Barnes, 1999; Allen and Durrieu de Madron, 2009; Liu et al., 2002). Numerous studies have reported enrichment along canyon axes supporting benthic biomass and diversity (e.g. Vetter and Dayton, 1998; De Leo et al., 2010).

Vertical profiles of SPM from within the canyon showed defined NL structure in comparison to those from the open slope. POC concentrations were within the ranges of enhanced POC values for other submarine canyons (e.g. Nazaré Canyon; Kiriakoulakis et al., 2011). Furthermore, samples from within the canyon branches appeared to have higher POC and SPM concentrations than those spatially adjacent and at similar depth ranges from the open slope area. However, neither POC nor SPM values from the two locations could be distinguished statistically. Higher POC values were only observed in comparisons by both methods with a bias towards canyon samples whereby, apparent enhancement of POC in the canyon was due to measurements on miniSAPS filters compared with (possibly) underestimates of POC by SAPS for open slope samples (Gardner et al., 2003). Direct comparisons of SPM and POC values within the branches and from the slope consistently showed higher concentrations within the canyon and, increased numerous of samples and replicates are likely needed to demonstrate this statically. Furthermore, large variations and standard deviations in the concentration of SPM in the canyon were driven by one low value.

Lipid analyses of sPOM were also limited to BNLs from within the canyon. It seems likely that enrichment within the Whittard Canyon can be attributed to the accumulation and retention of these components in the NLs and antedates the rapid delivery and redistribution of rich OM (Amaro et al., 2015). The extensive coverage by the INLs extending distances >25 km off slope could be laterally transporting material over a wider extent than if the material was simply deposited through downward propagation, thus channelling high quality material to deeper depths and promoting the conduit nature of the canyon. The rugged topography and continuous reflection of internal motions associated with the INLs here (Wilson et al., 2015a; Chapter 4), likely induces a continuous supply of

relatively fresh material. However, due to the limited number of samples and profiles from the open slope it is not clear whether enrichment by NLs is promoted by the complex topography and restricted to within the canyon and absent on the open slope. It is also possible that given the time of the survey, the settling of material from the surface through the shallower water column on the open slope area was sufficient to fuel and maintain small NLs there with moderate POC concentrations.

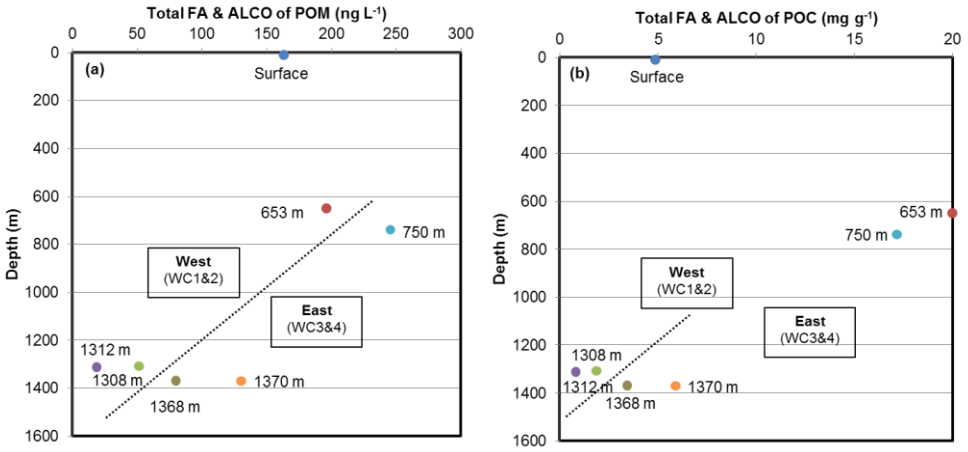

Figure 6.12. East-west divide in the compositional quality of sPOM at the Whittard Canyon. Concentrations of total lipids V water depth in (a) ng of lipids per L of filtered water and (b) mg lipids per g of organic carbon.

6.5.3.2 Compositional heterogeneity by an 'east-west' divide

The compositional nature of the sPOM in the BNLs and INLs showed heterogeneity in the concentration and quality due to a mixture of fresh and decayed OM from a variety of sources. This variability was observed between depth groups and across the four branches of the canyon. Spatial and temporal variation of the local supply from the surface and varying (energy) processes can affect the quantity and quality of OM and likely explain some of the variability observed. Indeed, a recent modelling study at the Whittard Canyon has shown considerable differences in the internal energy fluxes between the branches that can rework and resuspend material (Amaro et al. 2016 their Fig. 3).

Many studies have also suggested that there are varying levels of activity in western and eastern branches of the Whittard Canyon in terms of benthic communities (e.g. Amaro et al. 2016; Gunton et al., 2014 and references therein). It has been proposed that these variations can be attributed to differences in

canyon branch activity and the supply of fresh OM to these communities. A clear distinction in the quantity and quality of sPOM in eastern (WC1, WC2) and western branches (WC3, WC4) was also observed here (Fig. 6.12). Higher concentrations of total lipids were observed in the east rather than the west at both depth ranges (normalised to volume of water; Fig. 6.12a). BNLs at the deeper depth range consistently had higher concentrations in the east (normalised to g of OC; Fig. 6.12b). Although sPOM in the west had lower lipid concentrations, high levels of unsaturated fatty acids and contributions of labile material indicative of phytoplankton and zooplankton were found (mainly PUFAs in WC1 and MUFAs in WC2). In contrast, low lability with high contributions of SFAs and fatty alcohols with bacterial signatures indicative of a more degraded nature of the sPOM was observed in the east (WC3 and WC4).

Huvenne et al., (2011) detected unsaturated fatty acids in the western (WC1) and eastern branches (east of WC4) of the canyon in water depths >1702 m. Although they reported differences in the contributions of PUFAs (DHA and EPA mainly in the east) and MUFAs (in the west), both groups are indicators of fresh material. Similar to the variation in the upper reaches of the canyon identified here, these differences likely reflect the variation in the contributions from phyto and zooplankton from/at distinct locations. However, at the deeper depth range (~1350 m, shallower than Huvenne et al. 2011 data), sPOM from both eastern branches (WC3 and WC4) showed no contribution of compounds derived from phytoplankton or zooplankton.

Lower concentrations of labile compounds were also reported by Huvenne et al. (2011) at sites in the eastern branches (WC3, 4 and east of WC4 in their study). However, the semi-labile and refractory compounds they detected were attributed to reworking and resuspension of POM deeper in the canyon (> 3000 m). Although these measurements only provide a snap shot of the composition and temporal variability could not have been captured, the differences observed by Huvenne et al. (2011) were at different depth ranges and not within the same depth range acrossbranches, as observed here.

sPOM from both sides of the system (here) showed some degree of degradation, as would be excepted, however the highest contribution of bacterial biomarkers was detected in WC3 and lowest in WC4. These extreme values may suggest episodic activity causing sudden and dramatic changes to the natural

composition of the sPOM. Lower concentrations of labile material, low degradation and lack of phyto and zoo plankton signatures would suggest higher levels of sedimentary material and that resuspension processes are influencing the compositional components of sPOM in the BNL in WC4.

Recent studies in the Whittard Canyon have suggested that large amounts of SPM, high in sedimentary OC and N and poor in terms of fresh OM, are transported in episodic events down the canyon (Duineveld et al., 2001; Amaro et al., 2015). Sites affected by trawl-induced resuspension have been identified in WC3 and WC4 (Wilson et al., 2015b; Chapter 5) and it is possible that this activity diluted or altered the quality of OM in these branches at the time.

Concentrations of SPM in WC4 exceeded 3000 µg L^{-1} and showed the highest sPOC values. Combined with the lack of lability these results would imply that much of this material is refractory OC. Lower pigment concentrations detected in a surface sample above WC4 (20% chlorophyll *a* contribution compared to at least 75% in the other surface samples), may also be explained by trawl activity whereby sediment from the seabed was brought to the surface with the haul of trawling gear. Concentrations of SPM in WC3 were much lower (~300 µg L^{-1}), but the samples were taken within the trawling period (14th June 2013: cast #63 and #66; Wilson et al., 2015b; Chapter 5).

To discern the possibility of whether or not trawling could be altering the composition of sPOM normally transported in the BNLs; MDS and ANOSIM analysis were carried out (Fig. 6.13). For this, Euclidean distance similarity matrices were calculated with fourth root transformed values. Due to the limited number of samples, MDS analysis was carried out on all seven samples to differentiate whether depth groups could be identified with respect to 42 individual lipid compounds. Cluster analysis clearly showed distinction between the depth groups; ~700 m and ~1350 m (ANOSIM, R = 1, p = 0.038). Within the deeper depth group (i.e. 1350 m), normal BNLs and ENLs (i.e. trawl affected) were separated.

The contribution of variables (i.e. compounds) driving the dissimilarity between the depth groups were determined using SIMPER analysis and showed differentiation was primarily due to monounsaturated fatty alcohols and PUFAs. Specifically, $C_{22:1}$ and $C_{20:1}$ fatty alcohols and $C_{22:5}$, $C_{22:6}$, $C_{20:3}$ and $C_{20:5}$ fatty acids, markers of Calanoid copepods and phytoplankton (both diatom and

dinoflagellates), were driving the dissimilarity (Dalsgaard, 2003; Tolosa et al., 2003; Berg and Barnathan, 2005; Parish 2013). These compounds were completely absent in the ENL samples while they were present in the normal BNLs at ~1350 m. Therefore the apparent east-west divide between sPOM from BNLs in the four branches of the canyon at ~1350 m may be driven by the influence of trawl induced resuspension. If this is the case, the delivery of fresh OM via NLs and depositional settling will inevitably be affected with consequences for the associated faunal communities (Johnson et al. 2013; Appendix A).

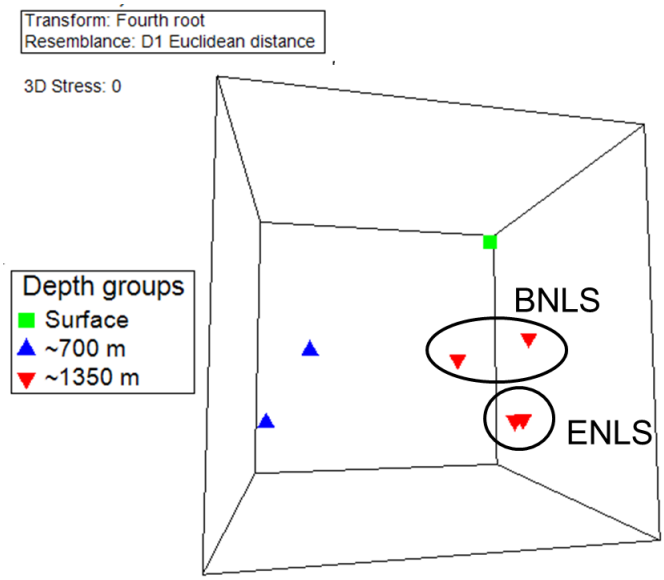

Figure 6.13. Multi-Dimensional Scaling (non-metric) plot of sPOM collected at two depth ranges (700 m-blue triangles & 1350 m-red triangles) in benthic nepheloid layers (BNLs) and enhanced nepheloid layer (ENLS i.e. induced by trawl activity) and the surface (green square) at the Whittard Canyon in June 2013. Total fatty acids and alcohols V water depth of sPOM in the Whittard Canyon.

6.6 Conclusion

This study provides a snapshot of the composition of POM in Whittard Canyon during a survey carried out in June 2013. The significant heterogeneity of sPOM reflects sources of both freshly settled and newly resuspended material. BNLs in the upper reaches of the canyon (650–750 m) are composed of high-quality OM by the accumulation of large quantities of freshly settled particles and cells from the surface. Highly labile material suspended in NLs in the upper reaches is probably re-distributed through internal wave reflection that induces numerous NLs throughout the canyon. Transformation of OM in the water column

with depth naturally decreases the quantity and composition of POM as observed in BNLs deeper in the canyon (1300–1400 m). However typical BNLs still showed a degree of lability and signatures of both phyto- and zoo- plankton. BNLs appear to be influencing the delivery of POC and labile OM to deeper parts of the canyon. Differential OM input conditions and variability to the freshness of OM and POC inevitably impact coral species and other assemblages in the Whittard Canyon. If episodic resuspension by trawling is diluting or altering the composition of material normally transported in NLs, these communities will be affected. This matter warrants further investigation, particularly as the Whittard Canyon hosts many unique mega- to meio- benthic and suspension feeding faunal communities. Resolving temporal changes and tracing sPOM in the NLs would augment our understanding and aid our address of questions surrounding spatial heterogeneity in the Whittard Canyon.

Acknowledgments

We thank the captain and crew of the RV Celtic Explorer and all the scientists involved in CE13008 for their dedication, generosity and assistance in collecting the samples used in this study. Technical support from Dave William, Hazel Clark and statistical advice from Rachel Jefferys and Mark Johnson are gratefully acknowledged. Alexandra Kraberg and Pauhla McGrane are gratefully acknowledged for their help with phytoplankton identifications and Emma Smith with lipid analysis. Fig. 6.11 was produced with the Giovanni online data system developed and maintained by the NASA GES DISC and the MODIS mission scientists and NASA personnel are acknowledged. This research was carried out under the Sea Change strategy with the support of the Marine Institute and the Marine Research Sub-Programme of the National Development Plan 2007 – 2013. A.M. Wilson was supported by the Hardiman Research Scholarship, NUI Galway and also received funding from the Thomas Crawford Hayes Award Trust and the Marine Institute Travel grant scheme to carry out this work.

References

Acker, J. G. and G. Leptoukh, Online Analysis Enhances Use of NASA Earth Science Data, Eos, Trans. AGU, Vol. 88, No. 2 (9 January 2007), pp. 14-17.

Alldredge, A.L. and Gotschalk, C.C., 1989. Direct observations of the mass flocculation of diatom blooms: characteristics, settling velocities and formation of diatom aggregates. Deep Sea Research Part A. Oceanographic Research Papers, 36, 159-171.

Allen, S.E. and Durrieu de Madron, X., 2009. A review of the role of submarine canyons in deep-ocean exchange with the shelf. Ocean Science, 5, 607-620.

Amaro, T., Huvenne, V.A.I., Allcock, A.L., Aslam, T., Davies, J.S., Danovaro, R., de Stigter, H.C., Duineveld, G.C.A., Gambi, C., Gooday, A.J., Gunton, L.M., Hall, R., Howell, K.L., Ingels, J., Kiriakoulakis, K., Kershaw, C.E., Lavaleye, M.S.S., Robert, K., Stewart, H., Van Rooij, D., White, M., Wilson, A.M., (2016). The Whittard Canyon-a case study of submarine canyon processes, Progress in Oceanography, 146, 38-57.

Amin, M. and Huthnance, J.M., 1999. The pattern of cross-slope depositional fluxes. Deep Sea Research Part I: Oceanographic Research Papers, 46, 1565-1591.

Antia, A.N., Maaßen, J., Herman, P., Voß, M., Scholten, J., Groom, S. and Miller, P., 2001. Spatial and temporal variability of particle flux at the NW European continental margin. Deep Sea Research Part II: Topical Studies in Oceanography, 48, 3083-3106.

Arar, E.J. and Collins, G.B., 1997. Method 445.0: In vitro determination of chlorophyll a and pheophytin a in marine and freshwater algae by fluorescence. United States Environmental Protection Agency, Office of Research and Development, National Exposure Research Laboratory.

Barlow, R.G., Mantoura, R.F.C., Gough, M.A. and Fileman, T.W., 1993. Pigment signatures of the phytoplankton composition in the northeastern Atlantic during the 1990 spring bloom. Deep Sea Research Part II: Topical Studies in Oceanography, 40, 459-477.

Bergé, J.P. and Barnathan, G., 2005. Fatty acids from lipids of marine organisms: molecular biodiversity, roles as biomarkers, biologically active compounds, and economical aspects. In Marine biotechnology I, Advances in Biochemical Engineering/Biotechnology, Springer Berlin Heidelberg (2005), pp. 49-125. DOI: 10.1007/b135782.

Bianchi, T.S., Johansson, B. and Elmgren, R., 2000. Breakdown of phytoplankton pigments in Baltic sediments: effects of anoxia and loss of deposit-feeding macrofauna. Journal of Experimental Marine Biology and Ecology, 251, 161-183.

Billett, D.S.M., Lampitt, R.S., Rice, A.L. and Mantoura, R.F.C., 1983. Seasonal sedimentation of phytoplankton to the deep-sea benthos. Nature, 302, 520-522.

Billett, D.S.M., Bett, B.J., Reid, W.D.K., Boorman, B. and Priede, I.G., 2010. Long-term change in the abyssal NE Atlantic: The 'Amperima Event'revisited. Deep Sea Research Part II: Topical Studies in Oceanography, 57, 1406-1417.

Boetius, A., Springer, B. and Petry, C., 2000. Microbial activity and particulate matter in the benthic nepheloid layer (BNL) of the deep Arabian Sea. Deep Sea Research Part II: Topical Studies in Oceanography, 47, 2687-2706.

Boon, A.R. and Duineveld, G.C.A., 1996. Phytopigments and fatty acids as molecular markers for the quality of near-bottom particulate organic matter in the North Sea. Journal of Sea Research, 35, 279-291.

Bosley, K. L., Lavelle, J. W., Brodeur, R. D., Wakefield, W. W., Emmett, R. L., Baker, E. T., & Rehmke, K. M., 2004. Biological and physical processes in and around Astoria submarine Canyon, Oregon, USA. Journal of Marine Systems, 50, 21-37.

Budge, S.M. and Parrish, C.C., 1998. Lipid biogeochemistry of plankton, settling matter and sediments in Trinity Bay, Newfoundland. II. Fatty acids. Organic Geochemistry, 29, 1547-1559.

Cacchione, D.A. and Drake, D.E., 1986. Nepheloid layers and internal waves over continental shelves and slopes. Geo-Marine Letters, 6, 147-152.

Cunningham, M.J., Hodgson, S., Masson, D.G., Parson, L.M., 2005. An evaluation of along- and down-slope sediment transport processes between Goban Spur and Brenot Spur on the Celtic Margin of the Bay of Biscay. Sedimentary Geology, 179, 99-116.

Dalsgaard, J., John, M.S., Kattner, G., Müller-Navarra, D. and Hagen, W., 2003. Fatty acid trophic markers in the pelagic marine environment. Advances in Marine Biology, 46, 225-340.

De Leo, F.C., Smith, C.R., Rowden, A.A., Bowden, D.A. and Clark, M.R., 2010. Submarine canyons: hotspots of benthic biomass and productivity in the deep sea. Proceedings of the Royal Society of London B: Biological Sciences, rspb20100462.

De Stigter, H.C., Boer, W., de Jesus Mendes, P.A., Jesus, C.C., Thomsen, L., van den Bergh, G.D., van Weering, T.C.E., 2007. Recent sediment transport and deposition in the Nazaré Canyon, Portuguese continental margin. Marine Geology, 246, 144–164.

Dell'Anno, A., Mei, M.L., Pusceddu, A. and Danovaro, R., 2002. Assessing the trophic state and eutrophication of coastal marine systems: a new approach based on the biochemical composition of sediment organic matter. Marine Pollution Bulletin, 44, 611-622.

Dickson, R.R. and McCave, I.N., 1986. Nepheloid layers on the continental slope west of Porcupine Bank. Deep Sea Research Part A. Oceanographic Research Papers, 33, 791-818.

Duineveld G., Lavaleye M.S.S., Berghuis E.M., de Wilde P., 2001. Activity and composition of the benthic fauna in the Whittard Canyon and the adjacent continental slope (NE Atlantic). Oceanologica Acta, 24, 69–83.

Duineveld, G.C.A., Jeffreys, R.M., Lavaleye, M.S.S., Davies, A.J. , Bergman, M.J.N. , Watmough, T. and Witbaard, R., 2012. Spatial and tidal variation in food supply to shallow cold-water coral reefs of the Mingulay Reef complex (Outer Hebrides, Scotland). Marine Ecology Progress Series, 444, 97-115.

Duros, P., Fontanier, C., Metzger, E., Pusceddu, A., Cesbron, F., de Stigter, H.C., Bianchelli, S., Danovaro, R., Jorissen, F.J., 2011. Live (stained) benthic foraminifera in the Whittard Canyon, Celtic margin (NE Atlantic). Deep-Sea Research Part I: Oceanographic Research Papers 58, 128–146.

Duros, P., Fontanier, C., de Stigter, H.C., Cesbron, F., Metzger, E., Jorissen, F.J., 2012. Live and dead benthic foraminiferal faunas from Whittard Canyon (NE Atlantic): focus on taphonomic processes and paleo-environmental applications. Marine Micropaleontology, 94, 25-44.

Durrieu De Madron, X.D., Castaing, P., Nyffeler, F. and Courp, T., 1999. Slope transport of suspended particulate matter on the Aquitanian margin of the Bay of Biscay. Deep Sea Research Part II: Topical Studies in Oceanography, 46, 2003-2027.

Gardner, W.D., 1989. Periodic resuspension in Baltimore Canyon by focusing of internal waves. Journal of Geophysical Research: Oceans, 94, 18185-18194.

Gardner, W.D., Richardson, M.J., Carlson, C.A., Hansell, D. and Mishonov, A.V., 2003. Determining true particulate organic carbon: bottles, pumps and methodologies. Deep Sea Research Part II: Topical Studies in Oceanography, 50, 655-674.

Gerritsen, H.D. and Lordan, C., 2014. Atlas of commercial fisheries around Ireland.

Giering, S.L., Sanders, R., Lampitt, R.S., Anderson, T.R., Tamburini, C., Boutrif, M., Zubkov, M.V., Marsay, C.M., Henson, S.A., Saw, K. and Cook, K., 2014. Reconciliation of the carbon budget in the ocean's twilight zone. Nature, 507, 480-483.

Gohin, F., Bryere, P. and Griffiths, J.W., 2015. The exceptional surface turbidity of the North-West European shelf seas during the stormy 2013–2014 winter: Consequences for the initiation of the phytoplankton blooms? Journal of Marine Systems, 148, 70-85.

Graf, G., Gerlach, S.A., Linke, P., Queisser, W., Ritzrau, W., Scheltz, A., Thomsen, L. and Witte, U., 1995. Benthic-pelagic coupling in the Greenland-Norwegian Sea and its effect on the geological record. Geologische Rundschau, 84, 49-58.

Gunton, L.M., Gooday, A.J., Glover, A.J., Bett, B.J., 2015. Macrofaunal abundance and community composition at lower bathyal depths in different branches of the Whittard Canyon and on the adjacent slope (3500m; NE Atlantic). Deep Sea Research Part I, 97, 29-39

Harwood, J.L. and Russell, N.J., 1984. Lipids in plants and microorganisms. George Allen & Unwin, London (1984).

Hayakawa, K., Handa, N. and Wong, C.S., 1997. Changes in the composition of fatty acids in sinking matter during a diatom bloom in a controlled experimental ecosystem. Journal of Experimental Marine Biology and Ecology, 208, 29-43.

Heinrich, A.K., 1962. The life histories of plankton animals and seasonal cycles of plankton communities in the oceans. Journal du Conseil, 27, 15-24.

Holt, J. and Thorpe, S., 1997. The propagation of high frequency internal waves in the celtic sea. Deep Sea Research Part I: Oceanographic Research Papers, 4, 2087-2116.

Hopkins, J.E., Stephenson, G.R., Green, J.A.M., Inall, M.E. and Palmer, M.R., 2014. Storms modify baroclinic energy fluxes in a seasonally stratified shelf sea: Inertial-tidal interaction. Journal of Geophysical Research: Oceans, 119, 6863-6883.

Hunter, W.R., Jamieson, A.J., Huvenne, V., Witte, U., 2013. Sediment community responses to marine vs. terrigenous organic matter in a submarine canyon. Biogeosciences, 10, 67-80.

Huvenne, V.A.I., Tyler, P.A., Masson, D.G., Fisher, E.H., Hauton, C., Hühnerbach, V., Le Bas, T.P., Wolff, G.A. 2011. A Picture on the Wall: Innovative Mapping Reveals Cold-Water Coral Refuge in Submarine Canyon. PLoS ONE 6, e28755.

Inthorn, M., Wagner, T., Scheeder, G. and Zabel, M., 2006a. Lateral transport controls distribution, quality, and burial of organic matter along continental slopes in high-productivity areas. Geology, 34, 205-208.

Inthorn, M., van der Loeff, M.R. and Zabel, M., 2006b. A study of particle exchange at the sediment–water interface in the Benguela upwelling area based on 234 Th/238 U disequilibrium. Deep Sea Research Part I: Oceanographic Research Papers, 53, 1742-1761.

Iversen, M.H. and Ploug, H., 2010. Ballast minerals and the sinking carbon flux in the ocean: carbon-specific respiration rates and sinking velocity of marine snow aggregates. Biogeosciences, 7, 2613-2624.

Johnson, D.R., Weidemann, A. and Pegau, W.S., 2001. Internal tidal bores and bottom nepheloid layers. Continental Shelf Research, 21, 1473-1484.

Johnson, M. P., White, M., Wilson, A., Würzberg, L., Schwabe, E., Folch, H., and Allcock, A. L., 2013. A vertical wall dominated by Acesta excavata and Neopycnodonte zibrowii, part of an undersampled group of deep-sea habitats. PLoS ONE, 8, e79917.

Joint, I., Wollast, R., Chou, L., Batten, S., Elskens, M., Edwards, E., Hirst, A., Burkill, P., Groom, S., Gibb, S. and Miller, A., 2001. Pelagic production at the Celtic Sea shelf break. Deep Sea Research Part II: Topical Studies in Oceanography, 48, 3049-3081.

Kiriakoulakis, K., Marshall,J.D., Wolff,G.A., 2000. Biomarkers in a lower Jurassic concretion from Dorset. Journal of Geological Society London, 157, 207–220.

Kiriakoulakis, K., Stutt, E., Rowland, S. J., Vangriesheim, A., Lampitt, R. S., Wolff, G. A., 2001. Controls on the organic chemical composition of settling particles in the Northeast Atlantic Ocean. Progress in Oceanography, 50, 65-87.

Kiriakoulakis, K., Bett, B.J., White, M. and Wolff, G.A., 2004. Organic biogeochemistry of the Darwin Mounds, a deep-water coral ecosystem, of the NE Atlantic. Deep Sea Research Part I: Oceanographic Research Papers, 51, 1937-1954.

Kiriakoulakis, K., Fisher, E., Wolff, G.A., Freiwald, A., Grehan, A. and Roberts, J.M., 2005. Lipids and nitrogen isotopes of two deep-water corals from the North-East Atlantic: initial results and implications for their nutrition. In Cold-Water Corals and Ecosystems (Eds.) Friewald, A. & Roberts, J.M. Springer Berlin Heidelberg. (2005), pp. 715-729.

Kiriakoulakis, K., Vilas, J.C., Blackbird, S.J., Arístegui, J., Wolff, G.A., 2009. Seamounts and organic matter-Is there an effect? The case of Sedlo and Seine seamounts, Part 2. Composition of suspended particulate matter. Deep-Sea Research II, 56, 2631-2645.

Kiriakoulakis K., Blackbird S., Ingels J., Vanreusel A., Wolff G.A., 2011. Organic geochemistry of submarine canyons: The Portuguese margin, Deep Sea Research Part II, 58, 2477-2488.

Lewis, K.B. and Barnes, P.M., 1999. Kaikoura Canyon, New Zealand: active conduit from near-shore sediment zones to trench-axis channel. Marine Geology, 162, 39-69.

Liu, J.T., Liu, K.J. and Huang, J.C., 2002. The effect of a submarine canyon on the river sediment dispersal and inner shelf sediment movements in southern Taiwan. Marine Geology, 181, 357-386.

Liu, Z., Stewart, G., Cochran, J.K., Lee, C., Armstrong, R.A., Hirschberg, D.J., Gasser, B. and Miquel, J.C., 2005. Why do POC concentrations measured using Niskin bottle collections sometimes differ from those using in-situ pumps? Deep Sea Research Part I: Oceanographic Research Papers, 52, 1324-1344.

Liu, Z., Cochran, J.K., Lee, C., Gasser, B., Miquel, J.C. and Wakeham, S.G., 2009. Further investigations on why POC concentrations differ in samples collected by Niskin bottle and in situ pump. Deep Sea Research Part II: Topical Studies in Oceanography, 56, 1558-1567.

Martín, J., Palanques, A., Vitorino, J., Oliveira, A., de Stigter, H.C., 2011. Near-bottom particulate matter dynamics in the Nazaré submarine canyon under calm and stormy conditions. Deep-Sea Research Part II, Topical Studies in Oceanography, 58, 2388-2400.

Masson, D.G., 2009. RRS James Cook Cruise 36, 19 Jul-28 Jul 2009. The Geobiology of Whittard Submarine Canyon.

Masson D.G., Huvenne V.A.I., de Stigter H., Wolff G.A., Kiriakoulakis K., Arzola R.G., Blackbird S., 2010. Efficient burial of carbon in a submarine canyon. Geology, 38, 831–834.

Mayer, L.M., 1994. Surface area control of organic carbon accumulation in continental shelf sediments. Geochimica et Cosmochimica Acta, 58, 1271-1284.

Meyers, P.A., 1997. Organic geochemical proxies of paleoceanographic, paleolimnologic, and paleoclimatic processes. Organic geochemistry, 27, 213-250.

Morris K.J., Tyler R.A., Masson D.G. Huvenne V.I.A. and Rogers A. 2013. Distribution of cold water corals in the Whittard Canyon NE Atlantic. Deep Sea Research II, 92, 136-144.

Mudge, S.M., 2005. Fatty alcohols-a review of their natural synthesis and environmental distribution. The Soap and Detergent Association, 132, 1-141.

Mudroch, A. and Mudroch, P., 1992. Geochemical composition of the nepheloid layer in Lake Ontario. Journal of Great Lakes Research, 18, 132-153.

Müller, P.J., 1977. CN ratios in Pacific deep-sea sediments: Effect of inorganic ammonium and organic nitrogen compounds sorbed by clays. Geochimica et Cosmochimica Acta, 41, 765-776.

Oliveira, A., Vitorino, J., Rodrigues, A., Jouanneau, J.M., Dias, J.A. and Weber, O., 2002. Nepheloid layer dynamics in the northern Portuguese shelf. Progress in Oceanography, 52, 195-213.

Parrish, C.C., 2013. Lipids in marine ecosystems. ISRN Oceanography, Article ID 604045, DOI: 10.5402/2013/604045

Pingree, R.D. and Le Cann, B., 1990. Structure, strength and seasonality of the slope currents in the Bay of Biscay region. Journal of the Marine Biological Association of the United Kingdom, 70, 857-885.

Pingree, R.D. and Le Cann, B., 1989. Celtic and Armorican slope and shelf residual currents. Progress in Oceanography, 23, 303-338.

Pingree, R. D., Sinha, B., Griffiths, C.R. 1999. Seasonality of the European slope current (Goban Spur) and ocean margin exchange. Continental Shelf Research, 19, 929-975.

Pollard, R. T., Griffttths, M. J., Cunningham, S. A., Read, J. F., Pérez, F. F., Ríos, A. F., 1996. Vivaldi 1991-A study of the formation, circulation and ventilation of Eastern North Atlantic Central Water. Progress in Oceanography, 37, 167-192.

Prentice, I.C., Farquhar, G.D., Fasham, M.J.R., Goulden, M.L., Heimann, M., Jaramillo, V.J., Kheshgi, H.S., LeQuéré, C., Scholes, R.J. and Wallace, D.W., 2001. The carbon cycle and atmospheric carbon dioxide. In Climate Change 2001: the Scientific Basis. Cambridge University Press, Cambridge, UK. pp 185 -237.

Puig, P., Company, J.B., Sardà, F. and Palanques, A., 2001. Responses of deep-water shrimp populations to intermediate nepheloid layer detachments on the Northwestern Mediterranean continental margin. Deep Sea Research Part I: Oceanographic Research Papers, 48, 2195-2207.

Puig, P., Palanques, A., Guillén, J. and El Khatab, M., 2004. Role of internal waves in the generation of nepheloid layers on the northwestern Alboran slope: implications for continental margin shaping. Journal of Geophysical Research: Oceans, 109, C09011. DOI: 10.1029/2004JC002394

Puig, P., Palanques, A., Martín, J., 2014. Contemporary Sediment-Transport Processes in Submarine Canyons. Annual Review of Marine Science, 6, 53-77.

Reid, G.S., Hamilton, D., 1990. A Reconnaissance Survey of the Whittard Sea Fan, Southwestern Approaches, British-Isles. Marine Geology, 92, 69–86.

Robert, K., D. O. B. Jones, P. A. Tyler, D. Van Rooij and V. A. I. Huvenne 2014. Finding the hotspots within a biodiversity hotspot: fine-scale biological predictions within a submarine canyon using high-resolution acoustic mapping techniques. Marine Ecology, 36, 1256-1276. DOI: 10.1111/maec.12228.

Sharples, J., Tweddle, J.F., Mattias Green, J.A., Palmer, M.R., Kim, Y.N., Hickman, A.E., Holligan, P.M., Moore, C., Rippeth, T.P., Simpson, J.H. and Krivtsov, V., 2007. Spring-neap modulation of internal tide mixing and vertical nitrate fluxes at a shelf edge in summer. Limnology and Oceanography, 52, 1735-1747.

Sharples, J., Scott, B.E. and Inall, M.E., 2013. From physics to fishing over a shelf sea bank. Progress in Oceanography, 117, 1-8.

Stephens, M.P., Kadko, D.C., Smith, C.R. and Latasa, M., 1997. Chlorophyll-a and pheopigments as tracers of labile organic carbon at the central equatorial Pacific seafloor. Geochimica et Cosmochimica Acta, 61, 4605-4619.

Stephenson, G. R., Jr., J. E. Hopkins, J. A. Mattias Green, M. E. Inall, and M. R. Palmer, 2015. Baroclinic energy flux at the continental shelf edge modified by wind-mixing, Geophysical Research Letters, 42, 1826–1833. doi: 10.1002/2014GL062627

Suess, E., 1973. Interaction of organic compounds with calcium carbonate-II. Organo-carbonate association in recent sediments. Geochimica et Cosmochimica Acta, 37, 2435-2447.

Tett, P.B., 1987. Plankton. In Biological Surveys of Estuaries and Coasts (eds.) Baker, J.M. and Wolff, J.W., Cambridge University Press, Cambridge (1987), pp. 280 – 341.

Tolosa, I., LeBlond, N., Copin-Montégut, C., Marty, J.C., de Mora, S. and Prieur, L., 2003. Distribution of sterol and fatty alcohol biomarkers in particulate matter from the frontal structure of the Alboran Sea (SW Mediterranean Sea). Marine chemistry, 82, 161-183.

Turnewitsch, R., Springer, B.M., Kiriakoulakis, K., Vilas, J.C., Arístegui, J., Wolff, G., Peine, F., Werk, S., Graf, G. and Waniek, J.J., 2007. Determination of particulate organic carbon (POC) in seawater: The relative methodological importance of artificial gains and losses in two glass-fiber-filter-based techniques. Marine Chemistry, 105, 208-228.

van Rooij, D., Iglesias, J., Hernández-Molina, F.J., Ercilla, G., Gomez-Ballesteros, M., Casas, D., Llave, E., De Hauwere, A., García-Gil, S., Acosta, J. and Henriet, J.P., 2010. The Le Danois Contourite Depositional System: interactions between the Mediterranean outflow water and the upper Cantabrian slope (North Iberian margin). Marine Geology, 274, 1-20.

Van Weering, T.C., Hall, I.R., de Stigter, H.C., McCave, I.N. and Thomsen, L., 1998. Recent sediments, sediment accumulation and carbon burial at Goban Spur, NW European Continental Margin (47–50 N). Progress in Oceanography, 42, 5-35.

Van Weering, T.C., de Stigter, H.C., Balzer, W., Epping, E.H., Graf, G., Hall, I.R., Helder, W., Khripounoff, A., Lohse, L., McCave, I.N. and Thomsen, L., 2001. Benthic dynamics and carbon fluxes on the NW European continental margin. Deep Sea Research Part II: Topical Studies in Oceanography, 48, 3191-3221.

Vetter, E.W. and Dayton, P.K., 1998. Macrofaunal communities within and adjacent to a detritus-rich submarine canyon system. Deep Sea Research Part II: Topical Studies in Oceanography, 45, 25-54.

Vilas, J.C., Arístegui, J., Kiriakoulakis, K., Wolff, G.A., Espino, M., Polo, I., Montero, M.F. and Mendonça, A., 2009. Seamounts and organic matter—Is there an effect? The case of Sedlo and Seine Seamounts: Part 1. Distributions of dissolved and particulate organic matter. Deep Sea Research Part II: Topical Studies in Oceanography, 56, 2618-2630.

Vlasenko, V., Stashchuk, N., Inall, M.E. and Hopkins, J.E., 2014. Tidal energy conversion in a global hot spot: On the 3-D dynamics of baroclinic tides at the Celtic Sea shelf break. Journal of Geophysical Research: Oceans, 119, 3249-3265.

Volkman, J.K. and Johns, R.B., 1977. The geochemical significance of positional isomers of unsaturated acids from an intertidal zone sediment. Nature, 267, 693-694. doi: 10.1038/267693a0

Volkman, J.K. and Tanoue, E., 2002. Chemical and biological studies of particulate organic matter in the ocean. Journal of oceanography, 58, 265-279.

Wakeham, S.G., Lee, C., Hedges, J.I., Hernes, P.J. and Peterson, M.J., 1997. Molecular indicators of diagenetic status in marine organic matter. Geochimica et Cosmochimica Acta, 61, 5363-5369.

Walsh, J.J., 1991. Importance of continental margins in the marine biogeochemical cycling of carbon and nitrogen. Nature, 350, 53-55.

White, M., 2007. Benthic dynamics at the carbonate mound regions of the Porcupine Sea Bight continental margin. International Journal of Earth Sciences, 96, 1-9.

White, M., Mohn, C., Kiriakoulakis, K., 2016 Environmental Sampling. In Biological Sampling in the Deep Sea, (Eds.) Malcolm, C., Mireille, C., Rowden, A., Wiley & Sons (2016), ISBN 978-0-470-65674-7, pp. 57-59.

Wilson, A.M., Raine, R., Mohn, C. and White, M., 2015a. Nepheloid layer distribution in the Whittard Canyon, NE Atlantic Margin. Marine Geology, 367, 130-142.

Wilson, A.M., Kiriakoulakis, K., Raine, R., Gerritsen, H.D., Blackbird, S., Allcock, A.L. and White, M., 2015b. Anthropogenic influence on sediment transport in the Whittard Canyon, NE Atlantic. Marine Pollution Bulletin, 101, 320-329.

Wollast, R. and Chou, L., 2001. The carbon cycle at the ocean margin in the northern Gulf of Biscay. Deep Sea Research Part II: Topical Studies in Oceanography, 48, 3265-3293.

Xu, W., Miller, P.I., Quartly, G.D. and Pingree, R.D., 2015. Seasonality and interannual variability of the European Slope Current from 20years of altimeter data compared with in situ measurements. Remote Sensing of Environment, 162, 196-207.

Yamamuro, M. and Kayanne, H., 1995. Rapid direct determination of organic carbon and nitrogen in carbonate-bearing sediments with a Yanaco MT-5 CHN analyzer. Limnology and Oceanography, 40, 1001-1005.

Zaragosi, S., Auffret, G.A., Faugères, J.C., Garlan, T., Pujol, C. and Cortijo, E., 2000. Physiography and recent sediment distribution of the Celtic Deep-Sea Fan, Bay of Biscay. Marine Geology, 169, 207-237.

Chapter 7
Synthesis

7.1 Summary of key findings

The primary intention of this study was to contribute to existing knowledge on the lateral transport of suspended particulate matter in nepheloid layers in the Whittard Canyon. With respect to the hypothesis and building on previous suggestions the importance of nepheloid layers as a physical delivery mechanism link between the pelagic and abyss at the Whittard Canyon had been clearly established here. The objectives of this study were set out with specific emphasis on addressing the generation, composition and implications of these in a spatial and temporal context. The most significant results of this study include;

- Local hydrodynamics and topographic interactions drive the distribution of nepheloid layers, with hotspots of formation at the boundaries of the permanent thermocline, MOW and regions of enhanced baroclinic energy
- Variations in the density stratification by both seasonal stratification and storm activity can cause temporal effects in distribution
- Both benthic and intermediate nepheloid layers are (generally) composed of high-quality organic material from heterogenic sources
- BNLs in the upper reaches of the canyon are particularly high in rich fresh and labile organic matter
- Fishing by bottom trawlers adjacent to the canyon branches can induce the transport of large amounts of material, altering the distribution and compositional nature of normal nepheloid layers

In establishing the distribution and means of both benthic and intermediate nepheloid layers across four branches of the canyon, the results presented here clearly illustrate the active nature of Whittard Canyon in terms of sediment transport. These observations build on the previous studies by de Stigter et al., 2008 and Huvenne et al., 2011 of BNLs in Whittard Canyon and along the Irish continental margin (e.g. Thorpe and White, 1988; Mc Cave et al., 2001) and in that further extend our knowledge on their distribution patterns and the generation mechanisms involved in their formation. Although the permant presence of NLs across the surveyed branches was established here, the processes generating NLs is likely to vary spatially across the dendritic system (i.e. baroclinic energy, distance of MOW from slope). Furthermore, these processes are likely to

experience temporal variation. Seasonal stratification and storm activity were found to influence NL distribution in the canyon, however large gaps in the temporal variation remains. As the data collected here were limited to late spring-summer season, questions regarding seasonality, both in terms of forcing and quality of material, frequency and lateral extent (on a temporal scale) cannot be address here.

The quantitative and qualitative assessment of the material transported within BNLs and INLs in this study, also builds on the data set of Huvenne et al., 2011; extensively increasing the elemental data set and the coverage of lipid biomarker data. The quality of particles in the water column also compliments sediment studies (e.g. Duineveld et al., 2001; Masson et al., 2010; Duros et al., 2011; Huvenne et al., 2011; Amaro et al., 2016; Appendix B). Based on the elemental and molecular data presented here, the deposition of size-sorted particles from INLs can explain increasing TOC with depth in the canyon (Amaro et al., 2016; Appendix B). Furthermore, higher concentrations of bioavailable organic matter in the canyon sediments compared to the adjacent slope (Duineveld et al., 2001) and higher concentrations of phytopigments in the upper canyon (Duros et al. 2011) can now be linked to the rich, labile OM suspended in BNLs in the upper reaches of the canyon described here. These findings further confirm suggestions by Amaro et al. (2015) regarding the lateral transport of phytodetritus and the accumulation of labile compounds in BNLs and adds further cause to previous suggestions for an association between vertical wall fauna and NLs (Johnson et al., 2011; Appendix A). Although, the data presented here adds more substance to these claims, it is still unclear the extent of this influence and/or actual affect of enhanced food avilabilty on canyon fauna.

Some insight into the consequences of near-by bottom trawling on the Whittard Canyon has been brought to light in this study. Building on publications regarding the scale of fishing impacts in Irish waters (e.g. Gerritsen et al., 2013) and work from other submarine canyons (e.g. Palanques et al., 2006; Puig et al., 2012; Martín et al., 2014), a clear link between large sediment transport events and local bottom trawling at the Whittard Canyon has been established. The triggering of episodic sediment flows, enhanced by the steep slope of the canyon and walls, by adjacent trawling has been showed to alter the natural distribution of BNL features here. This work further confirms suggestions that anthropogenic

activity may need to be considered as contempary sediment transport process (Puig et al., 2014). In addition, the dilution of rich, labile OM by refractory/degraded bulk material from the shelf by large episodic events as hypotheised by Amaro et al. (2015) appears to stand. While the evidence presented further highlights the conservational issues surrounding bottom trawling for deep-sea habitats, the influence of trawling impact has not been, and could not be assessed here.

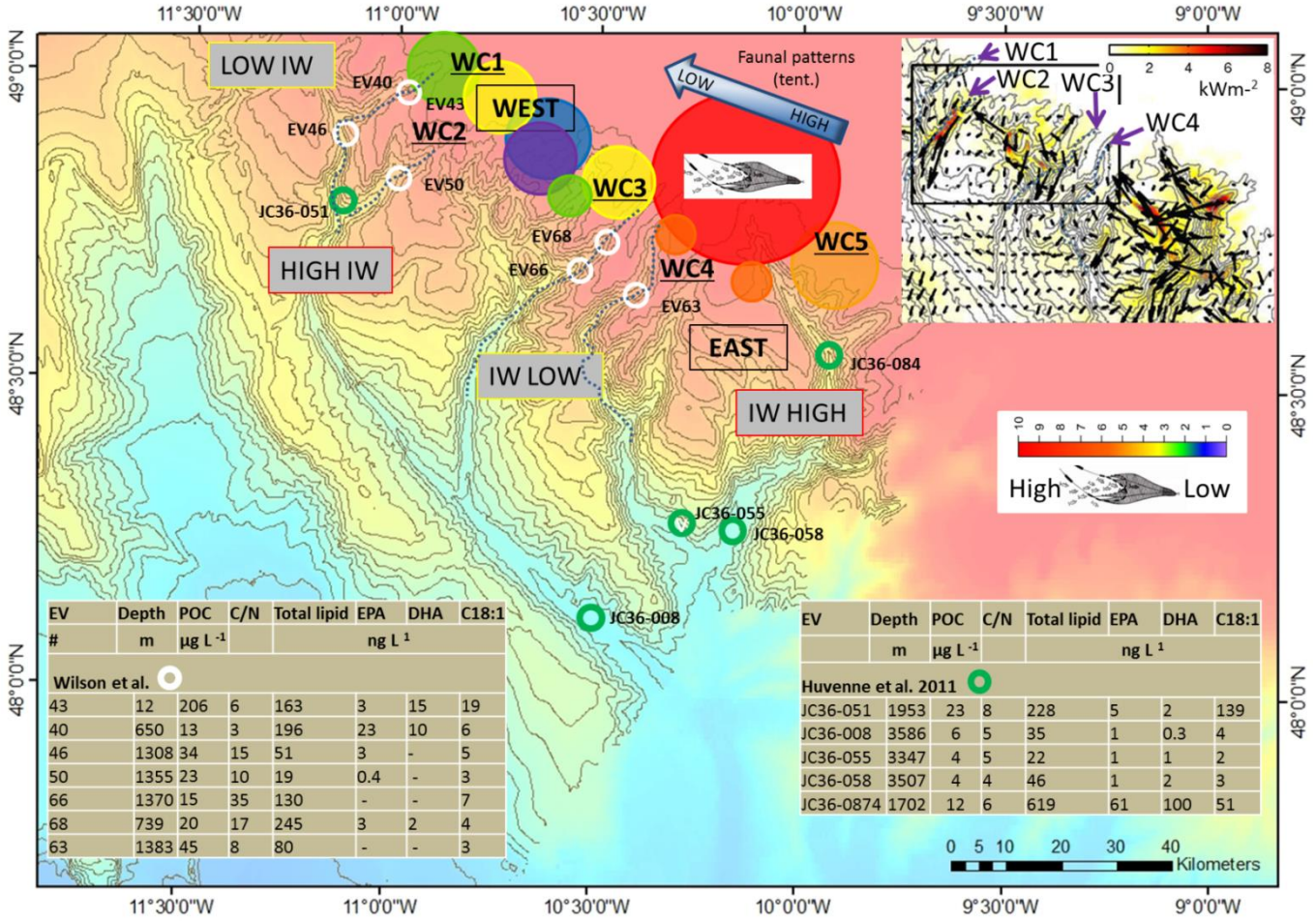

EV #	Depth m	POC µg L^{-1}	C/N	Total lipid ng L^{1}	EPA	DHA	C18:1
Wilson et al.							
43	12	206	6	163	3	15	19
40	650	13	3	196	23	10	6
46	1308	34	15	51	3	-	5
50	1355	23	10	19	0.4	-	3
66	1370	15	35	130	-	-	7
68	739	20	17	245	3	2	4
63	1383	45	8	80	-	-	3

EV	Depth m	POC µg L^{-1}	C/N	Total lipid ng L^{1}	EPA	DHA	C18:1
Huvenne et al. 2011							
JC36-051	1953	23	8	228	5	2	139
JC36-008	3586	6	5	35	1	0.3	4
JC36-055	3347	4	5	22	1	1	2
JC36-058	3507	4	4	46	1	2	3
JC36-0874	1702	12	6	619	61	100	51

Figure 7.1. Summary of the spatial heterogeneity observed at the Whittard Canyon. Location of sPOM data from Chapter 6 and from Huvenne et al. (2011)'s study are shown across five branches (WC1–5). sPOM results are summarised in inset tables with values of POC expressed in µg L^{-1} and total lipids, EPA, DHA and C18:1(n-9) expressed in ng L^{-1}. Insert map shows variable internal energy fluxes i.e. internal waves (IW) and branches are labelled high – low IW accordingly. (Amaro et al. 2016; Appendix B Fig. 3). The fishing activity relative to an annual mean of 0.03 d km^{-2} (Sharples et al., 2013) is indicated by coloured dots corresponding to colour bar. Decreasing faunal abundance and diversity from east to west are indicated with blue arrow.

7.2 Lateral transport through nepheloid layers

It has previously been established that nepheloid layers are significant contributors to the shelf edge exchange of material (e.g. van Weering et al., 1998; Amin and Huthnance, 1999; Puig et al. 2001). Research through large international projects, such as OMEX - along the NE Atlantic margin; have highlighted the importance of lateral transport processes in shelf export. Submarine canyons have also been noted as areas for increased transport and enhanced export of organic matter. The presence of nepheloid layers have been reported at many sites along the NE Atlantic margin and in the Whittard Canyon (e.g. Thorpe and White, 1988; McCave et al., 2001; Antia et al., 2001; Huvenne et al., 2011; Johnson et al., 2011; Appendix A) and, although implications of their presence have been hypothesised, their distribution and generation mechanisms (at some sites) are insufficiently known.

The first systematic description of the distribution of nepheloid layers (and suspended particulate matter) in the water column at the Whittard Canyon is presented here in Chapter 4. Repeated mapping of the layers has yielded a better representation of their extent and persistence. Durrieu de Madron, (1994) suggested that the mechanisms by which continental margins trap or bypass particulate material is closely related to the distribution and dynamics of particles. The mechanisms controlling particle distributions (i.e. PT, MOW boundaries and baroclinic motions) forming INLs extensions up to 25 km off slope in the Whittard Canyon have been successfully identified here. In this respect, the processes and dynamics (seasonal stratification and storms) affecting the nepheloid layers are likely to be similar in other areas where canyons incise the shelf edge and where similar dynamics have been observed (e.g. Sanchez-Vidal, et al., 2012).

Sediment distribution, characteristics and transport in nepheloid layers are directly related to local hydrodynamics (e.g. van Weering et al., 1998; Oliveria et al., 2002). Furthermore, the depth ranges of INL detachments can signify hotspots in energy fluxes and oceanographic processes. Previous studies have suggested varying activity in the branches of the Whittard Canyon (e.g. Duineveld et al., 2001; Huvenne et al., 2011; Hunter et al., 2013; see also supplementary data by Gunton et al., 2015). Spatial heterogeneity and the attributing processes hypothesised here are summarised in Fig. 7.1. The distribution of nepheloid layers

and variability in the SPM patterns agree with previous suggestions of variable energy fluxes in the canyon. Much of the spatial heterogeneity observed in the nepheloid layers can be explained by variability of internal energy fluxes (insert on Fig. 7.1 and Amaro et al. 2016; Appendix B Fig. 3).

Heterogeneity in the distribution of nepheloid layers between the open slope and within the canyon branches was also identified. Although less data (i.e. vertical profiles) were available for the open slope sites, the profiles did not show the defined distribution of SPM in NLs as seen inside the canyon branches and (integrated) concentrations of SPM were higher in the canyon. Inside the canyon branches, the walls and canyon axis slopes are much higher (up to 40 °) in comparison to the interfluves (0–4 °). These steeper slopes promote higher energy fluxes that (can) generate INLs. The presence of both benthic and intermediate layers confirms and demonstrates the active nature of the Whittard Canyon in terms of sediment transport in comparison to the adjacent open slope and interfluves. Furthermore, nepheloid layers in the Whittard Canyon contribute to the conduit nature of the canyon and provide a pathway for the lateral transport of SPM across the shelf edge.

The extensive coverage of both BNLs and INLs and the off slope extensions described here (Chapter 4) confirm that NLs are lateral transporters of material. The concentrations of material reported here provide sufficient additional (lateral) input of particles to promote higher fluxes (van Weering et al., 1998). Other studies have reported that the net sediment export and flow regime is in an up-canyon direction (Amaro et al., 2015; 2016; Appendix B). Although internal energy fluxes in this area are generated at the shelf break by across-slope tidal flow with some waves propagating onto the shelf and the semi-diurnal tide driving 28-48 W m^{-1} energy on-shelf (Holt and Thorpe, 1997; Hopkins et al., 2014); transport down the canyon will still prevail. The highly variable internal energy flux, up- down- and across the different canyon branches, is shown in the inset map in Fig. 7.1. According to the model, on-shelf fluxes are seen for example in the upper reaches of WC3 (site of *Acesta* community; Johnson et al., 2013; Appendix A). INLs associated with the reflection of internal waves have been detected (Chapter 4 and Johnson et al., 2013; Appendix A), however the material resuspended and transported in them will be transported off the slope and laterally to deeper depths. Granted these are high energy fluxes but gravitational

forces and the steep slope along the canyon axis will dominate the direction of transport. At the seabed, Amaro et al. (2015) reports that the sediment transport is driven by the semi-diurnal tidal currents, flowing alternately up- and down-canyon direction and indeed there is likely to be variation at the seabed boundary but the effects of the shelf edge current and processes in the BBL will naturally drive down-welling (Holt et al., 2009). Furthermore, Holt et al. (2009) showed that off the northwest European Continental Shelf (~52 °N), both large scale circulation and frictional processes (Ekman layer at the seabed) support the off shelf transport of carbon that is sufficiently quick to remove ~40% of the carbon sequestered by one growing season, further supporting down canyon and off slope transport. Instantaneous horizontal particulate fluxes from the BOBO lander data (at 1479 m) presented by Amaro et al. (2015; 2016) are calculated by multiplying suspended sediment concentrations with the instantaneous current speed to give point measurements of the SPM flux. However, the vertical component and integrated values of the water column both above and below the lander must also be considered to obtain the true concentration and direction of the net transport. Furthermore, the suggestion of net transport up the canyon at the seabed appears to be between May and June from their data (Amaro et al. 2015 Fig. 2; and Amaro et al., 2016; Appendix B, Fig. 4) and this, perhaps seasonal effect may only be true at the depth of the lander recording.

On the upper slope offshore Namibia, Inthorn et al. (2006a) has shown that effective seaward particle transport primarily along the BNL is a key process that promotes and maintains high local sedimentation rates, ultimately causing high preservation of organic carbon in the depocenter there. Their results indicate that lateral transport is the primary mechanism controlling supply and burial of organic carbon. These advective processes increase sedimentation rates and efficiently displace material from maximum production along the inner shelf toward the slope and possibly to the deep-sea. Recently, Amaro et al. (2015) suggested that the fresh organic matter found in the Whittard Channel mainly arrives though vertical deposition and local settling of phytodetritus produced during phytoplankton blooms. Before this, Duineveld et al. (2001) found indications for biological enrichment in the Whittard Canyon extending to the lower canyon reaches which they attributed to lateral transport of fresh organic matter down the canyon. In Amaro et al. (2015)'s study they also suggest that the

redistribution (by bottom currents) of aggregates of fresh phytodetritus deposited over the lower slope of Whittard Canyon and accumulations of this material in the topographic depressions formed by the Channel. Considering the results presented here, this seems likely and accumulations in NLs generated by such currents can explain the local enrichment of sediments with fresh organic matter. Elemental and lipid biomarker analysis here (Chapter 6) showed sPOM from benthic and intermediate nepheloid layers in the four surveyed branches had POC enrichment and contributions of labile compounds, albeit not at all sites. Material from the BNLs in the upper reaches of the canyon had the highest contributions of fresh rich material and lipid biomarker signatures of material of phytoplankton and zooplankton origin. Chlorophyll *a* at mid water depths, within the depth ranges of benthic and intermediate layers, clearly showed that (some) fresh material is accumulating along the density gradients present in the layers. Given the distribution of BNLs and the distance covered by the INL extensions delineated here, combined with the indications of POC rich material in the layers; redistribution of fresh phytodetritus by nepheloid layers can explain enrichment in the canyon described by others (e.g. Duineveld et al., 2001). Vertical settling of phytodetritus most certainly plays a role but lateral advection by nepheloid layers must be partially responsible for the delivery of rich OM to the Whittard Canyon. Even material transported by vertical settling can accumulate in nepheloid layers and be further transported by lateral advection to deeper depths. Inthorn et al. (2006a) suggests that in the geologic past, widespread downslope lateral transport of organic carbon may have been a primary driver of enhanced OC burial at the deeper continental slopes and abyssal basins. The implications of lateral transport by NLs are great and therefore quantification of this delivery mechanism should be addressed in future studies.

7.3 Trawl-induced sediment transport events

Large episodic turbidity flows have previously been recorded in the Whittard Channel but previous studies have offered no explanation other than that they are gravity flows (e.g. Amaro et al., 2015). Evidence that bottom trawling on the Celtic shelf and spurs of the Whittard Canyon may be inducing resuspension events is presented for the first time in Chapter 5. Concentrations of SPM detected in two branches exceeded those of the typical nepheloid layers by

at least an order of magnitude (based on two consecutive surveys and early measurements in the third survey). The exceptionally high SPM values were linked with bathymetric and VMS data revealing (for the first time) an association between bottom trawling activity and episodic transport events at the Whittard Canyon.

The data presented here related to trawl-induced resuspension events was collected over a five-day period but it is almost certain that these were not isolated events. In Western Europe 822,000 km^2 of seabed is utilised for bottom trawling (Oberle et al., 2016). In the northern Celtic Sea over two-thirds of the bottom area is impacted by trawling at least once per year, while some areas are impacted more than ten times per year (Gerritsen et al., 2013). Sharples et al. (2013) showed that the mean fishing activity in UK and Irish waters of the Celtic Sea based on VMS data between May to September 2005 was 0.03 d km^{-2}. Using the VMS data for the study area in Chapter 5 (428 points recorded at two hour intervals for June 2013 in the quadrangle: 48 ° 30' – 48° 55' N and 10° 35 – 10 ° 15' W; ~1200 km^2); the trawling activity was estimated to be 0.1–0.2 d km^{-2} (colour bar and corresponding circles in Fig. 7.1). These values agree with the estimates presented in Sharples et al. (2013) in their Fig. 3 which indicate orange/red for this area (values between 3.3 and 6.3, relative to the mean of 0.03 d km^{-2}).

At the NW Iberian shelf, the sediment flux induced by bottom trawling is estimated to be six times greater that the natural wave and current sediment flux (Oberle et al., 2016). In Oberle et al. (2016) it was shown that bottom trawl-induced changes to sediment transport that will have an impact on human time-scales. According to their calculations; 9.74 million km^2 of seabed is disturbed by bottom trawling activities and 21.87 Gt yr^{-1} of sediment is estimated to be resuspended.

Using the methods of Oberle et al. (2016; see their Fig. 4 and Table 3); the total bottom trawl-induced resuspension load for the trawled areas at the Whittard Canyon on June 13th, 14th, 15th and 16th 2013 have been calculated (Table 7.1 & Fig 7.2). The distance covered by the VMS data points of suspect trawlers present in Chapter 5 was computed using ERSI's ArcMap 10.0 and multiplied by the door spread of typical otter trawls (taken to be 80 m) and the mass resuspension (g m^{-2}) from previously published data (Chruchill, 1989; de Madron et al., 2005; Dellapenna et al., 2006; Dounas et al., 2007; O'Neill and Summerbell,

2011). As the sediment on the spurs of the canyon are known to be mixed (e.g. Cunningham et al., 2005; Stewart et al., 2014), the mean total resuspension for five sediment types were calculated and compared with the total mass of sediment on each of the days, estimated from the average summation of the SPM values from the vertical profiles over the water depth.

Table 7.1. Values for resuspended sediment mass calculated for four days at the Whittard Canyon in June 2013 for different sediment types detailed in Oberle et al. (2016).

June 2013	Distance (km)	Sand (kg)	Silty sand (kg)	Sand silt (kg)	Silt (kg)	Clayey silt (kg)	Mean for all sediment types (kg)
13	27.43	1.75E+06	3.39E+06	5.03E+06	6.26E+06	1.13E+06	3.51E+06
14	33.95	2.17E+06	4.20E+06	6.22E+06	7.74E+06	1.40E+06	4.35E+06
15	27.58	1.76E+06	3.41E+06	5.05E+06	6.29E+06	1.14E+06	3.53E+06
16	36.37	2.34E+06	4.53E+06	6.72E+06	8.36E+06	1.51E+06	4.69E+06

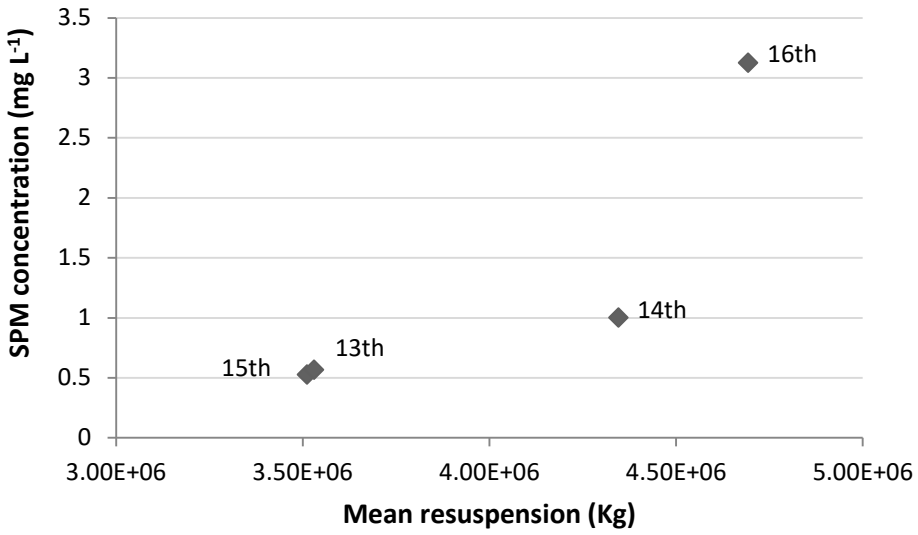

Fig. 7.2 Mean resuspension calculated from Oberle et al., 2016 versus sum of suspended particulate matter from vertical transmissometer profiles on June 13th, 14th, 15th and 16th 2013.

The mean SPM concentration in the ENLs from the four vertical profiles and the fishing effort based on the VMS data points during the trawling period in June 2013, where used to conservatively estimate (10 months of activity) the annual resuspension by trawling and found to be: 115168 kg m^{-2} yr^{-1}. Based on the average sediment transport recorded by BOBO landers at 3913 m in the Whittard Channel (3.15x10^{5} kg m^{-2} yr^{-1}; Amaro et al., 2015), the sediment resuspended by

trawling activity is approximately 4%. This value appears rather low in comparison to the estimates of Oberle et al. (2016) and requires some re-evalution; however it is clear that during trawling periods there is an increase in resuspension and concentrations of material in the canyon.

In recent years exploration and utilisation of the earth's resources has extended from terrestrial and coastal areas to beyond the shelf seas and now to the edge of the continental margin. Since 1950, the mass of ground fish caught by bottom trawling has increased globally on average by about 3% yr^{-1} (Pauly et al., 2002). Further increases are expected and with activity now at the edge of the steep continental slope and canyon rims that promote larger driving forces, artificial resuspension events are likely to increase and cause long-term alterations to shelf, slope and abyssal environments. Impacts of bottom trawling on the continental shelf can also lead to variable secondary consequences in the deep ocean. The mobilization of sediment by towed demersal fishing gears has been related to the release of nutrients, eutrophication, benthic infaunal mortality, smothering and the resuspension of phytoplankton cysts (including toxic species) and copepod eggs (O'Neill and Summerbell, 2011; Oberle et al., 2015). Although the impacts of bottom trawling range from insignificant to potentially detrimental, deep sea ecosystems tend to be much more vulnerable than their shallower counter parts, taking much longer to recover.

In the Mediterranean Sea, the smoothing of complex topography by increased sedimentation and mechanical dragging of heavy trawling gear has been shown (e.g. Puig et al., 2012). Reduced topographic complexity may decrease internal wave reflection and ultimately reduce energy fluxes at such sites. Indeed the energy flux model presented in Amaro et al. (2016; Appendix B Fig. 3) also shows lower fluxes in branches with flat slopes and rims.

Given the fishing intensity and width of the Celtic Sea shelf (e.g. Witt and Godley, 2007; Sharples et al., 2013) trawl-induced sediment transport requires much greater consideration. Spatial and temporal analyses of both natural and anthropogenic forces on sediment fluxes are needed. Currently natural wind and wave sediment fluxes for the Celtic Sea and Whittard Canyon area are limited with few long term data sets available. The global and human life scale of the anthropogenic forcing cannot be resolved before we fully understand and can first make accurate estimates of the natural mechanisms.

7.4 Heterogeneity of organic matter in the Whittard Canyon

Biogeochemical data of sPOM at the Whittard Canyon to date is limited to one other study; Huvenne et al. (2011; see inset table on Fig. 7.1). Significant heterogeneity was observed in the sPOM here in comparison to Huvenne et al. (2011)'s study (Fig. 7.1), although it is difficult to make direct comparisons between the data sets with regard to different branches and different depths. In that regard, the differences in sPOM at the Whittard Canyon (observed in both studies) can be explained most simply as the natural variability that will exist between different branches as is similarly seen at different seamounts (e.g. Christiansen & Wolff, 2009).

Previously, ecological studies have suggested that different flow regimes and levels of activity influence the (enhanced) delivery of organic matter and are hence responsible for faunal distributions (e.g. Duineveld et al., 2001; Duros et al., 2011; Ingels et al. 2011; Gunton et al., 2015; Gambi and Danovaro, 2016). Recent energy flux models (see insert on fig. 7.1; Amaro et al. 2016*;* Appendix B Fig 3; and also Aslam et al. 2014) provide new evidence confirming these suggestions of variable energy flows in the difference branches. The energy flux model shows areas of high activity (5–6 kW m^{-2}) in the eastern (WC1) and western branches (WC5) with lower values (2–3 kW m^{-2}) in the middle branches (WC3 and WC4) and thus emphasising the variability within the system.

Natural variability observed in the concentration of SPM in INLs and distributions between branches (section 3 in Amaro et al. 2016; Appendix B) can also be explained by variable energy fluxes and critical and supercritical reflective conditions for semi-diurnal internal tides (Chapter 4). The intensity, time and distance travelled and reflected in the stage of development of the NL will affect the concentration of material. The intermittent presence of INLs and (small) differences in depth ranges observed between branches (and years), (Amaro et al. 2016; Appendix B) is most likely due to variation in the density stratification influenced by seasonal and meteorological activity (Chapter 4). There is also seasonality in the supply of phytodetritus to vertical settling fluxes and material accumulating in NLs. Thus, naturally driven variability both spatial and temporal can drive changes in the oceanographic regimes and organic matter in NLs influencing the ecosystems in the canyon.

Faunal assemblage data (meiofauna, macrofauna and megabenthic filter feeders) presented in Amaro et al. (2016; Appendix B) suggested that abundance and diversity showed a gradient moving from east to west in the system. It would therefore be expected that these faunal distributions reflect the influence of organic enrichment (together with hydrodynamic activity). However, Huvenne et al. (2011) reported high amounts of essential fatty acids derived from phytoplankton (diatoms, dinoflagellates, coccolithophores and copepods; eicosapentaenoic acid (EPA); docosahexaenoic acids (DHA); 9(Z)-octadecenoic acid) in both eastern and western sides of the canyon. Higher energy fluxes in the eastern (WC5) and western sides (WC2) of the system were also predicted by the model relative to the lower fluxes in the middle branches (WC3,4) (see Fig.7.1). Elevated energy fluxes in the canyon do not show the same east to west gradient as observed in the faunal communities and thus some other process appears to be driving the apparent division in faunal assemblages or it may not exist at all.

Biogeochemical data (molar C/N, POC and lipid biomarkers) presented here (Chapter 6) showed a distinct east-west divide (Fig. 6.12 and 6.13). Lower energy fluxes in these middle branches (WC3 and WC4) relative to the western branches (WC1) may explain these results. However, trawl induced resuspension events in the eastern branches (WC3 and WC4) and absence in the western branches (WC1 and WC2) and the dilution of fresh rich organic material with degraded refractory material (Amaro et al., 2015) may also provide an explaination. Sharples et al. (2013) showed that the “shelf edge” area in their study which includes Whittard Canyon, fishing activity was between ~0.075–0.25 d km^{-2} (green to red on their Fig. 3) with the highest activity on the eastern side of the system and decreasing towards the west (see Fig. 7.1). Thus some of the variability (POM and faunal patterns) observed at the Whittard Canyon may be affected by non-natural variability and anthropogenic influence.

Statistical analysis of lipid data presented in Chapter 6 does suggest that the influence of bottom-trawling may be driving the apparent east-west divide in the study here rather than natural variation (Fig. 7.1). Due to the limited number of samples available; all seven samples were included in order to obtain statistically significant results. The statistics are somewhat crude and conjured to address whether or not trawl-induced resuspension may be involved, albeit they do illustrate that some other process is involved. It is certainly not established

beyond doubt but the results signify the possibility and warrants further investigation. Thus, heterogeneity between branches and within branches which are linked to organic matter and quality may be explained by variable NL patterns and the episodic influence of enhanced nepheloid layers that arise from the oceanographic processes and anthropogenic influence.

7.5 Implications for canyon ecosystem function, carbon cycling and the glocal canyon community

From a regional and global persecptive, the results presented here and in both appendices significantly contribute to the awareness and understanding of canyon ecosystems along the Irish continental margin. The discovery of new deep-sea faunal and faunal associations has proven successful in the novel bioactives in pharmaceutical manufacturing (e.g. Fenical et al., 2003; Skropeta, 2008; Rae et al., 2013). The data presented here adds to our understanding of the environmental settings inhabitated by such fauna which is important for the protection and appropriate use of Ireland ocean resources. Over the last decade, heightened interest in the deep-sea and developments in sampling technological (e.g. ROVs) have allowed for new discoveries and assessments of the submarine canyon occurrence in the context of their distribution, processes and significance thus offering guidance for their conservation. The observations here add to the knowledge on 'active' canyons (Harris and Whiteway, 2011), of which Whittard differs in its shelf-to-canyon sediment delivery mechanism due to the influence of tidal resuspension and down slope sediment flows in comparison to active systems that fed with regular river flows (e.g. Kaikoura Canyon, New Zealand; Zaire/Congo Canyon, SW Africa; Swatch-No-Ground Canyon, Bay of Bengal, India). Formed in the Plio-Pleistocene and with the deglaciation of the British and European ice-sheets contributing significant amounts of material and fluvial flux (Bourillet et al., 2003), understanding transport at Whittard Canyon may aid future exploration of Antarctic canyons as they undergo de-glaciation.

Recent publications from Norfolk and Baltimore Cayon on the North-West Atlantic (e.g. Brooke et al., 2016; Bourque et al., 2016) offer interesting insights and comparisons to Whittard Canyon. Coral distributions have been found to vary in both systems reflecting differences in environmental conditions, particularly turbidity (i.e. NLs). Similarly at the Whittard Canyon, the discovery of a unique

community of *Acesta excavata* bivalves and *Neopycnodonte zibrowii* oysters on a vertical wall was associated with BNLs and INLs (Johnson et al., 2011; Appendix A). High internal energy fluxes at this site in WC3, further affirm the presence of high energy in the area that when focused/reflected can suspend material and generate NLs (Amaro et al. 2016; Appendix B Fig. 3). In addition, data presented in Chapter 6 showed high contributions of essential fatty acids in BNLs at this depth range, with lateral advection of such components from BNL into the INL through their formation implied and complimented by elemental data from the INLs. These observtaions suggest that the distribution of suspension feeding fauna on the wall is dependent on the distribution of rich organic matter, suspended in NLs in the canyon, confirming previous suggestions and can be applied to other submarine canyons.

However, the actual affect of enhanced food availability on the canyon fauna have not been clearly deciphered. Communities of epistrate feeders in the canyon suggest the availability of fresh material derived from high surface productivity (Amaro et al., 2016; Appendix B). Furthermore, higher abundances of macro benthic fauna have been reported within the canyon in comparison to the slope and diversity within these communities has been linked to the quality and quantity of OM (e.g. Gunton et al., 2015). While higher abundances of suspension feeding fauna deeper in the canyon are belived to reflect a shift in feeding regime from the overall predominantanly deposit feeding communities, heterogeneity in the supply will have variable influences on benthic/infaunal/suspension feeding communities. Benthic foraminifera densities in the upper sediment layers at Whittard Canyon reflect a shallow oxygen penetration depth associated with high OM input and perhaps Whittard Canyon is undergoing a similar “enhancement paradox” as Norfolk/Baltimore Canyon (Robertson et al., 2014) with anoxic conditions promoting opportunistic species.

In comparison to the Meditereanean submarine canyons, the Whittard Canyon is much further offshore (e.g. 300 km V’s 4 km at Palamós Canyon; Palanques et al., 2006). However, evidence of similar trawl-induced sediment transport events has been presented here. With minimal terrestrial and fluvial inputs which bring regularity to flows and inputs in comparison to those on the Iberian margin or off the Gulf of Lion, the effects of sediment flows caused by

bottom trawling may be different at a canyon like Whittard which is predominantly influenced by tidal resuspension.

Irregular high concentration resuspension events induced by trawling can increase sedimentation rates, similar to those observed on the Ebro shelf (Palanques et al., 2014). Again, the exact implications of such events are unclear but certainly intense events may smother feeding and respiratory organs of suspension feeders and/or alter chemical compositions of organic matter food supply to benthic habitats. Elemental data (C/N) presented in Chapter 5 demonstrated the degraded nature of the sPOM in ENLs. Low nutritional quality of trawl affected sPOM is further suggested in the lipid biomarker results (Chapter 6). It is well established that faunal communities in the deep sea response to seasonal pulses of phytodetritus (e.g. Gooday, 1988), as has been shown in the Whittard Canyon (e.g. Gambi and Danovaro, 2016). Seasonally/climatically driven changes to phytodetritus at the Porcupine Abyssal Plain have also resulted in changes in the benthic community structure (Billett et al., 1983; Ramirez-Llodra et al., 2005; Glover et al., 2010). Thus if trawling is altering the seasonal and natural delivery of phytodetritus, is it possible that high inorganic particle loading may provide nutritionally unsuitable material to these habiatats and similar changes may be observed in community structures at the Whittard Canyon in the future.

Amaro et al. (2015) suggested that episodic events may be diluting fresh rich organic matter, however large quantities of lithogenic material may also act as a ballasting mechanism for OM. Suspended particulate organic carbon concentrations associated with trawl induced resuspension were more than an order of magnitude higher (Chapter 6) than in Huvenne et al. (2011)'s similar study (up to 690 µg L^{-1} *vs*. 12–23 µg L^{-1} at similar canyon depths; Tables inset on Fig. 7.1). Furthermore, TOC contents in the upper centimetre of the canyon sediments are double the values from the nearby open slope at Goban Spur (Amaro et al. 2016; Appendix B). Reduced oxygen exposure times at the seabed through large episodic events and higher sedimentation rates, may promote oportunisitc species communites. The population structures of Nematodes have also suggested sedimentary conditions which may be the result of sedimentary overflow on the interfluves of the canyon head (Ingels et al., 2011). A combination of increased resuspension by fishing activity and the conduit nature of Whittard may forge an environment for carbon burial.

Furthermore, such events may they may also increased burial efficiency of inorganic carbon and or degraded OM and have positive implications for the preservation of carbon. The transport of carbon below the permanent pycnocline is a key process in the sink of atmospheric CO_2 from shelf seas (Holt et al., 2009). ENLs in Chapter 5 were all observed at depths below the permanent thermocline. Similar to Dense Shelf Water Cascading Events (DSWC) in the Mediterranean Sea and Gulf of Lions, additional input of sediment can promote density driven turbidity flows that can transport large amounts organic matter to the deep ocean (Sanchez-Vidal et al., 2008; Canals et al., 2009; Canal et al., 2013). Similarl scouring of the shelf and shallower canyon spurs by trawling may suspend large amounts of organic and inorganic substances with rapid deposition to the deep promoted by the increased density, providing a mechanism for carbon sequestion.

Despite its distance offshore, sediment transport processes at the Whittard Canyon are influenced by both natural and anthropogenic means. Increased DSWC events at the Gulf of Lions margin and in submarine canyons in the northwest Mediterranean Sea are predicted to occur with future climate change (Canals et al., 2009). These events are unlikely to occur at the Whittard Canyon but increased storm depressions over the Bay of Biscay may induce similar high turbidity events and mass sediment flux processes (Xu et al., 2002; de Stigter et al., 2007; Amaro et al., 2015). Increased air temperatures over the NE Atlantic may see changes to seasonal stratification and the depth of the winter mixed layer, which have pronounced influence on the formation of NLs as seen in Chapter 4. Variation, both temporal and climatic, may therefore impact the generation of NLs and may have important implications for the delivery of material that they supply to the deep-sea and canyon ecosystems.

7.6 Recommendations for future work and developments

Although this study has made significant progress in determining the main controlling factors of permanent and temporal distributions of nepheloid layers, the duration that the material in the layers remains in suspension remains unknown. Knowledge of such time scales is essential in understanding biogeochemical cycles, food webs and the processing of sPOM in the system. A greater insight into the persistence of the processes inducing suspension and the persistence of trawl induced resuspension are important factors for future

consideration. Further research into this topic would include deployments of landers equipped with sensors to monitor the turbidity over a time series. Such investigations are expensive and long term deployments in deep-sea and canyon environments come with their own associated problems.

In terms of understanding biogeochemical cycling processes, laboratory experiments including mesocosms may provide a more cost effective way to investigate these processes. Aggregations of diatom blooms and bacterial mediation of carbon fluxes as well as size distributions have successfully been studied in this manner using similar techniques (i.e. optical measurements, chlorophyll *a*, POC, PN; e.g. Smith et al., 1995; Costello et al., 1995; Li and Logan, 1995; Alldredge et al., 1995).

The use of stable isotopes (e.g. ^{13}C, ^{15}N) to asses temporal variation (seasonal shifts) and/or tracing energy flow through trophic level studies is another important aspect for future study. Contour plots of the SPM distribution in the Whittard Canyon showed INLs extending off the slope for at least 25 km but it may be beneficial to trace the lateral advection of sPOM in order to assess the source to end point of the material and to understand the constant changes sPOM undergoes in nepheloid layers. Dating sPOM from nepheloid layers by radioactive isotopes would also aid our understanding if these processes. Combined with isotopic studies of the sediments from the shelf, questions related to the source of material, particularly in relation to the trawl induced resuspension events could be addressed. The use of ^{234}Th and^{210}Pb has been successful in the exploration of particle exchanges in other studies (Inthorn et al. 2006b; Owens et al., 2015; Marchal and Lam, 2012 and references therein). Ocean particles are subject to a wide variety of processes; precipitation, sinking, remineralisation or dissolution, (dis)aggregation, and transport by currents. Measurements of particle-reactive metals (such as thorium) can tell us a lot about these particle processes and sorption reactions in the ocean.

With further extension of fishing areas and the development of more intensive fishing methods, we may see an increase in trawl-induced resuspension events and/or increased activity at vulnerable canyon sites. As shown above, the extent of increased sediment transport by bottom trawling may have implications on a human time-scale. Thus there is an urgent need to further examine this issue in Irish waters. Analysis of VMS and AIS data (Oberle et al., 2015) from other sites

along the Irish continental margin would be of interest to assess the scale of trawling and its potential effects on the seabed topography, with AIS data offering far greater resolution (data point every 6 seconds in comparison to every 2 hours by VMS).

The application of Multi-Beam Echo Sounders for the quantification of suspended sediment concentration and flow velocities has recently been demonstrated (Simmons et al., 2009; Best et al. 2010; O'Neill et al., 2013), enabling the imaging of sediment dynamics across a two-dimensional swathe within the flow field. These instruments can also be used to quantify the sediment concentrations and the sediment loads that are mobilized into the water column in the wake of towed demersal fishing gears.

The the extent of the influence and/or actual affect of enhanced food avilabilty by NLs on canyon fauna is still unclear. An intergrated study, combining a larger suspended particulate organic matter data set with comparable gut analysis of the fauna would be required to make a more conviencing link similar to the work of Duineveld et al., 2012. Additional data addressing the temporal variability of the supply and extent of labile material to NLs would also be benefical in this regard.

The acquisition of models is becoming increasingly popular in modern day ocean science due to their lower costs, reduction in labour intensiveness (in terms of sample collection and lab work) and advances in computational software. The generation sites of nepheloid layers have been established here. Modelling these sites over large spatial scales is the next step. If the distribution of nepheloid layers could be successfully mapped (or modelled) this could assist with biological prediction and marine carbon cycling models. Temporal and seasonal variability of nepheloid layers still requires further investigation but the development of such models would be a step in the right direction and seasonal compositional changes could be address at modelled nepheloid layer hot spots.

Although models hold great potential, traditional observational science is still an important component to oceanography. In order for these models to be accurate and worthwhile, they must be validated with real data. Furthermore, fitting actual date into models can prove much more powerful than a model alone. Environmental data collected during the three research surveys here has been included in the energy fluxes models presented in Amaro et al. (2016;

Appendix B). Such models can often produce a wider view rather than once off snapshots of observational data. However, often observations often can complete the story told by these bigger pictures. Observations of trawlers while on station prompted the investigation into trawl-induced resuspension events as an explanation for the unusual data collected during the 2013 survey. Observing the environment and collecting samples and data therefore remains vitally important in producing good quality science. Identifying potential sites of interest through models could cut exploration costs substantially thus, I believe a balance between both is the key.

7.7 Conclusion

This study has revealed for the first time the distribution, dynamics and compositions of nepheloid layers within four branches of the Whittard Canyon. The interactions of oceanographic features and flow with the local topography are controlling factors on the distribution of particles in the system. Seasonal and temporal conditions influencing stratification patterns and the introduction of fresh organic matter also affect distribution, dynamics and compositional components. The results provide an explanation for presence of fresh labile OM at depth and faunal distributions that use this material as a food source. Heterogeneity in quality and quantity of organic matter can be naturally (both spatial and temporal) influenced but bottom trawl-induced resuspension may alter the composition of sPOM, with implications for carbon burial and food quality for suspension and benthic feeders.

As well as filling gaps in our knowledge on canyon ecosystem functioning and lateral transport, this study has also raised important questions and has highlighted the vitallity of multidisciplinary research for monitoring and conserving our ocean.

References

Alldredge, A.L., Gotschalk, C., Passow, U. and Riebesell, U., 1995. Mass aggregation of diatom blooms: Insights from a mesocosm study. Deep Sea Research Part II: Topical Studies in Oceanography, 42, 9-27.

Amaro, T., de Stigter, H., Lavaleye, M. and Duineveld, G., 2015. Organic matter enrichment in the Whittard Channel; its origin and possible effects on benthic megafauna. Deep Sea Research Part I: Oceanographic Research Papers, 102, 90-100.

Amaro, T., Huvenne, V.A.I., Allcock, A.L., Aslam, T., Davies, J.S., Danovaro, R., de Stigter, H.C., Duineveld, G.C.A., Gambi, C., Gooday, A.J., Gunton, L.M., Hall, R., Howell, K.L., Ingels, J., Kiriakoulakis, K., Kershaw, C.E., Lavaleye, M.S.S., Robert, K., Stewart, H., Van Rooij, D., White, M., Wilson, A.M. (2016) The Whittard Canyon-a case study of submarine canyon processes, Progress in Oceanography, 146, 38-57.

Amin, M., Huthnance, J.M., 1999. The pattern of cross-slope depositional fluxes. Deep Sea Research Part I: Oceanographic Research Papers, 46, 1565 – 1591.

Antia, A.N., Maaßen, J., Herman, P., Voß, M., Scholten, J., Groom, S. and Miller, P., 2001. Spatial and temporal variability of particle flux at the NW European continental margin. Deep Sea Research Part II: Topical Studies in Oceanography, 48, 3083-3106.

Aslam, T., Hall, R., Dye, S., 2014. Internal Waves in Whittard Canyon. Paper presented at 2nd International Symposium on Submarine Canyon, Edinburgh, October 2014.

Best, J., Simmons, S., Parsons, D., Oberg, K., Czuba, J. and Malzone, C., 2010. A new methodology for the quantitative visualization of coherent flow structures in alluvial channels using multibeam echo-sounding (MBES).Geophysical Research Letters, 37, L06405, DOI: 10.1029/2009GL041852.

Billett, D.S.M., Lampitt, R.S., Rice, A.L. and Mantoura, R.F.C., 1983. Seasonal sedimentation of phytoplankton to the deep-sea benthos. Nature, 302, 520-522.

Biscaye, P.E. and Anderson, R.F., 1994. Fluxes of particulate matter on the slope of the southern Middle Atlantic Bight: SEEP-II. Deep-Sea Research II, 41, 459-509.

Bourillet, J.F., Reynaud, J.Y., Baltzer, A. and Zaragosi, S., 2003. The 'Fleuve Manche': the submarine sedimentary features from the outer shelf to the deep-sea fans. Journal of Quaternary Science, 18, 261-282.

Canals, M., Danovaro, R., Heussner, S., Lykousis, V., Puig, P., Trincardi, F., Calafat, A., Durrieu de Madron, X., Palanques, A. and Sanchez-Vidal, A., 2009. Cascades in Mediterranean submarine grand canyons. Oceanography, 22, 26-43.

Canals, M., Company, J.B., Martin, D., Sanchez-Vidal, A. and Ramirez-Llodra, E., 2013. Integrated study Mediterranean deep canyons: novel results and future challenges. Progress in Oceanography, 118, 1-27.

Christiansen, B. and Wolff, G., 2009. The oceanography, biogeochemistry and ecology of two NE Atlantic seamounts: The OASIS project. Deep Sea Research Part II: Topical Studies in Oceanography, 56, 2579-2581.

Churchill, J.H., 1989. The effect of commercial trawling on sediment resuspension and transport over the Middle Atlantic Bight continental shelf.Continental shelf research, 9, 841-865.

Costello, D.K., Carder, K.L., Hou, W., 1995. Aggregation of diatom bloom in a mesocosm: Bulk and individual particle optical measurements. Deep Sea Research Part II: Topical Studies in Oceanography, 42, 29-45.

De Stigter, H.C., Boer, W., de Jesus Mendes, P. A. Jesus, C. C. Thomsen, L., van den Bergh, van Weering, T.C.E., 2007. Recent sediment transport and deposition in the Nazaré Canyon, Portuguese continental margin. Marine Geology, 246, 144 – 164.

Dellapenna, T.M., Allison, M.A., Gill, G.A., Lehman, R.D., Warnken, K.W., 2006. The impact of shrimp trawling and associated sediment resuspension in mud dominated, shallow estuaries. Estuarine, Coastal and Shelf Science, 69, 519-530.

Dounas, C., Davies, I., Triantafyllou, G., Koulouri, P., Petihakis, G., Arvanitidis, C., Sourlatzis, G., Eleftheriou, A., 2007. Large-scale impacts of bottom trawling on shelf primary productivity. Continental Shelf Research,27, 2198-2210.

Duineveld, G., Lavaleye, M., Berghuis, E., de Wilde, P., 2001. Activity and composition of the benthic fauna in the Whittard Canyon and the adjacent continental slope (NE Atlantic). Oceanologica acta, 24, 69 – 83.

Duineveld, G.C.A., Jeffreys, R.M., Lavaleye, M.S.S., Davies, A.J. , Bergman, M.J.N. , Watmough, T. and Witbaard, R., 2012. Spatial and tidal variation in food supply to shallow cold-water coral reefs of the Mingulay Reef complex (Outer Hebrides, Scotland). Marine Ecology Progress Series, 444, 97-115.

Duros, P., Fontanier, C., Metzger, E., Pusceddu, A., Cesbron, F., de Stigter, H.C., Bianchelli, S., Danovaro, R., Jorissen, F.J. 2011. Live (stained) benthic foraminifera in the Whittard Canyon, Celtic margin (NE Atlantic). Deep-Sea Research Part I: Oceanographic Research Papers, 58, 128–146.

Durrieu de Madron, X.D., 1994. Hydrography and nepheloid structures in the Grand-Rhône canyon. Continental Shelf Research, 14, 457-477.

Durrieu de Madron, X., Ferré, B., Le Corre, G., Grenz, C., Conan, P., Pujo-Pay, M., Buscail, R., Bodiot, O., 2005. Trawling-induced resuspension and dispersal of muddy sediments and dissolved elements in the Gulf of Lion (NW Mediterranean). Continental Shelf Research, 25, 2387-2409.

Fenical, W. and Jensen, P.R., 2006. Developing a new resource for drug discovery: marine actinomycete bacteria. Nature chemical biology, 2, 666-673.

Gambi, C. and Danovaro, R., 2016. Biodiversity and life strategies of deep-sea meiofauna and nematode assemblages in the Whittard Canyon (Celtic margin, NE Atlantic Ocean). Deep Sea Research Part I: Oceanographic Research Papers, 108, 13-22.

Gerritsen, H.D., Minto, C. and Lordan, C., 2013. How much of the seabed is impacted by mobile fishing gear? Absolute estimates from Vessel Monitoring System (VMS) point data. ICES Journal of Marine Science: Journal du Conseil, fst017.

Glover, A.G., Gooday, A.J., Bailey, D.M., Billett, D.S.M., Chevaldonné, P., Colaco, A., Copley, J., Cuvelier, D., Desbruyeres, D., Kalogeropoulou, V. and Klages, M., 2010. Temporal change in deep-sea benthic ecosystems: a review of the evidence from recent time-series studies. Advances in Marine Biology, 58, 1-95.

Gooday, A.J., 1988. A response by benthic foraminifera to the deposition of phytodetritus in the deep sea. Nature, 332, 70-73.

Gunton, L.M., Gooday, A.J., Glover, A.G. and Bett, B.J., 2015. Macrofaunal abundance and community composition at lower bathyal depths in different branches of the Whittard Canyon and on the adjacent slope (3500m; NE Atlantic). Deep Sea Research Part I: Oceanographic Research Papers, 97, 29-39.

Harris, P.T. and Whiteway, T., 2011. Global distribution of large submarine canyons: Geomorphic differences between active and passive continental margins. Marine Geology, 285, 69-86.

Holt, J. and Thorpe, S., 1997. The propagation of high frequency internal waves in the celtic sea. Deep Sea Research Part I: Oceanographic Research Papers, 4, 2087-2116.

Holt, J., Wakelin, S. and Huthnance, J., 2009. Down-welling circulation of the northwest European continental shelf: A driving mechanism for the continental shelf carbon pump. Geophysical Research Letters, 36, L14602, DOI: 10.1029/2009GL038997.

Hopkins, J. E., Stephenson, G. R., Green, J., Inall, M. E., and Palmer, M. R., 2014. Storms modify baroclinic energy fluxes in a seasonally stratified shelf sea: Inertial-tidal interaction. Journal of Geophysical Research: Oceans, 119, 6863-6883.

Hunter, W.R., Jamieson, A.J., Huvenne, V., Witte, U., 2013. Sediment community responses to marine vs. terrigenous organic matter in a submarine canyon. Biogeosciences, 10, 67-80.

Huvenne, V.A., Tyler, P.A., Masson, D.G., Fisher, E.H., Hauton, C., Hühnerbach, V., Le Bas, T.P. and Wolff, G.A., 2011. A picture on the wall: innovative mapping reveals cold-water coral refuge in submarine canyon. PLoS ONE, 6, e28755.

Ingels J., Tchesunov A.V., Vanreusel A. 2011. Meiofauna in the Gollum Channels and the Whittard Canyon, Celtic Margin - How Local Environmental Conditions Shape Nematode Structure and Function. PLoS ONE, 6, 1-15.

Inthorn, M., 2006. Lateral particle transport in nepheloid layers – a key factor for organic matter distribution and quality in the Benguela high-productivity area. Berichte, Fachbereich Geowissenschaften, Universität Bremen, No. 244, 124 pages, Bremen, 2006. ISSN 0931-0800.

Inthorn, M., Mohrholz, V. and Zabel, M., 2006b. Nepheloid layer distribution in the Benguela upwelling area offshore Namibia. Deep Sea Research Part I: Oceanographic Research Papers, 53, 1423-1438.

Inthorn, M., Wagner, T., Scheeder, G. and Zabel, M., 2006a. Lateral transport controls distribution, quality, and burial of organic matter along continental slopes in high-productivity areas. Geology, 34, 205-208.

Jahnke, R.A., Reimers, C.E. and Craven, D.B., 1990. Intensification of recycling of organic matter at the sea floor near ocean margins. Nature, 348, 50-54. doi: 10.1038/348050a0.

Johnson, M.P., White, M., Wilson, A., Würzberg, L., Schwabe, E., Folch, H., Allcock, A.L., 2013. A Vertical Wall Dominated by Acesta excavata and Neopycnodonte zibrowii, Part of an Undersampled Group of Deep-Sea Habitats. PLoS ONE, 8, e79917.

Li, X. and Logan, B.E., 1995. Size distributions and fractal properties of particles during a simulated phytoplankton bloom in a mesocosm. Deep Sea Research Part II: Topical Studies in Oceanography, 42, 125-138.

Marchal, O. and Lam, P.J., 2012. What can paired measurements of Th isotope activity and particle concentration tell us about particle cycling in the ocean? Geochimica et Cosmochimica Acta, 90, 126 – 148.

Masson D.G., Huvenne V.A.I., de Stigter H., Wolff G.A., Kiriakoulakis K., Arzola R.G., Blackbird S. (2010). Efficient burial of carbon in a submarine canyon. Geology, 38, 831–834.

McCave, I.N., Hall, I.R., Antia, A.N., Chou, L., Dehairs, F., Lampitt, R.S., Thomsen, L., van Weering, T.C.E., Wollast, R., 2001. Distribution, composition and flux of particulate material over the European margin at 47 ° –50 °N. Deep-Sea Research II, 48, 3107 – 3139.

Oberle, F.K., Storlazzi, C.D. and Hanebuth, T.J., 2015. What a drag: Quantifying the global impact of chronic bottom trawling on continental shelf sediment. Journal of Marine Systems, 159, 109-119.

Oliveira, A., Vitorino, J., Rodrigues, A., Jouanneau, J. M., Dias, J. A., Weber, O., 2002. Nepheloid layer dynamics in the northern Portuguese shelf. Progress in Oceanography, 52, 195 – 213.

O'Neill, F.G. and Summerbell, K., 2011. The mobilisation of sediment by demersal otter trawls. Marine Pollution Bulletin, 62, 1088-1097.

O'Neill, F.G., Robertson, M., Summerbell, K., Breen, M. and Robinson, L.A., 2013. The mobilisation of sediment and benthic infauna by scallop dredges.Marine Environmental Research, 90, 104-112.

Owens, S.A., S. Pike, and Buesseler, K.O., 2015. Thorium-234 as a tracer of particle dynamics and upper ocean export in the Atlantic Ocean. Deep Sea Research Part II: tropical Studies in Oceanography, 116, 42-59.

Palanques, A., Martín, J., Puig, P., Guillén, J., Company, J.B., Sardà, F., 2006a. Evidence of sediment gravity flows induced by trawling in the Palamós (Fonera) submarine canyon (northwestern Mediterranean). Deep Sea Research Part I: Oceanographic Research Papers, 53, 201 – 214

Pauly, D., Christensen, V., Guénette, S., Pitcher, T.J., Sumaila, U.R., Walters, C.J., Watson, R. and Zeller, D., 2002. Towards sustainability in world fisheries. Nature, 418, 689-695.

Puig, P., Company, J.B., Sardà, F. and Palanques, A., 2001. Responses of deep-water shrimp populations to intermediate nepheloid layer detachments on the Northwestern Mediterranean continental margin. Deep Sea Research Part I: Oceanographic Research Papers, 48, 2195-2207.

Puig, P., Canals, M., Company, J.B., Martín, J., Amblas, D., Lastras, G., Palanques, A. and Calafat, A.M., 2012. Ploughing the deep sea floor. Nature, 489, 286-289.

Rae, M., Folch, H., Moniz, M.B., Wolff, C.W., McCormack, G.P., Rindi, F. and Johnson, M.P., 2013. Marine bioactivity in Irish waters. Phytochemistry reviews, 12, 555-565.

Ramirez-Llodra, E., Reid, W.D.K. and Billett, D.S.M., 2005. Long-term changes in reproductive patterns of the holothurian Oneirophanta mutabilis from the Porcupine Abyssal Plain. Marine Biology, 146, 683-693.

Robertson, C.M., Demopoulos, A.J.W., Bourque, J.R., Mienis, F., Duineveld, G., Davies, A.J., Ross, S., Brooke, S. 2014. Distinct benthic community trends driven by an enrichment paradox in the Mid-Atlantic Bight Canyons, NW Atlantic, Paper presented at 2nd International Symposium on Submarine Canyon, Edinburgh, October 2014.

Sanchez-Vidal, A., Pasqual, C., Kerhervé, P., Calafat, A., Heussner, S., Palanques, A., Durrieu de Madron, X., Canals, M. and Puig, P., 2008. Impact of dense shelf water cascading on the transfer of organic matter to the deep western Mediterranean basin. Geophysical Research Letters, 35, L05605, DOI: 10.1029/2007GL032825

Sanchez-Vidal, A., Canals, M., Calafat, A.M., Lastras, G., Pedrosa-Pàmies, R., Menéndez, M., Medina, R., Hereu, B., Romero, J. and Alcoverro, T., 2012. Impacts on the deep-sea ecosystem by a severe coastal storm. PLoS ONE, 7, e30395.

Sharples, J., Scott, B.E. and Inall, M.E., 2013. From physics to fishing over a shelf sea bank. Progress in Oceanography, 117, 1-8.

Simmons, S.M., Parsons, D.R., Best, J.L., Orfeo, O., Lane, S.N., Kostaschuk, R., Hardy, R.J., West, G., Malzone, C., Marcus, J. and Pocwiardowski, P., 2009. Monitoring suspended sediment dynamics using MBES. Journal of Hydraulic Engineering, 136, 45-49.

Skropeta, D., 2008. Deep-sea natural products. Natural Product Reports, 25, 1131-1166.

Smith, D.C., Steward, G.F., Long, R.A. and Azam, F., 1995. Bacterial mediation of carbon fluxes during a diatom bloom in a mesocosm. Deep Sea Research Part II: Topical Studies in Oceanography, 42, 75-97.

Thorpe, S. A., and White, M., 1988. A deep intermediate nepheloid layer. Deep Sea Research Part A. Oceanographic Research Papers, 35, 1665 – 1671.

Van Weering, T.C., Hall, I.R., de Stigter, H.C., McCave, I.N. and Thomsen, L., 1998. Recent sediments, sediment accumulation and carbon burial at Goban Spur, NW European Continental Margin (47–50 N). Progress in Oceanography, 42, 5-35.

Witt, M.J. and Godley, B.J., 2007. A step towards seascape scale conservation: using vessel monitoring systems (VMS) to map fishing activity. PLoS ONE, 2, e1111.

Wollast, R. and Chou, L., 2000. The carbon cycle at the ocean margin in the northern Gulf of Biscay. Deep Sea Research Part II: Topical Studies in Oceanography, 48, 3265-3293.

Xu, J.P., Noble, M.A., Eittreim, S.L., Rosenfeld, L.K., Schwing, F.B., Pilskaln, C.H., 2002. Distribution and transport of suspended particulate matter in Monterey Canyon, California. Marine Geology 181, 215-234.

Appendix A:
A Vertical Wall Dominated by *Acesta excavata* and *Neopycnodonte zibrowii*, Part of an Undersampled Group of Deep-Sea Habitats.

Mark P. Johnson[1], Martin White[1], **Annette Wilson[1*],** Laura Würzberg[2], Enrico Schwabe[3], Helka Folch[4], A. Louise Allcock[1].

[1]Ryan Institute and School of Natural Sciences, National University of Ireland Galway, Galway, Ireland.

[2]Biocenter Grindel and Zoological Museum, University of Hamburg, Hamburg, Germany.

[3]Bavarian State Collection of Zoology, Munich, Germany.

[4]School of Biological Sciences, Queen's University Belfast, Belfast, United Kingdom.

Published: PLoS ONE 8(11): e79917.

***Role:** Contributed to sampling, collection and analysis of data, writing of paper and production of figures 5, 6 and 7.

Abstract

We describe a novel biotope at 633 to 762 m depth on a vertical wall in the Whittard Canyon, an extensive canyon system reaching from the shelf to the deep sea on Ireland's continental margin. We explored this wall with an ROV and compiled a photomosaic of the habitat. The assemblage contributing to the biotope was dominated by large limid bivalves, *Acesta excavata* (mean shell height 10.4 cm), and deep-sea oysters, *Neopycnodonte zibrowii*, at high densities, particularly at overhangs. Mean density of *N. zibrowii* increased with depth, with densities of the most closely packed areas of *A. excavata* also increasing with depth. Other taxa associated with the assemblage included the solitary coral *Desmophyllum dianthus*, cerianthid anemones, comatulid crinoids, the trochid gastropod *Margarites* sp., the portunid crab *Bathynectes longispina* and small fish of the family Bythitidae. The scleractinian coral *Madrepora oculata*, the pencil urchin *Cidaris cidaris* and a species of *Epizoanthus* were also common. Prominent but less abundant species included the flytrap anemone *Actinoscyphia saginata*, the carrier crab *Paramola cuvieri*, and the fishes *Lepidion eques* and *Conger conger*. Observations of the hydrography of the canyon system identified that the upper 500 m was dominated by Eastern North Atlantic Water, with Mediterranean Outflow Water beneath it. The permanent thermocline is found between 600 and 1000 m depth, i.e., in the depth range of the vertical wall and the dense assemblage of filter feeders. Beam attenuation indicated nepheloid layers present in the canyon system with the greatest amounts of suspended material at the ROV dive site between 500 and 750 m. A cross-canyon CTD transect indicated the presence of internal waves between these depths. We hypothesise that internal waves concentrate suspended sediment at high concentrations at the foot of the vertical wall, possibly explaining the large size and high density of filter-feeding molluscs.

Introduction

The continental margins, along with other parts of the deep oceans, still represent locations of discovery science [1], [2]. The novelty of deep-sea habitats is reflected by a habitat-discovery curve that does not yet have a plateau [3]. This relative lack of knowledge of deep-sea habitats is coupled with incompletely characterized, but important, ecosystem functions and services including nutrient recycling, carbon sequestration and nursery areas [4]. Sampling constraints have certainly restricted the description of deep-sea habitats. The vertical faces of canyon walls and other related habitats have only become accessible to survey with the availability of deep-water ROVs [5], [6].

The Whittard Canyon is one of the major submarine canyons along the Celtic margin, situated between the two main North Atlantic gyres. The region is an area of high primary production, with estimates of ca. 160 g C m^{-2} a^{-1} at the Goban Spur [7]. The Whittard Canyon floor has been found to be locally enriched in particulate organic carbon and phytodetritus (chl a) and labile lipids, suggesting high food quality in comparison to the open slope [8]. The NE Atlantic continental margin is characterized by a poleward flowing slope current, with typical long term mean flow in the vicinity of the Whittard Canyon of 5–10 cm s^{-1} [9] [10][11]. The Celtic Sea region, which the Whittard Canyon fringes, is characterized by high barotropic tidal energy, with subsequent conversion to baroclinic internal tides (e.g., [12], [13]). The region is one where internal waves are generated by the residual flow over the rough margin topography (e.g., [14]).

In the results presented here, we describe a novel biotope from a vertical wall in the Whittard Canyon system: vertical surfaces and overhangs at depths between 633 and 762 m covered by the bivalve *Acesta excavata* (Fabricius, 1779) and the giant deep-sea oyster N*eopycnodonte zibrowii* Gofas, Salas & Taviani, in Wisshak et al., 2009. The term biotope describes the combination of a characteristic suite of species with an associated physical habitat [15]. A suite of species found together is referred to as an assemblage throughout the current study. The term assemblage is sometimes considered synonymous with community when describing the species found together in the same location; however, we use assemblage and follow the convention that the use of the term community implies that more is known about biological interactions between species.

Acesta excavata is found in the North Atlantic between Mauritania and Norway with scattered Mediterranean records; typical depths are between 200 and 800 m [16]. Outside of Norwegian fjords, *A. excavata* is considered to be a component of reefs of the cold-water coral *Lophelia pertusa*, whereas vertical walls in fjords are often covered by attached *A. excavata* [16]. *Neopycnodonte zibrowii* is not generally recognized as associated with *L. pertusa* habitats, although the oyster may occur in relatively close proximity to cold-water corals. Extensive vertical reefs of *N. zibrowii* have been reported from the canyons of the Bay of Biscay [5].

In the current study we describe the occurrence of an *A. excavata -N. zibrowii* biotope on a vertical wall. This adds to the known diversity of deep-sea habitats, contributing to the habitat-based framework for conservation planning [17]. We analyse quantitative biological and oceanographic measurements to understand more about the cross-habitat variations in the assemblage. This identifies some of the constraints that may be operating to shape the occurrence and extent of the habitat identified.

Results

Habitat Scope and Inhabitants

On an ROV dive on 16th April 2012, at 48.761 °N, 10.461 °W (Figure 1) we encountered a vertical wall extending from 631 m depth to 780 m depth. On this wall we identified the presence of large numbers of *Acesta excavata* on the vertical faces.

Acesta excavata and *Neopycnodonte zibrowii* were found together, mostly between depths of 633 m and 762 m, with particularly high densities in the vicinity of small overhangs (Figure 2). Nine taxa apart from the bivalves were identifiable in more than 10% of photographs. The two most abundant species were the scleractinian corals *Desmophyllum dianthus* and *Madrepora oculata* (Table 1). Comatulid feather stars were also relatively abundant, although the resolution of the photographs was sufficient neither to identify the feather stars to species level nor to conclude that they comprised a single species. In order of decreasing abundance was a species of small pink fish of the family Bythitidae living in the cryptic habitat created by the bivalves and corals, a pink tube anemone of the family Cerianthidae, a trochid gastropod *Margarites* sp., a

portunid crab *Bathynectes longispina*, and the pencil urchin *Cidaris cidaris*. A species of *Epizoanthus* was also very abundant, being present on 24% of oyster shells.

Other species were present in less than 10% of the photographs. Some of these species were large and conspicuous despite occurring infrequently, for example, the bright orange flytrap anemone *Actinoscypha saginata* (Figure 3, bottom right), the carrier crab *Paramola cuvieri*, *Lepidion eques*, a characteristic fish species of deep waters in the region [18], and a conger eel, *Conger conger*, which was encountered at a depth of 681 m on the wall. Other crustaceans present in the photographs were squat lobsters Munidae sp., unidentified caridean shrimps and the euphausiid *Meganyctiphanes norvegica*. Apart from the crinoids and pencil urchin mentioned above, echinoderms in the photographs included four species of starfish. These comprised two poraniids, one almost certainly *Poranius pulvillus*, the other unidentified, a species of *Ceramaster* (Figure 3, upper left), and a stichastrellid, probably *Stichastrella rosea*. A second urchin species *Echinus* sp. (Figure 3, upper right) was also present. Other cnidarian species identified were the antipatharian coral *Stichopathes* sp. of which just two specimens were seen, a second species of zoanthid, *Parazoanthus anguicomis*, which was identified on a very small number of oyster shells, and the athecate hydrozoan *Tubularia indivisa*, which was more prevalent in shallower depths. Polychaetes are likely abundant in this cryptic habitat but are rarely visible in photographs. Two photographs capture Sabellidae sp. with their feeding tentacles displayed. This habitat is highly suitable for sabellids but it is likely that the turbulence caused by the ROV thrusters causes them to withdraw their characteristic tentacles making them hard to locate on photographs. Bryozoa were encountered relatively frequently but they were usually small and it was mostly not possible to identify them nor to elucidate the number of species present. However, a reticulate species of *Reteporella*, possibly *R. incognita*, was present, as as a cyclostome species that was probably *Tervia irregularis*. Sheet encrusting cheilostomes were occasionally present on oyster shells but could not be identified further. Distinctive sponges included the hadromerid *Weberella bursa*, the poecilosclerid *Mycale lingua* and an unidentified species of Tetractinellida. Two further sponge species were also tentatively identified from the upper part of the wall but the difficulty of sampling in overhang areas means

that no voucher specimens were collected for confirmation. Nevertheless the blue sponge (Figure 3, upper left) could be *Hymedesmia curvichela sensu* [19] (not *Hymedesmia curvichela* Lundbeck, 1910) which we encountered (and collected) on a previous cruise to a canyon system north of the Porcupine Seabight. The bright yellow crust (also Figure 3, upper left) is likely *Hexadella dedritifera* Topsent, 1913, although this has recently been shown to be a species complex [20].

Assemblage Structure

Size and density measurements in photographs were related to depth (Figure 4). The average height of *A. excavata* shells tended to increase with depth ($F_{1,20}$ = 5.41, $p < 0.05$, r^2 21%). The overall size distribution of measured shells was generally symmetrical around the mean of 10.5 cm (SE 0.37), with no obvious additional size classes. A linear regression of *A. excavata* density with depth was not significant; however, the highest densities in 20 m depth bands seemed to increase with depth. This observation was supported by quantile regression: coefficients for the 75% quantile were significant, indicating that upper density limits for *A. excavata* increased with depth. The maximum *A. excavata* density recorded was 25.2 m^{-2}. *Neopycnodonte zibrowii* also occurred at higher densities with increasing depth ($F_{1,20}$ = 4.6, $p<0.05$, r^2 19%). The maximum oyster density observed was 16.1 m^{-2}. The patterns of increasing density with depth ended abruptly, with the deepest individuals found at low densities (values not directly estimated due to reflections of the laser sights off the substrate).

Correlations between species in the assemblage suggest common responses to environmental gradients and/or a biological interaction. *Acesta excavata* and *N. zibrowii* densities were positively correlated ($r = 0.662$, $p<0.01$). Of the nine identifiable taxa frequently observed in photographs, six were positively correlated with *A. excavata* and/or oyster densities: *Desmophyllum dianthus,*

Cerianthidae sp, Comatulida sp(p)., Bythitidae sp., Bathynectes longispina and *Margarites sp.* (Table 1). The densities of two conspicuous species, the coral *Madrepora oculata* and the urchin *C. cidaris*, had no associations with *A. excavata* or *N. zibrowii.* Because of the nature of zoanthid colonies and the difficulties in

identifying discrete colonies, it was not possible to test whether these were positively correlated with bivalve densities.

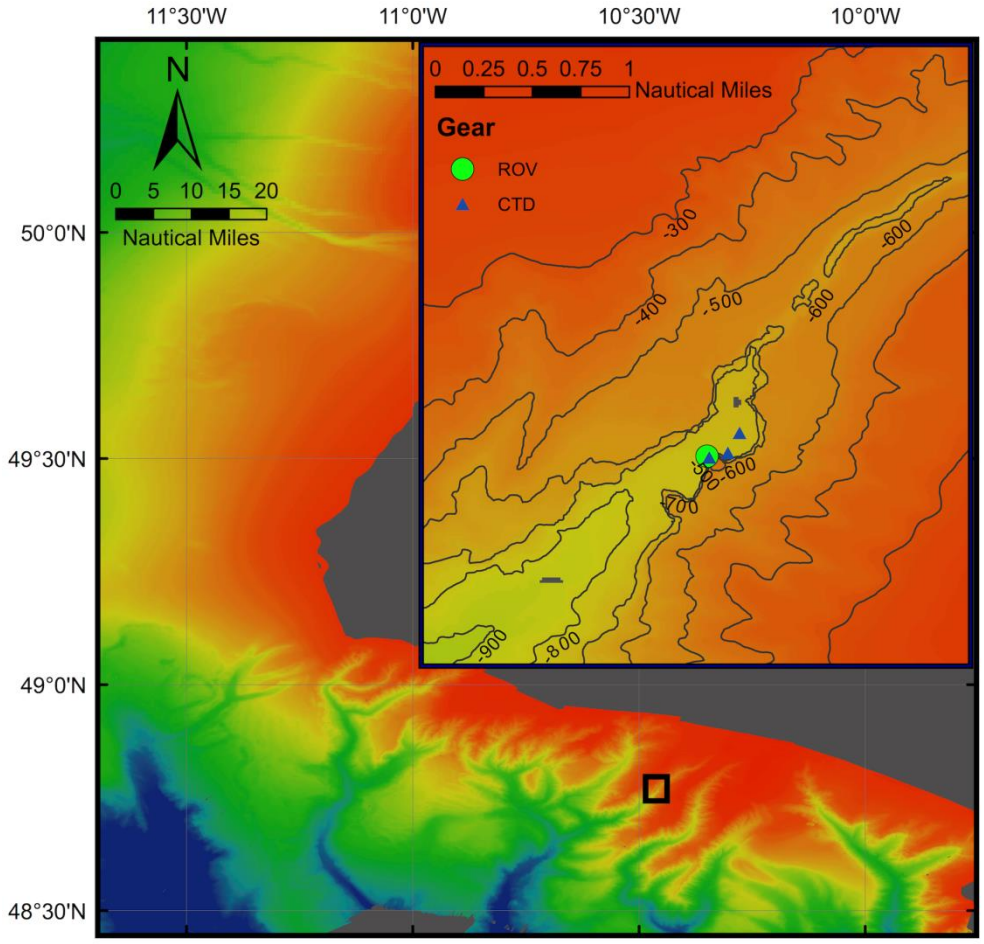

Figure 1. Location of the *A. excavata -N. zibrowii* biotope on the southern side of the surveyed canyon (green circle on inlay marked as 'ROV'). Deeper waters have cooler colours. doi:10.1371/journal.pone.0079917.g001

Figure 2. Photomosaic of *A. excavata-N. zibrowii* habitat at a depth of 666 m. Total area approximately 5 m^2. A prominent *N. zibrowii* is visible in the top left of the image, with other oyster individuals embedded in the matrix of *A. excavata* and other species. doi:10.1371/journal.pone.0079917.g002

Table 1. Correlations between taxa counted in photographs and the densities of *A. excavata* and *N. zibrowii.*

Taxon	Mean density (m^{-2}) ±SE	Correlation with *A. excavata*	Correlation with *N. zibrowii*
Desmophyllum dianthus	24.0±4.42	0.552**	0.438**
Madrepora oculata	3.10±0.397	0.214	0.112
Comatulida sp(p).	2.23±0.629	0.619**	0.348
Bythitidae sp.	0.50±0.137	0.372	0.564*
Cerianthidae sp.	0.45±0.163	0.482*	0.594**
Cidaris cidaris	0.25±0.071	−0.001	−0.190
Margarites sp.	0.16±0.062	0.461*	0.473*
Bathynectes longispina	0.12±0.058	0.492*	0.505*

Results are only shown for taxa recorded in over 10% of photographs; other taxa were seen in fewer than 10% of photographs. Significant correlations are indicated using *p<0.05, **p<0.01, ***p<0.001. Other taxa were seen in less than 10% of photographs and are listed in the results section.
doi:10.1371/journal.pone.0079917.t001

Other aspects of the habitat varied with depth. Most strikingly, the deepest part of the cliff had few *A. excavata* and the rest of the rock surface was relatively bare. This contrasts with shallower areas, where *A. excavata* was frequent, as were mobile species and colonies of corals, bryozoans, hydroids and sponges (Figure 3).

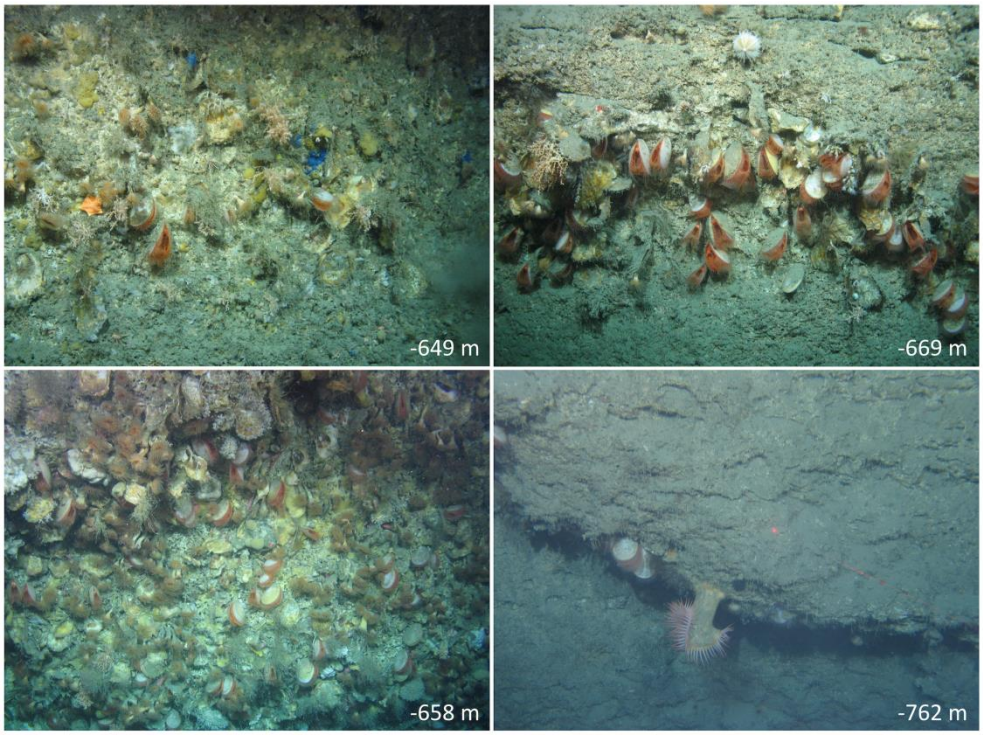

Figure 3. Images from different depths on the wall showing qualitative differences with depth, including more sponge cover at the shallowest depth, increased *A. excavata* and *N. zibrowii* with depth until the deepest, low biomass, section is reached. doi:10.1371/journal.pone.0079917.g003

Hydrography

The water masses at the Whittard Canyon region are dominated by Eastern North Atlantic Water (ENAW) in the upper 500 m (Figure 5A) with ranges of 8<T<18 °C, 35.2<S<36.7, and density, σ_t = 27–27.2 kg m^{-3}. Below this, lies Mediterranean Outflow Water (MOW, 2.6<T<11 °C, 35<S<36.2, with a core centred at σ_t = 27.5 kg m^{-3}), found principally off slope, although the influence of MOW can be seen extending into the canyon branches. Labrador Sea Water (LSW) is found at intermediate depths with a core between 1900–2000 m. Vertical profiles of temperature, salinity and density, σ_t (Figure 5B–D) indicated a weakly stratified surface layer down to 400 m; the spring timing of the survey had not permitted full seasonal stratification to be developed. Between 600–1000 m evidence of the permanent thermocline can be seen, with strong stratification of the water column in both profiles. The ROV dive site (water depth 750 m), and the depths of the wall where high densities of suspension feeders were found (640–740 m), are located within this permanent thermocline.

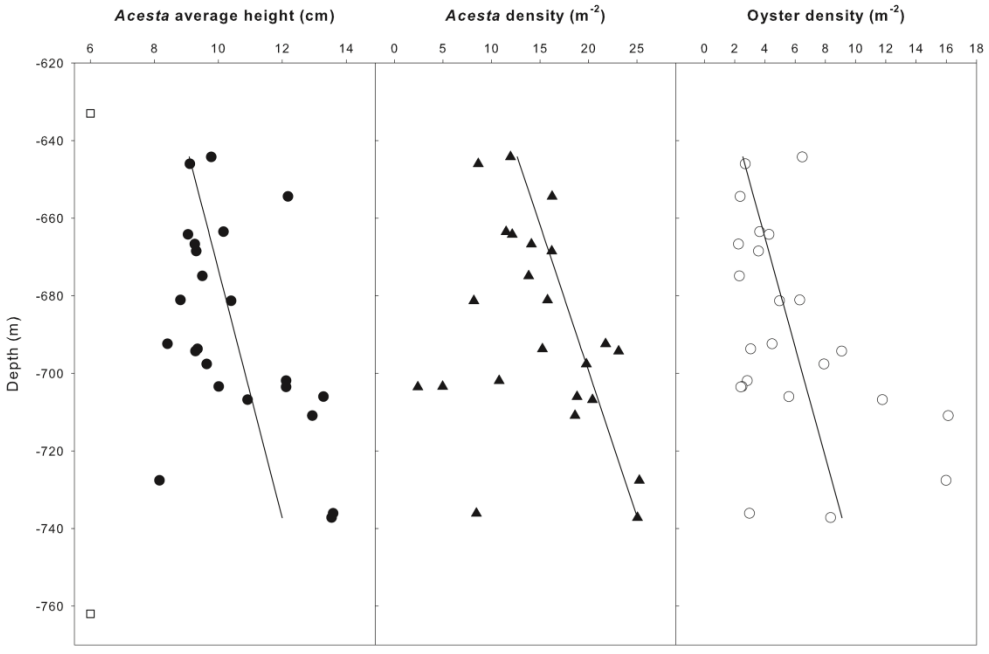

Figure 4. Variations in mean *A. excavata* shell height, *A. excavata* density and *N. zibrowii* density as a function of depth. The range of depths where *A. excavata* shells were observed on the wall was from 633 to 762 m (open square symbols). Lines are fitted linear regressions except for the panel displaying *A. excavata* densities where the line is a quantile regression estimating the position of the third quartile (0.75). Quantile regression coefficients were significantly different from zero when tested using bootstrap estimates of SE. doi:10.1371/journal.pone.0079917.g004

Vertical profiles of beam attenuation (m^{-1}), used as a proxy for suspended material concentration, revealed a strong benthic nepheloid layer (BNL) present and numerous intermediate nepheloid layers (INL) within the canyon (Figure 6). Overall beam attenuation (m^{-1}) was highest in BNLs at 750 and 1000 m water depths. At 1000 m water depth, the BNL extended >100 m above the seabed, possibly associated with impinging MOW core found at this depth. A 200 m thick INL centred at 1100 m in the adjacent, deeper, vertical profile (water depth 1320 m) was likely associated with the detachment of the BNL. At the ROV dive site, the vertical profile of beam attenuation (m^{-1}) indicated the highest values of suspended material extending from the seabed at 750 m to 500 m depth. INLs observed between 650–750 m water depth in the 1000 m and 1320 m profiles were also likely to be associated with the BNL found at the ROV site.

The rough topographic nature of canyons is likely to result in dynamics of a complex nature where energy will be extracted from barotropic tides to baroclinic internal wave motion. A 6–7 hour repeat cross-canyon channel CTD transect 3 km downcanyon from the dive site suggested the presence of internal waves in the depth range 400–700 m (Figure 7). Internal waves generated at the barotropic semi-diurnal tidal period will propagate as a beam through the water column, periodically stretching and squashing the isopycnal surfaces at the depths where the internal wave energy is concentrated. This is highlighted in Figure 7 which shows the displacement of isopycnals based on the repeat CTD profiles at six locations across the canyon. At this time the upper 200 m of the water column was well mixed due to a severe storm a few days previously and is not shown. Maximum isopyncal displacement occurred close to the seabed at the dive site side of the canyon at ~500 m and a secondary maximum was found at about 300 m on the opposite (northern) side. Relatively high isopycnal excursion occurred as a layer between these two maxima, as well as in a layer between 200–300 m which one might tentatively suggest emanated from the northern maximum. The band of high isopycnal excursion across the canyon between 300–500 m represented an angle (β) of ~3 degrees from the horizontal. The buoyancy frequency (N), determined from vertical density profiles, together with an internal wave frequency (σ) appropriate for the semi-diurnal tide and Coriolis parameter (f), would suggest that internal waves would indeed propagate in beams 3 degrees from the horizontal (e.g. $sin(\beta) = [(\sigma^2 - f^2/N^2 - f^2)]^{1/2}$,

[21]). This perhaps suggests that internal waves may have been generated at the top of the north canyon wall, with subsequent cross canyon propagation to a location immediately above ROV dive site wall. In addition there is high displacement at the foot of the canyon which may be due to tidal modulation of any bottom density flow or of any MOW water located between 800–1000 m. This would cause a change in density from horizontal advection rather than vertical displacements.

The resolution of the CTD transect was such that repeat profiles were made at water depths of 500 and 1000 m respectively, spanning the depth range of the vertical wall. The high calculated displacements above 300 m may also be the result of an internal wave beam originating from the same source, propagating up and reflecting from the surface mixed layer, where there are high displacements immediately below the bottom of the surface mixed layer. Again the propagation angles are consistent although the interpretation is somewhat speculative. Overall the repeat CTD transect suggests that a significant amount of baroclinic energy exists within the upper/mid canyon region. A BNL was generated at the depth of high displacement on the southern canyon wall (500 m) and an INL at that depth was present within the canyon (Figure 6). It is likely therefore that sediment mobilisation at depths above the wall and its associated fauna is a persistent process within the canyon.

Discussion

The *A. excavata-N. zibrowii* biotope has not been previously recognized and this habitat adds to the complexity and diversity of what is known from vertical faces at the continental margins. The group of six species associated with *A. excavata* or *N. zibrowii* also suggests a coherent assemblage responding to the same habitat cues. *Acesta excavata* has only previously been noted in such abundance from shallower depths on the sides of fjords [16]. High *N. zibrowii* cover has been observed in other canyon systems in the Bay of Biscay, but not in association with *A. excavata* [5]. The vertical face covered in *Lophelia pertusa* with occasional *A. excavata* described by Huvenne et al. [6] was at a deeper point of the Whittard Canyon system (1350 m). Other wall-associated assemblages seem likely, possibly including extensions of some of the rock assemblages identified by Howell et al. [17]. The source of debris in a gorge close to the Wyville-Thomson

ridge has been suggested to be from barnacle populations (*Bathylasma hirsutum*) on adjacent rock walls [22].

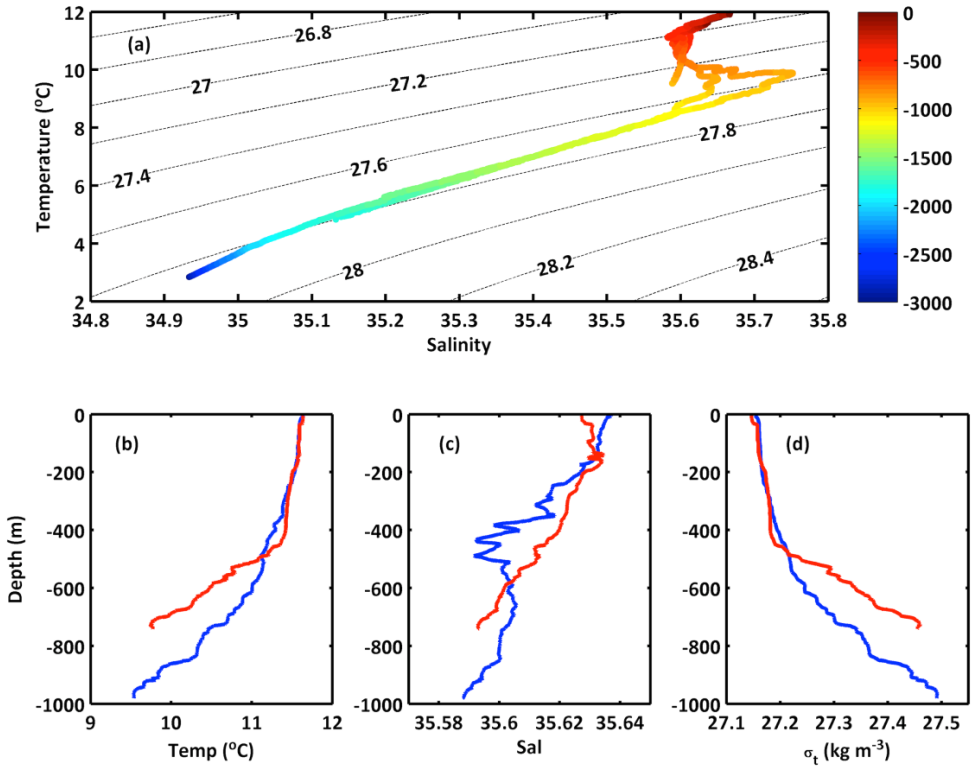

Figure 5. Water mass properties in the Whittard Canyon. **A** Temperature-salinity plots (CTD casts at 750 m, 1000 m, 1820 m, 3100 m). Isopycnals indicate potential density, σ_t (kg m^{-3}) and the colourbar indicates depth (m). **B** temperature (°C) profiles at 750 m (red line) and 1000 m (blue line). **C** salinity profiles at 750 m and 1000 m. **D** density, σ_t (kg m^{-3}) profiles at 750 m and 1000 m. doi:10.1371/journal.pone.0079917.g005

The variation in densities and mean shell size imply that there are relatively small-scale vertical variations in resource supply. Larger and more numerous filter feeders with depth suggest that there is more food at greater depths, up to the point where the biomass is much lower. Observation of the suspended particulate matter (SPM) concentrations in the canyon (Figure 6) indicated a general increase in SPM at the depths occupied by the biotope, which was located within the permanent thermocline. The depth range of this large vertical density gradient is one where both tidal and residual current energy are often enhanced (e.g., [21]). The rough topography associated with the canyon branches will likely be a source (and sink) of baroclinic energy (internal waves) generated by the enhanced currents found at the margin, for both residual flows (e.g., [5]) and those of tidal origin (e.g., [13], [14]). The canyon topography itself

will likely channel and focus internal waves, resulting in a complex spatial (vertical and horizontal) distribution of baroclinic energy within the canyon (e.g. Figure 7). For example, observations of periodic resuspension in Baltimore canyon were associated with the focussing of internal waves towards the canyon head, manifest as a cold-water bore propagating up the canyon [23]. Hotchkiss and Wunsch [24] also found focussing of internal wave energy in the bottom layer at the foot of the upper Hudson Canyon. It is plausible therefore that one might expect the highest suspended sediment concentrations to be found at the foot of the wall in the Whittard Canyon. The availability of suspended food resources may explain the increases in bivalve size and densities with depth, up to the point where disturbance may restrict the assemblage towards the base of the wall due to burial or abrasion.

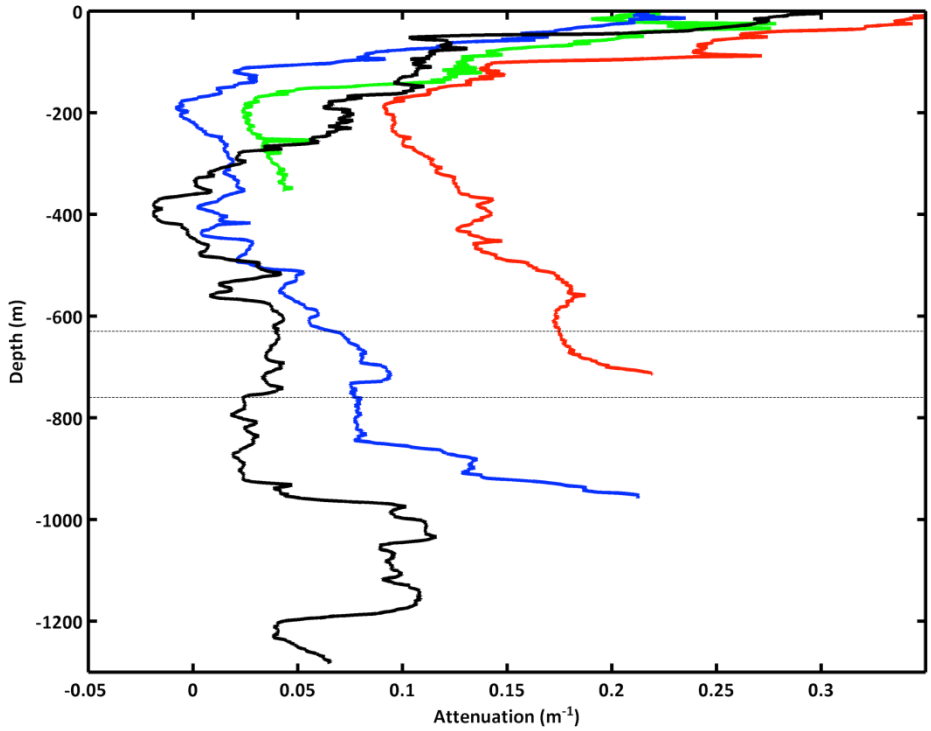

Figure 6. Light attenuation profiles (m^{-1}) in the eastern branch of the Whittard canyon at 375 m (green), 750 m (red), 1000 m (blue) and 1320 m (black) water depth. Dashed lines (620–740 m) indicate depth of wall where high densities of suspension feeders were found. doi:10.1371/journal.pone.0079917.g006

The different assemblages found on rock walls may be caused by environmental preferences. Variations in assemblage structure seem unlikely simply to be an expression of depth alone. For example, *L. pertusa* has a depth

range that completely overlaps the *A. excavata-N. zibrowii* association reported in the current study [25] and therefore might have been expected to be conspicuous on the surveyed habitat. The influences of substratum hardness, stability and texture on the settlement and survival of different species are unknown. Food quality and quantity may have a role to play in creating different assemblages. *Acesta excavata* has a high capacity for filter feeding and a low metabolic rate [26]. It is seems likely that, given heterogeneity in resource supply in the deep sea, other filter feeders may specialize on different resource availabilities to *A. excavata*. The greater filtering capacity of a bivalve may cope better with a highly episodic supply, while a coral may be more efficient with a more regular supply of food particles.

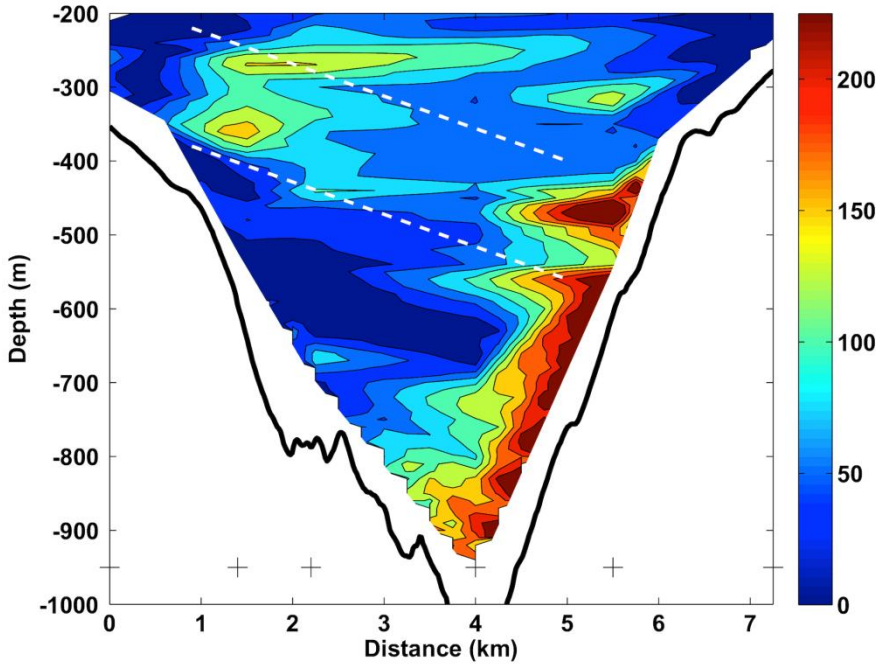

Figure 7. Transect of isopycnal displacement (absolute value in m) calculated from a 6–7 hr repeat transect across the canyon channel 4 km downstream of the ROV dive site. The southern side of the canyon (where the *A. excavata-N. pycnodonte* biotope was found) is on the right side of the figure. A scale is shown to the right, CTD locations by 'x' and the seabed by the black line. The parallel white lines across the transect indicate a possible beam of high isopycnal displacement associated with an internal wave emanating from the northern canyon wall. doi:10.1371/journal.pone.0079917.g007

Although different species may have environmental preferences for particular wall habitats, it is not clear whether direct competition for resources has a role in structuring wall assemblages. *Acesta excavata, N. zibrowii* and a number of other taxa were positively correlated on a small scale, which would not

support the hypothesis of competition for resources between species. If there are direct competitive interactions between different species found on walls, then the timescales may be long, given the apparent longevity of corals and *A. excavata* [16], [27]. The relatively large average size of *A. excavata* and the absence of clear size classes other than the mean size may indicate that the assemblage had one large recruitment event leading to *A. excavata* domination of the available rock surface. This could imply assemblages structured by space pre-emption. However, it is difficult to distinguish between a large recruitment at one point in time and a stable age structure topped up by a very low level of recruitment and a high survivorship. A greater number of growth rate estimates at different scales and in different topographic settings would help to develop a clearer basis for understanding the variation in wall assemblages.

Looking at the available bathymetry, it is clear that there may be many areas of near-vertical habitat in the canyons of the continental margin (e.g., [28]). As pointed out by Huvenne et al. [6], canyon walls may represent refuges from fishing-related disturbance for species that may be found across wider areas. The vertical habitats certainly contain structures that may act as nursery habitat for deep-sea fish and other mobile species. In our example, the three-dimensional microstructures created by the *A.excavata-N. zibrowii* assemblage provide diverse habitats for macrofaunal organisms, including the fish and mobile invertebrates visible in photographs. Comparative studies of canyon wall assemblages would provide excellent information about the supply and fate of organic matter at different scales along the continental margin.

Methods

Biological Observations

Observations were made using the deep-water ROV Holland I during a cruise on the RV Celtic Explorer to the Whittard Canyon system (cruise CE12006, Figure 1). ROV Holland I is a Quasar work class ROV rated to 3000 m. It is equipped with several video camera systems, an OE14-208 digital stills camera and has two robotic arms, a slurp sampler and storage boxes for collecting fauna. Material retained in the slurp chamber was sieved with a 0.5 mm sieve and used to verify identifications from photographs. ROV depth and position were

established via a Sonardyne Ranger USBL beacon system. Cruise CE12006 was targeting vertical walls in canyon systems as potential sites of high biomass. Potential wall areas were identified from the available INFOMAR bathymetry by targeting regions with high slope. The INFOMAR (Integrated Mapping for the Sustainable Development of Ireland's Marine Resource) project is a joint venture between the Geological Survey of Ireland and the Marine Institute and provides high quality bathymetry to 25 m resolution, interpolated from 100 m spaced point data (http://www.infomar.ie/data/). Suitable sites were dived with the ROV. On 16th April 2012, a dive at 48.761 °N, 10.461 °W (cruise CE12006, Event number 12) encountered a vertical wall extending from 631 m depth to 780 m depth. On this wall we identified the presence of large numbers of A. excavata on the vertical faces. On reaching the top of the wall, the ROV was flown to near the bottom of the wall to repeat a vertical pass while taking still photographs. Poor weather prevented any further dives on or near this site during the cruise.

Individual, non-overlapping, photographs were treated as individual quadrats to collect information on size distributions and densities of *A. excavata*. Size and area estimates were made for each photograph using paired laser guidelines orientated at 90 ° to the camera's focal plane and separated by 10 cm. Measurements, calibrated to that photograph's laser guideline separation, were made in imageJ, an open source Java-based image processing progamme (http://rsb.info.nih.gov/ij/). Counts of *A. excavata* and *N. zibrowii* were converted to densities m^{-2}. The attachment point of *A. excavata* shells to the substratum was taken as a basis for shell height measurements (the species has a straight dorsal margin). To minimize error, these measurements were only taken when the attachment point was clear and the shells were seen with a view of one valve or were seen in side view. *Neopycnodonte zibrowii* shells were similar in size to *A. excavata*, but the uneven nature of the oyster shells and the tendency for the edges of shells to overlap meant that shell sizes could not be confidently estimated. Quantile regressions were carried out using the quantreg package in R [29]. Overlapping photographs were mosaiced using check points added manually in the Hugin package (http: //hugin.sourceforge. net/) to provide larger images of the assemblage. Organisms associated with the habitat were identified, where possible, from the images.

Hydrographic Data

Sixty-six CTD casts were performed in two branches of the Whittard Canyon providing detailed hydrographic data. Vertical profiles of temperature, salinity, fluorescence and transmission were taken down to depths of 3150 m. Beam attenuation measurements were made using a 0.25 m path-length transmissometer (C-Star, WET Labs') operating at 650 nm. Data were processed using Seabird data-processing software and MATLAB (Matworks, R2007a). Beam attenuation was calculated using

$$c = -\ln(Tr) * {}^{1}/_{x}$$

where x is the pathlength of the transmissometer and Tr is the transmittance output from the instrument expressed as

$$Tr = \frac{Voltage\ (signal) - Voltage\ (dark\ value)}{Voltage\ (clean\ water\ calibration) - Voltage\ (dark\ vlaue)}$$

$Voltage\ (signal)$ is the output signal, $Voltage\ (dark\ value)$ is the dark offset for the instrument obtained by blocking the light path and $Voltage\ (clean\ water\ calibration)$ is the manufacturer's supplied value for output in clean water.

Isopycnal displacements were calculated from a 6–7 hour repeat survey across the canyon close to the ROV dive site. To achieve this, the individual profiles were averaged over 20 m vertical bins to obtain individual vertical profiles of density and the density difference between the profile pair (ρ'). To calculate the isopycnal displacement (Z) at any depth, each pair of repeat profiles was averaged to form a mean vertical density profile and ρ' was divided by the vertical density gradient of a range $\pm$ 40 m about each depth ($d\rho/dz$),

$$\text{i.e. } Z = \frac{\rho'}{d\rho/dz}$$

Acknowledgments

We are grateful to Christine Morrow (Queen's University Belfast), Bernard Picton (Ulster Museum), Ulrich Schliewen (Bavarian State Collection for Zoology), Estefania Rodriguez (American Museum of Natural History), Teresa Darbyshire (National Museum Wales) and Peter Hayward (formerly of Swansea University) for assistance in identifying fauna from the photographs. The INFOMAR team provided bathymetry data. We thank the captain and crew of the RV Celtic Explorer. This research survey was carried out under the Sea Change strategy with the support of the Marine Institute and the Marine Research Sub-programme of the National Development Plan 2007–2013. Images taken by the Irish deep-water ROV Holland I remain the property of the Marine Institute. We are grateful to Andre´ Freiwald, Jason Hall-Spencer, Veerle Huvenne and an anonymous reviewer for their constructive reviews.

Author Contributions

Conceived and designed the experiments: ALA MPJ MW. Performed the experiments: MPJ MW ALA AW ES LW HF. Analyzed the data: MPJ MW ALA AW ES LW HF. Contributed reagents/materials/analysis tools: MPJ MW ALA AW ES LW HF. Wrote the paper: MPJ MW ALA AW ES LW HF. Chief Scientist on cruise: ALA.

References

1. Menot L, Sibuet M, Carney RS, Levin LA, Rowe GT, et al. (2010) New perceptions of continental margin biodiversity. In: Life in the World's Oceans Diversity, Distribution and Abundance (Edited by Alistair D McIntyre) Wiley-Blackwell.
2. Webb TJ, Vanden Berghe E, O'Dor R (2010) Biodiversity's Big Wet Secret: The Global Distribution of Marine Biological Records Reveals Chronic Under-Exploration of the Deep Pelagic Ocean. PLoS ONE 5(8): e10223. doi:10.1371/journal.pone.0010223.
3. Ramirez-Llodra E, Brandt A, Danovaro R, De Mol B, Escobar E, et al. (2010) Deep, diverse and definitely different: unique attributes of the world's largest ecosystem. Biogeosciences 7: 2851–2899.
4. Levin LA, Sibuet M (2012) Understanding Continental Margin Biodiversity: A New Imperative. Ann Rev Mar Sci 4: 79–112.
5. Van Rooij D, De Mol L, Le Guilloux E, Wisshak M, Huvenne VAI, et al. (2010) Environmental setting of deep-water oysters in the Bay of Biscay. Deep-Sea Res 57: 1561–1572.
6. Huvenne VAI, Tyler PA, Masson DG, Fisher EH, Hauton C, et al. (2011) A Picture on the Wall: Innovative Mapping Reveals Cold-Water Coral Refuge in Submarine Canyon. PLoS ONE 6(12): e28755. doi:10.1371/journal.-pone.0028755.
7. Wollast R, Chou L (2001) Ocean Margin Exchange in the Northern Gulf of Biscay: OMEX I. An introduction. Deep-Sea Res 48: 2971–2978.
8. Duineveld G, Lavaleye M, Berghuis E, de Wilde P (2001) Activity andcomposition of the benthic fauna in the Whittard Canyon and the adjacent continental slope (NE Atlantic). Oceanologica Acta 24: 69–83.
9. Pingree RD, Le Cann B (1989) Celtic and Armorican slope and shelf residual currents. Prog Oceanogr 23: 303–339.
10. Pingree RD, Sinha B, Griffiths CR (1999) Seasonality of the European slope current (Goban Spur) and ocean margin exchange. Continental Shelf Res 19: 929–975.
11. Reid GS, Hamilton D (1990) A reconnaissance survey of the Whittard Sea Fan, southwestern approaches, British Isles. Mar Geol 92: 69–86.
12. Pingree RD, Mardell GT, New AL (1986) Propagation of internal tides from the upper slopes of the Bay of Biscay. Nature 321: 154–158.
13. Pingree RD, New LA (1989) Downward propagation of internal tidal energy into the Bay of Biscay. Deep-Sea Res 36: 735–758.
14. Holt JT, Thorpe SA (1997) The propagation of high frequency internal waves in the Celtic Sea. Deep-Sea Res 44: 2087–2116.
15. Connor DW, Allen JH, Golding N, Howell KL, Lieberknecht LM, et al. (2004) The Marine Habitat Classification for Britain and Ireland Version 04.05. JNCC, Peterborough ISBN 1 861 07561 8 (internet version) http://jncc.defra.gov.uk/MarineHabitatClassification.
16. Lo´pez Correa M, Freiwald A, Hall-Spencer J, Taviani M (2005) Distribution and habitats of Acesta excavata (Bivalvia: Limidae) with new data on its shell ultrastructure. In: Freiwald A, Roberts JM, editors. Cold-water Corals and Ecosystems. Berlin Heidelberg: Springer-Verlag. 173–205.

17. Howell KL, Davies JS, Narayanaswamy BE (2010) Identifying deep-sea megafaunal epibenthic assemblages for use in habitat mapping and marine protected area network design. JMBA UK 90: 33–68.
18. So¨ffker M, Sloman KA, Hall-Spencer JM (2011) In situ observations of fish associated with coral reefs off Ireland. Deep-Sea Research I 58: 818–825.
19. Stephens J (1921) Sponges of the coast of Ireland. II.-The Tetraxonida (Concluded). Fish Irel Sci Invest 1920 II [1921]: 1–75.
20. Reveillaud J, Remerie T, van Soest R, Erpenback D, Cardenas P, et al. (2010) Species boundaries and phylogenetic relationships between Atlanto-Mediterranean shallow-water and deep-sea coral associated Hexadella species (Porifera, Ianthellidae). Mol Phylogenet Evol 56: 104–114.
21. White M, Dorschel B (2010) The importance of the permanent thermocline to the cold water coral carbonate mound distribution in the NE Atlantic. Earth Plan Sci Lett 296: 395–402.
22. Gage JD (1986) The benthic fauna of the Rockall Trough - regional distribution and bathymetric zonation. Proc Roy Soc Edin B 88: 159–174.
23. Gardner WD (1989) Periodic resuspension in Baltimore Canyon by focusing of internal waves. J Geophys Res 94: 185–194.
24. Hotchkiss FS, Wunsch C (1982) Internal waves in Hudson Canyon with possible geological implications. Deep-Sea Res 29: 415–442.
25. Davies AJ, Guinotte JM (2011) Global Habitat Suitability for Framework- Forming Cold-Water Corals. PLoS ONE 6(4): e18483. doi:10.1371/journal.- pone.0018483.
26. Ja¨ rnegren J, Altin D (2006) Filtration and respiration of the deep living bivalve Acesta excavata (J.C. Fabricius, 1779) (Bivalvia; Limidae). J Exp Mar Biol Ecol 334:122–129.
27. Hall-Spencer J, Allain V, Fossa° JH (2002) Trawling Damage to Northeast Atlantic Ancient Coral Reefs. Proc Roy Soc B 269: 507–511.
28. Sacchetti F, Benetti S, Georgiopoulou A, Shannon PM, O'Reilly BM, et al. (2012) Deep-water geomorphology of the glaciated Irish margin from highresolution marine geophysical data. Mar Geol 291: 113–131.
29. R Development Core Team (2010) R: A language and environment for statistical computing. R Foundation for Statistical Computing, Vienna, Austria. ISBN 3-900051-07-0, URL http://www.R-project.org.

Appendix B:
The Whittard Canyon – a case study of submarine canyon processes

T. Amaro[1*], V.A.I. Huvenne[2], A.L. Allcock[3], T. Aslam[4,5], J.S. Davies[6], R. Danovaro[7,8], H.C. de Stigter[9], G.C.A. Duineveld[9], C. Gambi[7], A.J. Gooday[2], L.M. Gunton[2], R. Hall[4], K.L. Howell[6], J. Ingels[10], K. Kiriakoulakis[11], C.E. Kershaw[11], M.S.S Lavaleye[9], K. Robert[2], H. Stewart[12], D. Van Rooij[13], M. White[3], **A.M. Wilson.[3*]**

[1]Hellenic Center for Marine Research (HCMR), 710 03 Heraklion, Crete, Greece. [2]National Oceanography Centre, University of Southampton Waterfront Campus, Southampton, SO14 3ZH, UK. [3]Ryan Institute and School of Natural Sciences, National University of Ireland, Galway, University Road, Galway, Ireland.[4]Centre for Ocean and Atmospheric Sciences, School of Environmental Sciences, University of East Anglia, Norwich, UK. [5]Centre for Environment Fisheries and Aquaculture Sciences (Cefas), Lowestoft, UK. [6]Marine Biology & Ecology Research Centre, Marine Institute, Plymouth University, Plymouth, PL4 8AA, UK.[7] Dep Life and Environmental Sciences, Polytechnic University of Marche, Ancona, Italy. [8]Stazione Zoologica Anton Dohrn, Villa Comunale I, Napoli, Italia. [9]NIOZ Royal Netherlands Institute for Sea Research, Department of Ocean Systems Sciences, and Utrecht University, PO Box 59, 1790 AB, Den Burg, Texel, The Netherlands.[10]Plymouth Marine Laboratory, Prospect Place, West Hoe, PL1 3DH, Plymouth, UK [11]School of Natural Sciences and Psychology, Liverpool John Moores University, Liverpool, L3, 3AF [12]British Geological Survey, The Lyell Centre, Research Avenue South, Edinburgh EH9 3LA, UK. [13]Renard Centre of Marine Geology (RCMG), Department of Geology and Soil Science, Ghent University, Krijgslaan 281 S8, B-9000 Gent, Belgium

Published: Progress in Oceanography, 146 (2016) 38 – 57.

***Role:** Contributed to the interpretation of data, analysis, production of figure 3 and writing of oceanography and canyon activity sections (2b and 3).

Abstract

Submarine canyons are large geomorphological features that incise continental shelves and slopes around the world. They are often suggested to be biodiversity and biomass hotspots, although there is no consensus about this in the literature. Nevertheless, many canyons do host diverse faunal communities but owing to our lack of understanding of the processes shaping and driving this diversity, appropriate management strategies have yet to be developed. Here, we integrate all the current knowledge of one single system, the Whittard Canyon (Celtic Margin, NE Atlantic), including the latest research on its geology, sedimentology, geomorphology, oceanography, ecology, and biodiversity in order to address this issue. The Whittard Canyon is an active system in terms of sediment transport. The net suspended sediment transport is mainly up-canyon causing sedimentary overflow in some upper canyon areas. Occasionally sediment gravity flow events do occur, some possibly the result of anthropogenic activity. However, the role of these intermittent gravity flows in transferring labile organic matter to the deeper regions of the canyon appears to be limited. More likely, any labile organic matter flushed downslope in this way becomes strongly diluted with bulk material and is therefore of little food value for benthic fauna. Instead, the fresh organic matter found in the Whittard Channel mainly arrives through vertical deposition and lateral transport of phytoplankton blooms that occur in the area during spring and summer. The response of the Whittard Canyon fauna to these processes is different in different groups. Foraminiferal abundances are higher in the upper parts of the canyon and on the slope than in the lower canyon. Meiofaunal abundances in the upper and middle part of the canyon are higher than on adjacent slopes, but lower in the deepest part. Mega- and macrofauna abundances are higher in the canyon compared with the adjacent slope and are higher in the eastern than the western branch. These faunal patterns reflect the fact that the Whittard Canyon encompasses considerable environmental heterogeneity, related to a combination of organic matter trapping, current regimes (due to focused internal tides) and different substrates. We conclude that coordinated observations of processes driving faunal patterns are needed at a fine scale in order to understand the functioning of communities in this and other submarine canyons.

1. Introduction

More than 9450 large submarine canyons have been identified along the World's continental margins (Harris et al., 2011), making them important features that affect the geology, sedimentology, oceanography, biology and ecology of our oceans. Their presence gives rise to complex physical oceanographic conditions that locally enhance primary productivity and increase particulate matter concentrations (Bosley et al., 2004; Ryan et al., 2005; Skliris & Denidi, 2006). They provide the main transport pathways between the shelf and the deep ocean, funnelling sediments, nutrients and organic matter (OM) (Puig et al., 2014) as well as pollutants and litter (e.g. Palanques et al., 2008; Pham et al., 2014) into the deep sea. These phenomena eventually lead to an enrichment in abundance and diversity of biological communities (Schlacher et al., 2007, Danovaro et al., 2009; Bianchelli et al., 2010; Vetter et al., 2010) including commercially important stocks of fish and shellfish (Puig et al., 2012). However, the processes controlling these phenomena are only partly understood. The interactions between oceanography, sediment transport, biogeochemistry and the resulting spatial distributions of biological communities are particularly unclear.

Submarine canyons, with their steep morphology, variable current speeds and occasional catastrophic flows, are challenging environments to study. Recent technological advances (e.g., the use of Remotely Operated Vehicles, gliders and robust landers) have driven an increase in the number and geographical spread of submarine canyon studies. However, a more complete picture of the processes acting and interacting in submarine canyon settings can only be obtained from concerted studies of individual canyons (Huvenne & Davies, 2014). The aim of this overview is therefore to integrate current knowledge of processes operating in the Whittard Canyon, one of the main submarine canyons along the Celtic Margin, NE Atlantic.

The Whittard Canyon is an interesting case study for several reasons. Firstly, the canyon head is located approximately 300 km from land (Fig. 1). This means that terrestrial sediment input is strongly reduced compared to canyons receiving direct river input (e.g. Kaikoura Canyon, off the coast of New Zealand) or canyons that have their heads close to the shoreline and hence act as traps for along-shore sediment transport (e.g., Nazaré Canyon, Iberian Margin). Hence, from this perspective, this canyon may appear inactive (Toucanne et al., 2006).

However, the Whittard Canyon still encompasses the complexities of a shelf-incising submarine canyon (as defined by Harris & Whiteway, 2011): a dentritic morphology with multiple branches converging into a single deep-sea channel, topography (steep and vertical walls), rich and varied biological communities. Therefore, a broad range of typical canyon processes (e.g. internal waves, small-scale slope failures, sediment gravity flows, lateral transport, Allen & Durrieu de Madron, 2009; Puig et al., 2014) are still acting here and can be studied without being obscured by repeated throughputs of terrestrially-derived material. The Whittard Canyon has been the subject of a wide range of specific studies over the past 10–15 years, covering many aspects of submarine canyon research. By combining all the available data and insights obtained by these individual investigations (Table 1), we aim to advance our understanding, not only of the Whittard Canyon system as a whole but also of canyon processes in general. As a framework for this integration, this paper will tackle the following questions. 1) Is the Whittard Canyon active in terms of sediment transport? 2) If so, at which temporal and spatial scale? 3) What impact does this (in)activity have on the associated benthic fauna and their functioning?

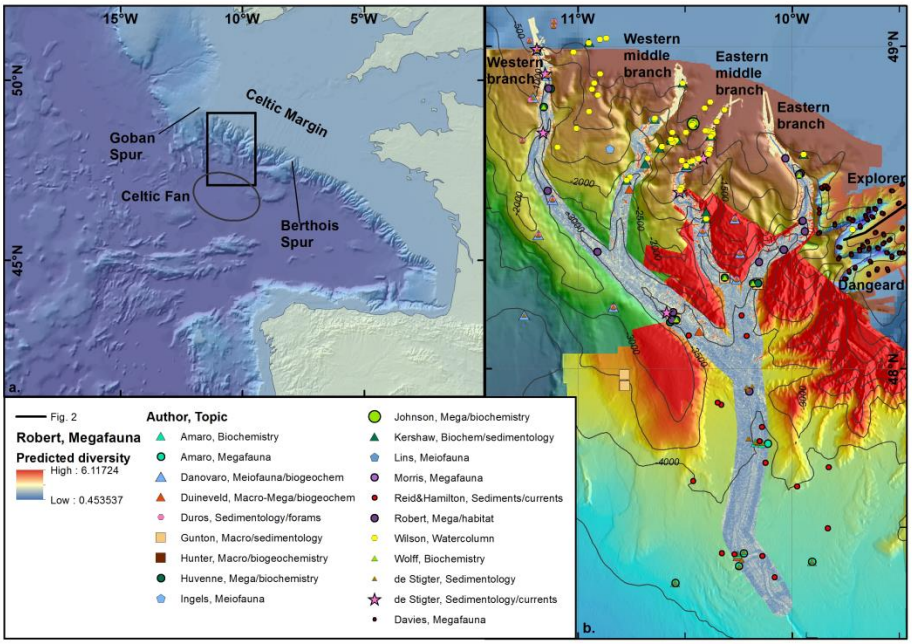

Figure 1. (a) Location map of the Whittard Canyon along the Celtic Margin, Bay of Biscay. Bathymetry data from GEBCO (2003). (b) multibeam bathymetric map of the Whittard Canyon and proximal part of the Whittard Channel and adjacent slopes, showing all the stations used for this paper, listed by author and data type (meio-, macro-, megafauna, biogeochemistry, sedimentology, watercolumn or current measurements). Bathymetry courtesy of the Geological Survey of Ireland (GSI Dublin) for the upper canyon, the HMS Scott for the lower canyon and Whittard Channel, and the MESH project for the Explorer & Dangeard Canyons.

Table 1 Datasets and published papers used as input for this overview paper. Sample locations are represented in Fig. 1c. Canyon branch: WC, Whittard Channel; W, western branch; WM, western middle branch; EM, eastern middle branch; E, eastern branch; S, open slope next to the canyon.

Reference	Subject	Sample type	Canyon branch	Depth range (m)
Amaro et al. (2015)	Biogeochemistry, megafauna	6 multicores, 5 video tows	WC	3900-4450
Gambi & Danovaro (2016)	Biogeochemistry, meiofauna	13 boxcores	W, EM, S	950-4000
Davies et al. (2014)	Megafauna	45 video tows	D, E	180-1060
de Stigter et al. (this study)	Sedimentology, Oceanography	27 multicores, 10 boxcores, 7 landers	W, EM, S, WC	175-4450
Duineveld et al. (2001)	Biogeochemistry, Macrofauna, Megafauna	3 boxcores, 1 Aggasiz trawl	W, WM, WC	2735-4375
Duros et al. (2011, 2012)	Sedimentology, foraminifera	18 multicores	W, EM, S	300-3000
Gunton et al. (2015a, 2015b)	Sedimentology, macrofauna	22 megacores	W, EM, E, S	3375-3670
Hunter et al. (2013)	Biogeochemistry, Macrofauna	2 ROV pushcore sites	W, E	3410-3595
Huvenne et al. (2011)	Biogeochemistry, megafauna	5 CTDs, 7 ROV pushcore sites, 14 ROV video tracks	W, E	1000-3650
Ingels et al. (2011a)	Meiofauna	2 megacores	WM	762-1160
Johnson et al. (2013)	Biogeochemistry, megafauna	1 ROV video site	WM	700
Kershaw et al. (this study)	Biogeochemistry, sedimentology	4 boxcores, 24 ROV pushcores	WM, EM, E, S	440-2820
Lins et al. (2013)	Meiofauna	3 megacores	WM	800-812
Morris et al. (2013)	Megafauna	13 ROV video tracks	W, E	1000-4000
Reid & Hamilton (1990)	Sedimentology, Oceanography	9 current meters, 3 grabs, 3 camera tows, 1 core	W, E, WC	3500-4500
Robert et al. (2015)	Megafauna	17 ROV video transects	W, E	1000-4000
Wilson et al. (2015a)	Oceanography	75 CTDs, 32 SAPS	WM, EM, S	200-2800
Wolff et al. (this study)	Biogeochemistry	5 CTDs, 5 SAPS	W, EM, E	1700-3370

2. Setting

a) Geology of the Celtic Margin

The Celtic Margin is a WNW-ESE oriented passive margin that extends from the Goban Spur to the Berthois Spur in the Bay of Biscay (Fig. 1). The adjacent continental shelf is wide, whereas its continental slope is steep (average slope 8 °). The entire margin is cut by approximately 35 submarine canyons, with the Whittard Canyon being the most westerly located (Bourillet et al., 2006; Mulder et al., 2012). The Celtic spurs and canyons are associated with submarine drainage basins (Grande Sole and Petite Sole), and feed the deep-sea Celtic fan through the Whittard and Shamrock Canyons (Bourillet et al., 2006). During the last glacial period, they were connected to an active palaeovalley system (Bourillet et al., 2003; Toucanne et al., 2008), but its activity is now much reduced due to its distance from the present-day shoreline (Reid and Hamilton, 1990). The canyon morphology was influenced by existing NNW-SSE trending fault systems, older buried canyons and natural depressions in the seafloor (Cunningham et al., 2005).

The Whittard Canyon is a deeply incising dendritic system, formed through headward erosion and retrogressive slope failure, starting in the Plio-Pleistocene, cutting deeply into Plio-Pleistocene aggradation and shelfal deposits, Miocene deltaic deposits (Fig. 2; Little Sole, Cockburn and Jones formations; Bourillet et al., 2003; Stewart et al., 2014) and the Cretaceous/Paleocene chalks (Evans, 1984; Cunningham et al., 2005). The most recent phase of canyon incision into the continental slope commenced during a number of episodic sea level lowstands in Plio-Pleistocene times (Fig. 2; Bourillet etal., 2003; Evans, 1990; Evans and Hughes, 1984). Fluvial connections to the Grande Sole and the Petite Sole drainage basins were via the Celtic Sea and Fleuve Manche respectively, resulting in multiple sediment sources for the Celtic deep-sea fan (Bourillet et al., 2003). Massive deglaciation of the British and European ice-sheets (ca. 20–13 ka) resulted in a significant increase in the fluvial flux to the Grande Sole drainage basin, and hence the Whittard Canyon, with terrigenous input prolonged until 7000 years ago by glacio-hydroisostatic uplift of the British Isles (Bourillet et al., 2003; Lambeck, 1996). The linear tidal sand ridges that developed on the outer continental shelf of the Celtic Sea (Praeg et al., 2015) between 20 and 12 ka years

ago (Scourse et al., 2009) are also proposed as a sediment source to the Celtic deep-sea fan through strong tidal transport of sediments into the canyon heads (Bourillet et al., 2006; Scourse et al., 2009). However, recent current measurements and oceanographic modelling results suggest an opposite sediment transport direction (see below, and also in Cunningham et al., 2005).

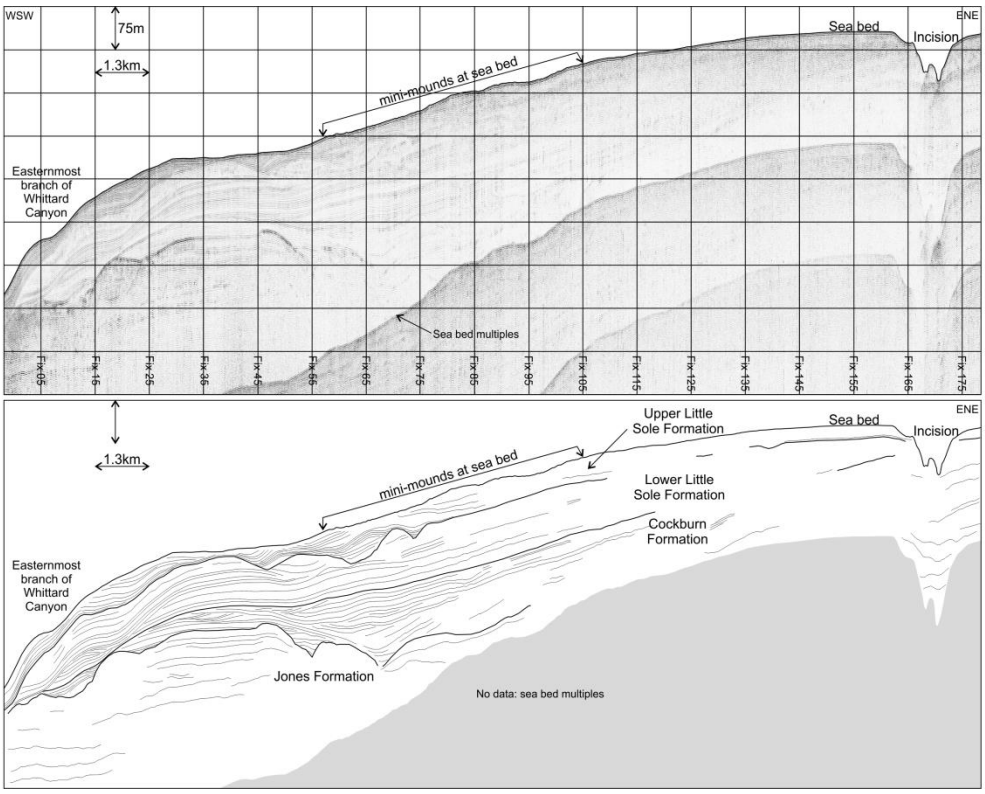

Figure 2. Sparker profile 2007/06/09 over Explorer interfluve, part of the eastern Whittard Canyon System, showing interpreted Neogene formations and the subtle sea-bed expression of the Explorer cold-water coral mini-mound province. Location of the profile is indicated in Fig. 1.

The Whittard Canyon system has four main V-shaped branches (Fig. 1), which connect with the broad shelf at approximately 200 m water depth and merge at 3500 m into the wide flat-bottomed or U-shaped Whittard Channel, that flows out to the Celtic Fan at 4500 m depth (Reid and Hamilton, 1990; Cunningham et al., 2005). The orientation of the canyon branches at the shelf edge is predominantly NNW-SSE and NNE-SSW (Cunningham et al., 2005). The canyon slope angles may increase to 40 ° within the canyon heads and flanks, or possibly steeper, featuring steep cliffs and overhangs (Huvenne et al., 2011; Robert et al., 2015; Stewart et al., 2014). Typically, the upper flanks have complicated gully networks and numerous headwall scars from slumps and slope

failures, which caused gravity driven flows that widened the canyon by retrogressive canyon wall failure. The seabed substratum is generally coarse-grained or mixed on the interfluves, whereas towards the flanks, the sediment becomes muddy, but with outcropping rocks within gullies or scars (Cunningham et al., 2005; Stewart et al., 2014). Additionally, Stewart et al. (2014) reported small mounds built of dead cold-water coral fragments on the Explorer and Dangeard interfluves (Eastern branches). In contrast to the morphologically diverse canyon walls, the canyon thalwegs are predominantly characterized by flat areas of soft sediment (Robert et al., 2015).

b) Oceanography of the Celtic Margin

The structure of the upper-water column (1500 m) along the Celtic Margin is characterised by central and intermediate water masses originating from sub-tropical latitudes. Relatively warm and saline Eastern North Atlantic Water (ENAW), a winter mode water with a source in the SW Bay of Biscay region, occupies the layer above the permanent thermocline (e.g. Perez et al., 1995; Pollard et al., 1996) with Mediterranean Outflow Water (MOW) present below the ENAW (e.g. van Aken, 2000; Van Rooij et al., 2010a). Flow characteristics are dominated by the European Slope Current (ESC) carrying ENAW (Pingree and Le Cann, 1990; Xu et al., 2015), and boundary flows associated with the MOW (Van Rooij et al., 2010a). The ESC is typically directed northwest (poleward) with mean flow speeds of 0.05–0.1 ms^{-1} (Pingree and LeCann, 1989; 1990) and varies seasonally, with a minimum in the principal driving mechanism during the summer months (Xu et al., 2015). Spring and autumn loss of slope-current continuity in the Whittard and Goban Spur region, through slope-ocean exchange and mean current reversals, has been reported and termed the SOMA (Sept-Oct-March-Apr) response (Pingree et al., 1999). Near the seabed, observed currents generally have a tidally induced downslope mean component balanced by Stoke transports (Pingree and LeCann, 1989). The possibility of cascading cold dense water from the shelf edge in winter and early spring was reported by Cooper and Vaux (1949), but has not subsequently been observed. In deeper adjacent waters, significant mesoscale variability exists within the MOW boundary flow and deeper (1600-2200 m) Labrador Sea Water layers (Bower et al., 2002).

Along the Celtic Sea shelf edge, internal waves and tides are generated at the shelf break by across-slope tidal flow (Pingree and Mardell, 1985; Holt and Thorpe, 1997). However, the direction of the propagating internal waves onto the shelf is quite random (Holt and Thorpe, 1997), in contradiction to the generally accepted view that across-shelf internal wave energy flux is controlled by the orientation of the shelf break (Garrett and Kunze, 2007). This is likely due to the highly corrugated nature (e.g. Nash et al., 2004) of the Celtic Sea shelf edge. Understanding the effect of the Whittard Canyon on the internal wave field is therefore important in understanding the internal wave dynamics within the larger Celtic Sea region. The semi-diurnal tide has been observed to drive 28–48W m^{-1} of energy on-shelf (Hopkins et al., 2014), with the positive on-shelf energy flux modulated by nonlinear interaction between the vertical velocity associated with the semi-diurnal internal tide, and the vertical shear of inertial oscillations, leading to an increase of 25–43% in the energy flux. Internal solitary waves with amplitudes reaching a maximum of 105 m have also been reported (Vlasenko et al., 2014). The internal tide generated at the shelf break has been observed as a coherent signal up to 170 km onto the Celtic Sea shelf (Inall et al., 2011). However, an estimated shoreward energy decay scale of 42 km implies that much of the energy generated at the shelf edge is dissipated at or near the shelf break.

Primary productivity along the Celtic Sea margin is reasonably high, with estimates between 100–250 g C m^{-2} yr^{-1} reported (Joint et al., 1986; Rees et al., 1999; Wollast and Chou, 2001). Near the Whittard region, Wollast and Chou (2001) report a value of 200 g C m^{-2} yr^{-1} decreasing to 140 g C m^{-2} yr^{-1} in deeper water 150 km from the shelf edge, with potentially 30 g C m^{-2} yr^{-1} exported to the open slope and deep ocean. Mixing by internal tides at the shelf edge is recognised as a significant driver of nutrient fluxes and fuelling enhanced primary productivity (e.g. Holligan et al., 1985; Sharples, 2007). Sharples et al. (2007) found a spring-neap modulation in vertical nitrate fluxes across the seasonal thermocline. Neap tide fluxes were sufficient to sustain significant new production, but a 3–6 increase in fluxes at spring tide provided excess available nitrate.

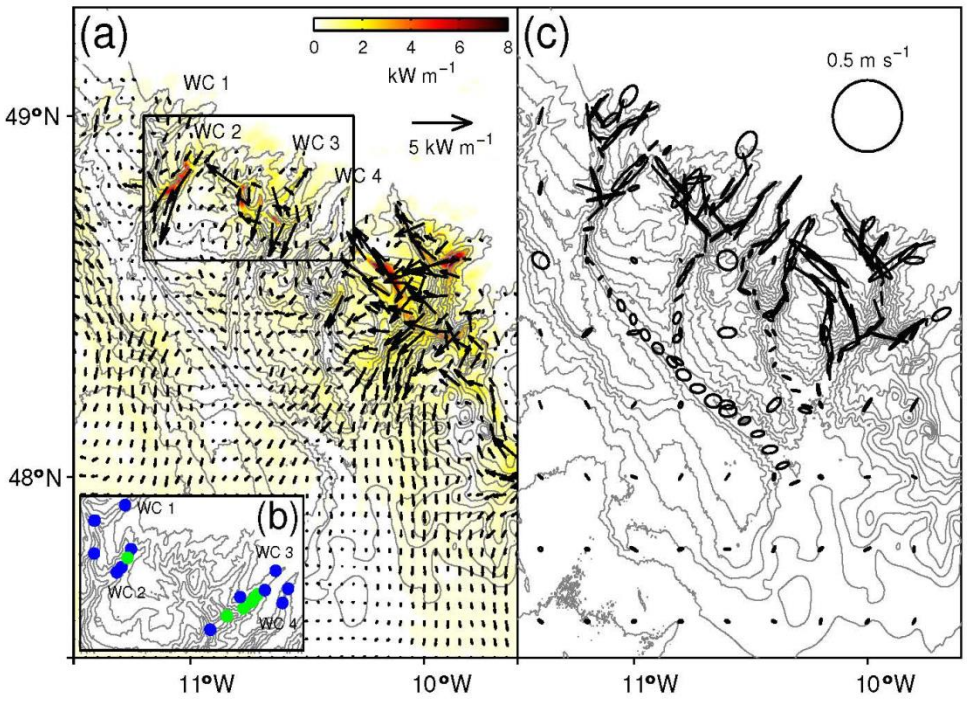

Figure 3. (a) Depth-integrated baroclinic M_2 energy flux in the Whittard Canyon region. Vectors are plotted every 10 model grid points (≈ 5 km) in each direction. The underlying colour is the energy flux magnitude. (b) Location of intermediate nepheloid layers observed along four canyon branches (WC1-4), 2011–2014. Observations from repeats years are green, single observations are blue. (c) Near-bottom M_2 tidal current ellipses from the same model as (a). Flux vectors and current ellipses shallower than 300 m are omitted for clarity. Depth contours are plotted every 300 m.

b.1) Surface tides

Tides play an important role in submarine canyons, leading to rectified barotropic flows, enhanced currents and mixing (Allen and Durrieu de Madron, 2009). Measurements of the barotropic tide close to Whittard Canyon (48 ° 34.59' N, 9 ° 30.69' W) over a spring-neap cycle show a variable depth-mean tidal current regime, 0.2 m s^{-1} during neap and 0.5 m s^{-1} during spring (Sharples et al., 2007). The semi-major axis of the depth-mean tidal flow is aligned approximately perpendicular (NE-SW) to the orientation of the isobaths at the sampling location and is confirmed by the TPXO 7.1 inverse model (Egbert, 1997; Egbert and Erofeeva, 2002). This across-slope alignment facilitates internal tide generation at the shelf edge and the upper reaches of the Whittard Canyon. In the Celtic Sea region, about 90% of the total kinetic energy of currents is contained in semi-diurnal frequencies, of which 75% can be attributed to the principal lunar semi-diurnal component

(M_2) (Pingree, 1980). This distribution of tidal energy is also applicable to the Whittard Canyon.

b.2) Internal tides

The complex sloping topography associated with submarine canyons can result in both the generation and reflection of internal waves and tides (Hickey, 1995). Scattering of barotropic (surface) tides from the sloping topography can generate baroclinic (internal) tides (Baines, 1982), whilst reflection of existing internal waves can lead to trapping and focusing of internal wave energy from outside the canyon (Gordon and Marshall, 1976; Hotchkiss and Wunsch, 1982). The type of reflection that occurs can be predicted from the topographic slope gradient (S_{topog}) and the internal wave characteristic slope gradient (S_{wave}), the latter dependant on local stratification, internal wave frequency and latitude (Thorpe, 2005). Steep canyon walls typically cause supercritical reflection (S_{topog}/S_{wave} >1) resulting in internal waves above the canyon rim being focused towards the canyon floor. Gently sloping canyon floors typically cause subcritical reflection (<1) resulting in offshore internal waves being focused toward the canyon head. During both types of reflection, the separation between adjacent internal wave characteristics narrows, focusing the wave energy into a smaller volume and hence increasing energy density. In the case of near-critical reflection (≅1), the energy is trapped against the boundary resulting in nonlinear effects such as wave breaking, internal bores and turbulent mixing (e.g. Nash et al., 2004).

Initial high-resolution simulations of the M_2 tide in Whittard Canyon using a modified version of the Princeton Ocean Model (as used by Hall and Carter, 2011 and Hall et al., 2013 for Monterey Canyon) show that the depth-integrated baroclinic energy flux within the canyon is elevated, but variable in different branches (Fig. 3a) and that there is a significant flux from certain canyon branches onto the shelf. Enhancement of near-bottom tidal currents is also seen within the canyon (Fig. 3c), with peak velocities >0.4 m s^{-1} in the upper reaches, and the current ellipses highly rectilinear along the canyon axes. In the lower reaches, current velocities are lower, around 0.1 m s^{-1}, and the current ellipses more circular. Enhanced tidal currents and breaking internal waves within the canyon drive turbulent mixing, both in the bottom boundary layer and the interior of the water column. Elevated bottom boundary

layer mixing may increase sediment and OM resuspension and along-canyon transport, potentially generate nepheloid layers, and has implications for benthic biology and ecology. Meanwhile, elevated interior mixing has the potential to enhance nutrient fluxes over the canyon, helping to fuel the enhanced primary productivity observed at the Celtic Sea margin.

3. Canyon Activity

a) Nepheloid layers

Nepheloid layers are cloudy layers of suspended particulate material largely driven by energetic hydrodynamics. They induce high turbidity compared to the surrounding clear waters contributing significantly to the shelf edge exchange of sediment (McCave, 1986; Amin and Huthnance, 1999). They serve as a physical link between productive shallow environments and the deep abyss (Puig and Palanques, 1998), transporting biogenic and lithogenic material, supporting unique benthic ecosystems and contributing to the deposition of carbon in marine sediments.

Benthic (BNL) and intermediate nepheloid layers (INL) line the branches of the Whittard Canyon (de Stigter et al., 2008a; Huvenne et al., 2011; Wilson et al., 2015a). Wilson et al. (2015a) report INLs that occur at depths where the benthic source could be attributed to enhanced seabed currents, particularly associated with near-critical internal wave reflection, or the presence of the permanent thermocline, and at depths where MOW cores impinge on the slope (e.g. Van Rooij et al., 2010a). Locations of INLs sourced at the seabed in four branches of Whittard Canyon based on observations from four consecutive surveys (2011–2014) are highlighted in Fig. 3b. Extensive BNLs cover the upper reaches of the branches down to 2500 m, likely maintained by canyon-enhanced near-bottom tidal currents (Fig. 3c). Intermittent INL observations in some of the branches of the Whittard Canyon (INLs observed in one survey only) may possibly be related to lower internal tide energy fluxes (Fig. 3 b).

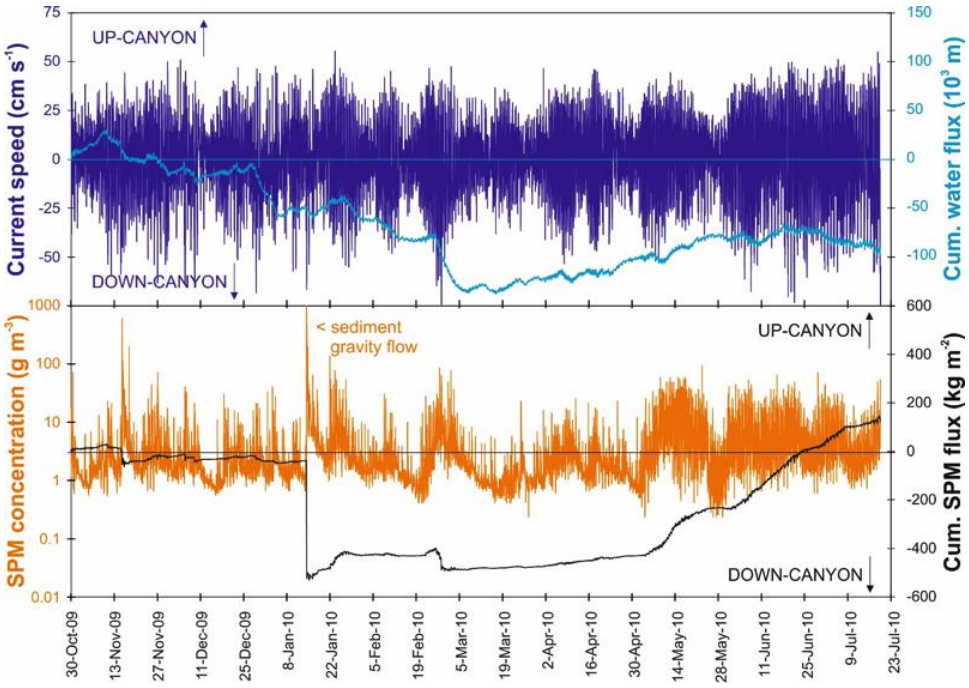

Figure 4. Near-bed, along-canyon current velocity and cumulative water flux (upper panel) and suspended particulate matter (SPM) concentration and cumulative SPM flux (lower panel), recorded by the BOBO lander at 1479 m water depth in the western branch of the Whittard Canyon, between 30 October 2009 and 23 June 2010. Note sediment gravity flow event at the 14th January 2010.

b) Current dynamics and tidally driven sediment transport

Near bottom current dynamics, in combination with temperature, salinity, turbidity and sediment flux, were recorded at various locations within the Whittard Canyon and Channel using the BOBO (BOttom BOundary; van Weering et al., 2000) and ALBEX (Duineveld et al., 2004) benthic landers. A number of deployments were carried out between 2007 and 2012 and lasted from a few days up to an entire year (Fig. 1). The lander records show that in the upper canyon reaches, extending from the shelf edge to about 2500 m depth, the near-bed current regime is indeed dominated by moderate to strong semi-diurnal tidal currents, flowing alternately in up- and down-canyon direction. Bottom water turbidity is generally observed to increase during periods of enhanced current speed, indicating that bottom sediment is resuspended and entrained by the tidal current (Fig. 4). Instantaneous horizontal particulate fluxes, calculated by multiplying suspended sediment concentrations with instantaneous current speed, reached values in the order of several grams m^{-2} s^{-1} during tidal current peaks. Net suspended sediment transport driven by tidal currents appeared to be generally in up-canyon direction, supporting the oceanographic modelling results

(Fig. 4). At greater depths in the canyon (deployments at 3566 and 3569 m) and in the adjacent deep-sea channel (4166 m), semi-diurnal tidal currents appear very weak, not exceeding 0.1–0.15 m s^{-1} and with no sign of resuspension of bottom sediment (Amaro et al., 2015). As also observed at shallower sites, net water flow at deeper sites was in an up-canyon direction, once more indicating that tidal currents do not contribute to down-canyon sediment transport (Mulder et al., 2012, Amaro et al., 2015). Low current speeds in the lower reaches of the canyon and the adjacent deep-sea fan area have previously been reported from short-term current meter deployments by Reid and Hamilton (1990).

c) Recent sediment gravity transport

Apart from the prevailing tidal currents, the BOBO landers deployed at 1479 and 4166 m recorded several events of significant down-canyon suspended sediment transport, which we interpret as representing sediment gravity flows (Fig. 4, Amaro et al., 2015). Typically, these events were marked by a sharp increase in suspended particulate matter (SPM) concentration, followed by a gradual decrease to normal values in the course of several days. Sediment trap samples encompassing these particular events recorded elevated sediment fluxes. In some cases the initial sharp increase in SPM was also accompanied by a marked increase in current speed and change to down-canyon flow. As illustrated by the 10-month BOBO record obtained at 1479 m depth in the western branch of Whittard Canyon (Fig. 4), sediment gravity flows occurring in the upper canyon reaches may be masked by the overall high concentrations of SPM and high current speeds. On several occasions the current speed at 1 m above bottom exceeded 0.7 m s^{-1}. Two high current speed events, however, recorded on 15 November 2009 and 14 January 2010, showed characteristics of a sediment gravity flow. During the most intense event in January 2010, the instantaneous near-bottom sediment flux during the peak of the event was estimated to be in excess of 3.2×10^6 kg m^{-2} y^{-1} in down-canyon direction. For comparison, the typical average rate of sediment accumulation at that depth as determined from ^{210}Pb in sediment cores is in the order of 10 kg m^{-2} y^{-1}. During the last recorded high current speed event on 19 July 2010, probably representing another sediment gravity flow, the lander was dislodged from its anchors and was later recovered drifting at the surface.

In the more quiescent lower canyon, where background suspended matter concentrations is very low, the turbidity peaks representing sediment gravity flows were obvious. In a 12-month record obtained from 4166 m depth in the Whittard Channel, two sediment gravity flow events were recorded on 22nd March and 1st July 2011, marked by sharp increases in bottom water turbidity together with a strong increase in sediment deposition (Amaro et al., 2015). Very similar high-turbidity events also accompanied by high mass sediment flux have been reported from other canyon systems considered to be active (e.g. Xu et al., 2002; de Stigter et al., 2007; Martín et al., 2011). In the Whittard Canyon, storm depressions, common over the Bay of Biscay, may be the most likely trigger for these events, comparable to processes observed in other canyons (e.g. Martín et al., 2011; Sanchez-Vidal et al., 2012).

d) Recent sediment deposition

Surface sediments from major branches of the Whittard Canyon (western and eastern middle branch) and from the Whittard Channel, as well as from adjacent slope and interfluve areas, were studied in boxcores and multicores collected between 2007 and 2011 (Fig. 1). Sediments from the upper reaches of the western and eastern central branches and from the adjacent upper slope, down to depths of about 500 m, appeared very similar, consisting of structureless silty sand composed for three quarters of lithogenic material (Fig. 5) and about one quarter of $CaCO_3$. Toward greater depths, sediments on the slope adjacent to the western canyon branch become progressively depleted in lithogenic material, whilst $CaCO_3$ content increases until constituting more than half of bulk sediment at depths below 3000 m on the lower slope. Most likely the observed trend reflects a decreasing input of lithogenic material with increasing distance from the shelf edge. In contrast to this, along the axis of the western and eastern middle canyon branches, lithogenic fine sand and silt consistently constitute the dominant sediment component down to 4000 m depth, suggesting ongoing transport of shelf-derived material down to the lower canyon reaches. On the interfluve adjacent to the eastern middle branch, lithogenic contents are also relatively high, possibly indicating sediment spillover from the adjacent canyon branches. Beyond 4000 m depth, where the lower canyon extends into the Whittard Channel, lithogenic fine sand and silt occurs as thin layers of a few mm

thick, alternating with more carbonate-rich hemipelagic ooze. This indicates that down-canyon transport occurs episodically by sediment gravity flows, punctuating prolonged intervals of hemipelagic deposition. Sediment dating with ^{210}Pb in a core from the proximal Whittard Channel showed that a number of these turbiditic layers were deposited within the last century. Thin turbidite layers were also observed in surface sediments draping the low banks to the east of the Whittard Channel, indicating spillover of turbidity currents from the main channel (Amaro et al., 2015). The fact that sediments on both sides of Whittard Channel contain distinctly more lithogenic material than lower slope sediments from west of the Whittard Canyon is another indication that spillover of turbidity currents contributes significantly to sediment deposition beyond the bounds of Whittard Channel. Apart from the afore-mentioned thin-bedded turbidites, one core from 4392 m depth in Whittard Channel contained a coarse sandy turbidite layer and debris flow deposit, in which abundant fragments of scleractinian corals were found. These corals must have been transported from the upper reaches of the canyon and slope at 250–2000 m depth, where both living and dead corals have been reported from ROV and towed video frame explorations (van Rooij et al., 2010a, Huvenne et al., 2011, Johnson et al. 2013, Davies et al., 2014).

e) Organic matter (OM)

e.1. Suspended Particulate Organic Matter (sPOM)

Huvenne et al. (2011) showed that near bottom (<10 m altitude) sPOM concentrations, measured using stand-alone pumps (SAPS – Challenger Oceanic), were 2 to 3 times higher in the upper parts of the canyon (<2000 m depth) than in the deeper and more central parts (three stations >3000 m depth). These values were comparable to those found in canyons from the Iberian Margin (Tyler et al., 2009; Kiriakoulakis et al., 2011). The observed decrease in sPOM concentrations with water depth was attributed to the less dynamic nature of deeper parts of the canyon. sPOM appeared to be fresh and phytoplankton-derived as suggested by the low molar C/N ratios (4.1–7.7). In addition, they showed that the nutritional quality of sPOM was higher in the upper canyon, as illustrated by the elevated concentrations of essential fatty acids, docosahexaenoic fatty acid (DHA) and eicosapentaenoic fatty acid (EPA). EPA and DHA are biosynthesized primarily by phytoplankton and are pivotal in aquatic ecosystem functioning, as they greatly

affect trophic transfer efficiency to higher trophic levels (Muller-Navarra et al., 2004; Kiriakoulakis et al., 2004, 2011).

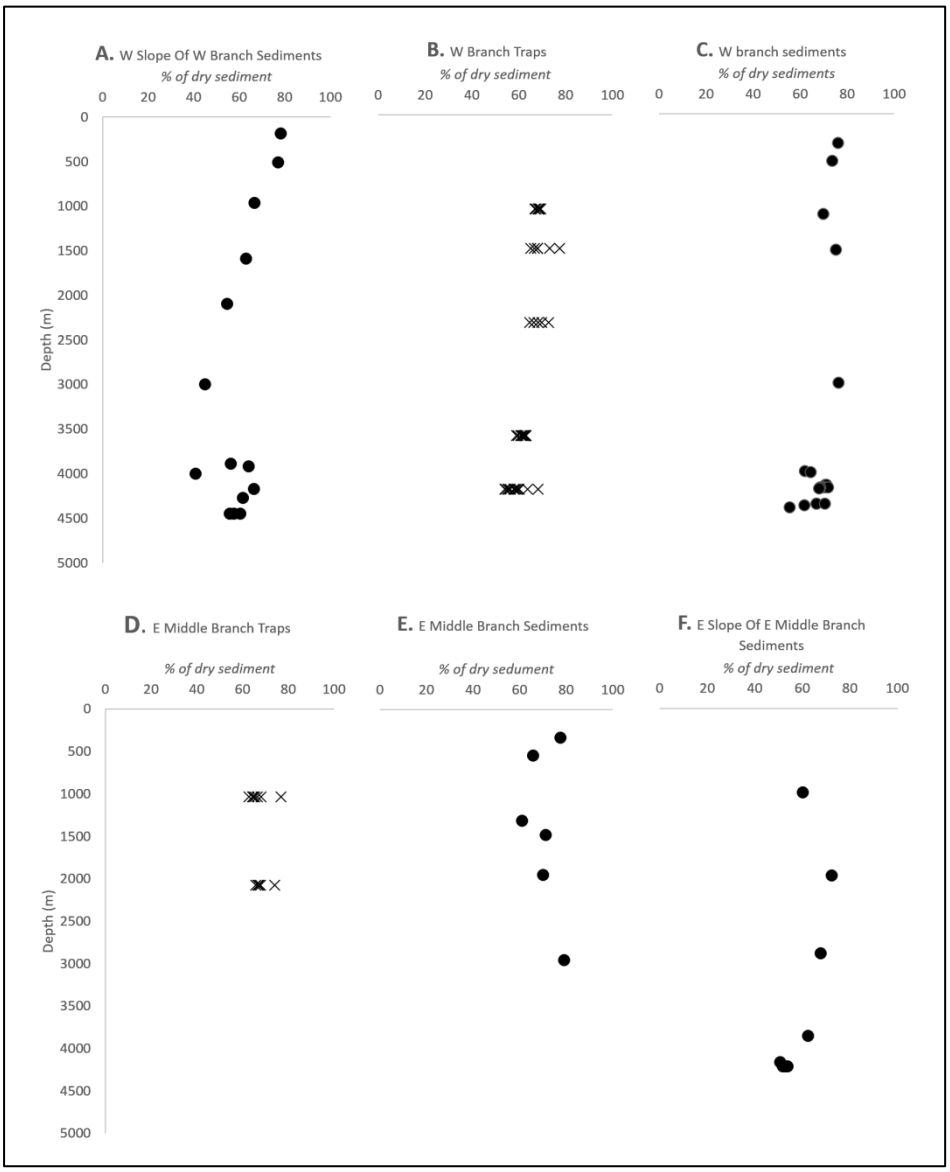

Figure 5. Lithogenic content (as % of dry sediment) of surface sediments (0–1 cm) and sediment traps (mounted on benthic landers) from the Whittard Canyon branches (for location details see Fig. 1). Details of sampling stations given in Table 1. The samples were collected during several cruises from 2007 to 2013.

Recently Wilson et al. (2015b) also investigated the sPOM in the intermediate and bottom nepheloid layers in the central upper branches of the Whittard Canyon. Data were collected in early summer 2013, mainly by filtering water from CTDs and to a lesser extent, from SAPS. Peaks in turbidity were detected with unusually high concentrations of SPM, in some cases greater than

an order of magnitude higher than maximum values typically found in NLs. sPOM from these nepheloid layers was strikingly different from that reported by Huvenne et al. (2011) both in concentration and elemental composition. The suspended particulate organic carbon (sPOC) concentrations were more than an order of magnitude higher in the Wilson study (up to 690 µg L^{-1}; *vs*. 12–23 µg L^{-1} in similar canyon depths), indicating that an episodic event had possibly taken place. The molar C/N ratios of the sPOM from these NLs were highly variable, ranging from 1 to 27. Although care needs to be exercised in comparing data from different sampling techniques (i.e. SAPS vs CTDs; see Turnewitsch et al. 2007). The results clearly show that sPOM collected during this study was highly heterogeneous, with possible contributions from clay-trapped inorganic nitrogen, bacteria and zooplankton (see references in Kiriakoulakis et al. 2011) and degraded material (C/N ratios above 10 indicate degraded OM in the absence of terrestrial inputs) in comparison to Huvenne et al. (2011). It is interpreted that these NL are possibly influenced by bottom trawling (see section 5).

A further insight on OM fluxes in the canyon system was provided by Amaro et al. (2015) based on the sediment trap record obtained from a one-year lander deployment at 4166 m depth in the Whittard Channel. Sediment traps provide a time series of particle fluxes suitable for investigating sinking material (White et al., 2015). The study by Amaro et al. (2015) concluded that the highest flux of fresh OM arriving in the Whittard Channel was due to local vertical settling and lateral transport of phytodetritus, after the spring phytoplankton bloom, rather than through gravity-driven episodic events, which provided material of low nutritional quality.

e.2. Sedimentary organic matter (SOM)

Canyons may act as ‘traps’ of organic matter (OM) as has been observed in the Nazaré Canyon off the coast of Portugal (e.g. Masson et al., 2010). The high sedimentation rates in Nazaré Canyon promote carbon burial by reducing the oxygen exposure time of the sediment (Kiriakoulakis et al., 2011). Evidence about the potential of other European canyons, such as the Whittard Canyon, to act as OM (and hence carbon) sinks can be derived from total organic carbon (TOC) contents and the elemental (i.e. C/N ratios; e.g. Meyers 1997) and molecular (e.g. Duineveld et al., 2001; Kiriakoulakis et al., 2011; Amaro et al., 2015) composition of OM in the sediment.

Duineveld et al. (2001) measured sedimentary TOC and total nitrogen (TN) content in the upper 5 cm at three stations in the middle-lower central branches of the Whittard Canyon (2735–4375 m water depth) and found that TOC (and TN) contents in the upper cm of the canyon sediments were double the values than at corresponding depths on the nearby open slope (Goban Spur). The shallowest station (2735 m) had highest overall TOC and TN content throughout the upper 5 cm, whereas at the two deeper stations levels sharply dropped below 2-3 cm. Duineveld et al. (2001) attributed this drop in TOC and TN at the deeper stations to a subsurface layer of coarse sand most likely originating from a gravity flow event. In general, coarser grains increase oxygen exposure and thus oxidation of SOM (Hedges and Keil 1995).

Extensive surveys of SOM in surface sediments (0–1 cm) along the axes of the western and eastern middle branches of Whittard Canyon showed that TOC and TN content generally increases towards the deeper part (~4000 m) of the canyon and decreases from the proximal to more distal areas of the Whittard Channel and adjacent deep-sea fan area (Fig. 6). This apparent increase of the TOC content in the deeper locations could be due to a corresponding decrease of the sediment particle size. However, no significant relationship was found between median grain size and TOC in cores from seven locations in the canyon axes of the upper middle branches, which were sectioned every cm down to 10 cm (Spearman's Test, $r = 0.450$, $p = 0.224$). Alternatively, the higher TOC contents in the lower canyon reaches and proximal part of the Whittard Channel could be explained by intermittent sediment gravity flows flushing fine-grained sediments enriched in SOM down the canyon. Less frequent occurrence of sediment gravity flows further down the Whittard Channel could then explain the decreasing OC contents towards more distal areas. However, in some locations within the Whittard Canyon (depths between 650 to 4450 m from eastern to western branches), surficial sediments are practically indistinguishable from open slope values at the same depth (0.1–0.7% TOC of dry sediment) (Huvenne et al. (2011). TOC content presented in (Fig. 6) of surface sediments and sediment traps from the Whittard Canyon branches in part supports the analyses presented by Amaro et al., (2015). This could be due to the complexity and spatial and temporal variability of the canyon processes that are as yet poorly understood.

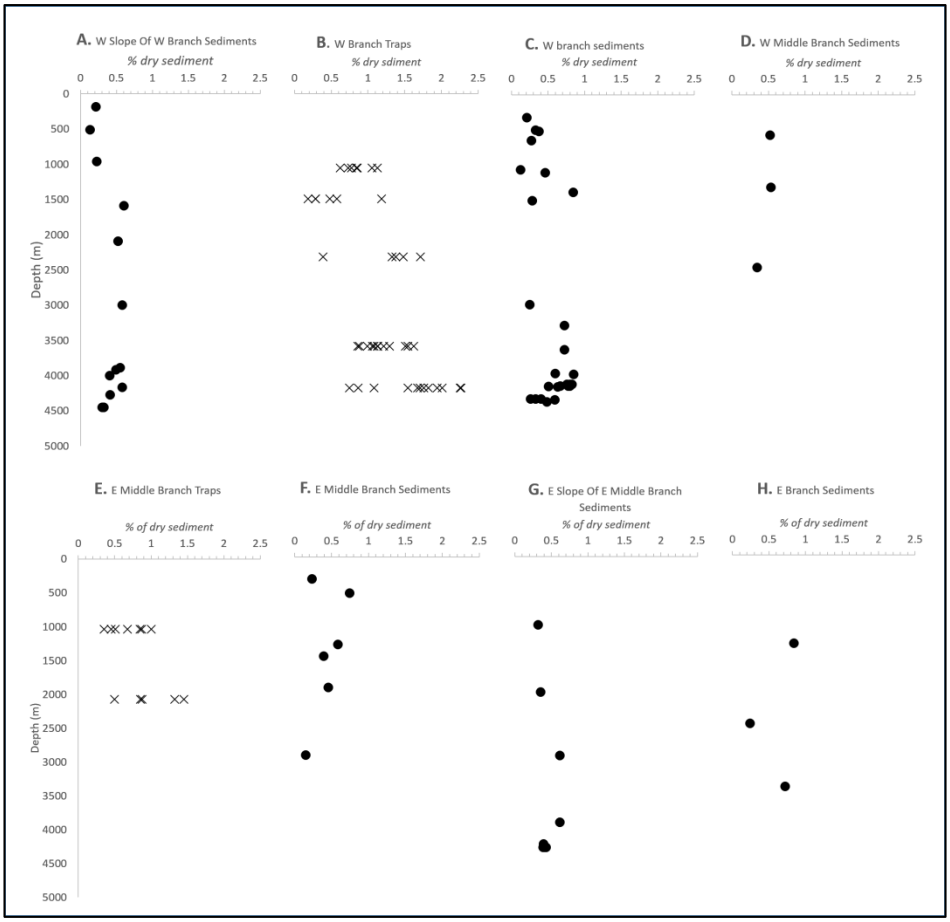

Figure 6. Total organic carbon (TOC) content (as % of dry sediment) of surface sediments (0–1 cm) and sediment traps (mounted on benthic landers) from the Whittard Canyon branches (for location details see Fig. 1). Details of sampling stations given in Table 1. The samples were collected during several cruises from 2007 to 2013.

As a crude measure of lability of SOM its molar C/N ratios from various locations in and outside the Whittard Canyon has been investigated by several authors (Duineveld et al., 2001; Huvenne et al., 2011; Ingels et al., 2011; Amaro 2015; de Stigter et al., 2008b). Molar C/N ratios of surface sediments show no consistent differences between canyon and slope sites, nor any consistent trends from the upper canyon and slope to the lower canyon and slope (Fig. 7). This, in combination with consistently low C/N ratios, suggests that the bulk of the OC preserved in surface sediments is broadly of relatively unaltered marine origin (Meyers 1997 and reference therein). The TOC contents of particulate matter collected in sediment traps close to the seabed in the western and eastern middle branches were significantly higher than in the nearby surface sediments (1.09 ± 0.51 and 0.47 ± 0.20 respectively; T-test, $p<0.05$), while molar C/N ratios were

significantly (if only slightly and still indicating marine origin) lower (8.12 ± 1.23 and 8.80 ± 1.68 respectively; T-test, $p<0.05$). It is unclear, however, whether the differences are due to modification of settling OM by benthic organisms, as suggested by Amaro et al., (2015), or by dispersal of slightly degraded OM from the shelf across the canyon and slope or a combination of both processes.

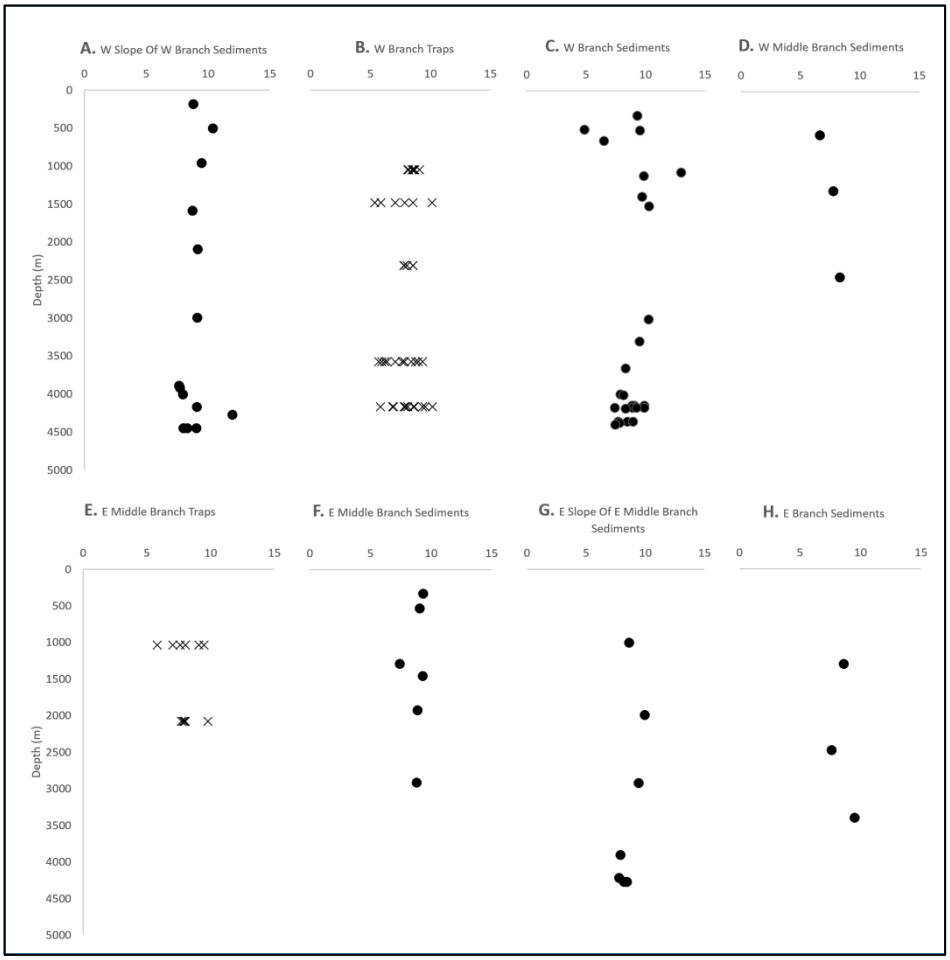

Figure 7. Mean molar (organic) Carbon to (total) Nitrogen ratio, of surface sediments (0–1 cm) and sediment traps (mounted on benthic landers) from the Whittard Canyon branches (for location details see Fig. 1). Details of sampling stations given in Table 1. The samples were collected during several cruises from 2007 to 2013.

Few studies have investigated phytopigments, nucleic and fatty acids (and hence the bioavailability of sedimentary organic matter) in the Whittard Canyon. Duineveld et al. (2001) showed that concentrations of phytopigments and nucleic acids decreased, both down slope and down core within the canyon, suggesting a lowering of OM bioavailability with canyon and core depth. In contrast to bulk

sediment and TOC distributions and concurrent with the observations described for sPOM, there is not yet any evidence for systematic down-canyon transport of labile organic material. Whilst current meter and fluorometer data recorded with a benthic lander in the upper canyon indicate resuspension and transport of phytodetritus by oscillating tidal currents (Fig. 8), the net transport of resuspended material appears to be in up- rather than in down-canyon direction. Up-canyon transport of phytodetritus, as well as proximity to shelf surface production, may well contribute to the high phytopigment concentrations reported by Duros et al. (2011) from the upper canyon. Even where intermittent gravity flows have been recorded, such as in the proximal Whittard Channel (Amaro et al., 2015), their role in transferring labile OM to lower slope regions appears very limited. More likely, the labile organic material flushed down-canyon by gravity flows, becomes strongly diluted with bulk sediment entrained by the flow, rendering it of little value for consumption by fauna in the area of deposition. Gravity flows through the canyon occasionally detected in sediment traps, resulted in accumulation of low quality degraded material.

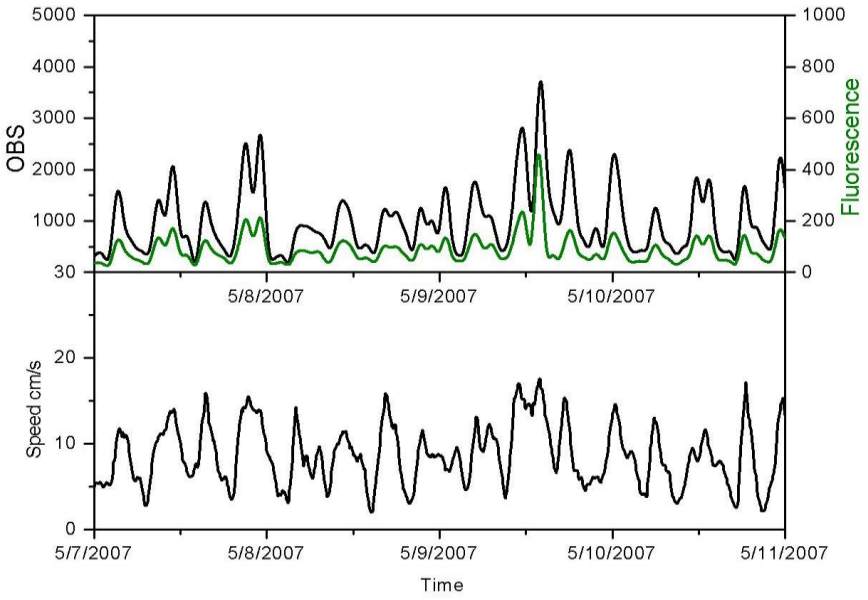

Figure 8. Fluctuations in turbidity (measured as optical backscatter – in black) and chlorophyll (measured as fluorescence – in green) near the bottom of the Whittard Canyon (A) clearly correlate with fluctuations in near-bed current speed (B), indicating that bottom sediment and phytodetritus are resuspended by tidal currents in the canyon. Data recorded with an ALBEX bottom lander at 2064 m depth in the eastern middle branch of Whittard Canyon.

4. Faunal Assemblages

a) Foraminifera

Most of the information on foraminifera in the Whittard Canyon and adjacent areas derives from the study of Duros et al. (2011), who analysed sediment samples obtained from 18 stations for benthic foraminifera (>150 µm fraction). (Fig.1, Table 1). Densities of Rose-Bengal stained foraminifera, indicating living specimens, were positively related to phytopigment concentrations and to proxies for food availability, leading to higher standing stocks in the upper parts of the canyon and on the slope than in the lower canyon (Duros et al., 2011). Many of these upper canyon stations (328–525 m, 1109 m) were characterised by a dominance of species (notably *Bolivina* spp., *Bulimina marginata*, *Cassidulina carinata*, *Trifarina angulosa* and *Uvigerina peregrina*) that are typical for organically enriched settings. The deepest site (3002 m in the western branch) was dominated (62% of fauna) by *Quinqueloculina seminula*. Agglutinated species (*Reophax* spp., *Lagenammina difflugiformis*) typical of tranquil deep-water environments are common together with *Bulimina costata* and *B. inflata*. At shallower sites (mainly <600 m) in both canyon branches, particularly the eastern branch, there was a strong concentration of stained foraminifera in the upper 0.5 cm sediment layer, reflecting the shallow oxygen penetration depth associated with a high OM input. At deeper sites, stained foraminifera followed oxygen in tending to penetrate further into the sediment. However, shallow-infaunal species, which typically occur in surficial sediment layers, were also encountered in deeper core layers, for example, at 515 m in the western branch and 328 m in the eastern middle branch. This is probably a result of bioturbation by macro- and mega-fauna.

Foraminiferal densities decreased with water depth on the slope adjacent to the eastern and western branches. Assemblage composition changed accordingly and was largely different from that observed in the canyon, particularly at shallower depths. *Uvigerina mediterranea* (considered to be an opportunistic species that responds to phytodetritus pulses) was dominant (48%) at 498 m depth on the western slope, *U. mediterranea*, *U. peregrina* and *Melonis barleeanum* were abundant around 1000 m on both slopes, *U. peregrina* was joined by *Hoeglundina elegans*, *Cibicidoides kullenbergi*, *Gavelinopsis translucens*

and *Gyroidina orbicularis* at 1500–2000 m, while the deepest slope sites (2950–3000 m) were characterised by species of *Reophax*, *Lagenammina* and *Ammobaculites agglutinans*. This sequence reflects increasingly food-depleted conditions with increasing water depth, as is typical on continental margins. The distribution of stained specimens within the sediment profile is more consistent with depth on the slope than in the canyon. However, as expected, sediment penetration still tended to be deeper at the deeper sites. Comparison between stained and dead assemblages reveals evidence for the transport of dead foraminiferal tests within the canyon (Duros et al., 2012). Species that are confined to the stained assemblage in the upper canyon are found as dead tests at deeper sites. In addition, the dead tests of species (*Ammonia beccarii* and *Haynesina germanica*) that are restricted to coastal settings occur at shallow (328 and 535 m) sites in the eastern canyon branch. These have probably been carried into the upper canyon by bottom currents, gravity flows or transported on floating algae. Differences between stained and dead assemblages in the area of the Whittard Canyon can also reflect seasonal population fluctuations. Thus, *Epistominella exigua*, an opportunistic species that responds with rapid population growth to inputs of phytodetritus (Gooday, 1988), represents 13% of the dead fauna, but only 2% of the living fauna collected at 2995 m on the western slope in June 2007 (Duros et al., 2012). Many of these dead tests are presumed to have been generated during a reproductive burst earlier in the year.

An earlier study by Weston (1985) provided species-level information on benthic foraminifera from the Whittard Canyon in a study that also encompassed the nearby Shamrock Canyon and Meriadzek Terrrace and the more tranquil environment of the Porcupine Seabight. Weston (1985) studied Rose Bengal-stained and dead assemblages (>125-µm fraction) in grab and anchor dredge samples collected at depths between 255 m and around 2000 m depth in the canyon. Standing stocks of stained tests were considerably higher in the Whittard Canyon than at comparable depths in the Porcupine Seabight and there were substantial differences in both the stained and dead faunas from the two areas. For example, certain species, notably *Cassidulina carinata* but also *Trifarina angulosa*, *T. bradyi*, *Brizalina spathulata* and *B. subaenariensis*, were considerably more abundant in the stained assemblage, and occurred at greater depths, in the Whittard Canyon than in the Porcupine Seabight. As a result, the latter area

displayed a much clearer zonation of species with depth than the canyon. Many of the species reported by Weston from the Whittard Canyon are the same as those in Duros et al. (2011, 2012). However, she also records attached species (*Cibicides lobatulus*, *C. refulgens*, *Planulina ariminensis*, *Paromalina crassa*), not reported by Duros et al. (2011, 2012), living on various hard substrates (e.g. pebbles, ascidians, agglutinated foraminiferan tubes, sponge spicules) between 700 and 1400 m depth.

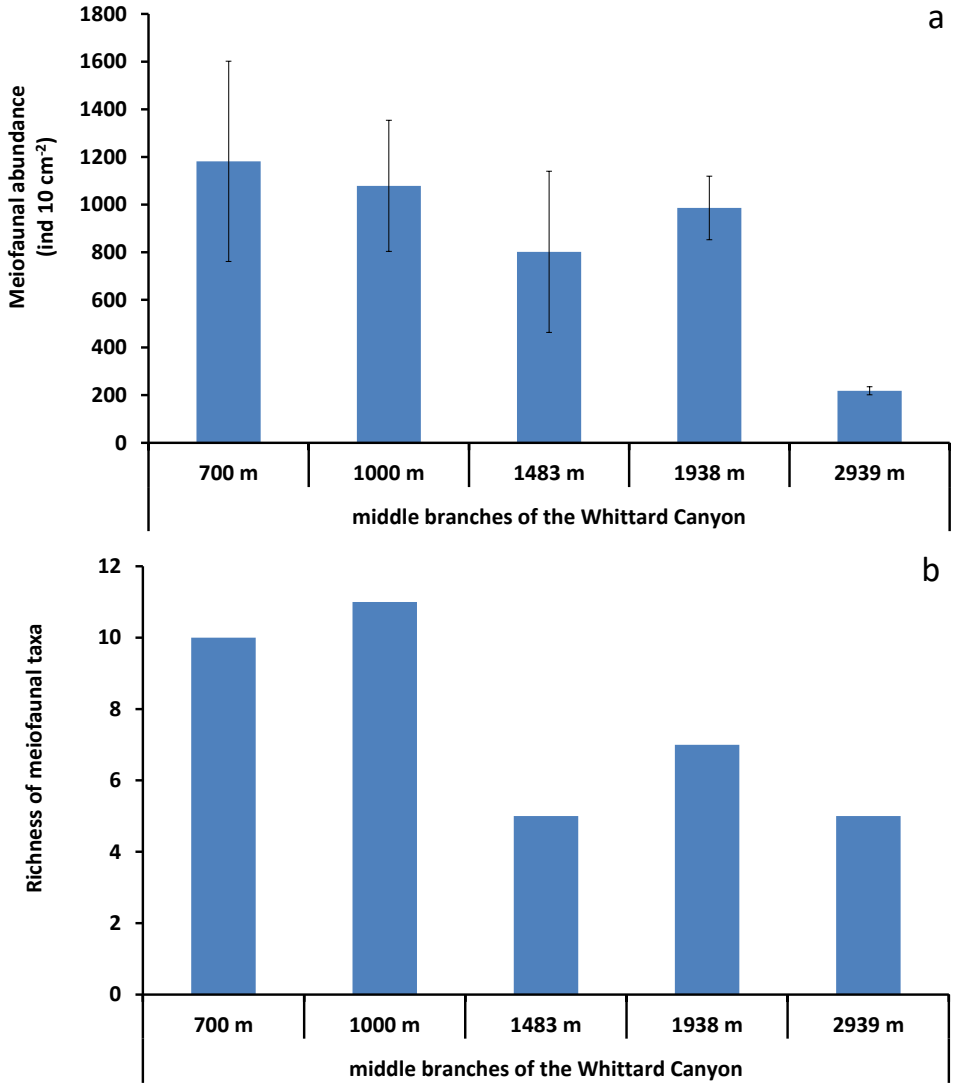

Figure 9. Meiofaunal abundance (a) and diversity as number of taxa (b) along a bathymetric transect in the middle branches of the Whittard Canyon. Data at 700 and 1000 m are published in Ingels et al. (2011) while data from 1483 to 2939 m are summarized from Gambi and Danovaro (2016).

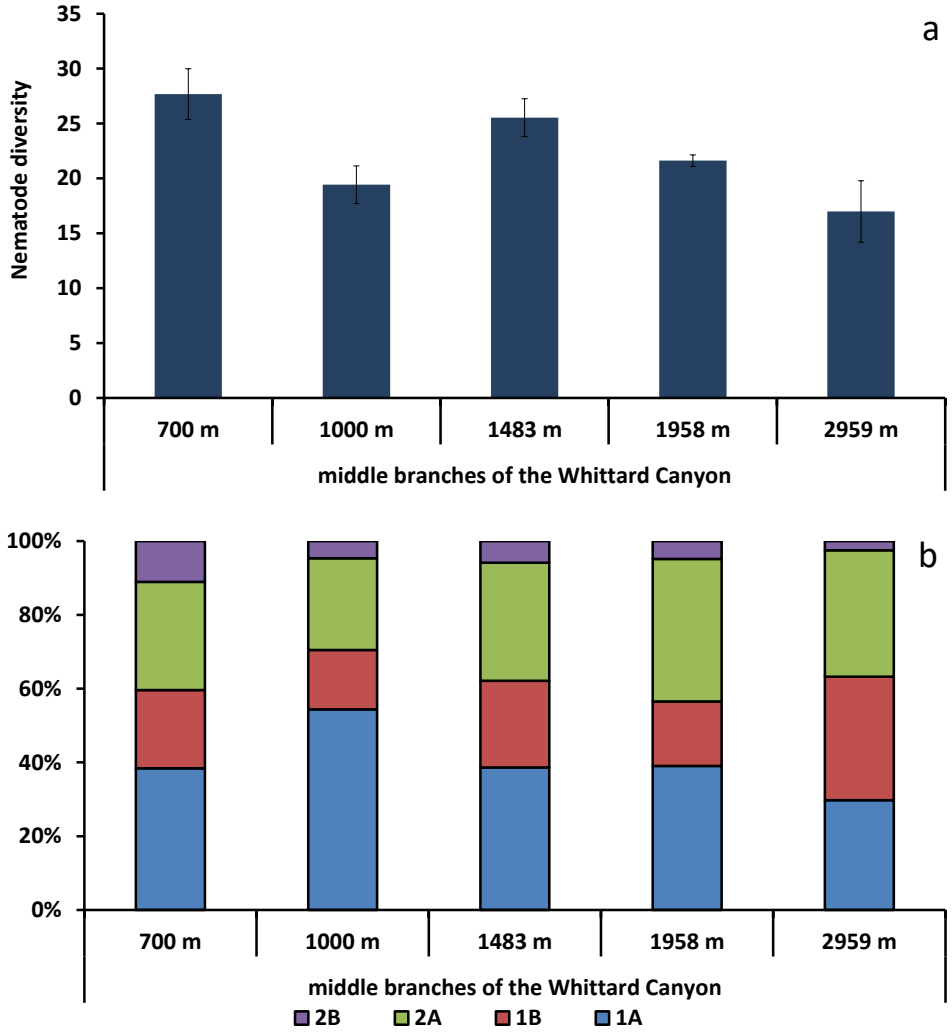

Figure 10. Nematode diversity as expected genera number EG(51) (a) and trophic structure (b) along a bathymetric transect in the middle branches of the Whittard Canyon. Reported are: 1A (selective deposit feeders); 1B (non-selective deposit feeders); 2A (epigrowth feeders) and 2B (predators/omnivores). Data at 700 and 1000 m are published in Ingels et al. (2011) while data from 1483 to 2939 m are summarized from Gambi and Danovaro (2016).

b) Meiofauna

Ingels et al. (2011a) reported meiofaunal abundance and biodiversity (as nematode genera) at two stations (ca. 700 and 1000 m depth), within the western middle branch of the Whittard Canyon. Data collected by Gambi and Danovaro (2016) between 1000 and 3000 m in the eastern middle branch have allowed to identify meiofaunal patterns along a wider bathymetric range in the middle branches of the Whittard canyon. Meiofaunal abundance does not change between 700 and 2000 m depth (PERMANOVA pair-wise tests, between 700m and 3000m and between 1483m and 3000m $p<0.05$; between 1000m and 3000m and

between 2000m and 3000m $p<0.01$; Fig. 9a). Meiofaunal abundances in the upper and middle part of the Whittard Canyon are generally higher than those reported from the open slopes of the Atlantic Ocean (Celtic and Portuguese margins) and of the Mediterranean Sea (Catalan and South Adriatic margins) (Bianchelli et al., 2010; Ingels et al., 2009, 2011a, b, c, 2013a; Romano et al., 2013) at similar depths. Meiofaunal abundances at 3000 m depth in the Whittard Canyon are lower than values reported at comparable depths in Nazaré and Cascais Canyons along the Portuguese margin (Ingels et al. 2009, 2011b, c). Meiofaunal diversity (at the level of higher taxa) did not display a clear spatial pattern with increasing water depth (Fig. 9b). This lack of bathymetric pattern has been observed in several canyons, independent of geographical region or canyon-scale environmental conditions (Bianchelli et al., 2010; Ingels et al., 2013a; Romano et al., 2013; Leduc et al., 2014; Pusceddu et al., 2013) and is likely reminiscent of canyon heterogeneity and associated environmental variability exerting influence on benthic assemblages. More important are small-scale environmental conditions that act on the scale of meiofauna and nematodes, such as those associated with sediment grain size and sediment depth, or the amount and availability of food (Ingels et al., 2013b, Leduc et al., 2012, 2014b). Ingels et al. (2011) supported the former observation by showing that small-scale (vertical) heterogeneity in SOM quality (expressed mainly as relative contributions of phytopigments) within the same core could explain much of the variation of the meiofaunal communities of the canyon. In the middle branches of the Whittard Canyon fourteen meiofaunal taxa have been identified: Nematoda, Copepoda (including their nauplii), Polychaeta, Kinorhyncha, Bivalvia, Ostracoda, Turbellaria, Oligochaeta, Tardigrada, Gastrotricha, Isopoda, Tanaidacea, Acarina and Aplacophora. Meiofaunal community structure displays a typical composition of deep-sea assemblages with few dominant taxa: nematodes dominate (92–96%) all stations, followed by copepods (3–7%), kinorhynchs (0–3%) and polychaetes (0-1%). All other taxa can be considered as rare (*sensu* Bianchelli et al., 2010), since their contribution to the overall community composition is <1%, and their number displays a clear decreasing pattern at depth >1000 m. Contrary to the spatial pattern observed for meiofaunal diversity in general, nematode diversity (as expected richness of genera for 51 individuals) decreases between 700 m and 1000m (PERMANOVA pair-wise tests, $p<0.05$), among 700 m and all other

sampling depths, expect for 1483 m, and progressively between 1483 m and 2939m, except for between 1939 m and 2939 m (PERMANOVA pair-wise tests, $p<0.05$; Fig. 10a). No differences in nematode diversity at species level (both as species richness and expected species number for 51 individuals) are observed between 1483 m and 2939 m in the middle eastern branch of the Whittard Canyon (Gambi and Danovaro, 2016). The present analysis of nematode assemblages in the middle branches of the Whittard Canyon reveals the presence of 119 nematode genera among a total of ca. 1400 individuals investigated from ca. 100 individuals from each of three replicate samples of each station. Ingels et al. (2011) reported the dominance of the genera *Leptolaimus* and *Molgolaimus* at 700 m-depth and *Astomonema* at 1000 m depth, respectively while in the deepest stations the dominant genera are: *Halalaimus* (16%), *Acantholaimus* (8%) and *Daptonema* (6%). Differences in genus dominance between the investigation by Gambi and Danovaro (2016), and Ingels et al. (2011a) are mostly caused by differences in bathymetric ranges considered in the two studies. These results are consistent with the patterns observed along other canyon systems and open slopes in which, the turnover of nematode genera (and species) is generally very high among sampling sites at greater water depths (Danovaro et al., 2009, 2014, Ingels et al., 2011, Gambi and Danovaro, 2016). Different drivers can be invoked to explain these patterns. Ingels et al (2011), indeed, revealed that the high variability of nematode genera composition was mainly explained by grain size and food availability (both quality and quantity) inside the canyon system. The analysis of nematode trophic structure at genus level does not display clear patterns along the bathymetric gradient in the middle branches of the Whittard Canyon (Fig.10b). Deposit feeders are always the dominant trophic guild, as observed for deep-sea sediments worldwide (Soetaert and Heip, 1995; Gambi et al., 2003; Vanhove et al., 2004; Danovaro et al., 2008; Vanreusel et al., 2010; Gambi et al., 2014). However, epistrate feeders contribute substantially to trophic composition at all stations and this could be related to the amount of “fresh” material in the canyon system deriving from the highly productive surface waters of the Celtic margin (Joint et al., 2001, Duros et al., 2011 and this manuscript). The relative contribution of predators is low and decreases progressively with increasing water depth. Predators represent a limited portion of the overall nematode trophic structure in the Whittard Canyon in comparison to their

relevant contribution observed in the adjacent open slopes (Gambi and Danovaro, 2016) and in the oligotrophic sediments of the deep Mediterranean Sea (Danovaro et al., 2008, Gambi et al., 2014). Interesting to note is also the relatively high numbers of chemosynthetic *Astomonema* nematodes, particularly at 1000 m water depth, suggesting reduced sedimentary conditions akin to seep environments. These conditions may be caused by very high sedimentation rates and consequent enhanced respiration and organic carbon burial conditions, which allow these nematodes to thrive (Ingels et al., 2011a, Tchesunov et al., 2012). Such sedimentary conditions may be caused by sedimentary overflow on the interfluves of the canyon head.

c) Macrofauna

Duineveld et al. (2001) published the first study of macrofauna from the Whittard Canyon. Samples obtained at 2735 and 3760 m water depth yielded similar densities (2717 ind m^{-2} and 1339 ind m^{-2}) to those found on the nearby Goban Spur, c. 150 km northeast of the canyon (3039 ind m^{-2} at 2200 m and 2420 ind m^{-2} at 3600 m). The same was true for the sample taken on the canyon fan at 4375 m depth (canyon fan 696 ind m^{-2}; Goban Spur 807 ind m^{-2} at 4500 m) (Duineveld et al. 2001, Fig. 11). On the other hand, biomass values were elevated inside the canyon (4739, 1877 and 1592 mg m^{-2} wet weight at 2735, 3760 and 4375 water depth, respectively) compared with the Goban Spur (3039, 1256, 886 mg m^{-2} wet weight at 2200, 3600 and 4500 m water depth, respectively). This increase was consistent with higher levels of OM and pigments found in the surface sediments of the canyon compared with the slope.

In a recent study, Gunton et al. (2015b) compared macrofauna assemblages at 3500 m water depth in three different branches of the Whittard Canyon (Fig. 1) and the adjacent slope to the west of the canyon. The canyon had a higher macrofaunal density than the slope (canyon average 4536 ± SD 1676 ind m^{-2}; slope 2744 ± SD 260 ind m^{-2}). Density varied throughout the branches of the canyon, increasing across the sites from west to east (western branch 2900 ± 538 ind m^{-2}; eastern middle branch 4461 ± SD 856 ind m^{-2}; eastern branch 6249 ± SD 1363 ind m^{-2}). This is consistent with the data of Hunter et al. (2013) who sampled macrofauna at a similar water depth (3500 m) in the canyon. They recorded higher macrofaunal densities in the eastern branch (5352 ± SD 2583 ind m^{-2})

compared with the western branch (3416 ± SD 2069 ind m^{-2}) (Fig. 11). As seen in section 3, disturbance regimes and the quantity and quality of OM vary throughout the canyon branches and this may have led to the different faunal densities reported in both studies. However, as the stations analysed for the quantity and quality of OM (section 3) are different from those where macrofauna were sampled, we can only make assumptions and a more coordinated sampling programme should be carried out in the future, so that observations from all disciplines can be better integrated.

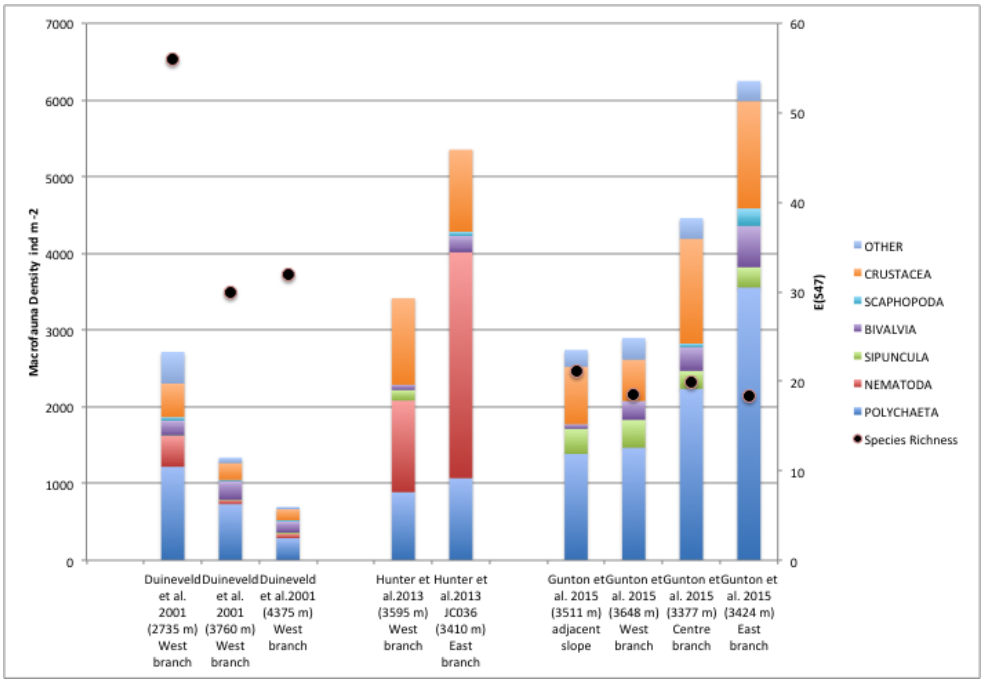

Figure 11. Macrofauna abundance in Whittard Canyon (ind m^{-2}).

Gunton et al. (2015b) also found that the Whittard Canyon macrofauna exhibited considerable variability at the higher taxon level. Polychaeta was the dominant taxon at 3500 m and represented >50% of the assemblage in the three main canyon branches. However, the ranking of the second and third most abundant taxa varied between branches and were respectively Sipunculida (12.5%) and Bivalvia (8.4%) in the western branch; Isopoda (16.2%) and Tanaidacea (7.3%) in the eastern middle branch; Isopoda (10.7%) and Bivalvia (8.6%) in the eastern branch. Hunter et al. (2013) also noted a difference in macrofaunal composition between canyon branches at 3500 m. In the eastern branch macrofaunal-sized nematodes (>50%) and polychaetes (cirratulids and spionids) contributed most to the assemblage, whereas in the western branch

crustaceans (tanaids and harpacticoid copepods) and polychaetes dominated. The differences between the two studies may reflect the sampling gear and sampling processing techniques used. Gunton et al. (2015b) used a megacorer and a 300 µm sieve, whereas Hunter et al. (2013) used ROV push cores and a 250 µm sieve. A megacorer will collect a larger sediment sample, while a larger sieve would retain fewer animals. Furthermore, Hunter et al. (2013) included nematodes in their macrofaunal analysis, but Gunton et al. (2015b) only included macrofauna *sensu stricto*. Polychaete family assemblage composition also varied throughout the canyon. Hunter et al. (2013) reported that the western branch had a high proportion of Amphinomidae, whereas Cirratulidae and Spionidae contributed most to the assemblage in the eastern branch. Gunton et al. (2015b) reported high numbers of Amphinomidae (all *Paramphinome jeffreysii*) in the western, central and eastern branches. The abundance of *P. jeffreysii* increased across sites from the western (21.2%) to the eastern branch (39.6%) (Gunton et al., 2015a). *Aurospio* sp. was ranked second in the western and eastern middle branches whereas juvenile Opheliidae were ranked second in the eastern branch. This within-canyon faunal heterogeneity is probably explained by a combination of variable organic enrichment and hydrodynamic activity, both of which can be influenced by the topographic profile of individual canyon branches (Gunton et al. 2015b and section 3 of this paper).

Although the macrofauna at all three stations in the study by Duineveld et al. (2001) were numerically dominated by deposit-feeders, the proportion of filter-feeders (mainly sabellid polychaetes) was highest at the deeper canyon station (3760 m). This was unexpected since more quiescent conditions, favouring deposit feeders rather than filter feeders, would normally be expected at greater depths. At slightly shallower depths (3500 m), polychaete feeding groups displayed a shift across the canyon, with a higher abundance of omnivores and macrophagous feeders reported in the eastern branch compared with more microphagous feeders in the western branch (L. Gunton unpublished observations). Macrofaunal-sized nematodes displayed a similar trend, the eastern branch was characterised by high numbers of predators and scavengers (e.g. *Paramesacanthion*) and the western branch by epigrowth feeders. Again, this shift in feeding groups may be linked to the different environmental characteristics of individual branches, as mentioned above.

Local macrofaunal diversity appears to be depressed inside the Whittard Canyon compared with the adjacent slope (Gunton et al., 2015a). Rarefied polychaete richness was similar in the western ($E[S_{47}]$ = 18.5), eastern middle ($E[S_{47}]$= 19.9) and eastern ($E[S_{47}]$ = 18.4) branches, but higher at the slope site to the west of the canyon ($E[S_{47}]$ = 21.2). The Simpson (1-λ') and Shannon (H' (log_2)) indexes were likewise highest at the slope site (1-λ' = 0.918, H' (log_2) = 4.104), intermediate in the western and eastern middle branches (1-λ' = 0.880 and 0.856, H' (log_2) = 3.706 and 3.891, respectively) and lowest in the eastern branch (1-λ' = 0.814, H' (log_2) = 3.656). Dominance was also higher inside the canyon (Rank 1 dominance canyon average 33.1, slope 18.7). Depressed diversity and increased dominance may be caused by high numbers of opportunistic species. As mentioned above, *P. jeffreysii* and juvenile Opheliidae were particularly abundant in the eastern branch of the canyon, perhaps as a result of an opportunistic response to a possible recent input of OM. Forty-six polychaete species that were not present on the open slope, were found in the Whittard Canyon, suggesting that the canyon may enhance diversity at a regional scale (Gunton et al., 2015a). However, the sampling effort on the adjacent slope was not sufficient to confirm that the canyon acts to increase regional diversity.

d) Megafauna

Megafaunal abundances have been found to be higher in the eastern as opposed to the western branch of the Whittard Canyon, but species richness appears to be similar (Ismail, 2016). Only one Agassiz trawl sample is available from the Whittard Canyon. A single trawl at a similar depth (3700 m) on the Goban Spur in 1995, repeated in 1996, revealed only minor differences in overall megafauna density, biomass and indeed the distribution of feeding guilds on the open slope as compared to the Whittard Canyon (Duineveld et al., 2001). By combining visual (ROV) observations on megafauna with habitat characteristics in General Additive Models (GAMs), higher megafauna abundance in the Whittard Canyon was found at shallower depths (<1000m), with small peaks at ~2200 and 3000m, while a peak in species richness occurred at ~1200 m (Robert et al. 2015). Some of these peaks may be associated with the interface of water masses present within the region (van Aken, 2000a, b; section 2 of this paper). At a finer scale, increased abundance, species richness and diversity were associated with

steep slopes and topographic highs, and decreased towards the thalweg (5). Video analysis of 17 transects (500-4000 m in depth) identified ~210 morphospecies (5), of which 31 putative species were corals (based on 13 transects). The most commonly observed species in the outer branches of the Whittard Canyon were xenophyophores (probably *Syringammina fragilissima*), *Pentametrocrinus* sp., *Acanella* sp., *Lophelia pertusa*, cerianthids and *Anthomastus* sp. (Robert et al. 2015). Examination of beta diversity indicated a high species turnover with transects showing species similarities below 40% (Robert et al. 2015), but many of these species have also been reported from other nearby banks, canyons and continental slopes, and are likely not to represent distinct communities (Tyler and Zibrowius 1992, Roberts et al. 2008, Howell 2010, Narayanaswamy et al. 2013, Davies et al. 2015). In terms of cold-water corals (CWC), the most abundant coral species found in a series of dive transects covering depths from 520–4703 m were *Acanella* sp., *Anthomasthus* sp. and *L. pertusa* (Morris et al., 2013). Although Morris et al. (2013) did not have a stratified random sampling scheme, the transects studied did cover a wide range of depths throughout the canyon and the coral distribution appeared to be driven by substratum type. The highest density of corals has been found along an overhanging vertical wall (1600 m long x 120 m high) at 1350 m water depth, mapped by Huvenne et al. (2011), where faunal coverage, mostly *L. pertusa*, was estimated at ~70%. Despite corals on vertical walls representing the habitat with the highest abundance and species richness, octocoral richness tended to be low (Morris et al. 2013, Robert et al. 2015). Species commonly found in this habitat included; the bivalve *Acesta excavata*, unidentified feather stars and an anemone species, possibly *Actinauge* sp. The frequently observed crinoids found in association with *L. pertusa*, (Robert et al., 2015) may represent a variant of the described '*L. pertusa* and crinoids on bedrock' biotope as listed by Davies et al. (2014). At depths between 633–762 m, *A. excavata* was found to be highly abundant and form a different vertical-wall assemblage with the deep-sea oyster *Neopycnodonte zibrowii* (Johnson et al. 2013). Other commonly observed species found within this assemblage included the cup coral *Desmophyllum dianthus*, unidentified feather stars and unidentified pink cerianthids. Another smaller wall has been found in the western branch at ~1650 m, colonised by *Primnoa* sp. and possibly *Solenosmilia variabilis* (Huvenne et al., 2011). At the foot of these walls, high concentrations of SPM and the

presence of bottom nepheloid layers have been recorded (Huvenne et al., 2011, Johnson et al., 2013). The potential increased mixing following the occurrence of down-canyon sediment gravity flows or the presence of internal waves (Wilson et al., 2015a) may explain why *Lophelia* within Whittard Canyon tend to occur outside the sigma-theta density envelope of 27.35–27.65kg m^{-3} proposed by Dullo et al. (2008) and Flögel et al. (2014) for optimal *Lophelia* growth (Whittard Canyon coral wall: ~27.80 kg m^{-3}; Huvenne et al. 2011). Moreover and as mentioned in section 3, Huvenne et al. (2011) showed appreciable concentrations of essential fatty acids (EPA and DHA) in the surficial sediments from several areas of the upper and middle parts of the canyon, which can explain the presence of CWCs in the same areas. Protection against excessive sedimentation and increased food availability were suggested as potential drivers for the colonisation of vertical cliffs; cliff habitats may act as refuges from fishing activities, play a role in providing nursery habitats and protection against predation, and add complexity beneficial for other filter feeders (Huvenne et al. 2011, Johnson et al. 2013).

In the deepest part of the canyon (4166–4349 m) and in the Whittard Channel (4321–4448m), dense aggregations of elpidiid holothurians have been observed (Duineveld et al., 2001; Amaro et al., 2015). Since members of the *Amperima*/*Peniagone* species complex are among those deep-sea organisms that select the freshest type of phytodetritus (FitzGeorge-Balfour et al. 2010), their presence is most likely associated with favourable quantities of trophic resources (Amaro et al., 2010; Billett et al., 2010; Jamieson et al. 2011) and their high densities in areas like the Whittard Channel confirm the presence of highly valuable food for the rest of the deep-sea benthos. As discussed above, this fresh OM is most probably derived from vertical settling, transported by bottom currents from adjacent lower slope areas and trapped in the topographic depressions incised by the canyon and channel rather than being flushed down-canyon by gravity flows, which appear to dilute the organic matter with bulk sediment.

The Dangeard and Explorer canyons (SW Approaches) are shallower canyons which feed into the Whittard Canyon (Fig. 1; Stewart et al., 2014). Davies et al. (2014) identified and mapped 12 megabenthic assemblages (biotopes) from imagery data (acquired between 184–1059 m), which revealed that these canyons are dominated by soft sediment assemblages. Although no similar biotope

analysis is available for the Whittard Canyon, dense sea pen aggregations (particularly *Kophobelemnon*) and *Lophelia* and/or *Madrepora* cold-water coral reef structures have also been observed between 400 and 1050 m water depth in the eastern middle branch (van Rooij et al., 2010a; ICES WGDEC 2012; Robert et al., 2014, Ingels et al., unpublished data). *Kophobelemnon stelliferum* has been recorded from the neighbouring Porcupine Seabight and so is not restricted to the canyons (Rice et al., 1992).

Many of the coral species observed in the Whittard Canyon have been also observed in the Dangeard and Explorer canyons including *Acanella* sp., *Anthomasthus* sp. and *L. pertusa*. Although CWC reef structures have been observed in the main branches of the Whittard Canyon, only one highly sedimented '*L. pertusa* reef' (795–940 m) has been observed on a steep flute feature on the floor of Explorer Canyon.

Interestingly areas of cold-water coral mini-mounds (up to 3 m high and 50–150 m in diameter) were found on the interfluves of Dangeard and Explorer canyons (250–410 m); but such features have not been recorded from the Whittard Canyon itself. Mini-mound provinces have also been recorded from the Guilvinec Canyon (2008, Armorican margin, De Mol et al., 2011) and between the Ferrol and A Coruña Canyon (van Rooij et al., 2009, Cantabrian margin, unpublished data) and so may be related to presence of the canyon, however mini-mounds have also been documented from the Porcupine Seabight upper slope (2003, Irish margin, Wilson et al., 2006).

5. Anthropogenic influences

Recorded litter densities in Whittard Canyon are lower than in other nearby canyons of the same continental margin. Derelict fishing gear represents ~28% of the observed litter suggesting anthropogenic impacts in this canyon system might be substantial, although in nearby Dangeard and Explorer Canyons this figure reached 72%. Approximately 42% of the litter was plastic, which will degrade slowly (Pham et al. 2014).

For nearly a decade, the influence of anthropogenic activity (i.e. bottom trawling) on sediment transport has been highlighted in numerous studies in Mediterranean canyon systems (e.g. Martín et al., 2008; Puig et al., 2012; Martín et al., 2014). Recently, evidence has been presented suggesting that trawling

similarly may influence SPM concentrations at the Whittard Canyon (Wilson et al., 2015b). ROV video survey footage (van Rooij et al., 2010c; Robert et al., 2015) has shown areas in the upper canyon (448–1119 m) that are draped by fine, loose sediment. This could suggest high rates of sedimentation and potentially overflow from sediment gravity events or tidal-driven sediment suspension, but could also be indicative of anthropogenic activity (i.e. bottom trawling). During a survey in 2013, concentrations of SPM in enhanced nepheloid layers (ENLs) were significantly higher (typical an order of magnitude) than the mean maximum in nepheloid layers normally observed in the Whittard Canyon (Wilson et al., 2015a). Wilson et al. (2015b) showed that vessel monitoring system (VMS) data indicated high spatial and temporal activity of trawling vessels coinciding with the occurrence of ENLs. Although only one study, the data would suggest that bottom trawling on the smooth adjacent spurs is triggering sediment gravity flows at the steeper rims of the canyon. The increased resuspended sediment induced by such activity maybe the cause of the episodic events detected by Amaro et al. (2015) and may explain the higher C/N ratios of sPOM suggestive of degradation detected during the Wilson study in comparison to Huvenne et al., (2011). Episodic trawl-induced resuspension events could potentially have detrimental effects on local ecosystems, introducing high inorganic particle loading, which smothers filter feeders and provides nutritional unsuitable material (Puig et al., 2012).

6. Conclusion and future directions

The following main conclusions emerge from the research results reviewed here.

1) The Whittard Canyon is currently still active in terms of sediment transport, although less so than during the last deglaciation. Intermediate and bottom nepheloid layers can be found throughout the (upper) canyon reaches, and benthic landers have recorded significant volumes of transported material, even in the deep Whittard Channel.

2) The net suspended sediment transport is mainly up-canyon, but sediment gravity flow events do occur (potentially due to anthropogenic activities) and carry shallow-water sediments and foraminiferal tests to greater depths. However, the down-canyon transport of labile OM by means of gravity flows

appears to be limited. The fresh OM found in deeper regions, particularly the Whittard Channel, appears to arrive through the vertical deposition and lateral transport of settling phytodetritus from phytoplankton blooms that occur during spring and summer.

3) The active sediment transport and trapping of OM influences the benthic fauna. In general, meiofauna, macrofauna and foraminifera showed increased abundances and/or biomass inside the canyon compared to the continental slope (adjacent slope, Goban Spur or nearby Porcupine Seabight), although this pattern could not be conclusively demonstrated for the megafauna. Similarly meiofaunal and foraminiferal abundances were higher in the upper than in the lower canyon. These patterns are related to a local increase of OM, food availability or food quality in the canyon compared to on the slope and in the upper canyon compared to the lower cayon. Megabenthic filter feeders, such as sponges, anemones, crinoids and corals, are found in higher densities inside the canyon (especially on the walls) than on the open slope. They are higher in the eastern than in the western branch. A similar east-west pattern has been reported for macrofauna, and again appears to be linked to OM quality and quantity. There is no evidence for a contrast in megafaunal densities inside versus outside the canyon, although data are very limited to a single trawl sample and should be treated with caution.

4) Biodiversity patterns are less consistent than abundance patterns between faunal groups and seem more influenced by local effects within the canyon branches. Nematode diversity at genus level decreased progressively with increasing water depth in the western middle branch of the Whittard Canyon; this was not the case for meiofauna higher taxa diversity. Local macrofaunal diversity appeared to be depressed inside the Whittard Canyon compared to the adjacent slope, but was characterised by an increase in opportunistic species not seen on the slope. This suggests that the canyon may still enhance diversity at a regional scale and exert an important influence on macrofaunal abundance, biomass and diversity patterns both locally and regionally. The multiple patterns of biodiversity compared to the open slope are generated by the complex, localised interactions of several environmental drivers and the different response of organisms and populations. Megafauna diversity increased on steep slopes and topographic highs and decreased towards the thalweg. However, there is little evidence of a

canyon endemic megafauna. Most species observed in the canyon also occur on the neighbouring continental slope, although comparative studies are needed to conclusively test this.

5) Elevated current velocities keep food for filter feeders in suspension and also expose hard substrata to which organisms can attach. Constriction of across-canyon tidal currents by the steep canyon walls and compensating amplification of along-canyon velocities is one mechanism by which elevated and spatially variable current regimes may occur. A second is enhancement of near-bottom currents associated with the focusing of internal tides in the canyon. The complex bathymetry of Whittard Canyon (with sub-, super- and near-critical reflection regimes) and the likely presence of short but energetic nonlinear waveforms means that the internal tide field needs to be observed and modelled at high resolution in order to map current variability at the same scale as biological observations. Further complications arise from temporal changes to the internal tide field in response to the spring-neap cycle and on longer timescales in response to mesoscale activity and seasonal changes in stratification.

6) The continuous sediment resuspension due to fishing, specifically bottom trawling in the Whittard Canyon can gradually reshape seafloor community structure and biodiversity (i.e. enhancing SPM fluxes, which smothers filter feeders and provides nutritional unsuitable material) reducing its original complexity.

Overall, this review has shown that perhaps the definition of an 'active' submarine canyon should not just be linked to the frequency of large-volume sediment flows and to unidirectional sediment transport from shallow waters to the deep-sea. A wide range of more frequent physical processes is 'active' in Whittard Canyon, both in terms of oceanography and sediment dynamics. Those equally contribute to the canyon formation and maintenance, and have a direct influence on the ecosystem functioning. It can be argued that those (tidal, seasonal) processes may be as important as, if not even more important than, large episodic events in shaping communities in submarine canyons. The spatial and temporal scales at which they occur are closer to the intrinsic scales of the biological patterns and ecological functioning within canyons, even if the latter ones are not well known yet. It is precisely a better insight in these intrinsic scales of biological patterns that is now urgently needed in order to fully understand the

interaction between physical processes and biological observations, between environmental drivers and community distributions. Some of the complex patterns observed in Whittard Canyon are difficult to interpret based on existing observations. Further coordinated studies are therefore necessary to clarify the processes responsible for these highly variable faunal distributions. Sampling along bathymetric transects within branches of the Whittard Canyon and across the adjacent open slopes is limited, inconsistent between disciplines and faunal groups, and often confined to a single time point. Further advances will require concerted interdisciplinary research based on samples and observations made at the same locations, as well as better temporal coverage based on long-term observation and time-series programs. Ultimately, other submarine canyon systems, potentially with different 'activity' regimes, need to be investigated through similar large, multi-scale, multidisciplinary and well-coordinated studies to allow global insights in canyon processes to be reached. Although seemingly homogenous, nearby canyons may differ tremendously.

A good understanding of the fundamental active processes governing submarine canyons, including their spatial and temporal scale, is also of major importance in order to correctly evaluate the impact of human activities. Although most active canyons may exhibit broad ecosystem patterns similar to those observed in the Whittard Canyon, the shelf-to-canyon sediment delivery mechanisms are often different. The Whittard Canyon head is located ~300 km from land, which means terrestrial sediment input is reduced compared to, for example, the Nazaré or Kaikoura Canyon. The effects of nepheloid layers and sediment flows caused by bottom trawling on canyon flanks may be very different in submarine canyons like Whittard Canyon, that are driven by tidal resuspension and limited downslope sediment flows, compared to systems with regular flows such as river-fed canyons. Equally, more indirect human impacts such as changes in water column temperature and density structure, caused by global warming, may have different impacts on the generation and propagation of internal tides, and hence on the crucial canyon 'activity' driving biodiversity and ecosystem functioning. Also acidification, reduced oxygen levels and the introduction of chemical pollutants are expected to have major effects on submarine canyon systems, and may cause reductions in faunal biomass and diversity. Major decreases in biomass will cause a widespread change in benthic ecosystems and

the functions and services they provide, causing unprecedented challenges for the sustainable management of canyon systems. The more insights can be obtained into the activity and functioning of submarine canyons by means of integrated studies, the better such challenges can be answered in the future.

7. Acknowledgments

This study was partially supported by Marie Curie Actions through the project CEFMED (project number 327488) and HERMES (contract number GOCE-CT 2005-511234-1). VAIH and KR are supported by the ERC Starting Grant project CODEMAP (Grant no 258482) and the NERC NC MAREMAP programme. AMW is funded by a Hardiman Research Scholarship, NUI Galway. RD and CG acknowledge the support of the programme RITMARE. JI was partially supported by a Marie Curie Intra-European Fellowship (MESMEC, Grant Agreement FP7-PEOPLE-2011-IEF no. 00879)

References

Allen, S. and Durrieu de Madron, X. (2009). A review of the role of submarine canyons in deep-ocean exchange with the shelf. Ocean Science, 5, 607-620.

Amaro, T., Bianchelli, S., Billett, D. S. M., Cunha, M. R., Pusceddu, A, and Danovaro, R. (2010). The trophic biology of the holothurian *Molpadia musculus*: implications for organic matter cycling and ecosystem functioning in a deep submarine canyon. Biogeosciences, 7: 1-14.

Amaro, T., de Stigter, H., Lavaleye, M. & Duineveld, G. (2015). Organic matter enrichment in the Whittard Channel (northern Bay of Biscay margin, NE Atlantic); its origin and possible effects on benthic megafauna. Deep-Sea Research Part I. 102, 90-100.

Amin, M. and Huthnance, J.M. (1999). The pattern of cross-slope depositional fluxes. Deep Sea Research Part I: Oceanographic Research Papers, 46, 1565-1591.

Baines, P. G. (1982). On internal tide generation models. Deep Sea Research Part A. Oceanographic Research Papers, 29,307-338.

Bianchelli S, Gambi C, Zeppilli D, Danovaro, R. (2010) Metazoan meiofauna in deep-sea canyons and adjacent open slopes: a large-scale comparison with focus on the rare taxa. Deep-Sea Research I, 57: 420-433.

Billett, D.S.M., Bett, B.J., Reid, W.D.K., Boorman, B., Priede, M. (2010). Long-term change in the abyssal NE Atlantic: The 'Amperima Event' revisited, Deep-Sea Research II 57, 1406–1417.

Bourillet, J.F., Reynaud, J.Y., Baltzer, A., Zaragosi, S. (2003). The 'Fleuve Manche': the submarine sedimentary features from the outer shelf to the deep-sea fans. Journal of Quaternary Science 18, 261-282.

Bourillet, J.F., Zaragosi, S., Mulder, T. (2006). The French Atlantic margin and deep-sea submarine systems. Geo-Marine Letters 26, 311-315.

Bosley, K. L., Lavelle, J. W., Brodeur, R. D., Wakefield, W. W., Emmett, R. L., Baker, E. T., & Rehmke, K. M. (2004). Biological and physical processes in and around Astoria submarine Canyon, Oregon, USA. Journal of Marine Systems, 50(1), 21-37.

Bower, A. S., Lecann, B., Rossby, T., Zenk, W., Gould, J, Speer, K, Richardson, P.L., Prater, M.D. and Zhang, H.-M (2002). Directly measured mid-depth circulation in the northeastern North Atlantic Ocean. Nature, 419, 603-607.

Brooke, S. and Ross, S.W. (2014). First observations of the cold-water coral *Lophelia pertusa* in mid Atlanctic canyons of the USA. Deep-sea research II, 104, 245-251.

Cooper L.H.N. and Vaux D. (1949). Cascading over the continental slope of water from the Celtic Sea. Journal of the Marine Biology Association of the United Kingdom, 28, 719–750.

Cunningham, M.J., Hodgson, S., Masson, D.G., Parson, L.M. (2005). An evaluation of along- and down-slope sediment transport processes between Goban Spur and Brenot Spur on the Celtic Margin of the Bay of Biscay. Sedimentary Geology 179, 99-116.

Danovaro R, Bianchelli S, Gambi C, Mea M, Zeppilli, D. (2009) α-, β-, γ-, δ and ε-diversity of deep-sea nematodes in canyons and open slopes of E-Atlantic and Mediterranean margins. Marine Ecology Progress Serie, 396: 197-209.

Danovaro R, Gambi C, Lampadariou N, Tselepides, A. (2008) Deep-sea biodiversity in the Mediterranean Basin: testing for longitudinal, bathymetric and energetic gradients. Ecography 31: 231-244.

Davies, J. S.,. Howell, K. L ; Stewart, H. A. , Guinan, J. and Golding, N. (2014). Defining biological assemblages (biotopes) of conservation interest in the submarine canyons of the South West Approaches (offshore United Kingdom) for use in marine habitat mapping. Deep Sea Research II, 104, 208-229.

Davies, J.S., Stewart, H.A., Narayanaswamy, B.E., Jacobs, C., Spicer, J., Golding, N., Howell, K.L. (2015). Benthic assemblages of the Anton Dohrn Seamount (NE Atlantic): defining deep-sea biotopes to support habitat mapping and management efforts with a focus on Vulnerable Marine Ecosystems. PLoS ONE. . DOI: 10.1371/journal.pone.0124815.

de Graciansky, P.C., Poag, C.W. and Foss, G. (1985). Drilling on the Goban Spur: objectives, regional geological setting, and operational summary, in: de Graciansky, P.C., Poag, C.W., Cunningham, R., Loubere, P., Masson, D.G., Mazzullo, J.M., Montadert, L., Müller, C., Otsuka, K., Reynolds, L.A., Sigal, J., Snyder, S.W., Vaos, S.P., Waples, D. (Eds.), Initial Reports of the Deep Sea Drilling Project. U.S. Government Printing Office, Washington, pp. 5-13.

De Mol, L., Van Rooij, D., Pirlet, H., Greinert, J., Frank, N., Quemmerais, F. and Henriet, J.-P. (2011). Cold-water coral habitats in the Penmarc'h and Guilvinec Canyons (Bay of Biscay): Deep-water versus shallow-water settings. Marine Geology, 282 (1-2), 40-52.

Derégnaucourt, D. and Boillot, G. (1982). Structure géologique du golfe de Gascogne. Bull. BRGM 2, 149-178.

De Stigter, H.C., Boer, W., de Jesus Mendes, P.A., Jesus, C.C., Thomsen, L., van den Bergh, G.D., van Weering, T.C.E. (2007). Recent sediment transport and deposition in the Nazaré Canyon, Portuguese continental margin. Marine Geology 246, 144–164.

De Stigter, H., Lavaleye, M., Duineveld, G. and van Weering, T. (2008a). Sediment dynamics of the Whittard Canyon, Celtic Margin. Presentation at the 3rd HERMES workshop, Carvoeiro, Portugal, March 2008.

De Stigter, H.C. and shipboard scientific party (2008b). Report of cruise 64PE269 with RV Pelagia, Portimão – Cork, 19 May – 11 June 2007. Dispersal of anthropogenic lead in submarine canyons. NIOZ – Royal Netherlands Institute for Sea Research, Texel, The Netherlands, 65 pp.

Dingle, R.V., Scrutton, R.A. (1979). Sedimentary succession and tectonic history of a marginal plateau (Goban Spur, Southwest of Ireland). Marine Geology 33, 45-69.

Duineveld G., Lavaleye M.S.S., Berghuis E.M., de Wilde P. (2001). Activity and composition of the benthic fauna in the Whittard Canyon and the adjacent continental slope (NE Atlantic). Oceanologica Acta, 24, 69–83.

Dullo, W.-C., S. Flögel, and A. Rüggeberg (2008). Cold-water coral growth in relation to the hydrography of the Celtic and Nordic European continental margin. Marine Ecology Progress Series, 165-176.

Duros, P., Fontanier, C., Metzger, E., Pusceddu, A., Cesbron, F., de Stigter, H.C., Bianchelli, S., Danovaro, R., Jorissen, F.J. (2011). Live (stained) benthic foraminifera in the Whittard Canyon,

Celtic margin (NE Atlantic). Deep-Sea Research Part I: Oceanographic Research Papers 58, 128–146.

Duros, P., Fontanier, C., de Stigter, H.C., Cesbron, F., Metzger, E., Jorissen, F.J. (2012). Live and dead benthic foraminiferal faunas from Whittard Canyon (NE Atlantic): focus on taphonomic processes and paleo-environmental applications. Marine Micropaleontology 94-95: 25-44.

Egbert, G. D. (1997). Tidal data inversion: interpolation and inference. Progress in Oceanography, 40, 53-80. Tidal Science In Honour of David E.Cartwright.

Egbert, G. D. and Erofeeva, S. Y. (2002). Efficient inverse modeling of barotropic ocean tides. Journal of Atmospheric and Oceanic Technology, 19,183-204.

Evans, C.D.R. (1990). The geology of the western English Channel and its western approaches. HMSO for the British Geological Survey, London.

Evans, C.D.R., Hughes, M.J. (1984). The Neogene succession of the South Western Approaches, Great Britain. Journal of the Geological Society of London 141, 315-326.

Flögel, S., Dullo, W. C., Pfannkuche, O. Kiriakoulakis, K. and Rüggeberg, A. (2014). Geochemical and physical constraints for the occurrence of living cold-water corals. Deep Sea Research Part II: Topical Studies in Oceanography 99:19-26.

Gambi, C., Vanreusel, A., Danovaro, R. (2003). Biodiversity of nematode assemblages from deep-sea sediments of the Atacama Slope and Trench (Southern Pacific Ocean). Deep-Sea Research I, 50, 103-117.

Gambi C, Pusceddu A, Benedetti-Cecchi L, and Danovaro R (2014). Species richness, species turnover, and functional diversity in nematodes of the deep Mediterranean Sea: searching for drivers at different spatial scales. Global ecology and biogeography, 23, 24-39.

Gambi C., Danovaro R. (2016). Biodiversity and life strategies of deep-sea meiofauna and nematode assemblages in the Whittard canyon (Celtic margin, NE Atlantic Ocean). Deep Sea Research Part I 108, 13-22.

Garrett, C. and Kunze, E. (2007). Internal tide generation in the deep ocean. Annual Review. Fluid Mech., 39, 57-87.

Gooday, A.J. (1988). A response by benthic foraminifera to phytodetritus deposition in the deep sea. Nature, 332: 70-73.

Gordon, R. L. and Marshall, N. F. (1976). Submarine canyons - internal wave traps. Geophysical Research Letters, 3, 622-624.

Gunton, L.M., Gooday, A.J., Glover, A.J., Bett, B.J. (2015a) Macrofaunal abundance and community composition at lower bathyal depths in different branches of the Whittard Canyon and on the adjacent slope (3500m; NE Atlantic). Deep Sea Research Part I 97, 29-39.

Gunton, L.M., Neal, L., Gooday, A.J., Bett, B.J., Glover, A.G. (2015b). Local and regional variation in deep-sea polychaete diversity: canyon influence (Whittard Canyon system, NE Atlantic). Deep Sea Research Part I 106, 42-54.

Hall, R. A. and Carter, G. S. (2011). Internal Tides in Monterey Submarine Canyon. Journal of Physical Oceanography, 41, 186-204.

Hall, R. A., Alford, M. H., Carter, G. S., Gregg, M. C., Lien, R.-C., Wain, D. J., and Zhao, Z. (2014). Transition from partly standing to progressive internal tides in Monterey Submarine Canyon. Deep-Sea Research II 104, 164-173.

Harris, P.T., Whiteway, T., (2011). Global distribution of large submarine canyons: geomorphic differences between active and passive continental margins. Marine Geology 285, 69-86.

Haughton, P. (2009) Hybrid sediment gravity flow deposits - Classification, origin and significance. Marine and Petroleum Geology, 26, 1900-1918.

Hedges J.I., Keil R.G., 1995. Sedimentary organic matter preservation: an assessment and speculative synthesis. Marine Chemistry, 49, 81–115.

Hickey, B. M. (1995). Coastal submarine canyons. Topographic effects in the ocean. SOEST Special publications, 95-110.

Holligan, P. M., Pingree, R. D., & Mardell, G. T. (1985). Oceanic solitons, nutrient pulses and phytoplankton growth. Nature, 314, 348-350.

Holt, J. and Thorpe, S. (1997). The propagation of high frequency internal waves in the celtic sea. Deep Sea Research Part I: Oceanographic Research Papers, 4, 2087-2116.

Hopkins, J. E., Stephenson, G. R., Green, J., Inall, M. E., and Palmer, M. R. (2014). Storms modify baroclinic energy uxes in a seasonally stratified shelf sea: Inertial-tidal interaction. Journal of Geophysical Research: Oceans, 119, 6863-6883.

Hotchkiss, F. S. and Wunsch, C. (1982). Internal waves in hudson canyon with possible geological implications. Deep-Sea Research Part a-Oceanographic Research Papers, 29,415-442.

Howell, K. L. (2010). A benthic classification system to aid in the implementation of marine protected area networks in the deep/high seas of the NE Atlantic. Biological Conservation 143:1041-1056.

Hunter, W.R., Jamieson, A.J., Huvenne, V., Witte, U. (2013). Sediment community responses to marine vs. terrigenous organic matter in a submarine canyon. Biogeosciences 10, 67-80.

Huvenne, V.A.I., Tyler, P.A., Masson, D.G., Fisher, E.H., Hauton, C., Hühnerbach, V., Le Bas, T.P., Wolff, G.A. (2011). A Picture on the Wall: Innovative Mapping Reveals Cold-Water Coral Refuge in Submarine Canyon. (J.M. Roberts, Ed.). PLoS ONE 6, e28755.

Huvenne, Veerle A.I.; Davies, Jaime S. (2014). Towards a new and integrated approach to submarine canyon research. Introduction. Deep Sea Research Part II: Topical Studies in Oceanography, 104. 1-5.

Inall, M., Aleynik, D., Boyd, T., Palmer, M., and Sharples, J. (2011). Internal tide coherence and decay over a wide shelf sea. Geophysical Research Letters, 38, L23607, doi:10.1029/2011GL049943.

Ingels, J., Kiriakoulakis, K., Wolff, G.A., Vanreusel, A. (2009). Nematode diversity and its relation to the quantity and quality of sedimentary organic matter in the deep Nazare Canyon, Western Iberian Margin. Deep-Sea Research Part I-Oceanographic Research Papers 56(9), 1521-1539.

Ingels J., Tchesunov A.V., Vanreusel A. (2011a) Meiofauna in the Gollum Channels and the Whittard Canyon, Celtic Margin - How Local Environmental Conditions Shape Nematode Structure and Function. PLoS ONE 6 (5), 1-15.

Ingels, J., Billett, D., Van Gaever, S., Vanreusel, A. (2011b) An insight into the feeding ecology of deep-sea canyon nematodes - Results from field observations and the first in-situ C-13 feeding experiment in the Nazare Canyon. Journal of Experimental Marine Biology and Ecology 396(2), 185-193.

Ingels, J., Billett, D.S.M., Kiriakoulakis, K., Wolff, G.A., Vanreusel, A. (2011c). Structural and functional diversity of Nematoda in relation with environmental variables in the Setúbal and Cascais

canyons, Western Iberian Margin. Deep Sea Research Part II: Topical Studies in Oceanography 58(23-24), 2354-2368.

Ingels, J., Vanreusel, A., Romano, C., Coenjaerts, J., Mar Flexas, M., Zúñiga, D., Martin, D., 2013a. Spatial and temporal infaunal dynamics of the Blanes submarine canyon-slope system (NW Mediterranean); changes in nematode standing stocks, feeding types and gender-life stage ratios. Progress in Oceanography 118, 159-174.

Ingels, J., Vanreusel, A., 2013b. The importance of different spatial scales in determining structural and functional characteristics of deep-sea infauna communities. Biogeosciences 10(7), 4547-4563.

Ismail, K., 2016. Marine landscape mapping in submarine canyons. University of Southampton, Ocean & Earth Science, Doctoral Thesis, 154 pp.

Ivanov V.V., Shapiro G.I., Huthnance J.M., Aleynik D.L., Golovin P.N. (2004). Cascades of dense water around the world ocean. Progress in Oceanography, 60, 47–98.

Joint, I.R., Owens, N.J.P. and Pomroy, A.J. (1986). Seasonal production of photosynthetic picoplankton and nanoplankton in the Celtic Sea. Marine Ecology Progress Series, 28, 251-258.

Joint I, Wollast R, Chou L, Batten S, Elskens M, et al. (2001) Pelagic production at the Celtic Sea shelf break. Deep-Sea Research Part II: Topical Studies in Oceanography 48: 3049–3081.

Jamieson, A.J., Kilgallen, N.M., Rowden, A.A., Fujii, T., Horton, T., Lorz, A.-N., Kitazawa, K. and Priede, I.G. (2011). Bait-attending fauna of the Kermadec Trench, SW Pacific Ocean: evidence for an ecotone across the abyssal-hadal transition zone. Deep-Sea Research Part I 58, 49–62.

Johnson, M. P.; White, M.; Wilson, A.; Würzberg, L.; Schwabe, E.; Folch, H. and Allcock, A. L. (2013). A vertical wall dominated by Acesta excavata and Neopycnodonte zibrowii, part of an undersampled group of deep-sea habitats. PLoS ONE 8:e79917.

Kershaw, C., Whitfield, E., Wilson, A., White, M., Kirby, J, and Kiriakoulakis, K. (2015) Sedimentation and organic biogeochemistry in the Whittard Canyon, NE Atlantic. Inaugural Meeting of the Deep-Sea Ecosystems Special Interest Group, Challenger Society for Marine Science, Liverpool, July 2015.

Kiriakoulakis K., Blackbird S., Ingels J., Vanreusel A., Wolff G.A. (2011). Organic geochemistry of submarine canyons: The Portuguese margin, Deep Sea Research Part II, 58, 2477-2488.

Lambeck, K., (1996). Glaciation and sea-level change for Ireland and the Irish Sea since Late Devensian/Midlandian time. Journal of the Geological Society of London 153, 853-872.

Lavaleye M., Duineveld G., Lundälv T., White M., Guihen D., Kiriakoulakis K., Wolff G.A. (2009). Cold-Water Corals on the Tisler Reef. Preliminary observations on the dynamic reef environment. Oceanography, 22, 76-84.

Lavaleye, M. and shipboard scientific crew. (2009). CORALFISH-HERMIONE Cruise Report, Cruise 64PE313, Galway-Lisbon, 16 Oct - 5 Nov 2009, Belgica Mound Province (CoralFISH & HERMIONE), Whittard Canyon (HERMIONE) and Galicia Bank area (BIOFUN). NIOZ - Royal Netherlands Institute for Sea Research, Texel, The Netherlands, 46 pp.

Leduc, D., Rowden, A.A., Probert, P.K., Pilditch, C.A., Nodder, S.D., Vanreusel, A., Duineveld, G.C.A., Witbaard, R. (2012). Further evidence for the effect of particle-size diversity on deep-sea benthic biodiversity. Deep Sea Research Part I: Oceanographic Research Papers, 63, 164-169.

Leduc, D., Rowden, A., Nodder, S., Berkenbusch, K., Probert, P., Hadfield, M. (2014). Unusually high food availability in Kaikoura Canyon linked to distinct deep-sea nematode community. Deep Sea Research Part II: Topical Studies in Oceanography 104, 310-318.

Lins, L., Vanreusel, A., van Campenhout, J., Ingels, J. (2013). Selective settlement of deep-sea canyon nematodes after resuspension - an experimental approach. Journal of Experimental Marine Biology and Ecolology, 441, 110-116.

Martín, J., Puig, P., Palanques, A., Masqué, P., García-Orellana, J. (2008). Effect of commercial trawling on the deep sedimentation in a Mediterranean submarine canyon. Marine Geology 252, 150-155.

Martín, J., Palanques, A., Vitorino, J., Oliveira, A., de Stigter, H.C. (2011). Near-bottom particulate matter dynamics in the Nazaré submarine canyon under calm and stormy conditions. Deep-Sea Research Part II, Topical Studies in Oceanography 58, 2388-2400.

Martín, J., Puig, P., Palanques, A., and Ribó, M. (2014). Trawling-induced daily sediment resuspension in the flank of a Mediterranean submarine canyon. Deep Sea Research Part II: Topical Studies in Oceanography, 104, 174-183.

Masson D.G., Huvenne V.A.I., de Stigter H., Wolff G.A., Kiriakoulakis K., Arzola R.G., Blackbird S. (2010). Efficient burial of carbon in a submarine canyon. Geology, 38, 831–834.

McCave, I.N. (1986). Local and global aspects of the bottom nepheloid layers in the world ocean. Netherlands Journal of Sea Research 20, 167-181.

Meyers, P. A. (1997) Organic geochemical proxies of paleoceanographic, paleolimnologic and paleoclimatic processes. Organic Geochemistry, 27, 213–250

Morris K.J., Tyler R.A., Masson D.G. Huvenne V.I.A. and Rogers A. (2013). Distribution of cold water corals in the Whittard Canyon NE Atlantic. Deep Sea Research II, 92, 136-144.

Muller-Navarra D.C., Brett M.T., Liston A.M. and Goldman C.R. (2000). A highly unsaturated fatty acid predicts carbon transfer between primary producers and consumers. Nature, 403, 74–77.

Mulder, T., Zaragosi, S., Garlan, T., Mavel, J., Cremer, M., Sottolichio, A., Sénéchal, N., Schmidt, S. (2012). Present deep-submarine canyons activity in the Bay of Biscay (NE Atlantic). Marine Geology, 295–298, 113-127.

Narayanaswamy, B. E., Hughes, D. J., Howell, K. L., Davies, J., and Jacobs, C. (2013). First observations of megafaunal communities inhabiting George Bligh Bank, Northeast Atlantic. Deep Sea Research Part II: Topical Studies in Oceanography.

Nash, J. D., Kunze, E., Toole, J. M., and Schmitt, R. W. (2004). Internal tide reflection and turbulent mixing on the continental slope. Journal of Physical Oceanography, 34,1117-1134.

Pérez, F. F., Ríos, A. F., King, B. A., Pollard, R. T. (1995). Decadal changes of the θ− S relationship of the Eastern North Atlantic Central Water. Deep Sea Research Part I: Oceanographic Research Papers, 42, 1849-1864.

Pham, C.K., Ramirez-Llodra, E.R., Alt, C., Amaro, T., et al. (2014) Marine litter distribution and density in European seas, from the shelves to deep basins. PLoS ONE 9(4):e95839.

Pingree, R. (1980). Physical oceanography of the celtic sea and english channel. Elsevier Oceanography Series, 24, 415-465.

Pingree, R. and Mardell, G. (1985). Solitary internal waves in the celtic sea. Progress in Oceanography, 14, 431-441.

Pingree R.D. and LeCann, B. (1989). Celtic and Armorican slope and shelf residual currents Progress in Oceanography, 23, 303–338.

Pingree, R. D., Sinha, B., Griffiths, C.R. (1999). Seasonality of the European slope current (Goban Spur) and ocean margin exchange. Continental Shelf Research 19, 929-975.

Pingree, R.D. and Le Cann, B. (1990). Structure, strength and seasonality of the slope currents in the Bay of Biscay region. Journal of the Marine Biological Association of the United Kingdom, 70, 857-885.

Pollard, R. T., Griffttths, M. J., Cunningham, S. A., Read, J. F., Pérez, F. F., Ríos, A. F. (1996). Vivaldi 1991-A study of the formation, circulation and ventilation of Eastern North Atlantic Central Water. Progress in Oceanography, 37,167-192.

Praeg, D., McCarron, S., Dove, D., Ó Cofaigh, C., Scott, G., Monteys, X., Facchin, L., Romeo, R., Coxon, P. (2015). Ice sheet extension to the Celtic Sea shelf edge at the Last Glacial Maximum. Quaternary Science Reviews, 111, 107-112.

Puig, P. and Palanques, A., (1998). Temporal variability and composition of settling particle fluxes on the Barcelona continental margin (Northwestern Mediterranean). Journal of Marine Research, 56, 639-654.

Puig, P., Canals, M., Company, J.B., Martín, J., Amblas, D., Lastras, G., Palanques, A., Calafat, A.M. (2012). Ploughing the deep sea floor. Nature 489, 286–289.

Puig, P., Palanques, A., Martín, J. (2014). Contemporary Sediment-Transport Processes in Submarine Canyons. Annual Review of Marine Science, 6, 53-77.

Pusceddu A, Mea M, Canals M, Heussner S, Durrieu de Madron X, Sanchez-Vidal A, Bianchelli S, Corinaldesi C, Dell'Anno A, Thomsen L, Danovaro R (2013) Major consequences of an intense dense shelf water cascading event on deep-sea benthic trophic conditions and meiofaunal biodiversity. Biogeosciences 10(4): 2659-2670.

Reid, G.S., Hamilton, D. (1990). A Reconnaissance Survey of the Whittard Sea Fan, Southwestern Approaches, British-Isles. Marine Geology 92, 69–86.

Rees, A.P., Joint, I. and Donald. K.M. (1999). Early spring bloom phytoplankton-nutrient dynamics at the Celtic Sea Shelf Edge. Deep Sea Research, 46, 483-510.

Rice, A. L., Tyler, P. A., & Paterson, G. J. L. (1992). The pennatulid *Kophobelemnon stelliferum* (Cnidaria: Octocorallia) in the porcupine seabight (north-east Atlantic Ocean). Journal of the Marine Biological Association of the United Kingdom, 72(02), 417-434.

Roberts, J. M., L. A. Henry, D. Long, and J. P. Hartley (2008). Cold-water coral reef frameworks, megafaunal communities and evidence for coral carbonate mounds on the Hatton Bank, north east Atlantic. Facies, 54, 297-316.

Robert, K., D. O. B. Jones, P. A. Tyler, D. Van Rooij and V. A. I. Huvenne (2015). Finding the hotspots within a biodiversity hotspot: fine-scale biological predictions within a submarine canyon using high-resolution acoustic mapping techniques. Marine Ecology, 36(4), 1256-1276. DOI: 10.1111/maec.12228.

Romano, C., Coenjaerts, J., Mar Flexas, M., Zúñiga, D., Vanreusel, A., Company, J.B., Martin, D. (2013). Spatio-temporal variability of meiobenthic density in the Blanes submarine canyon (NW Mediterranean). Progress in Oceanography 118, 144-158.

Ryan, J. P., Chavez, F. P., & Bellingham, J. G. (2005). Physical-biological coupling in Monterey Bay, California: topographic influences on phytoplankton ecology. Marine Ecology Progress Series, 287, 23-32.

Sanchez-Vidal, A., Canals, M., Calafat, A.M., Lastras, G., Pedrosa-Pàmies, R., Menéndez, M., Medina, R., Company, J.B., Hereu, B., Romero, J., Alcoverro, T. (2012). Impacts on the Deep-Sea Ecosystem by a Severe Coastal Storm. PlosOne 71, e30395.

Scourse, J., Uehara, K., Wainwright, A. (2009). Celtic Sea linear tidal sand ridges, the Irish Sea Ice Stream and the Fleuve Manche : palaeotidal modelling of a transitional passive margin depositional system. Marine Geology, 259, 102-111.

Sharples, J., Tweddle, J. F., Mattias Green, J., Palmer, M. R., Kim, Y.-N., Hickman, A. E., Holligan, P. M., Moore, C. M., Rippeth, T. P., Simpson, J. H., et al. (2007). Spring-neap modulation of internal tide mixing and vertical nitrate fluxes at a shelf edge in summer. Limnology and Oceanography, 52, 1735-1747.

Sibuet, J.-C., Monti, S., Loubrieu, B., Mazé, J.-P., Srivastava, S. (2004). Carte bathymétrique de l'Atlantique nord-est et du golfe de Gascogne. Bulletin du Société Géologique de France 175, 429–442.

Soetaert, K. and Heip, C. (1995) Nematode assemblages of deep-sea and shelf break sites in the North Atlantic and Mediterranean Sea. Marine Ecology Progress Series 125: 171-183

Skliris, N. and Denidi, S. (2006). Plankton dynamics controlled by hydrodynamic processes near a submarine canyon off NW corsican coast: a numerical modelling study. Continental Shelf Research, 26, 1336-1358.

Stewart, H.A., Davies, J.S., Guinan, J.C., Howell, K.L. (2014). The Dangeard and Explorer Canyons, South-West Approaches, UK: Geology, sedimentology and newly discovered cold-water coral mini-mounds. Deep-Sea Research II 104, 230-244.

Tchesunov, A.V., Ingels, J., Popova, E.V. (2012). Marine free-living nematodes associated with symbiotic bacteria in deep-sea canyons of north-east Atlantic Ocean. Journal of the Marine Biological Association of the United Kingdom 92(6), 1257-1271.

Thorpe, S. A. (2005). The Turbulent Ocean. Cambridge University Press.

Toucanne, S., Zaragosi, S., Bourillet, J.F., Naughton, F., Cremer, M., Eynaud, F., Dennielou, B., (2008). Activity of the turbidite levees of the Celtic-Armorican margin (Bay of Biscay) during the last 30,000 years: Imprints of the last European deglaciation and Heinrich events. Marine Geology, 247, 84-103.

Turnewitsch R., Springer B. M., Kiriakoulakis K., Vilas J. C., Arístegui J., Wolff G. A., Peine F., Werk S., Graf G., Waniek. J. (2007). Approaching the true concentration of particulate organic carbon in seawater: the relative methodological importance of artificial organic carbon gains and losses in two-filtration-based techniques. Marine Chemistry, 105, 208-228.

Tyler, P. A., and H. Zibrowius (1992). Submersible observations of the invertebrate fauna on the continental-slope southwest of ireland (NE atlantic-ocean). Oceanologica Acta 15:211-226.

Tyler P., Amaro T., Azorla R., Cunha M., de Stigter H., Gooday A., Huveene V., Ingels J., Kiariakoulakis K., Lastras G., Masson D., Oliveira A., Pattenden A., Vanreusel A., van Weering T., Vitorino J., Witte U., Wolff G.A. (2009). Europe's 'Grand Canyon': the Nazaré Submarine Canyon. Oceanography, 22, 46-57.

Vanhove, S., Vermeeren, H. and Vanreusel, A., (2004). Meiofauna towards the south Sandwich Trench (750-6300 m), focus on nematodes. Deep-Sea Research Part II, 51, 1665-1687.

Vanreusel, A., Fonseca, G., Danovaro, R., da Silva, M., Esteves, A., Ferrero, T., Gad, G., Galtsova, V., Gambi, C., Genevois, V., Ingels, J., Ingole, B., Lampadariou, N., Merckx, B., Miljutin, D., Miljutina, M., Muthumbi, A., Netto, S., Portnova, D., Radziejewska, T., Raes, M., Tchesunov, A., Vanaverbeke, J., Van Gaever, S., Venekey, V., Bezerra, T., Flint, H., Copley, J., Pape, E., Zeppilli, D., Martinez, P., Galeron, J. (2010). The contribution of deep-sea macrohabitat heterogeneity to global nematode diversity. Marine Ecology-an Evolutionary Perspective 31(1), 6-20.

van Aken, H. M. (2000a). The hydrography of the mid-latitude northeast Atlantic Ocean: I: The deep water masses. Deep Sea Research Part I: Oceanographic Research Papers 47:757-788.

van Aken, H. M. (2000b). The hydrography of the mid-latitude Northeast Atlantic Ocean: II: The intermediate water masses. Deep Sea Research Part I: Oceanographic Research Papers 47:789-824.

van Rooij, D., Iglesias, J., Hernández-Molina, F.J., Ercilla, G., Gomez-Ballesteros, M., Casas, D. Llave, E., De Hauwere, A., Garcia-Gil, S., Acosta, J. and Henriet, J.P. (2010a). The Le Danois Contourite Depositional System: interactions between the Mediterranean outflow water and the upper Cantabrian slope (North Iberian margin). Marine Geology, 274, 1-20.

van Rooij, D., de Mol, L., Ingels, J., Versteeg, W., Ruggeberg, A., Jauniaux, T., party, the shipboard scientific party (2010b) Cruise Report Belgica 10/17b, Belgica BiSCOSYSTEMS II, Leg 2, Whittard Canyon. Renard Centre of Marine Geology & Marine Biology Research Group, Ghent University, Belgium, pp. 39.

Van Weering, T.C.E., Thomsen, L., van Heerwaarden, J., Koster, B., Viergutz, T. (2000). A seabed lander and new techniques for long term in situ study of deep-sea near bed dynamics. Sea Technology 41, 17–27.

Vlasenko, V., Stashchuk, N., Inall, M. E., and Hopkins, J. E. (2014). Tidal energy conversion in a global hot spot: On the 3-d dynamics of baroclinic tides at the celtic sea shelf break. Journal of Geophysical Research: Oceans, 119(6):3249-3265.

Weston, J. (1985). Comparison between Recent benthic foraminiferal faunas of the Porcupine Seabight and Western Approaches continental slope. Journal of Micropaleontology. 4: 165-183.

White M., Mohn C., Kiriakoulakis K., 2015. Environmental Sampling. In: Biological sampling in the deep-sea: An (illustrated) manual of tools and techniques (eds: Clark M., Consalvey M., Rowden A.) Wiley-Blackwell.

Wilson, M.F.J., O'Connell, B., Brown, C., Guinan, J.C. & Grehan, A.J. (2007). Multiscale Terrain Analysis of Multibeam Bathymetry Data for Habitat Mapping on the Continental Slope. Marine Geodesy, 30, 3-35.

Wilson, A.M., Raine, R., Mohn,C. and White, M. (2015a). Nepheloid layer distribution in the Whittard Canyon, NE Atlantic Margin. Marine Geology, 367,130-142.

Wilson, A.M., Raine, R., Gerritsen, H., Kiriakoulakis, K., Blackbird, B., Allcock, L. and White, M. (2015b) Anthropogenic influence on sediment transport in the Whittard Canyon, NE Atlantic. Marine Pollution Bulletin 101, 320-329.

Wollast, R. and Chou, L. (2001). The carbon cycle at the ocean margin in the northern Gulf of Biscay. Deep Sea Research Part II, 48, 3265-3293.

Xu, J.P., Noble, M.A., Eittreim, S.L., Rosenfeld, L.K., Schwing, F.B., Pilskaln, C.H., 2002. Distribution and transport of suspended particulate matter in Monterey Canyon, California. Marine Geology 181, 215-234.

Zaragosi, S., Bourillet, J.F., Eynaud, F., Toucanne, S., Denhard, B., Van Toer, A., Lanfumey, V., 2006. The impact of the last European deglaciation on the deep-sea turbidite systems of the Celtic-Armorican margin (Bay of Biscay). Geo-Marine Letters 26, 317-329.

Acknowledgments

Over the last 4 year and 9 months, on the PhD rollercoaster, I have been fortunate enough to work alongside the most amazing people and they are all due some thanks!

First and foremost, I want to thank my supervisors (official and unofficial). To Martin White, for your continuous support, guidance and enthusiasm, I am forever grateful. I will miss hearing “do you know what we could…” as the light bulbs have a disco in your head. You have always had great confidence in me and paid great attention to my development as a researcher and to the project. Thank you for teaching me to see the tree in the forest!! To Robin Raine, for welcoming me to the A-team. This journey would never have begun without your support, generosity and positivity. I will always be grateful. To Kostas Kiriakoulakis, for your patience and general air of calmness, particularly during the turbulent days of a data panic! You were always at the end of an email with an answer! Thanks for everything and for introducing me to the lovely world of lipids!

To my GRC panel, Prof. Mark Johnson and Dr. Rachel Cave, for your support, helpful advice and funny stories! Many times during the write up I have reminded myself of your beaver story Mark.

The department of Earth and Ocean Sciences and the Ryan Institute, all the technical staff, particularly to Sheena Fennel- you are wonder woman! Thank you for all the chats, crocheting tutorials and all your help.

To my fellow post grads-past and present! Ellen for all the dinners, debrief sessions after a hard day and for the motivational pictures! To the ladies –Aimee and Sineád, for the copious amounts of tea and baked goods! To Cossie and Gary, for all the good times in 301, 305 and along our corridor! I miss you both!! Ye are both an inspiration for what is ahead! To Clynt (on)! For being such a great office buddy over the last few weeks! Thanks for all the snacks! Your support and generosity has made the last hurdle so much easier. To Nico for your helpful advice always!

To all the staff at Liverpool John Moore's University that made me feel so welcome. To Emma, Cat, Milly and Liz – you are all so amazing! Thanks for everything while I was in Liverpool, particularly Emma for finding me places to live and sleep including on your couch.

To the crew of the Celtic Explorer, you are all so wonderful. I would also like to thank all the scientists that helped me collect my samples-all that filtering!! Particularly Sorcha and Morag and, Cossie for being human SAPS! To chief scientist Louise Allcock, for mentoring me both on board and on land, I am so grateful for your guidance.

To my Polarstern family, for the most inspiring six weeks of my life that I will never, ever forget. And to all the amazing scientists I have meet on this journey.

To my friends, for being so supportive and understanding over the last few years. A big shout out to Áine and Rose, for all the phone calls, skypes and milestone celebrations – I couldn't ask for better people. Rose for also putting me up in Liverpool and Áine for knowing what a nepheloid layer is! To 'Nom' for all the laughs, especially to Jenny for all your support during the early days. To the Ballygoran ladies for keeping it real and the marine girls for your inspiration! Conor for all the good times – soon I will have the floppy hat! Fran for your friendship and love always.

To the Corrigans, there are no words to describe your generosity and kindness. Ger and Louis, I am so grateful for everything over the last few years.

To my family. I wouldn't have got this far without ye. Thanks for all your love and support and reminders to "keep the faith!" when times were tough. I can't wait for Sunday dinner! Bring on the cheese and port!

To my wonderful boyfriend Ronan. You have more than earned your honorary degree! Thank you for your encouragement, patience, good humour, dinner making, gifts of wifi and proof reading! I'll stop talking about PhD chapters now so we can start our next chapter.

Go raibh míle maith agaibh!!!!